

UTRECHT STUDIES IN EARTH SCIENCE

Nr. 24

**Biogeochemistry of selenium isotopes:
processes, cycling and paleoenvironmental applications**

Kristen Mitchell

Cover: The image on the cover is was taken by the Galileo spacecraft on December 7, 1992 on its way to explore the Jupiter system in 1995-97. This file is in the public domain because it was created by NASA. NASA copyright policy states that "NASA material is not protected by copyright unless noted".This image was downloaded from Wikimedia Commons (commons.wikimedia.org) a database of 13,327,537 freely usable media files to which anyone can contribute under Creative Commons license (creativecommons.org)

Printed by **CPI Wöhrmann Print Service.**

ISBN: 978-90-6266-312-5

Biogeochemistry of selenium isotopes: processes, cycling and paleoenvironmental applications

Biogeochemie van selenium isotopen: processen, cycli en paleo-
milieu toepassingen
(met een samenvatting in het Nederlands)

Proefschrift

ter verkrijging van de graad van doctor aan de Universiteit Utrecht op
gezag van de rector magnificus, prof.dr. G.J. van der Zwaan,
ingevolge het besluit van het college voor promoties in het openbaar
te verdedigen op donderdag
15 november 2012 des middags te 12.45 uur
door

Kristen Ann Mitchell
geboren op 5 oktober 1982 te Pennsylvania, USA

Promotor:
Prof. dr. Philippe Van Cappellen

Co-promotor:
Dr. Paul R.D. Mason

Members of the dissertation committee:

Prof. dr. Laurent Charlet

University of Grenoble

Prof. dr. Gregory A. Cutter

Old Dominion University

Prof. dr. Thomas M. Johnson

University of Illinois at Urbana-Champaign

Prof. dr. Timothy W. Lyons

University of California at Riverside

Prof. dr. Jack J. Middelburg

Utrecht University

A GOOD TRAVELER HAS NO FIXED PLANS
AND IS NOT INTENT UPON ARRIVING.
A GOOD ARTIST LETS HIS INTUITION
LEAD HIM WHEREVER IT WANTS.
A GOOD SCIENTIST HAS FREED HIMSELF OF CONCEPTS
AND KEEPS HIS MIND OPEN TO WHAT IS.

THUS THE MASTER IS AVAILABLE TO ALL PEOPLE
AND DOESN'T REJECT ANYONE.
HE IS READY TO USE ALL SITUATIONS
AND DOESN'T WASTE ANYTHING.
THIS IS CALLED EMBODYING THE LIGHT.

WHAT IS A GOOD MAN BUT A BAD MAN'S TEACHER?
WHAT IS A BAD MAN BUT A GOOD MAN'S JOB?
IF YOU DON'T UNDERSTAND THIS, YOU WILL GET LOST,
HOWEVER INTELLIGENT YOU ARE.
IT IS THE GREAT SECRET.

~LAO TZU

Table of Contents

TABLE OF CONTENTS	I
SUMMARY	V
SAMENVATTING IN HET NEDERLANDS	XI
CHAPTER 1 GENERAL INTRODUCTION	1
1.1 Aims and scope of thesis	3
1.2 Introduction	4
1.3 Chemistry of selenium	7
1.3.1 Analytical chemistry of Se	9
1.3.2 Marine cycle of Se.....	10
1.4 Biological redox pathways	13
1.4.1 Biological uptake of Se	13
1.4.2 Assimilatory reduction	15
1.4.3 Selenoprotein functionality	17
1.4.4 Dissimilatory reduction	21
1.4.5 Microbial oxidation	25
1.4.6 Volatilization.....	25
1.5 Abiotic redox pathways.....	26
1.5.1 Reduction by iron (II) compounds	26
1.5.2 Reduction by sulfide compounds	27
1.5.3 Reduction in hydrothermal settings.....	28
1.5.4 Photochemical transformations of Se.....	29
1.6 Selenium stable isotope chemistry	29
1.6.1 Selenium isotope mass spectrometry	30
1.6.2 Selenium stable isotope fractionation	32
1.7 Organization and structure of thesis.....	41
References	43
CHAPTER 2 MARINE BIOGEOCHEMICAL CYCLE OF SELENIUM	55
Abstract	57
2.1 Selenium as micronutrient.....	58
2.2 Biogeochemistry of Selenium: analog of sulfur, or not? ...	59

2.3	Biological cycling of Se and S	65
2.3.1	Assimilatory reduction	67
2.3.2	Dissimilatory reduction	70
2.4	Isotope fractionation.....	71
2.4.1	Fractionation associated with assimilatory reduction	71
2.4.2	Fractionation associated with dissimilatory reduction	72
2.5	biochemical evolution of selenium	75
2.6	Genetics: the UGA codon and tRNA	76
2.7	Selenocysteine containing proteins and their functionality	78
2.7.1	Nickel–iron–selenium hydrogenase	81
2.7.2	Thioredoxin Reductase.....	82
2.7.3	Gluthione peroxidase.....	83
2.8	Geological evolution	83
2.9	Integrated biological and geological evolution	89
	References	92

CHAPTER 3 SELENIUM ISOTOPE DISTRIBUTION IN THE OCEANS103

	Abstract	105
3.1	Introduction	106
3.2	Model	108
3.2.1	Model parameters	108
3.2.2	Sensitivity Analysis and response times	116
3.3	Results and discussion.....	117
3.3.1	Sensitivity analysis and response time	117
3.3.2	Model scenarios.....	120
3.4	Conclusions	127
	References	129

CHAPTER 4 SELENIUM AS PALEO-OCEANOGRAPHIC PROXY133

Abstract	135
4.1 Introduction and background	137
4.2 Materials	144
4.2.1 Marine plankton	144
4.2.2 Black Sea: modern euxinic basin	145
4.2.3 Arabian Sea: modern oxygen minimum zone (OMZ)	145
4.2.4 Demerara Rise and Cape Verde Basin: OAE2.....	146
4.2.5 Posidonia Shale: Early Jurassic (Toarcian Oceanic Anoxic Event).....	147
4.2.6 New Albany Shale: stratified basin	149
4.2.7 Alum Shale: Late Cambrian SPICE	149
4.3 Methods	150
4.3.1 Sample digestion	150
4.3.2 Analytical techniques	151
4.4 Results	155
4.5 Discussion	159
4.6 Conclusions	171
References	174
Supplemental information	185
4.7 Site data	185
4.7.1 Black Sea	185
4.7.2 Arabian Sea	186
4.7.3 Demerara Rise and Cape Verde Basin	188
4.7.4 Posidonia Shale	190
4.7.5 New Albany Shale.....	191
4.7.6 Alum Shale.....	192
4.8 Selenium isotope analytical interferences and double spike calculations.....	194
4.8.1 Isobaric interferences	194
4.8.2 Double isotope spike and data reduction.....	196
References	199

CHAPTER 5 SELENIUM SORPTION AND ISOTOPE FRACTIONATION.....201

Abstract	203
5.1 Introduction	204
5.2 Methods	206
5.2.1 Iron minerals	206
5.2.2 Experiments	208
5.2.3 Analytical techniques	209
5.2.4 Data analysis	213
5.3 Results	216
5.3.1 Reaction kinetics	216
5.3.2 Selenium isotope fractionations	221
5.4 Discussion	224
5.5 Conclusions	228
References	229
Supplemental information	233
CHAPTER 6 CONCLUSIONS AND FUTURE RESEARCH DIRECTIONS...	235
6.1 Conclusions	237
6.2 Future work	239
References	242
ACKNOWLEDGEMENTS	243
CURRICULUM VITAE	245

SUMMARY

Selenium (Se) is an essential trace element, which, with multiple oxidation states and six stable isotopes, has been suggested as a potentially powerful environmental tracer and paleoenvironmental proxy. This thesis investigates the biogeochemical cycling of Se and Se isotope fractionation from a paleoenvironmental perspective.

A general introduction to the chemistry and biogeochemical cycling is presented in **Chapter 1** of the thesis. This detailed literature review considers the Se cycle in a new light, instead of in the shadow of the sulfur (S) cycle. While the Se cycle does share some similarities with the S cycle, there are major differences that become apparent from a synthesis of the existing literature, we therefore further compare the oceanic cycles of Se and S in **Chapter 2**.

Due to selenium's redox sensitive behavior and chemical similarity to sulfur, the biogeochemical cycle of Se and Se stable isotopes have recently enjoyed renewed interest. The marine biogeochemical cycles of S and Se are fundamentally different because of differences in concentration, distribution, speciation and residence times that impact the use and interpretation of Se isotope data. The differences between the S and Se cycles are analyzed in relation to their distributions in the oceans, their role in biochemical cycles and the isotope fractionations that occur during biological uptake and reduction. The biochemical function of Se is reviewed in

an evolutionary context. The geological evolution of the S cycle and the S isotopic record are then used as a framework for discussing the Se isotopic compositions observed in marine sedimentary rocks spanning geological history.

Selenium concentrations in marine shales are generally very low averaging around 5 ppm and cover a very limited isotopic range ($\delta^{82/76}\text{Se}$: -2 to +2‰). This suggests that assimilatory uptake and nutrient recycling has controlled the Se cycle throughout geologic time, despite biological evolution and major perturbations in the composition of the oceans and atmosphere. In **Chapter 3**, the conceptual biogeochemical Se cycle model constructed in **Chapter 2** is expanded to include isotope compositions and isotope fractionation mechanisms. The isotopic model highlights the insensitivity of global sedimentary Se isotope signatures to changes in marine Se cycling. Because of the short residence time of Se in the oceans, the signatures recorded in marine sediments are most sensitive to changes in the isotopic composition of the Se inputs. The stability of the Se isotope system even when the oceans undergo major changes is consistent with the narrow range of Se isotope compositions that are observed in the sedimentary rock record.

In **Chapter 4** a more detailed analysis Se isotope compositions in marine sediments and sedimentary rocks is undertaken. Bulk Se concentrations and Se isotopic compositions are analyzed in a suite of about 120 samples of fine-grained marine sedimentary rocks and sediments spanning the entire Phanerozoic. While the Se

concentrations vary greatly (0.22 to 72 ppm), the $\delta^{82/76}\text{Se}$ values fall in a fairly narrow range from -1 to +1‰, with the exception of laminated black shales from the New Albany Shale formation (Late Devonian), which have $\delta^{82/76}\text{Se}$ values of up to +2.20‰. Black Sea sediments (Holocene) and sedimentary rocks from the Alum Shale formation (Late Cambrian) have Se to total organic carbon ratios (Se/TOC) and $\delta^{82/76}\text{Se}$ values close to those found in modern marine plankton ($1.72 \pm 0.15 \times 10^{-6}$ mol/mol and 0.42 ± 0.22 ‰). For the other sedimentary sequences and sediments, the Se/TOC ratios show Se enrichment relative to modern marine plankton. Additional input of isotopically light terrigenous Se may explain the Se/TOC and $\delta^{82/76}\text{Se}$ data measured in recent Arabian Sea sediments (Pleistocene). The very high Se concentrations in sedimentary sequences that include the Cenomanian-Turonian Oceanic Anoxic Event (OAE) 2 may reflect an enhanced input of volcanogenic Se to the oceans. As the latter has an isotopic composition not greatly different from marine plankton, the volcanogenic source does not impart a distinct signature to the sedimentary Se isotope record. The lowest average $\delta^{82/76}\text{Se}$ values are observed in the OAE2 samples from Demerara Rise and Cape Verde Basin cores ($\delta^{82/76}\text{Se} = -0.14 \pm 0.45$ ‰) and could reflect fractionation associated with microbial or chemical reduction of Se oxyanions in the euxinic water column. In contrast, a limiting availability of seawater Se during periods of increased organic matter production and burial may be responsible for the elevated $\delta^{82/76}\text{Se}$ values and low Se/TOC ratios in the black shales of the New Albany Shale formation.

Overall, our results indicate that to unlock the full proxy potential of marine sedimentary Se records, we need to gain a much more detailed understanding of the sources, chemical speciation, isotopic fractionations and cycling of Se in the marine environment.

The isotopic compositions found in the sedimentary rock record prompted the investigation of other processes that may impart Se isotope fractionations. In **Chapter 5**, Se sorption and abiotic reduction processes are investigated because 1) they are important processes influencing the mobility and cycling of Se in natural environments and 2) they have received relatively little attention, particularly with respect to the associated isotopic fractionations. In this chapter, we determined the rates of reaction and isotopic fractionations of Se(IV) and Se(VI) during sorption to iron oxides (2-line ferrihydrite, hematite and goethite) and iron sulfides (mackinawite and pyrite) at pH 7 and room temperature (22±2°C). More than 80% of aqueous Se(IV) was removed from solution in the presence of the mineral phases, except for hematite where only 40% of aqueous Se(IV) was sorbed. In contrast, less than 20% of aqueous Se(VI) was removed in the mineral suspensions, except for 2-line ferrihydrite where approximately 50% removal was observed. While XANES spectra revealed no change in Se oxidation state when Se(IV) and Se(VI) sorbed to iron oxides, they showed evidence of reduction in the presence of iron sulfides. Selenium isotopic fractionations, expressed as $\epsilon^{82/76}\text{Se}$, were always less than 1‰ in the experiments with iron oxides (mean $\epsilon^{82/76}\text{Se}$: 0.2‰). Fractionations were

significantly higher in the experiments with iron sulfides, with $\epsilon^{82/76}\text{Se}$ values of up to $\sim 10\text{‰}$ in the Se(IV)-pyrite system, and a mean $\epsilon^{82/76}\text{Se}$ value of 2.3‰ for all sorption experiments with iron sulfides combined. The larger fractionations in the experiments with iron sulfides reflect the chemical reduction of Se(IV) and Se(VI). The highest isotope fractionation observed in the Se(IV)-FeS₂ system (9.7‰) is comparable to that previously reported for Se(VI) reduction by green rust (11.1‰).

Finally, **Chapter 6** summarizes the main conclusions of the thesis and gives suggestions for future work. Chapter 6 emphasizes that the marine Se cycle is dominated by biological cycling in surface waters. This cycling is so rapid that Se isotopes are homogenized on very short timescales, and marine sediments record changes almost instantaneously. Therefore, most of the recorded changes are due to local or regional variations in Se inputs, rather than global changes in ocean circulation and biogeochemical dynamics. Thus, future work must be formulated carefully to ensure a meaningful use of Se isotopes as a paleo-proxy.

SAMENVATTING IN HET NEDERLANDS

Selenium (Se) is een essentieel sporenelement dat, met meerdere oxidatiestaten en zes stabiele isotopen, een potentiële, veelvermogende milieu-merkstof en paleomilieu aanduider kan zijn. Dit proefschrift onderzoekt de biochemische kringloop van Se en Se isotoop fractionatie, gezien vanuit een paleomilieuperspectief.

Een algemene introductie in de scheikundige en biochemische kringloop is gepresenteerd in **Hoofdstuk 1** van dit proefschrift. Deze gedetailleerde literatuurstudie zet de Se cyclus in een nieuw licht, in plaats van in de schaduw van de zwavel (S) cyclus. Hoewel de Se cyclus verscheidene overeenkomsten heeft met de S cyclus, zijn er grote verschillen die naar voren kwamen tijdens het samenstellen van een overzicht van de bestaande literatuur. In **Hoofdstuk 2** zullen we daarom verder gaan met het maken van een vergelijking tussen de oceanische cycli van Se en S.

De biochemische kringlopen van stabiele Se isotopen hebben recentelijk hernieuwde interesse ontvangen vanwege het redoxgevoelige gedrag van Se en de chemische overeenkomsten met zwavel. De mariene biochemische kringlopen van S en Se zijn fundamenteel verschillend door verschillen in concentratie, distributie, speciatie en verblijftijden, welke het gebruik en de interpretatie van Se isotoopgegevens beïnvloeden. De verschillen tussen de S en Se cycli zijn bestudeerd in relatie tot hun verspreiding in de oceanen, hun rol in biochemische cycli, alsmede de isotoop fractionatie die plaats vindt

tijdens biologische opname en reductie. De biochemische functie van Se wordt vanuit een evolutionaire context besproken. De geologische evolutie van de S cyclus en het S isotopen gegevensrecord zijn vervolgens gebruikt als een raamwerk voor het bespreken van Se isotoopsamenstellingen die, verspreid door de geologische geschiedenis, geobserveerd zijn in mariene, sedimentaire gesteenten.

Selenium concentraties in mariene schalies zijn over het algemeen erg laag, gemiddeld rond de 5 ppm, en omvatten een zeer nauw isotopenbereik ($\delta^{82/76}\text{Se}$: -2 to +2‰). Dit suggereert dat door de geologische tijd, assimilatieve opname en veelvuldig hergebruik de Se kringloop heeft beheerst, ondanks biologische evolutie en grote verstoringen in de samenstelling van de oceanen en de atmosfeer. In **Hoofdstuk 3** wordt het conceptuele biochemische Se kringloopmodel, dat in **Hoofdstuk 2** is geconstrueerd, uitgebreid zodat het ook isotoopsamenstellingen en isotoop fractionatiemechanismen aankaart. Het isotopenmodel belicht de ongevoeligheid van de wereldwijde, sedimentaire Se isotopensignatuur voor veranderingen in de mariene Se kringloop. Vanwege de korte verblijftijd van Se in de oceanen zijn de signaturen die opgeslagen zijn in mariene sedimenten het meest gevoelig voor veranderingen in de isotoopsamenstelling van de Se invoer. Zelfs wanneer de oceanen grote veranderingen ondergaan komt de stabiliteit van het Se isotopensysteem overeen met het smalle bereik van Se isotoopsamenstellingen gevonden in het sedimentaire gesteenterecord.

In **Hoofdstuk 4** volgt een meer gedetailleerde analyse van de Se isotoopsamenstellingen gevonden in mariene sedimenten en sedimentaire gesteenten. Voor een verzameling van ongeveer 120 monsters, bestaande uit fijn-korrelige mariene, sedimentaire gesteenten en sedimenten uit het Phanerozoicum, zijn bulk Se concentraties en Se isotoopsamenstellingen geanalyseerd. Terwijl de Se concentraties sterk variëren (0.22 tot 72 ppm), vallen de $\delta^{82/76}\text{Se}$ waarden binnen een smal bereik van -1 tot +1‰, met uitzondering van gelamineerde, zwarte shalies uit de New Albany Shale formatie (laat Devoon), welke $\delta^{82/76}\text{Se}$ waarden tot +2.20‰ laten zien. Zwarte Zee sedimenten (Holoceen) en sedimentaire gesteenten van de Alum Shale formatie (laat Cambrium) hebben Se-totaal organische koolstof verhoudingen (Se/TOC) en $\delta^{82/76}\text{Se}$ waarden die overeenkomen met die voor hedendaags mariene plankton ($1.72 \pm 0.15 \times 10^{-6}$ mol/mol en $0.42 \pm 0.22\%$, respectievelijk). Voor de overige sedimentaire opeenvolgingen en sedimenten laten de Se/TOC ratios een relatieve Se-verrijking zien ten opzichte van hedendaagse, mariene plankton. Aanvullende invoer van isotopisch licht, terrigeen Se kan een verklaring zijn voor de Se/TOC en $\delta^{82/76}\text{Se}$ waarden gemeten in recente Arabische Zee sedimenten (Pleistoceen). De zeer hoge Se concentraties in sedimentaire opeenvolgingen, die het Cenomanien-Turonien Oceanische Anoxische Event (OAE) 2 omvatten, laten een verhoogde aanvoer van vulkanisch Se naar de oceanen zien. Aangezien vulkanisch Se een isotoopsamenstelling heeft die geen grote verschillen heeft ten opzichte van mariene plankton, betekent

een vulkanische bron geen onderscheidende signatuur in het sedimentaire Se isotopenrecord. De laagste, gemiddelde waarden voor $\delta^{82/76}\text{Se}$ werden geobserveerd in OAE2 monsters genomen van Demerara Rise en Cape Verde Basin kernen ($\delta^{82/76}\text{Se} = -0.14 \pm 0.45\text{‰}$) en zouden een weerspiegeling kunnen zijn van fractionatie geassocieerd met microbiële of chemische reductie van Se oxy-anionen in de euxinische waterkolom. Daarentegen, een beperkte beschikbaarheid van zeewatergerelateerd Se tijdens periodes van verhoogde productie van organisch materiaal en begraving zouden verantwoordelijk kunnen zijn voor de verhoogde $\delta^{82/76}\text{Se}$ waarden en lage Se/TOC ratios in de zwarte schalies van de New Albany Shale formation. Over het algemeen laten onze resultaten zien dat we een veel gedetailleerder begrip van de bronnen, isotoop fractionatie en kringloop van Se in het mariene milieu nodig hebben om de volledige potentie van mariene, sedimentaire Se records te ontsluiten.

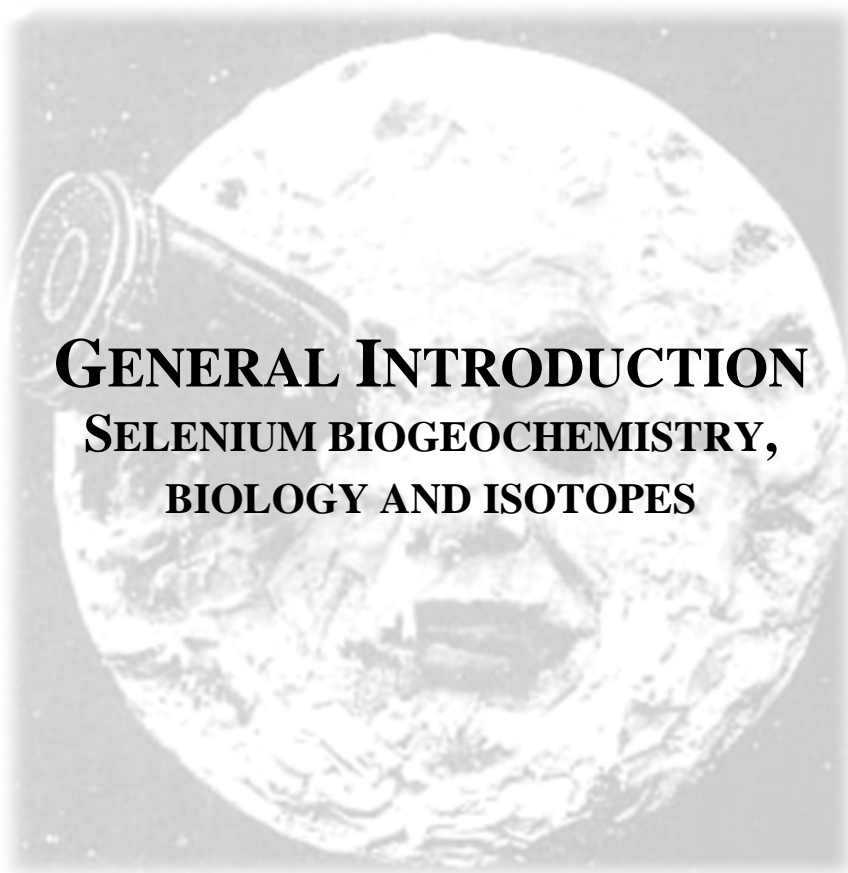
De isotoopsamenstellingen aangetroffen in sedimentaire gesteenten leidde tot het onderzoeken van andere processen die Se fractionatie kunnen beïnvloeden. In **Hoofdstuk 5**, zijn Se sorptie en abiotische processen onderzocht omdat 1) zij belangrijke processen zijn die de mobiliteit en kringloop van Se in natuurlijke milieus beïnvloeden, en omdat 2) zij relatief weinig aandacht hebben ontvangen, specifiek ten opzichte van de geassocieerde isotoop fractionaties. In dit hoofdstuk bepalen we de snelheden van reactie en isotoop fractionatie van Se(IV) en Se(VI) gedurende sorptie aan ijzeroxiden (2-lijns ferrihydriet, hematiet en goethiet) en ijzersulfiden

(mackinawiet en pyriet), bij een pH van 7 en bij kamertemperatuur ($22\pm 2^\circ\text{C}$). In de aanwezigheid van de genoemde mineraalfasen was meer dan 80% van het opgeloste Se(IV) verwijderd van de oplossing, behalve in het geval van hematiet, waaraan slechts 40% van het opgeloste Se(VI) was geadsorbeerd. Daarentegen, in dezelfde mineraalsuspensies, minder dan 20% van het opgeloste Se(IV) was verwijderd, behalve voor de 2-lijns ferrihydriet oplossing, waarvoor ongeveer 50% was verwijderd. Terwijl XANES spectra geen verandering laten zien in de Se-oxidatiestaat tijdens Se(IV) en Se(VI) adsorptie aan ijzeroxides, laten ze wel bewijs zien van reductie in de aanwezigheid van ijzersulfiden. Selenium isotoop fractionatie, weergegeven als $\epsilon^{82/76}\text{Se}$, was altijd minder dan 1‰ in experimenten met ijzeroxides (gemiddelde $\epsilon^{82/76}\text{Se}$: 0.2‰). Fractionatie was significant hoger in de experimenten met ijzersulfides, met $\epsilon^{82/76}\text{Se}$ waarden tot ~10‰ in het Se(IV)-pyriet systeem, en een gemiddelde $\epsilon^{82/76}\text{Se}$ waarde van 2.3‰ voor alle sorptie experimenten met ijzersulfides tesamen. De grotere fractionatie in de experimenten met ijzersulfides reflecteert de chemische reductie van Se(IV) en Se(VI). De hoogste isotoop fractionatie geobserveerd in het Se(IV)-FeS₂ systeem (9.7‰) is vergelijkbaar met voorgaande, gerapporteerde waarden voor Se(VI) reductie door groene roest mineralen (11.1‰).

Uiteindelijk, **Hoofdstuk 6** vat de hoofdconclusies van het proefschrift samen en geeft suggesties voor toekomstig onderzoek. **Hoofdstuk 6** benadrukt dat de mariene Se kringloop gedomineerd wordt door biologische processen in oppervlaktewateren. Deze cycli

zijn zo snel dat Se isotopen gehomogeniseerd worden op zeer korte tijdschaal en dat mariene sedimenten vrijwel instantaan van samenstelling veranderen. Daardoor zijn de meeste van de geregistreerde veranderingen veroorzaakt door lokale of regionale veranderingen in Se invoer, in plaats van wereldwijde veranderingen in zeewatercirculatie en biochemische dynamiek. Dus, toekomstig onderzoek zal voorzichtig geformuleerd moeten worden om een bruikbare toepassing van Se isotopen als paleo-proxy te waarborgen.

CHAPTER 1



GENERAL INTRODUCTION SELENIUM BIOGEOCHEMISTRY, BIOLOGY AND ISOTOPES

SELENIUM IS NAMED AFTER THE GREEK *σελήνη*, *selene*
MEANING MOON.

THE IMAGE ON THE PREVIOUS PAGE IS FROM THE 1902 FILM *LE VOYAGE DANS LA LUNE* (*A TRIP TO THE MOON*) WRITTEN AND DIRECTED BY GEORGES MÉLIÈS. THIS WORK IS IN THE PUBLIC DOMAIN IN THE UNITED STATES BECAUSE IT WAS PUBLISHED (OR REGISTERED WITH THE U.S. COPYRIGHT OFFICE) BEFORE JANUARY 1, 1923.

1.1 AIMS AND SCOPE OF THESIS

This project began with the intention of developing selenium (Se) isotopes as a tracer for early life. The initial questions we planned to address were the following.

- 1) Can Se isotope variations recorded in sediments and sedimentary rocks serve as robust biomarkers?
- 2) More specifically, can Se isotopes be used at environmentally relevant (i.e. low) Se concentrations to infer microbial activity and hence expand the potential to trace ancient microbial life?
- 3) How different are microbially mediated Se isotope fractionations from those within the sulfur (S) system? Can the two isotope systems be combined more reliably to differentiate biogenic from inorganic processes in ancient sedimentary rocks?
- 4) Is there a relationship between the cell specific selenate reduction rate and Se isotope fractionation factor? In other words, do Se isotopes reflect activity?

As the research progressed it became apparent that we first needed to understand the biogeochemical cycling of Se further before we could assess the potential utility of the Se isotope proxy. Looking at the Se cycle in a holistic way shifted our focus away from microbially mediated selenium oxyanion reduction to the interpretation of Se isotopic fractionations found in the rock record, in terms of the key processes in the oceanic Se cycle. The research objectives were therefore redefined as follows.

- 1) Develop an updated biogeochemical Se cycle for the oceans based on recent advances in the Se literature and compare and

contrast Se biogeochemical cycle and isotope geochemistry with that of S.

- 2) Construct an isotopic mass balance model to assess our understanding of the Se isotope signatures that are observed in the marine geologic record.
- 3) Evaluate the utility of Se isotope signatures in sedimentary rocks as a paleo-tracer for life and redox conditions.
- 4) Determine the contribution of abiotic reactions to Se isotope fractionation.

1.2 INTRODUCTION

Selenium was discovered by two Swedish scientists, J.J. Berzelius and J.G. Gahn, in 1817 (Crystal, 1973). The two researchers analyzed a residual slime that was formed during the oxidation of sulfur dioxide from copper pyrites. The residue was initially thought to be tellurium, named from the Latin, *tellus*, meaning earth. Tellurium had been discovered approximately 35 years before. However, upon further investigation it proved to be a unique element, and was named after the Greek (σελήνη) *selene* meaning moon. Note, however, that a work by Arnold of Villanova the “Rosarius Philosophorum”, from the fourteenth century, refers to a red sulfur deposit (*sulfur rubeum*) discovered on the inside walls of an oven where vapor from crude sulfur had condensed (Crystal, 1973). This may have been the first recorded observation of selenium.

Selenium is one of the rarest trace elements in the earth’s crust with an average abundance of $0.05 \mu\text{g g}^{-1}$ (Taylor, 1964). It is also unevenly distributed on the surface of the Earth (Oldfield, 2002).

Selenium can accumulate to high concentrations in ore deposits (e.g. coal), hydrothermal formations and fluids, as well as in the run-off from irrigated seleniferous soils and in wastewaters generated by anthropogenic activity (Plant et al., 2003).

Selenium has long been an element of environmental and public health interest due to its dual role as an essential element and a toxin (Schwartz, 1977). Selenium toxicity and deficiency is apparent in humans as well as livestock and wildlife. Selenium deficiency in animals becomes apparent at levels between 0.05 and 0.10 mg/kg and toxicity effects occur at levels exceeding 5 to 15 mg/kg (Milne, 1998). Selenium, mainly as selenocysteine, the 21st amino acid, is essential for the synthesis of over 20 known selenoproteins (Hatfield and Gladyshev, 2002). The bioavailability of selenium is highly dependent on its oxidation state. Selenium has several oxidation states, the main ones being (-II), (0), (IV) and (VI). In solution, selenium generally occurs as selenate, SeO_4^{2-} , and selenite SeO_3^{2-} . Selenium toxicity can result from ingestion of food or water, but also through inhalation of dust particles or gaseous forms. Hydrogen selenide is toxic to humans at a concentration as low as 1.5 ppm (Lide, 2006).

Areas of unusually high or low concentrations exist in several places on Earth, including areas of the United States, the United Kingdom, and China (Oldfield, 2002). These areas often become areas of interest due to the diseases that can result from selenium toxicity or deficiency in livestock and or humans. These diseases include Kashin-Beck disease (a joint disorder) and Keshan disease (a heart disorder)

in humans both of which are caused by selenium deficiency, whereas selenosis is typically found in areas with high levels of selenium. Water, agricultural and medical issues associated with selenium have been extensively studied, especially in China where areas experiencing both selenium deficiency and toxicity may be closely located relative to one another.

Selenium isotopes have a long history among the ‘heavy stable isotopes’ or ‘non-traditional’ stable isotopes, the first study being carried out by Krouse and Thode (1962). However, the rigors of the analytical process proved too difficult for the techniques to become commonplace. Because of recent analytical advances selenium isotopes have begun to experience a renaissance. With the advent of the multi-collector inductively coupled plasma mass spectrometer (MC-ICP-MS), sample sizes have decreased dramatically allowing for a wider range of applications (Rouxel et al., 2002). Selenium isotopes are now being used as environmental and geological tracers (Johnson et al., 1999; Johnson et al., 2000; Rouxel et al., 2002; Rouxel et al., 2004; Wen et al., 2007; Clark and Johnson, 2008; Clark and Johnson, 2010; Wen and Carignan, 2011; Schilling et al., 2011a, b; Mitchell et al., 2012). The early studies of Se isotopes focused on constraining some of the predicted equilibrium isotopic fractionations, as well as measuring values of selenium isotope fractionation during chemical reduction (Krouse and Thode, 1962; Rees and Thode, 1966; Rashid and Krouse, 1985). More recent studies of selenium isotope systematics are interested in more environmentally relevant selenium isotope fractionation pathways (Johnson et al., 1999; Johnson et al.,

2000; Rouxel et al., 2002; Johnson and Bullen, 2003; Ellis et al., 2003; Rouxel et al., 2004; Wen et al., 2007; Clark and Johnson, 2008; Clark and Johnson, 2010; Wen and Carignan, 2011; Schilling et al., 2011a, b; Mitchell et al., 2012). These studies have substantially expanded our knowledge of Se isotope systematics in nature.

Many comparisons are drawn between the selenium isotope system and the sulfur isotope system. However, there are some very important differences that need to be investigated further. For instance, the preservation of the isotopic signals of Se and S differ significantly. One major form of sulfur preserved in the sedimentary record is iron sulfide, whereas for selenium it is a combination of elemental Se, organically associated Se and, to a lesser extent iron selenides. Sulfate is found in abundance in evaporite minerals such as anhydrite and barite, unlike Se, which is nearly undetectable in these deposits (Nriagu, 1989b; Rouxel et al., 2004). Furthermore, there are a host of reactions that have the potential to fractionate selenium isotopes, including abiotic reduction, photo-redox reactions, adsorption, and microbial reduction. Elucidating the fractionations associated with these reactions may potentially allow selenium isotopes to be used as a tool to trace reaction pathways in the biogeochemical cycle of Se.

1.3 CHEMISTRY OF SELENIUM

On the periodic table, Se is situated between sulfur and tellurium in Group VIA. Its atomic number 34 puts it in period four between arsenic and bromine with an atomic weight of 78.96. Even though Se is characterized as a non-metal it has physical and chemical

properties that are intermediate between those of metals and non-metals. There are different allotropes of elemental Se, three of which are generally accepted (Lide, 2006). Elemental Se can have either an amorphous or crystalline structure. Amorphous Se is red in powder form or black in vitreous form and crystalline monocyclic Se is dark red, crystalline hexagonal Se is a metallic grey and also the most stable form of Se (Lide, 2006). The melting point, boiling point and specific gravity of crystalline hexagonal Se (grey) are 221°C, 685 °C, 4.79 respectively. Selenium exhibits photovoltaic and photoconductive action; it can convert a.c. power to d.c. power and is also a p-type semiconductor (Lide, 2006). These chemical properties make Se important in electronics, photography, and solar energy production. The use of selenium in these industries is widespread and contributes significantly to the anthropogenic flux of selenium in the global biogeochemical cycle of Se. Other anthropogenic sources include mining byproducts, copper smelting, coal and nuclear power plant waste.

Selenium has several oxidation states which are stable in nature, the main ones being -II, 0, IV and VI. In solution Se generally occurs as selenate (SeO_4^{2-}), and selenite oxyanions (SeO_3^{2-}). Multiple oxidation states of Se are often found together in nature, for instance elemental Se found in oxic surface waters along with Se(IV) and Se(VI), though theoretically elemental Se is not stable under these conditions (Tokunaga et al., 1991; Zhang and Moore, 1996; Zawislanski, 1998; Figure 1.1). Selenium(IV) is also found in suboxic and anoxic waters, though at very low concentrations (Cutter, 1982;

Rue et al., 1997). Organic selenides are also found in the photic zone of oxic surface waters in the ocean (Cutter, 1982, 1992).

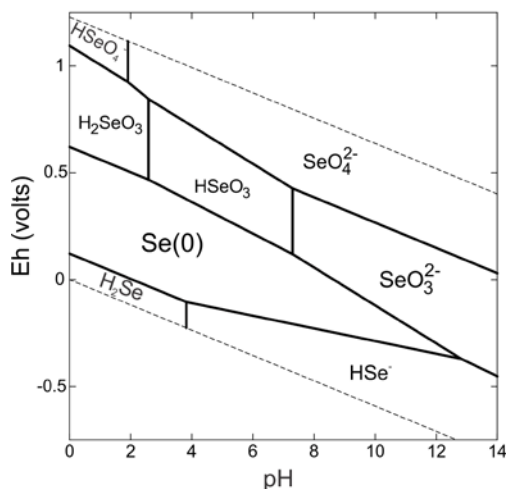


Figure 1.1 Thermodynamic stability diagram for Se, at a total Se concentration of 10^{-8} M, 25°C and 1 bar. Redrawn after Johnson and Bullen (2004).

1.3.1 ANALYTICAL CHEMISTRY OF SE

Numerous methods have been used to determine concentrations and speciation of Se in various materials, including water samples, plant material, and sediments. Traditional methods include neutron activation analysis, fluorometry, gas chromatography, mass spectrometry and atomic absorption spectrometry. Solid Se samples can be characterized using XANES (X-ray Absorption Near Edge-Edge Structure), XAS (X-ray Absorption Spectroscopy) and EXAFS (Extended X-ray Absorption Fine-Structure). Measurements of total Se and Se species have become more sensitive with the advent of techniques such as hydride generation mass spectrometry or hydride generation atomic fluorescence spectrometry, which can be

coupled with high performance liquid chromatography for more rapid and direct speciation measurements (Cutter, 1978).

One drawback of using hydride generation methods however is that only Se in the 4+ oxidation state can be measured, while other oxidation states of selenium must be determined by chemically altering the original sample. The most common procedure for aqueous sample preparation is heating with 4 M or 5M HCl (Cutter, 1978; Pettersson and Olin, 1991) . In these preparations only Se(IV) and Se(VI) are actually measured so the organic fraction can be underestimated. This can be dealt with by measuring the total Se concentrations after oxidation of the sample with hydrogen peroxide and nitric acid. Total selenium is defined as $\text{Se}(-\text{II}+0+\text{IV}+\text{VI})$. Organic selenide is then calculated as $\text{Se}(-\text{II}+0)=\text{Total Se} - \text{Se}(\text{IV}+\text{VI})$. This procedure, however, may include solid elemental selenium that is oxidized during chemical oxidation. Thus, the organic selenide fraction of environmental samples can easily be over- or under-estimated, which still represents a major obstacle to the detailed understanding of the biogeochemical cycling of Se.

1.3.2 MARINE CYCLE OF SE

In contrast to sulfate, seawater Se concentrations are very low (<1 nM or <0.08 ppb) and can be spatially variable (Cutter and Bruland, 1984). Selenium exhibits nutrient-like behavior, with very low concentration at the surface due to biological uptake and regeneration below the photic zone (e.g. Measures et al., 1983; Cutter and Cutter, 1995; Johnson, 2004). This is significantly different from the behavior of ocean sulfate, which does not display much variability

with depth. In addition to the inorganic forms of dissolved Se, organic selenide may be taken up by marine phytoplankton as a recycling mechanism in the surface ocean (Baines, 2001). The two main sources of selenium to ocean sediments are deposition of organic matter from the overlying water column (Wrench and Measures, 1982; Cutter and Bruland, 1984; Ohlendorf, 1989; Baines and Fisher, 2001) and particulate matter delivered by rivers, generally under the form of adsorbed Se(IV) or detrital organic matter. Organically-bound Se that settles out of the surface ocean is rapidly recycled at a rate of $1.6 \text{ pmol Se L}^{-1} \text{ year}^{-1}$ (Cutter and Bruland, 1984). Therefore, only a small fraction of the total assimilated Se reaches marine sediments. The present-day deposition flux of selenium to the seafloor is estimated to range from 7.4×10^9 to 1×10^{10} g Se/year (Wrench and Measures, 1982).

Little is known about the fate of organic selenium that ultimately reaches the seafloor. The usual assumption is that it is mainly preserved under the form of sulfides or selenides, although there may be other more important phases such as elemental selenium (Belzile et al., 2000). A study of riverine sediments suggests that the predominant Se species may be recalcitrant organic selenium or Se(IV) adsorbed to organic materials (Oram et al., 2008). Other studies of the reduction of selenium by ferrous iron suggest that nanoparticulate elemental selenium is an important product, and thus Se(0) could be the major oxidation state found in sediments (Charlet et al., 2007). To summarize: selenium in marine sediments can exist as iron selenides, elemental selenium, organic Se and oxidized Se sorbed to organic matter, iron oxides, or clays.

Adsorption of Se anions is also a possible supply mechanism of selenium to marine sediments. Selenate and selenite anions are known to sorb to organic matter, iron oxides and iron sulfides (Balistreri and Chao, 1987; Bruggeman et al., 2005; Scheinost and Charlet, 2008). Selenite has been shown to form strong inner-sphere complexes with α -FeOOH (goethite), making it more immobile than selenate, which forms weak outer-sphere complexes with goethite (Hayes et al., 1987). The adsorption of Se oxyanions on goethite depends on several factors including other anions present, especially phosphate and organic acids (Balistreri and Chao, 1987). The pH during deposition also plays a large role in Se mobility: selenite strongly adsorbs at low pH and becomes more mobile with increasing alkalinity up to pH 11 when it becomes completely desorbed (Howard III, 1977; Neal et al., 1987). Selenite, but not selenate, has been shown to sorb to humic substances; humic substances appear to disrupt the formation of Se(0) (Bruggeman et al., 2005; Bruggeman et al., 2007). Sorption of selenite on pyrite (FeS_2) results in the subsequent reduction to Se(0) (Bruggeman et al., 2005). Selenite also adsorbs to mackinawite (FeS) and is reduced to either Se(0) or Se(-II) in the form of FeSe depending mainly on pH (Scheinost and Charlet, 2008). Adsorption of selenite to siderite only causes minimal reduction to Se(0), with most of the selenite remaining in the original oxidation state (Scheinost and Charlet, 2008). Magnetite reduces selenite to Se(-II) after adsorption forming an unidentified mixed valence (Fe(II)-Fe(III)) iron selenide (Scheinost and Charlet, 2008).

Biological processes are a major source of selenium emissions to the atmosphere. Both land plants and phytoplankton emit volatile selenium compounds including dimethyl selenide (DMSe) and dimethyl diselenide (DMDS₂). Production of methylated selenium compounds by the marine biosphere represents the main input of selenium to the atmosphere, with a flux from $5\text{-}35 \times 10^9 \text{ g Se yr}^{-1}$ (Mosher and Duce, 1987; Amouroux and Donard, 1996; Amouroux et al., 2001). Dimethyl selenide is thought to be the main form of volatile selenium that reaches the atmosphere (Wen and Carignan, 2007). Dimethyl selenide is highly reactive and the residence time for DMSe in the atmosphere is estimated to be just 6 hours (Atkinson et al., 1990). The present day Se/S ratio of volatile components (1.5×10^{-4}) (Amouroux et al., 2001) is similar to historical values (800 B.C. to 1892) of Se/S found in Greenland ice cores (1.4×10^{-4}) (Weiss et al., 1971). After 1892, the ratio of Se/S decreased to 0.7×10^{-4} , presumably due to increasing use of petroleum products which have lower Se/S ratios ($0.1\text{-}0.5 \times 10^{-4}$) (Weiss et al., 1971; Amouroux et al., 2001).

1.4 BIOLOGICAL REDOX PATHWAYS

1.4.1 BIOLOGICAL UPTAKE OF SE

Organic selenides, including selenomethionine and selenocysteine, appear to be highly bioavailable forms of Se, along with selenite (Se(IV)) and to a lesser degree selenate (Se(VI)) oxyanions (Heider and Bock, 1993; Baines, 2001). However, this order does seem to vary depending on Se speciation, the organism and environmental conditions. Organic selenides have been shown to be

bioavailable to several types of phytoplankton including diatoms, cyanobacteria and algae (Gobler et al., 1997; Baines, 2001).

The enzyme selenocysteine lyase is thought to be the main functional enzyme in the recycling of micronutrient Se from degraded selenoproteins that contain selenocysteine as a main functional component (Stadtman, 1990; Omi et al., 2010; Mihara and Esaki, 2012). This enzyme is found in anaerobic amino acid fermenting bacteria and decomposes D-selenocysteine into pyruvate, ammonia and elemental Se. Selenocysteine lyase, unlike cysteine desulfurases which catalyze the release of S and Se from cysteine and selenocysteine, only catalyzes the degradation of selenocysteine but is inert to cysteine (Mihara and Esaki, 2012). These selenocysteine lyases have thus far only been isolated from bacteria and mammals, but it is likely that they are as widespread as their selenoprotein counterparts.

Elemental Se has long been thought to be one of the least bioavailable forms of Se. However, uptake of elemental Se has been reported in two types of bivalves, *Macoma baltica* and *Potamocorbula amurensis*, as well as in carp, catfish and Medaka fish (Luoma et al., 1992; Wang and Lovell, 1997; Schlekat et al., 2000; Li et al., 2008; Zhou et al., 2009). In mice and rats nanoparticulate Se(0) has been shown to exhibit similar bioavailability as selenomethionine and selenite, but with less toxicity than selenomethionine (Zhang et al., 2001; Wang et al., 2008). Dissimilatory reduction of Se(0) occurs in several microorganisms. Presumably this reaction occurs after uptake of Se(0) into the cell

(Woolfolk and Whiteley, 1962; Herbel et al., 2003; Pearce et al., 2008). There are only three known organisms that can oxidize elemental selenium to selenite and selenate; *Bacillus megaterium*, *Thiobacillus ASN-1*, and *Leptothrix MNB-1* (Sarathchandra and Watkinson, 1981; Dowdle and Oremland, 1998). This oxidation occurs enzymatically, thus, again, the Se(0) is likely taken up into the cell.

1.4.2 ASSIMILATORY REDUCTION

Selenate, selenite and selenomethionine are all readily assimilated, though even elemental Se shows some bioavailability, as described above (Schlekat et al., 2000; Zhang et al., 2004; Wang et al., 2007). Assimilatory reduction of selenate resulting in incorporation into selenocysteine follows essentially the same pathway as sulfate for dissimilatory sulfate reduction (Figure 1.2). The uptake of selenite appears to be more complex with multiple possible uptake pathways.

Se(IV) must be reduced to Se(-II) for incorporation into biomolecules: it is assumed that the thioredoxin-glutathione system is involved in this initial step (Heider and Bock, 1993). There is no direct evidence that selenite is taken into the cell without reduction; however, some organisms seem to have non-specific mechanisms to take up selenite while others have specific mechanisms (Milne, 1998). Non-specific uptake results mainly in the excessive substitution of selenocysteine for cysteine and may be the cause for the toxicity of selenite (Heider and Bock, 1993).

Most evidence points to active transport of selenite but the mode of transport of selenite into the cell appears to be organism

dependent. Selenite can be taken up into the sulfate reduction mechanism but only at elevated concentrations. After uptake into the cell selenate and selenite are reduced to selenide or selenophosphate, presumably through either the sulfate reduction pathway or the glutathione pathway, but other unknown pathways may also be important (Stadtman, 1974; Schrauzer, 2000).

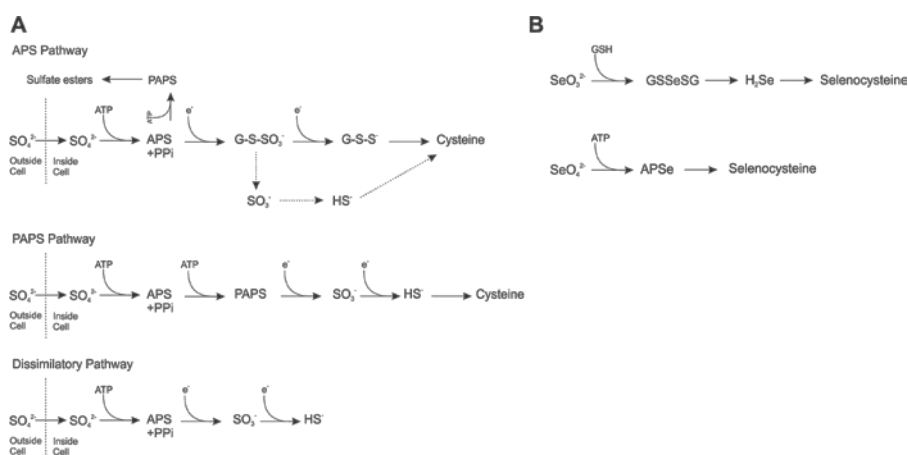


Figure 1.2A) Uptake and reduction of sulfate. The steps shown above are thought to be fundamentally the same for the uptake and incorporation of selenate into selenated proteins, essentially where Se is substituted for sulfur in cysteine or methionine (Stadtman, 1974; Milne, 1998; Böck et al., 2006). The PAPS pathway is mainly used by archaea and bacteria. Figure drawn after Canfield et al. 2005 (APS, adenosine phosphosulfate; G-S-SO₃⁻; organic thiosulfate; G-S-S⁻; reduced organic sulfur; PP_i, pyrophosphate; PAPS, phosphoadenosine-5'-phosphosulfate). **B) Selenocysteine biosynthesis in plants, marine algae, and brewer's yeast,** figure modified from Schrauzer (2000). This process may be slightly different in bacteria but follows the same general pathways. (GSH, glutathione; GSSeSG, selenogluthathione trisulfide; APSe, adenosine phosphoselenate).

Selenocysteine is the first organic selenium compound formed which can eventually be converted to selenomethionine. Selenocysteine and selenomethionine can be incorporated into

proteins and enzymes depending on function. At increased levels of ambient Se, selenomethionine is the dominant organic form of Se.

Selenium can also be taken up in the form of dissolved organic compounds, such as selenomethionine and selenocysteine. Uptake of selenocysteine by the cysteine transport system in *E.coli* can be quite toxic (Heider and Bock, 1993). Selenomethionine is also readily taken up and exchanged for methionine but this appears to be less toxic for cells and does not inhibit growth of *E. coli* (Heider and Bock, 1993). It is unclear how organic Se is transported across the cell. Although transport of organic S species across the cell membrane can occur through ABC (ATP-binding cassette) transporters these are only active at low sulfate concentrations (Bykowski et al., 2002). The high sulfate concentrations in the oceans likely inhibit this pathway for S but there may be similar pathways for the uptake of organic Se. Organic Se is the most abundant form of Se in the surface ocean. In addition, the uptake of organic selenium by phytoplankton has been observed, hence it may be the dominant pathway of Se uptake in marine surface waters (Wrench and Measures, 1982; Cutter and Bruland, 1984; Cutter and Cutter, 1995; Baines, 2001).

1.4.3 SELENOPROTEIN FUNCTIONALITY

There are 23 known selenoproteins and they all have the shared feature of redox catalysis, (Hatfield and Gladyshev, 2002). For those selenoproteins with known functions all are classified as oxidoreductases, which, as the name implies, catalyze oxidation-reduction reactions (Hatfield and Gladyshev, 2002; Gladyshev, 2006;

Gladyshev and Hatfield, 2010). However, there are many other selenoproteins whose functions are yet unknown.

Selenocysteine provides an advantage over cysteine due to increased catalytic capabilities attributed to the increased nucleophilicity and lower pKa (5.2) of SeH compared with SH (9.1) in cysteine (Harris and Turner, 2002; Copeland, 2005; Kim et al., 2006; Salinas et al., 2006). In some cases cysteine may not be reactive enough and therefore is replaced by selenocysteine. In other cases selenocysteine may be too reactive and thus toxic, in which case cysteine is the preferred protein (Gladyshev and Hatfield, 2010). It has recently been found that cysteine can be synthesized through the selenocysteine biosynthetic pathway (Turanov et al., 2011). Selenium has the ability to easily donate and accept electrons which is evident from the fact that it possesses photoelectric properties, and is influenced by the presence of light (Hengeveld and Fedonkin, 2007). This ability to easily donate and accept electrons allows selenocysteine to resist inactivation, which gives it two specific properties: 1) it can easily be recycled to its original reduced form after oxidation, and 2) it is not oxidized by most oxidants to its highest VI+ oxidation state which would inactivate the enzyme, and which occurs with cysteine because S(IV) is unstable in most conditions, unlike Se(IV) (Ruggles et al., 2012). The first quality would make Se advantageous over its S homolog cysteine in the aerobic world, while the second property, which does not require the presence of free oxygen, explains why selenocysteine usage could have originated in the anaerobic world (Ruggles et al., 2012).

Selenium occurs in selenoproteins in two main forms, as a labile cofactor and as the amino acid selenocysteine. Selenium can also be incorporated non-specifically into proteins through the cysteine or methionine biosynthetic pathways, resulting in the incorporation of selenocysteine in place of the S counterpart. This misincorporation of Se may be the cause of Se toxicity (Hatfield and Gladyshev, 2002). Proteins with Se inserted post-translationally as a dissociable cofactor are a relatively rare form of selenium in proteins, and have only been found in Mo-containing enzymes (Hatfield and Gladyshev, 2002).

Xanthine dehydrogenase, nicotinic acid hydroxylase (NAH) and purine hydroxylase (PH) are enzymes of the molybdenum hydroxylase class (Rother, 2012). The xanthine dehydrogenase isolated from *Clostridium stricklandii* has similar properties to mammalian xanthine oxidases, which contain Mo and Fe. The main function of the enzyme is the reduction of uric acid to xanthine. Nicotinic acid hydroxylase was the first molybdenum hydroxylase containing a selenium labile cofactor, and was isolated from *Clostridium barkeri*. NAH catalyzes the first step in the fermentation of nicotinic acid to ammonia, propionate, acetate and carbon dioxide (Gladyshev et al., 1996). Another selenium-dependent molybdenum hydroxylase is purine hydroxylase (PH) isolated from *Clostridium purinolyticum* (Self et al., 2003) which catalyzes the hydroxylation of hypoxanthine to xanthine.

Selenocysteine containing proteins include nickel–iron–selenium hydrogenases, thioredoxin and glycine reductases,

glutathione peroxidases, and formate dehydrogenases. All [NiFeSe] hydrogenases are either periplasmic or membrane associated, and belong to one of 4 following classes of organisms: 1) δ -proteobacteria, 2) *Clostridia*, 3) *Methanococci*, and 4) *Methanopyrus*. The one exception is *Thermodesulfovibrio yellowstonii* from the Nitrospira class which is deep branching (Baltazar et al., 2011). Thus all organisms containing [NiFeSe] hydrogenases are either sulfate reducing bacteria or methanogenic archaea (Baltazar et al., 2011). Thioredoxin reductase (TR) and thioredoxin compose a major cellular redox system found in all organisms (Arnér and Holmgren, 2000; Novoselov and Gladyshev, 2003). Due to its universal incorporation thioredoxin reductase is the best candidate for an essential selenoprotein (Hatfield and Gladyshev, 2002). Glycine reductase is mainly found in gram positive bacteria, it was first found in the bacteria *C. stricklandii* which utilizes amino acids as carbon and energy sources (Stadtman, 1996). Glycine reductase reduces glycine to acetate while producing ATP, and serves as a terminal electron acceptor for amino acid fermenting anaerobic bacteria (Stadtman, 1980). Glutathione peroxidase (GPx) is found in all domains of life with the selenocysteine containing active sites found mainly in vertebrates, while most terrestrial plants, yeasts, protozoa and bacteria have cysteine substituted glutathione peroxidases (Flohé and Brigelius-Flohé, 2012). The selenium containing formate dehydrogenase is 300 times more catalytically active than its S homolog (Stadtman, 1996). Table 1.1 summarizes some of the best understood selenoproteins and their functions.

Table 1.1 Important selenoproteins and their functions.

Selenoprotein	Function	Additional information	References
<i>Proteins with labile Se cofactors</i>			
Xanthine dehydrogenase (XDH)	catalyzes oxidation of hypoxanthine and xanthine		(Schröder et al., 1999)
Nicotinic acid hydroxylase (NAH)	Reduces NADP ⁺ to NADPH	First step in fermentation of nicotinic acid to ammonia, propionate, acetate and CO ₂	(Stadtman, 1980; Gladyshev et al., 1996)
Purine hydroxylase (PH)	Fermentation of purines to CO ₂ , ammonia, acetate and formate		(Rother, 2012)
<i>Selenocysteine containing selenoproteins</i>			
[NiFeSe] hydrogenases	Catalyzes the reversible oxidation of molecular hydrogen	Found in sulfate reducing or methanogenic microorganisms	(Baltazar et al., 2011)
Thioredoxin reductase (TR)	NADPH-dependent reduction of thioredoxin	Present in all organisms; used in redox signaling	(Arnér and Holmgren, 2000; Williams et al., 2000)
Glycine Reductase (selenoprotein A)	Reduces glycine to acetate	Only selenoprotein with no cysteine homolog	(Stadtman, 1996)
Glutathione peroxidase (GPx)	Reduces H ₂ O ₂	Part of the large glutathione peroxidase family	(Flohé and Brigelius-Flohé, 2012)
Formate Dehydrogenase	Oxidizes formate	Mainly found in methanogens	(Stadtman, 1980)

1.4.4 DISSIMILATORY REDUCTION

Microorganisms capable of growth with selenium (IV, VI) as terminal electron acceptor can be placed in four groups, based on growth conditions and phylogeny: hyperthermophilic archaea, thermophilic bacteria, mesophilic gram-negative bacteria, and γ -, δ -

and ϵ -proteobacteria, shown in Figure 1.3 (J.S. Geelhoed, personal communication, 2007). The (hyper)thermophilic selenium reducers are able to use an autotrophic growth mechanism with H_2 or reduced sulfur compounds as electron donor, and *Bacillus sp.* ML-SRAO reduces Se(VI) with arsenite as electron donor.

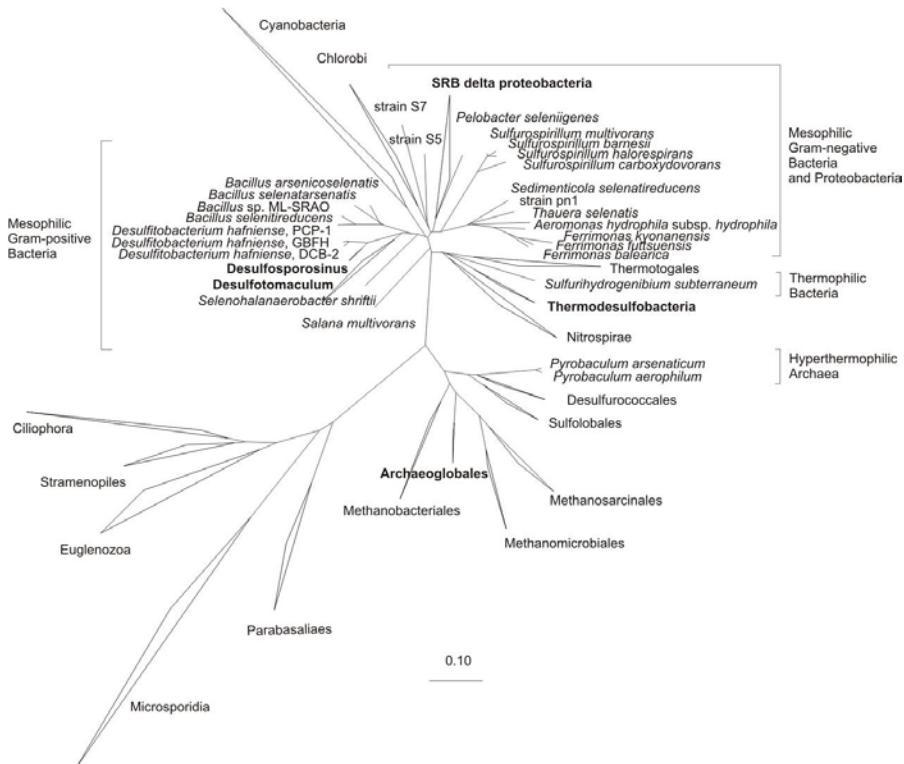


Figure 1.3 Phylogenetic tree showing all known Se reducing microorganisms that couple Se oxyanion reduction to growth (figure created by J.S. Geelhoed). Species names are shown in italics.

Of the mesophilic organisms, *Sulfurospirillum* species may use an inorganic electron donor in the form of hydrogen, but require an organic carbon source for growth. Thus far, the selenate reductase enzyme has only been isolated from *Thauera selenatis* (Schroder et al., 1997).

Another mechanism by which selenium oxyanions are reduced is co-metabolic reduction. For this process, energy in the form of an electron donor is required, however, the selenium reduction process is not coupled to growth (e.g. Tomei et al., 1995). Several mechanisms have been proposed and these include the reduction of selenium oxyanions by the activity of reduction enzyme systems for other anions, such as nitrite and nitrate reductases, and the reduction of Se(IV) by glutathione (DeMoll-Decker and Macy, 1993; Kessi and Hanselmann, 2004). Reduction of selenium oxyanions by a non-specific reduction pathway has also been shown for some species of sulfate reducing bacteria affiliated with the δ -proteobacteria (Zehr and Oremland, 1987; Hockin and Gadd, 2006). Experiments with strains of *Desulfovibrio desulfuricans* and *Desulfomicrobium* suggest that selenate disrupts the sulfate uptake mechanism and thus it is likely reduced via the same pathway (Newport and Nedwell, 1988).

The predominant end product of the reduction of selenium oxyanions is red amorphous elemental selenium. However, formation of considerable amounts of Se(-II) has been observed for selenite reduction by *Bacillus selenitireducens*, *Citrobacter freundii* and *Veillonella atypica* (formerly known as *Micrococcus lactilyticus*) (Woolfolk and Whiteley, 1962; Herbel et al., 2003; Zhang et al., 2004; Pearce et al., 2008). The latter two organisms are able to reduce selenium oxyanions, but are unable to conserve energy for growth from this conversion. Production of Se(-II) occurs only after all selenite has been converted to Se(0).

Elemental selenium is mainly deposited outside the cell. Therefore, it is possible that further reduction of Se(0) to Se(-II) is achieved via a mechanism of extracellular electron transfer. This may involve electron shuttle compounds or extracellular proteins. The use of conductive pili structures for electron transfer has been proposed as well (see reviews by Lovley and Phillips, 1994; Stams, 2006; Gralnick and Newman, 2007). Electron shuttle compounds are present in the natural environment, e.g. in the form of humic substances, reduced sulfur compounds, Fe-colloids, and compounds produced by microorganisms, e.g. phenazines and flavins.

Geobacter sulfurreducens is well known to use extracellular proteins (c-type cytochromes and multicopper proteins) to transfer electrons to Fe-oxides and electrodes (Lovley, 2006). Although *G. sulfurreducens* does not respire selenium oxyanions, it can reduce Se(IV) to Se(-II) (Pearce et al., 2008). In addition, the presence of the electron shuttle compounds and the humic acid analogue anthraquinone disulfonic acid (AQDS) has been shown to speed up the reduction of selenite by *V. atypica* (Pearce et al., 2008). *Shewanella putrefaciens* strain 200 is known to reduce selenite (Taratus, 2000), and adsorb and subsequently reduce selenate at pH<6 (Kenward et al., 2006). The mechanism of reduction of selenite and adsorption of selenate are currently unknown for this organism. *S. putrefaciens* is also known to use c-type cytochromes to transfer electrons to Fe-oxides (DiChristina et al., 2005). It is possible that selenite reduction in *S. putrefaciens* could be carried out enzymatically or more likely is a result of reduction by iron (II)

produced by electron shuttling (Taratus, 2000; T.J. DiChristina, personal communication).

1.4.5 MICROBIAL OXIDATION

There are only three known microorganisms that can oxidize elemental selenium to selenite and selenate; *Bacillus megaterium*, *Thiobacillus ASN-1*, and *Leptothrix MNB-1* (Lipman and Waksman, 1923; Sarathchandra and Watkinson, 1981; Dowdle and Oremland, 1998). The aerobic (oxidative) cycle of selenium does not seem to compete with that of sulfur, but Se(0) oxidation appears to be a co-metabolic process (Dowdle and Oremland, 1998). Microbial oxidation of Se(0) is very slow when compared to the reduction of selenate (Dowdle and Oremland, 1998).

1.4.6 VOLATILIZATION

Detoxification of selenium compounds by some organisms such as humans, rats and bacteria is well known: dimethyl selenide and trimethyl selenonium ion are common in excretory products (Stadtman, 1990; and references therein). There are five main forms of volatile selenium; hydrogen selenide (H_2Se), methane selenol (CH_3SeH), dimethyl selenide (CH_3SeCH_3 ; DMSe), dimethyl selenenyl sulfide ($\text{CH}_3\text{SeSCH}_3$) and dimethyl diselenide ($\text{CH}_3\text{SeSeCH}_3$; DMDS₂) (Chasteen, 1998). The first two forms are rapidly oxidized under atmospheric conditions. The last two forms have a low vapor pressure at low temperatures therefore selenium is not thought to be volatilized in these forms. This leaves dimethyl selenide as the key compound for selenium mobility in the environment (Chasteen, 1998).

Bacteria, phytoplankton, and fungi appear to be major sources of volatilized selenium to the atmosphere. Land plants are often divided into selenium accumulator plants and non-accumulator plants. Selenium accumulator plants can reach internal levels of selenium 100-10,000 times the levels found in non-accumulator plants. It has been postulated that the volatilization may not be a process conducted by the plants at all, but may be due to the degradation of the plant tissues by bacteria (Gamboa-Lewis, 1976; Chasteen, 1998); however this is still a point of debate. Mechanisms for selenium volatilization may be similar to or the same as those that methylate sulfur (Challenger and North, 1934; Gamboa-Lewis, 1976; Reamer and Zoller, 1980; Ansedo and Yoch, 1997).

1.5 ABIOTIC REDOX PATHWAYS

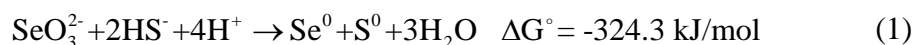
1.5.1 REDUCTION BY IRON (II) COMPOUNDS

Selenate and selenite can be reduced by Fe(II,III) oxides (green rust) that are found in suboxic sediments and soils (Myneni et al., 1997). However, green rust minerals are rarely abundant in natural reductive environments due to their metastability with respect to magnetite and siderite (Charlet et al., 2007). A recent study of selenite reduction by mackinawite, siderite and magnetite found multiple reaction products including FeSe, Se(0) and mixed valence iron selenides (Scheinost and Charlet, 2008). Reaction of selenite with magnetite is fairly fast, occurring within hours. The specific surface areas of the Fe(II) mineral phases appear to be one of the controlling factors of the reaction rates. Though reaction rates are very fast under experimental conditions it is likely that they are in competition with

other processes such as adsorption on clay minerals or humic substances in natural settings and thus reaction rates may be slower (Bruggeman et al., 2005; Scheinost and Charlet, 2008).

1.5.2 REDUCTION BY SULFIDE COMPOUNDS

The precipitation of elemental selenium and sulfur has been observed in cultures of *Desulfomicrobium norvegicum*, which was isolated from an estuarine sediment (Hockin and Gadd, 2003). However, it was proposed that the reduction mechanism was abiotic reduction of selenite ions by aqueous sulfide as shown in Equation 1, rather than reduction by ferrous iron:



It was further argued that the reduction of selenite is favored over the formation of iron mono-sulfide. Reaction 1 has been independently verified by mixing Na_2SeO_3 and Na_2S in a carbonate buffered solution at pH 8.2 (Breynaert et al., 2008).

Iron sulfides also appear to reduce selenite in solution given a sufficient equilibration time of 2-3 weeks (Breynaert et al., 2008). The reduction of selenite by FeS appears to be the result of the dissolution of FeS and subsequent reaction between selenite and sulfide in solution which produces suspended colloidal Se(0) as an intermediate, with an end product attributed to FeSe_x species (Breynaert et al., 2008). Reduction of selenite by mackinawite produces different end products depending on the starting pH; at pH 4.4 FeSe forms, and at pH 6.3 elemental selenium forms. This suggests that the solubility of mackinawite at different pH values supplies the Fe(II) in solution for the precipitation of FeSe. The solubility of mackinawite is highly

sensitive to pH, with the solubility increasing with decreasing pH (Rickard, 2006).

The reaction with FeS_2 appears to produce monoclinic elemental selenium, as opposed to trigonal elemental selenium (Breynaert et al., 2008). It is unclear what the exact mechanism for reduction is in the presence of pyrite, although surface precipitation was ruled out by these authors as there was no iron in the final product (Breynaert et al., 2008). However, in a recent study using a mixture of nano-pyrite and greigite, principle component analysis (PCA) and least squares fitting (LSF), revealed FeSe_2 as a primary reaction product for the reaction between FeS_2 and Se(IV) and Se(VI) for the first time (Charlet et al., 2012).

1.5.3 REDUCTION IN HYDROTHERMAL SETTINGS

There are few robust analyses of trace elements in hydrothermal vent environments, especially those that precipitate with metal sulfides, including Se (German and Von Damm, 2003a). Available data show that Se concentrations in hydrothermal sulfide minerals are highly variable, ranging from 1 ppm to over 1000 ppm (Rouxel et al., 2004). Depending on the type of hydrothermal deposit, Se concentrations can vary over a wide range. The highest Se concentrations are generally found in chalcopyrites which have higher Se content than pyrites (Auclair, 1987). All Se in pyrite and chalcopyrite is found to be in solid solution with sulfur, thus no Se is found as individual selenides (Auclair, 1987). Selenium concentrations in high temperature vent fluids ($\sim 350^\circ\text{C}$) are relatively

low, 80 μM , and Se precipitates more readily from high temperature vent fluids than cooler ones (Von Damm et al., 1985a; Auclair, 1987).

1.5.4 PHOTOCHEMICAL TRANSFORMATIONS OF SE

Photo-oxidation of Se(IV) oxyanions by UV radiation has been observed in the laboratory at a wavelength of 300 nm by Chen et al. (2005). These authors investigated the oxidation of Se(IV) in several different matrices, including pure water, HNO_3 , HCl and a mixture of HCl and HNO_3 . In pure water the rate of oxidation was relatively slow, with only 60% oxidation observed after 5 hours. In contrast, in 1% (v/v) HNO_3 oxidation was 100% complete within 60 minutes. The relative roles of pH and nitrate on the photochemical oxidation kinetics remain to be determined.

The photo-reduction of selenium oxyanions has been studied in more detail than its photo-oxidation counterpart (Tan et al., 2003a, b, c; Nguyen et al., 2005). The existing studies demonstrate that selenate and selenite ions can be photo-chemically reduced to Se(0) at wavelengths below 380 nm, in the presence of formic acid and using TiO_2 as a catalyst (Kikuchi and Sakamoto, 2000), with the reaction proceeding through several steps. Experiments for either photo-oxidation or photo-reduction which are representative of natural conditions have not yet been carried out to our knowledge.

1.6 SELENIUM STABLE ISOTOPE CHEMISTRY

There are six stable isotopes of selenium which are shown with their percent natural abundance in Table 1.2. ^{82}Se has a half-life of 1.08×10^{20} years, and is therefore included with the stable isotopes. It is one of the 35 Se isotopes that undergo a double beta decay ($\beta^- \beta^-$),

producing ^{82}Kr . There is one other radioactive isotope of selenium, ^{79}Se , which is a fission product, with a half-life of 3.27×10^5 years. This isotope undergoes beta decay (β^-) producing ^{79}Br . Twenty-three other unstable Se isotopes have also been identified.

Table 1.2 Natural abundance of selenium stable isotopes (Fischer, 1978).

Mass Se	Abundance (%)
74	0.87
76	9.02
77	7.58
78	23.52
80	49.82
82	9.19

1.6.1 SELENIUM ISOTOPE MASS SPECTROMETRY

Selenium isotopes have been measured since the early 1960s by gas source mass spectrometry as SeF_6 (Krouse and Thode, 1962). This technique was relatively sensitive but it required large sample quantities ($>10 \mu\text{g}$) and took over 1 hour for each analysis, thus this technique has not been widely used. During the 1990s, Wachsmann and Heumann (1992) began to develop a Thermal Ionization Mass Spectrometer (TIMS) method that formed negative ions for sulfur, selenium and tellurium. This method, while effective, poses a challenge for selenium because selenium volatilizes at relatively low temperatures ($\text{Se}(0)$ vaporizes at $648 \text{ }^\circ\text{C}$). The sample sizes for Negative ion-TIMS (N-TIMS) is significantly less than for gas source mass spectrometry ($\sim 500\text{ng}$), however there is a large amount of instrument bias. This method was later amended by Johnson et al. (1999), using a double spike technique to improve precision.

The Multi-Collector Inductively-Coupled-Plasma Mass-Spectrometer (MC-ICP-MS) has allowed for more isotopes, over a wider range to be analyzed simultaneously, hence simplifying isotope analysis of heavier elements. The method developed by Rouxel et al., (2002) has decreased the sample size dramatically while maintaining precision by analyzing standards between samples as the TIMS method. This technique suffers from instrumental bias but it can be overcome by either sample standard bracketing and/or double-spike addition to samples. Hydride generation (HG) permits the use of small sample sizes, and has been widely employed in concentration measurements. Selenium forms hydrides (H_2Se) which ionize readily, requiring less material to be injected into the instrument. During hydride generation other hydride forming elements (i.e. Ge, As and Br) can produce isobaric interferences on the Se isotopes of interest, thus these interferences must be minimized for analysis. Chapter 4 provides a more detailed discussion of isobaric interferences and data reduction for hydride generation MC-ICP-MS.

1.6.1.1 SELENIUM ISOTOPE STANDARDS

There have been a number of selenium isotope standards in the relatively short history of selenium isotope measurements. These include Cañon Diablo Triolite (CDT), MH-495, MERCK and NIST SRM 3149. Cañon Diablo Triolite was used as the isotope standard in the earliest selenium isotope studies (Krouse and Thode, 1962; Rees and Thode, 1966; Carignan and Wen, 2007). It is also the standard for sulfur isotope work and was thought to be representative of Se isotope ratios as well. MH-495 was used by Johnson et al. (1999), as well as in their subsequent studies (Johnson et al., 1999; Johnson et al., 2000;

Herbel et al., 2000; Herbel et al., 2002; Johnson and Bullen, 2003; Clark and Johnson, 2008). Yet another standard, a MERCK Titrisol solution (SeO_2 in HNO_3) was used by Rouxel (2002). This standard was measured against the MH-495 standard from Johnson et al. (1999) plus a standard made from selenium metal CRPG. Good external precision was found when the three standards were compared.

Finally, in 2007 Carignan and Wen (2007) proposed that the NIST SRM 3149 become the accepted inter-laboratory selenium isotope standard. Each internal standard from the individual laboratories was measured against the NIST SRM 3149, yielding the following $\delta^{82/76}\text{Se}$ values were proposed relative to the NIST SRM 3149: MERCK= 1.54 ± 0.20 ‰, CRPG= -2.01 ± 0.15 ‰ and MH-495= -3.04 ± 0.50 ‰.

1.6.2 SELENIUM STABLE ISOTOPE FRACTIONATION

1.6.2.1 SELENIUM ISOTOPE FRACTIONATION THEORY

The isotope notation used for the selenium system is identical to that used by Canfield (2001b) for the sulfur system. The fractionation factor is defined as follows:

$$\alpha_{(A-B)} = \frac{\left(\frac{{}^{82}\text{Se}}{{}^{76}\text{Se}} \right)_A}{\left(\frac{{}^{82}\text{Se}}{{}^{76}\text{Se}} \right)_B} \quad (2)$$

where A is the reactant and B is the product. Isotopic compositions are expressed in per mil (‰) and are presented in the standard delta notation reporting the 82/76 ratio relative to the NIST SRM 3149 standard:

$$\delta^{82/76}\text{Se}_{\text{NIST}} = \left[\frac{\left(\frac{^{82}\text{Se}}{^{76}\text{Se}} \right)_{\text{Sam}}}{\left(\frac{^{82}\text{Se}}{^{76}\text{Se}} \right)_{\text{Std}}} - 1 \right] \quad (3)$$

Fractionations are expressed in terms of ϵ , also with units of (‰):

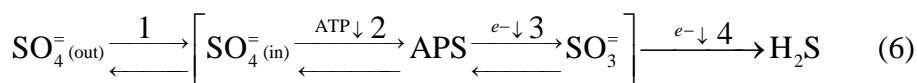
$$\epsilon = (\alpha_{\text{A-B}} - 1)$$

The epsilon notation is convenient because ϵ is roughly equal to the difference between the δ values for of the reactant and product:

$$\epsilon \cong \delta^{82/76}\text{Se}_\text{A} - \delta^{82/76}\text{Se}_\text{B} \quad (5)$$

The ϵ reported here correspond to the 82/76 ratios relative to the NIST SRM 3149 standard ($\epsilon^{82/76}\text{Se}$).

The majority of redox reactions that impart relatively large isotope fractionations are kinetic, multi-step reactions at low temperatures. Such is the case for selenium isotope fractionation. The mechanisms of selenium oxyanion reduction are not well understood, especially for dissimilatory reduction of selenate and selenite (see section 1.4.2). However, much of selenium isotope theory is based on that of sulfur isotopes, specifically following the Rees (1973) model, which has been further expanded upon by others (Canfield, 2001b; Canfield et al., 2006a; Hoek et al., 2006; Mitchell et al., 2009). Only a simplified model is considered here, (see the aforementioned references for further discussion), based on the following reaction scheme:



In the reaction scheme, the cell actively takes up sulfate via membrane-bound transport proteins (Equation 6; step 1), and this step is thought to be reversible (Cypionka, 1991), allowing exchange of sulfate in and out of the cell. A small isotope effect of -3‰ ($\epsilon_{\text{SO}_4(\text{out})-\text{SO}_4(\text{in})}$) is associated with this step (Rees, 1973). Once sulfate is inside the cell it is activated by ATP via ATP sulfurylase to form adenosine 5'-phosphosulfate (APS) (Equation 6; step 2), which is reduced to sulfite by adenylylsulfate reductase (Equation 6; step 3). These two steps are also considered to be reversible. No fractionation is expected during the activation of sulfate, but a fairly large isotopic fractionation ($\epsilon_{\text{SO}_4(\text{in})-\text{SO}_3}$) of around 25‰ accompanies to APS reduction (Harrison and Thode, 1957; Harrison and Thode, 1958). The final reduction of sulfite to hydrogen sulfide is performed by sulfite reductase (Equation 6; step 4). A 25‰ isotope fractionation ($\epsilon_{\text{SO}_3-\text{H}_2\text{S}}$) has been ascribed to this step (Kemp and Thode, 1968; Rees, 1973). This model thus yields a maximum fractionation of (-3+25+25=) 47‰. It is assumed that the dissimilatory reduction of selenate (and selenite) anions follows a similar multi-step enzymatic pathway, and therefore the same model has been applied to the selenium isotope system (Johnson and Bullen, 2004).

Krouse and Thode (1962) calculated equilibrium isotope fractionations for selenium isotopes undergoing various redox transformations. At 25°C, equilibrium fractionation ($\epsilon^{82/76}\text{Se}$) for the transformation between selenate and selenide is on the order of 33‰. This is significantly smaller than the equilibrium fractionation of 75‰ for the reaction of sulfate to sulfide (Tudge and Thode, 1950). The

theoretical isotope calculations thus suggests that the kinetic isotope fractionation observed for selenium should be smaller than of sulfur because it is much heavier than sulfur (Schauble, 2004). Thus far observed selenium isotope fractionations support this prediction.

1.6.2.2 BIOTIC FRACTIONATION

1.6.2.2.1 FRACTIONATION ASSOCIATED WITH ASSIMILATORY REDUCTION

Assimilatory processes often impart only small isotope fractionations because of the lack of exchange between internal and external pools of an element (Rees, 1973; Canfield, 2001b). For sulfur, for example, assimilatory reduction indeed produces small fractionation (1-5‰). Few studies of Se assimilatory reduction have produced isotope fractionation data to date, however. Algal uptake of selenium in the freshwater species *Chlamydomonas reinhardtii*, produces fractionations of ($\epsilon^{82/76}\text{Se}$) from 1.5 to 3.9‰ (Hagiwara, 2000). Assimilatory fractionations are summarized in Table 1.3, along with other biotic fractionations. Selenium extracted from wetland plant tissues exhibit an isotopic fractionation ($\epsilon^{82/76}\text{Se}$) of <1.5‰. In **Chapter 4**, we measured the Se isotope composition of an oligotrophic marine plankton sample, hence adding to the small body of assimilatory Se fractionation values.

1.6.2.2.2 VOLATILIZATION

Volatilization of selenium shows equally small of fractionation, with maximum ($\epsilon^{82/76}\text{Se}$) values of 0.9‰ and 1.7‰, reported for soil microbes and cyanobacteria, respectively (Johnson et al., 1999; Herbel et al., 2002; Johnson and Bullen, 2004). Volatilization by the fungus *Alternaria alternata* is associated with a

slightly larger Se isotope fractionation of up to 6‰ (Schilling et al., 2011a).

1.6.2.2.3 FRACTIONATION ASSOCIATED WITH DISSIMILATORY BACTERIAL REDUCTION

Selenium isotopic fractionations associated with dissimilatory reduction by microorganisms are larger than for assimilatory reduction, as expected. Most studies of isotope fractionation during dissimilatory selenate and selenite reduction have been done using pure cultures, which show large selenium isotope fractionations. Herbel et al. (2000) performed selenate and selenite experiments using growing cultures of *Sulfurospirillum barnesii* strain SES-3, *Bacillus selenitireducens* strain MLS10 and *Bacillus arenicoselenatis* strain EH1. In these experiments, low fractionations were observed at the beginning of the experiments on the order of ($\epsilon^{82/76}\text{Se}$) 0.3-1‰. Fractionation, however, increased as the reaction proceeded. The final fractionation observed was 7.5‰ ($\epsilon^{82/76}\text{Se}$) in the selenate experiments and up to ($\epsilon^{82/76}\text{Se}$) 13.65‰ in the selenite experiments. Sediment slurry experiments of selenite reduction by Ellis et al. (2003) yielded fractionations that are similar to those measured in the pure culture studies ($\epsilon^{82/76}\text{Se}$; 8.25‰). The selenium concentrations used in the slurry experiments were much lower, the lowest being 230 nmol/L. The latter value, however, is still well above the seawater concentration of selenium (~1 nmol/L). There also appeared to be no dependence of fractionation on the concentration of selenium. This is a significant finding, as the selenium isotope theory is based heavily on that for sulfur isotope fractionation, and a dependence on the

sulfate concentration for sulfur isotope fractionation has been demonstrated (Habicht et al., 2002b).

A study with an intact sediment core and mixed and unmixed sediment slurries found much less fractionation than previous slurry experiments and microbial cultures (Clark and Johnson, 2008). The mixed slurries exhibited fractionation ($\epsilon^{82/76}\text{Se}$) from 1.11 to 2.69‰ for the aqueous selenate fraction (i.e. the selenate became heavier). The unmixed slurries produced even smaller fractionation ($\epsilon^{82/76}\text{Se}$) 0.79‰.

Table 1.3 Selenium isotope fractionations associated with biotic reduction of selenium oxyanions

Reduction	Organism	Fractionation ($\epsilon^{82/76}\text{Se}$, ‰)	References
Assimilatory	algae; <i>Chlamydomonas reinhardtii</i>	1.5-3.9	Clark, 2007; Hagiwara et al., 2000
Assimilatory	higher plants	<1.5	Clark, 2007
Volatilization	soil microbes	max 0.9	Herbel et al., 2002; Johnson & Bullen, 2004
Volatilization	cyanobacteria	max 1.7	Johnson, 1999
Dissimilatory Se(IV) → Se(0)	<i>S. barnesii</i> strain SES-3, <i>B. arsenicoselenatis</i> strain EH1 and <i>B.</i> <i>selenitireducens</i>	max 13.65	Herbel et al., 2000
Dissimilatory Se(VI) → Se(IV)	<i>S. barnesii</i> strain SES-3, <i>B. arsenicoselenatis</i> strain EH1 and <i>B. selenitireducens</i>	max 7.5	Herbel et al., 2000
Dissimilatory	sediment slurry (mixed)	8.25	Ellis et al., 2003
Dissimilatory	sediment slurry (mixed)	1.11 to 2.69	Clark & Johnson, 2008
Dissimilatory	sediment slurry (un- mixed)	0.79	Clark & Johnson, 2008
Dissimilatory	Intact sediment core	-0.11 to 1.06	Clark & Johnson, 2008

The intact sediment core was supplied with two separate loadings of selenium. In the first loading the fractionation was quite small ($\epsilon^{82/76}\text{Se} = -0.11\%$) and in the second loading the fractionation was closer to the mixed slurries ($\epsilon^{82/76}\text{Se} = 1.06\%$). This study is important because it shows the importance of using environmentally relevant samples and relatively low selenium concentrations (960 nmol/L).

1.6.2.3 ABIOTIC FRACTIONATION

Although there have been several measurements of fractionation caused by abiotic reactions (Table 1.4), most of these reactions were conducted using strong acids under conditions that are not particularly environmentally relevant (Krouse and Thode, 1962; Rees and Thode, 1966; Rashid and Krouse, 1985; Johnson et al., 1999).

Johnson and Bullen (2003) conducted the first reductive abiotic fractionation study on an environmentally relevant reaction to date. They investigated the reduction of selenite by green rust, an Fe(II)-and Fe(III) bearing mineral with sulfate layers (see section 1.5.1).

Table 1.4 Abiotic selenium isotope transformations and associated isotope fractionations

Se transformation	Method	Fractionation ($\epsilon^{82/76}\text{Se}, \%$)	References
Se(VI)→Se(IV)	8 M HCl @ 25°C	18	Rees & Thode, 1966
Se(VI)→Se(IV)	4N HCl @ 70°C	8.25	Johnson, 1999
Se(VI)→Se(IV)/Se(0)	Green Rust	11.1	Johnson, 2003
Se(IV)→Se(0)	Ascorbic acid or NH ₂ OH	15-19	Rees & Thode, 1966; Krouse & Thode, 1962; Rashid & Krouse, 1985; Webster, 1972
Se(IV) adsorption	Fe(OH) ₃ in H ₂ O	0.8	Johnson, 1999
Se(IV)→Se(VI)	1M NaOH, 30% H ₂ O ₂ 24°C	~0	Johnson, 2004

A fractionation of $\varepsilon^{82/76}\text{Se}=11.1\%$, was observed in these reduction experiments, and was highly reproducible in repeated experiments. No relationship between reaction rate and isotope fractionation was observed by Johnson and Bullen (2003). Adsorption of selenite to amorphous iron oxyhydroxide causes a very small isotope fractionation (Table 1.4). The chemical oxidation of selenite to selenate has been shown to have no isotope fractionation associated with it. In **Chapter 5** we expand this data set to include sorption of Se(IV) and Se(VI) to three additional iron(III) oxides as well as two iron(II) sulfide minerals.

1.6.2.3.1 SELENIUM ISOTOPE COMPOSITIONS IN MARINE HYDROTHERMAL SYSTEMS

Isotopic compositions as low as -4.75% ($\delta^{82/76}\text{Se}$) have been observed in hydrothermal systems (Rouxel et al., 2002; Rouxel et al., 2004), however, it is inconclusive where the isotope fractionation occurs. For all ranges of Se/S values, sulfides show enrichment in light Se isotopes relative to basalts (Rouxel et al., 2004). There is no apparent relationship between Se concentration and Se isotope fractionation in these hydrothermal systems. The Se/S ratios seem to be too small to be accounted for by hydrothermal fluids only, thus a second source of selenium depleted water is needed to explain the concentration data. It is possible that fractionations could be occurring due to abiotic redox processes when seawater mixes with hydrothermal fluid or by biotic reduction carried out by microbes at lower temperatures (Rouxel et al., 2004).

The present and past selenium isotopic composition of seawater is currently unknown which complicates the interpretation of Se isotope signatures observed in marine sedimentary rocks. Sample

size and oxidation state considerations hamper efforts to determine the Se isotopic value of modern sea water. Selenium does not readily form selenate minerals, thus it is also difficult to constrain the marine isotopic signature of Se through geological time, as its concentration in barite, etc., is extremely low (<20 ppb Se) (Rouxel et al., 2004).

1.6.2.3.2 SELENIUM ISOTOPIC COMPOSITIONS OF GEOLOGICAL MATERIALS

The archive of Se isotope composition from geological materials is relatively small, and shows a limited range of Se of $\delta^{82/76}\text{Se}$ which are summarized in Table 1.5. There are, however, a few geological materials that fall outside of the narrow range. The largest range of Se isotope compositions are found in the Yutangba Selenium Deposit, Hubei Province, China, with $\delta^{82/76}\text{Se}$ ranging between -14.20‰ and 9.13‰ (Wen et al., 2007; Zhu et al., 2008). A model, as follows, has been proposed to account for the large selenium isotopic fractionation found in these samples. Selenium is mobilized via oxidation in the soil zone and along fast-flowing fractures to an unknown depth below the soil (~1 m). As the selenium seeps downward, eventually the water becomes anoxic, and precipitates as Se(-II) producing a selenium enriched layer. Over time, the oxic front migrates downward as the land surface is eroded and selenium is mobilized near the top and re-deposited deeper, and the total amount of accumulated selenium increases. It is likely the selenium in the high selenium layer has been remobilized several times which may increase the isotopic contrast and explain the unusually high selenium isotope fractionations observed in these samples. Drill core samples show the isotopic variation decreasing and minimizing to ~0‰ at

about 50 m depth (Wen and Carignan, 2007; Zhu et al., 2008; Wen and Carignan, 2011).

Table 1.5 Selenium isotopic compositions of geological samples.

Sample Type	$\delta^{82/76}\text{Se}$ (‰)	References
Hydrothermal	-4.75 to 3.40	Rouxel et al., 2002, 2004
Carbonaceous shale	-14.20 to 9.13	Wen and Carignan, 2007, 2011; Zhu et al., 2008
Carbonaceous chert	-12.86 to 4.93	Wen and Carignan, 2011
Kerogen	-6.92 to 7.52	Wen and Carignan, 2011
Marine sediments	-1.08 to 3.40	Rouxel et al., 2002
Marine sediments	-1.43 to 0.00	Hagiwara, 2000
Altered shale	-7.20 to 0.66	Hagiwara, 2000
Shale (outcrop)	-1.58 to 4.56	Hagiwara, 2000
Shale (core)	-1.67 to 0.53	Hagiwara, 2000
Chalk (core)	1.46	Hagiwara, 2000

Rouxel et al. (2002) found isotopic variation in marine sediments ranging from -1.08 to 3.40‰ ($\delta^{82/76}\text{Se}$). Hagiwara (2000) investigated altered and unaltered shale, and marine sediments and found $\delta^{82/76}\text{Se}$ values ranging between -7.2 and 4.56‰. These data sets are probably more representative of the fractionation that is imparted by fewer consecutive redox transformations that is seen in the Chinese shale samples. In the rest of the thesis our data will add considerably to the body of existing Se isotope compositions in natural samples (**Chapter 2** and **Chapter 4**).

1.7 ORGANIZATION AND STRUCTURE OF THESIS

Chapter 1 is a general introduction to and history of the study of selenium and the selenium cycle. **Chapter 2** discusses the evolution of the Se cycle and Se biochemistry in the context of Se isotopes and in comparison with S. **Chapter 3** incorporates Se isotopes into the model of marine Se cycling presented in **Chapter 2**. **Chapter 4** presents a large data set of Se isotopic compositions in

shale samples spanning the Phanerozoic, in order to assess the utility of Se isotopes as a paleo-oceanographic proxy. **Chapter 5** presents isotopic fractionations, kinetic data, and solid state speciation of Se during sorption to iron oxides and iron sulfides. **Chapter 6** presents a summary and synthesis of the thesis with recommendations of future research directions for Se research.

REFERENCES

- Amouroux D., Donard O.F.X. (1996) Maritime Emission of Selenium to the Atmosphere in Eastern Mediterranean seas. *Geophys. Res. Lett.* **23**.
- Amouroux D., Liss P.S., Tessier E., Hamren-Larsson M., Donard O.F.X. (2001) Role of oceans as biogenic sources of selenium. *Earth. Planet. Sci. Lett.* **189**, 277-283.
- Ansele J.H., Yoch D.C. (1997) Comparison of selenium and sulfur volatilization by dimethylsulfoniopropionate lyase (DMSP) in two marine bacteria and estuarine sediments. *FEMS Microbiol. Ecol.* **23**, 315-324.
- Arnér E.S.J., Holmgren A. (2000) Physiological functions of thioredoxin and thioredoxin reductase. *Eur. J. Biochem.* **267**, 6102-6109.
- Atkinson R., Aschmann S.M., Hasegawa D., Thompson-Eagle E.T., Frankenberger W.T. (1990) Kinetics of the atmospherically important reactions of dimethyl selenide. *Environ. Sci. Technol.* **24**, 1326-1332.
- Auclair G., Fouquet, Y. and Bohn, M. (1987) Distribution of selenium in high-temperature hydrothermal sulfide deposits at 13° north, East Pacific Rise. *Can. Mineral.* **25**, 577-587.
- Baines S.B., Fisher N.S. (2001) Interspecific differences in the bioconcentration of selenite by phytoplankton and their ecological implications. *Mar. Ecol. Prog. Ser.* **213**, 1-12.
- Baines S.B., Fisher, N.S., Doblin, M.A., Cutter, Gregory A. (2001) Uptake of dissolved organic selenides by marine phytoplankton. *Limnol. Oceanog.* **46**, 1936-1944.
- Balistreri L.S., Chao T.T. (1987) Selenium adsorption by goethite. *Soil Sci. Soc. Am. J.* **51**, 1145-1151.
- Baltazar C.S.A., Marques M.C., Soares C.M., DeLacey A.M., Pereira I.A.C., Matias P.M. (2011) Nickel–Iron–Selenium Hydrogenases – An Overview. *Eur. J. Inorg. Chem.* **2011**, 948-962.
- Belzile N., Chen Y.W., Xu R. (2000) Early diagenetic behaviour of selenium in freshwater sediments. *Appl. Geochem.* **15**, 1439-1454.
- Böck A., Rother M., Leibundgut M., Ban N. (2006) Selenium metabolism in prokaryotes, in: Hatfield, D.L., Berry, M.J., Gladyshev, V.N. (Eds.), *Selenium*. Springer US, pp. 9-28.
- Breynaert E., Bruggeman C., Maes A. (2008) XANES–EXAFS analysis of Se solid-phase reaction products formed upon contacting Se(IV) with FeS₂ and FeS. *Environ. Sci. Technol.* **42**, 3595-3601.
- Bruggeman C., Maes A., Vancluysen J. (2007) The interaction of dissolved Boom Clay and Gorleben humic substances with selenium oxyanions (selenite and selenate). *Appl. Geochem.* **22**, 1371-1379.
- Bruggeman C., Maes A., Vancluysen J., Vandemussele P. (2005) Selenite reduction in Boom clay: Effect of FeS₂, clay minerals and dissolved organic matter. *Environ. Pollut.* **137**, 209-221.
- Bykowski T., Ploeg J.R.v.d., Iwanicka-Nowicka R., Hryniewicz M.M. (2002) The

- switch from inorganic to organic sulphur assimilation in *Escherichia coli*: adenosine 5'-phosphosulphate (APS) as a signalling molecule for sulphate excess. *Mol. Microbiol.* **43**, 1347-1358.
- Canfield D.E. (2001) Biogeochemistry of sulfur isotopes, in: Valley, J.W., Cole, D.R. (Eds.), *Stable Isotope Geochemistry*. Mineralogical Society of America, Washington, DC., pp. 607-636.
- Canfield D.E., Olesen C.A., Cox R.P. (2006) Temperature and its control of isotope fractionation by a sulfate-reducing bacterium. *Geochim. Cosmochim. Acta* **70**, 548-561.
- Carignan J., Wen H. (2007) Scaling NIST SRM 3149 for Se isotope analysis and isotopic variations of natural samples. *Chem. Geol.* **242**, 347-350.
- Challenger F., North H.E. (1934) The production of organo-metalloidal compounds by micro-organisms. Part II. Dimethyl selenide. *J. Chem. Soc.*, 68-71.
- Charlet L., Kang M., Bardelli F., Kirsch R., Géhin A., Grenèche J.-M., Chen F. (2012) Nanocomposite Pyrite-Greigite Reactivity toward Se(IV)/Se(VI). *Environ. Sci. Technol.* **46**, 4869-4876.
- Charlet L., Scheinost A.C., Tournassat C., Grenèche J.M., Gehin A., Fernandez-Martínez A., Coudert S., Tisserand D., Brendle J. (2007) Electron transfer at the mineral/water interface: Selenium reduction by ferrous iron sorbed on clay. *Geochim. Cosmochim. Acta* **71**, 5731-5749.
- Chasteen T.G. (1998) Volatile Chemical Species of Selenium, in: Frankenberger Jr., E., R.A. (Ed.), *Environmental Chemistry of Selenium*. Marcel Dekker, New York, pp. 589-612.
- Chau Y.K., Wong P.T.S., Silverberg B.A., Luxon P.L., Bengert G.A. (1976) Methylation of Selenium in the Aquatic Environment. *Science* **192**, 1130-1131.
- Chen Y.-W., Zhou X.-L., Tong J., Truong Y., Belzile N. (2005) Photochemical behavior of inorganic and organic selenium compounds in various aqueous solutions. *Anal. Chim. Acta* **545**, 149-157.
- Clark S.K. (2007) Selenium stable isotope ratios in wetlands: Insights into biogeochemical cycling and how a diffusive barrier affects the measured fractionation factor. PhD Thesis, University of Illinois at Urbana-Champaign.
- Clark S.K., Johnson T.M. (2008) Effective isotopic fractionation factors for solute removal by reactive sediments: A laboratory microcosm and slurry study. *Environ. Sci. Technol.* **42**, 7850-7855.
- Clark S.K., Johnson T.M. (2010) Selenium stable isotope investigation into selenium biogeochemical cycling in a lacustrine environment: Sweitzer Lake, Colorado. *Journal of Environmental Quality* **39**, 2200-2210.
- Copeland P. (2005) Making sense of nonsense: the evolution of selenocysteine usage in proteins. *Genome Biology* **6**, 221.
- Crystal R.G. (1973) Elemental Selenium: structure and

- properties, in: Klayman, D.L.a.G., W.H.H. (Ed.), *Organic selenium compounds: their chemistry and biology*. John Wiley & Sons, Inc., New York.
- Cutter G.A. (1978) Species determination of selenium in natural waters. *Anal. Chim. Acta* **98**, 59-66.
- Cutter G.A. (1982) Selenium in Reducing Waters. *Science* **217**, 829-831.
- Cutter G.A. (1992) Kinetic controls on metalloid speciation in seawater. *Mar. Chem.* **40**, 65-80.
- Cutter G.A., Bruland K.W. (1984) The marine biogeochemistry of selenium: A re-evaluation. *Limnol. Oceanog.* **29**, 1179-1192.
- Cutter G.A., Cutter L.S. (1995) Behavior of dissolved antimony, arsenic, and selenium in the Atlantic Ocean. *Mar. Chem.* **49**, 295-306.
- DeMoll-Decker H., Macy J.M. (1993) The periplasmic nitrite reductase of *Thauera selenatis* may catalyze the reduction of selenite to elemental selenium. *Arch. Microbiol.* **160**, 241-247.
- DiChristina T.J., Fredrickson J.K., Zachara J.M. (2005) Enzymology of Electron Transport: Energy Generation With Geochemical Consequences. *Reviews in Mineralogy and Geochemistry* **59**, 27-52.
- Dowdle P.R., Oremland R.S. (1998) Microbial oxidation of elemental selenium in soil slurries and bacterial cultures. *Environ. Sci. Technol.* **32**, 3749-3755.
- Ellis A.S., Johnson T.M., Herbel M.J., Bullen T.D. (2003) Stable isotope fractionation of selenium by natural microbial consortia. *Chem. Geol.* **195**, 119-129.
- Fischer R., Zeeman, J and Leutwein (1978) Selenium, in: Wedepohl, K.H. (Ed.), *Handbook of Geochemistry*. Springer-Verlag, Berlin-Heidelberg, pp. 34-A-31 - 34-O-31.
- Flohé L., Brigelius-Flohé R. (2012) Selenoproteins of the Glutathione Peroxidase Family, in: Hatfield, D.L., Berry, M.J., Gladyshev, V.N. (Eds.), *Selenium*. Springer New York, pp. 167-180.
- Gamboa-Lewis B.A. (1976) Selenium in Biological Systems, and Pathways for its Volatilization in Higher Plants, in: Nriagu, J.O. (Ed.), *Environmental Biogeochemistry*. Ann Arbor Science, Ann Arbor, pp. 389-409.
- German C.R., Von Damm K.L. (2003) 6.07 - Hydrothermal Processes, in: Editors-in-Chief: Heinrich, D.H., Karl, K.T. (Eds.), *Treatise on Geochemistry*. Pergamon, Oxford, pp. 181-222.
- Gladyshev V. (2006) Selenoproteins and selenoproteomes, in: Hatfield, D.L., Berry, M.J., Gladyshev, V.N. (Eds.), *Selenium*. Springer US, pp. 99-110.
- Gladyshev V.N., Hatfield D.L. (2010) Selenocysteine Biosynthesis, Selenoproteins, and Selenoproteomes, in: Atkins, J.F., Gesteland, R.F. (Eds.), *Recoding: Expansion of Decoding Rules Enriches Gene Expression*. Springer New York, pp. 3-27.
- Gladyshev V.N., Khangulov S.V., Stadtman T.C. (1996) Properties of the Selenium- and Molybdenum-Containing Nicotinic Acid Hydroxylase from *Clostridium barkeri*. *Biochemistry* **35**, 212-223.
- Gobler C.J., Hutchins D.A., Fisher N.S., Cosper E.M., Sanudo-

- Wilhelmy S.A. (1997) Release and bioavailability of C, N, P, Se, and Fe following viral lysis of a marine chrysophyte. *Limnol. Oceanogr.* **42**, 1492-1504.
- Gralnick J.A., Newman D.K. (2007) Extracellular respiration. *Mol. Microbiol.* **65**, 1-11.
- Habicht K.S., Gade M., Thamdrup B., Berg P., Canfield D.E. (2002) Calibration of Sulfate Levels in the Archean Ocean. *Science* **298**, 2372-2374.
- Hagiwara Y. (2000) Selenium isotope ratios in marine sediments and algae. A reconnaissance study., MSc Thesis, University of Illinois at Urbana-Champaign.
- Harris T.K., Turner G.J. (2002) Structural Basis of Perturbed pKa Values of Catalytic Groups in Enzyme Active Sites. *IUBMB Life* **53**, 85-98.
- Hatfield D.L., Gladyshev V.N. (2002) How Selenium Has Altered Our Understanding of the Genetic Code. *Mol. Cell. Biol.* **22**, 3565-3576.
- Hayes K.F., Roe A.L., Brown G.E., JR., Hodgson K.O., Leckie J.O., Parks G.A. (1987) In Situ X-ray Absorption Study of Surface Complexes: Selenium Oxyanions on α -FeOOH. *Science* **238**, 783-786.
- Heider J., Bock A. (1993) Selenium Metabolism in Micro-organisms, in: Rose, A.H. (Ed.), *Advances in Microbial Physiology*. Academic Press, pp. 71-109.
- Hengeveld R., Fedonkin M. (2007) Bootstrapping the Energy Flow in the Beginning of Life. *Acta Biotheoretica* **55**, 181-226.
- Herbel M.J., Blum J.S., Oremland R.S., Borglin S.E. (2003) Reduction of elemental selenium to selenide: Experiments with anoxic sediments and bacteria that respire Se-oxyanions. *Geomicrobiol. J.* **20**, 587-602.
- Herbel M.J., Johnson T.M., Oremland R.S., Bullen T.D. (2000) Fractionation of selenium isotopes during bacterial respiratory reduction of selenium oxyanions. *Geochim. Cosmochim. Acta* **64**, 3701-3709.
- Herbel M.J., Johnson T.M., Tanji K.K., Gao S.D., Bullen T.D. (2002) Selenium stable isotope ratios in California agricultural drainage water management systems. *J. Environ. Qual.* **31**, 1146-1156.
- Hockin S.L., Gadd G.M. (2003) Linked redox precipitation of sulfur and selenium under anaerobic conditions by sulfate-reducing bacterial biofilms. *Appl. Environ. Microbiol.* **69**, 7063-7072.
- Hockin S.L., Gadd G.M. (2006) Removal of selenate from sulfate-containing media by sulfate-reducing bacterial biofilms. *Environ. Microbiol.* **8**, 816-826.
- Hoek J., Reysenbach A.-L., Habicht K.S., Canfield D.E. (2006) Effect of hydrogen limitation and temperature on the fractionation of sulfur isotopes by a deep-sea hydrothermal vent sulfate-reducing bacterium. *Geochimica et Cosmochimica Acta: A Special Issue Dedicated to Robert A. Berner* **70**, 5831-5841.
- Howard III J.H. (1977) Geochemistry of selenium: formation of ferroselite and selenium behavior in the vicinity of oxidizing sulfide and uranium deposits. *Geochim. Cosmochim. Acta* **41**, 1665-1678.

- Johnson T.M. (2004) A review of mass-dependent fractionation of selenium isotopes and implications for other heavy stable isotopes. *Chem. Geol.* **204**, 201-214.
- Johnson T.M., Bullen T.D. (2003) Selenium isotope fractionation during reduction by Fe(II)-Fe(III) hydroxide-sulfate (green rust). *Geochim. Cosmochim. Acta* **67**, 413-419.
- Johnson T.M., Bullen T.D. (2004) Mass-Dependent Fractionation of Selenium and Chromium Isotopes in Low-Temperature Environments. *Reviews in Mineralogy and Geochemistry* **55**, 289-317.
- Johnson T.M., Bullen T.D., Zawislanski P.T. (2000) Selenium stable isotope ratios as indicators of sources and cycling of selenium: Results from the northern reach of San Francisco Bay. *Environ. Sci. Technol.* **34**, 2075-2079.
- Johnson T.M., Herbel M.J., Bullen T.D., Zawislanski P.T. (1999) Selenium isotope ratios as indicators of selenium sources and oxyanion reduction. *Geochimica Et Cosmochimica Acta* **63**, 2775-2783.
- Kenward P.A., Fowle D.A., Yee N. (2006) Microbial Selenate Sorption and Reduction in Nutrient Limited Systems. *Environ. Sci. Technol.* **40**, 3782-3786.
- Kessi J., Hanselmann K.W. (2004) Similarities between the Abiotic Reduction of Selenite with Glutathione and the Dissimilatory Reaction Mediated by *Rhodospirillum rubrum* and *Escherichia coli*. *J. Biol. Chem.* **279**, 50662-50669.
- Kikuchi E., Sakamoto H. (2000) Kinetics of the Reduction Reaction of Selenate Ions by TiO₂ Photocatalyst. *J. Electrochem. Soc.* **147**, 4589-4593.
- Kim H.-Y., Fomenko D.E., Yoon Y.-E., Gladyshev V.N. (2006) Catalytic Advantages Provided by Selenocysteine in Methionine-S-Sulfoxide Reductases†. *Biochemistry* **45**, 13697-13704.
- Krouse H.R., Thode H.G. (1962) Thermodynamic properties and geochemistry of isotopic compounds of selenium. *Can. J. Chem.* **40**, 367-375.
- Li H., Zhang J., Wang T., Luo W., Zhou Q., Jiang G. (2008) Elemental selenium particles at nano-size (Nano-Se) are more toxic to Medaka (*Oryzias latipes*) as a consequence of hyper-accumulation of selenium: A comparison with sodium selenite. *Aquat. Toxicol.* **89**, 251-256.
- Lide D.R. (2006) *CRC Handbook of Chemistry and Physics*, 87 ed. CRC Press, Boca Raton.
- Lipman J.G., Waksman S.A. (1923) The Oxidation of Selenium by a New Group of Autotrophic Micro-Organisms. *Science* **57**, 60.
- Lovley D.R. (2006) Bug juice: harvesting electricity with microorganisms. *Nature Reviews Microbiology* **4**, 497-508.
- Lovley D.R., Phillips E.J.P. (1994) Novel Processes for Anaerobic Sulfate Production from Elemental Sulfur by Sulfate-Reducing Bacteria. *Applied Environmental Microbiology* **60**, 2394-2399.

- Luoma S.N., Johns C., Fisher N.S., Steinberg N.A., Oremland R.S., Reinfelder J.R. (1992) Determination of selenium bioavailability to a benthic bivalve from particulate and solute pathways. *Environ. Sci. Technol.* **26**, 485-491.
- Measures C.I., Grant B.C., Mangum B.J., Edmond J.M. (1983) The relationship of the distribution of dissolved selenium IV and VI in three oceans to the physical and biological process, in: Wong, C.S., Boyle, E., Bruland, K.W., Burton, J.D., Goldberg, E.D. (Ed.), *Trace Metals In Seawater*. Plenum Press, New York.
- Mihara H., Esaki N. (2012) Selenocysteine Lyase: Mechanism, Structure, and Biological Role, in: Hatfield, D.L., Berry, M.J., Gladyshev, V.N. (Eds.), *Selenium*. Springer New York, pp. 95-105.
- Milne J.B. (1998) The Uptake and Metabolism of Inorganic Selenium Species, in: Frankenberger Jr., W.T., Engberg, R.A. (Ed.), *Environmental Chemistry of Selenium*. Marcel Dekker, New York, pp. 459-477.
- Mitchell K., Heyer A., Canfield D.E., Hoek J., Habicht K.S. (2009) Temperature effect on the sulfur isotope fractionation during sulfate reduction by two strains of the hyperthermophilic *Archaeoglobus fulgidus*. *Environ. Microbiol.* **11**, 2998-3006.
- Mitchell K., Mason P.R.D., Van Cappellen P., Johnson T.M., Gill B.C., Owens J.D., Diaz J., Ingall E.D., Reichart G.-J., Lyons T.W. (2012) Selenium as paleo-oceanographic proxy: A first assessment. *Geochim. Cosmochim. Acta* **89**, 302-317.
- Mosher B.W., Duce R.A. (1987) A Global Atmospheric selenium budget. *Journal of Geophysical Research* **92**, 13,289-213,298.
- Myneni S.C.B., Tokunaga T.K., Brown G.E., Jr. (1997) Abiotic Selenium Redox Transformations in the Presence of Fe(II,III) Oxides. *Science* **278**, 1106-1109.
- Neal R.H., Sposito G., Holtzclaw K.M., Traina S.J. (1987) Selenite Adsorption on Alluvial Soils: I. Soil Composition and pH Effects. *Soil Sci Soc Am J* **51**, 1161-1165.
- Newport P.J., Nedwell D.B. (1988) The mechanisms of inhibition of Desulfotomaculum and Desulfotomaculum. *J. Appl. Bacteriol.* **65**, 419-423.
- Nguyen V.N.H., Beydoun D., Amal R. (2005) Photocatalytic reduction of selenite and selenate using TiO₂ photocatalyst. *Journal of Photochemistry and Photobiology A: Chemistry* **171**, 113-120.
- Novoselov S.V., Gladyshev V.N. (2003) Non-animal origin of animal thioredoxin reductases: implications for selenocysteine evolution and evolution of protein function through carboxy-terminal extensions. *Protein science : a publication of the Protein Society* **12**, 372-378.
- Nriagu J. (1989) Selenium in Geological Materials, in: Inhat, M. (Ed.), *Occurrence and Distribution of Selenium*. CRC Press, Boca Raton.
- Ohlendorf H.M. (1989) Bioaccumulation and Effects of Selenium on Wildlife, in: Jacobs, L.W. (Ed.), *Selenium in Agriculture and the Environment*.

- American Society of Agronomy, Madison, pp. 133-177.
- Oldfield J.E. (2002) Selenium World Atlas. *Selenium-Tellurium Development Association*.
- Omi R., Kurokawa S., Mihara H., Hayashi H., Goto M., Miyahara I., Kurihara T., Hirotsu K., Esaki N. (2010) Reaction Mechanism and Molecular Basis for Selenium/Sulfur Discrimination of Selenocysteine Lyase. *J. Biol. Chem.* **285**, 12133-12139.
- Oram L.L., Strawn D.G., Marcus M.A., Fakra S.C., Möller G. (2008) Macro- and Microscale Investigation of Selenium Speciation in Blackfoot River, Idaho Sediments. *Environ. Sci. Technol.* **42**, 6830-6836.
- Pearce C.I., Coker V.S., Charnock J.M., Patrick R.A.D., Mosselmans J.F.W., Law N., Beveridge T.J., Lloyd J.R. (2008) Microbial manufacture of chalcogenide-based nanoparticles via the reduction of selenite using *Veillonella atypica*: an in situ EXAFS study. *Nanotechnology* **19**, 155603.
- Pettersson J., Olin A. (1991) The rate of reduction of selenium(VI) to selenium(IV) in hydrochloric acid. *Talanta* **38**, 413-417.
- Plant J.A., Kinniburgh D.G., Smedley P.L., Fordyce F.M., Klinck B.A., Heinrich D.H., Karl K.T. (2003) Arsenic and Selenium. *Treatise on Geochemistry* **9**, 17-66.
- Rashid K., Krouse H.R. (1985) Selenium isotopic fractionation during SeO_3^{2-} reduction to Se^0 and H_2Se . *Can. J. Chem.* **63**, 3195-3199.
- Reamer D.C., Zoller W.H. (1980) Selenium Biomethylation Products from Soil and Sewage Sludge. *Science* **208**, 500-502.
- Rees C.E. (1973) A steady-state model for sulphur isotope fractionation in bacterial reduction processes. *Geochim. Cosmochim. Acta* **37**, 1141-1162.
- Rees C.E., Thode H.G. (1966) Selenium isotope effects in the reduction of sodium selenite and of sodium selenate. *Can. J. Chem.* **44**, 419-427.
- Rickard D. (2006) The solubility of FeS. *Geochim. Cosmochim. Acta* **70**, 5779-5789.
- Rother M. (2012) Selenium Metabolism in Prokaryotes, in: Hatfield, D.L., Berry, M.J., Gladyshev, V.N. (Eds.), *Selenium*. Springer New York, pp. 457-470.
- Rouxel O., Fouquet Y., Ludden J.N. (2004) Subsurface processes at the lucky strike hydrothermal field, Mid-Atlantic ridge: evidence from sulfur, selenium, and iron isotopes. *Geochim. Cosmochim. Acta* **68**, 2295-2311.
- Rouxel O., Ludden J., Carignan J., Marin L., Fouquet Y. (2002) Natural variations of Se isotopic composition determined by hydride generation multiple collector inductively coupled plasma mass spectrometry. *Geochim. Cosmochim. Acta* **66**, 3191-3199.
- Rue E.L., Smith G.J., Cutter G.A., Bruland K.W. (1997) The response of trace element redox couples to suboxic conditions in the water column. *Deep Sea Res. I Oceanogr. Res. Pap.* **44**, 113-134.
- Ruggles E.L., Snider G.W., Hondal R.J. (2012) Chemical Basis for the Use of Selenocysteine

- Selenium, in: Hatfield, D.L., Berry, M.J., Gladyshev, V.N. (Eds.), Springer New York, pp. 73-83.
- Salinas G., Romero H., Xu X.-M., Carlson B., Hatfield D., Gladyshev V. (2006) Evolution of selenocysteine decoding and the key role of selenophosphate synthetase in the pathway of selenium utilization, in: Hatfield, D.L., Berry, M.J., Gladyshev, V.N. (Eds.), *Selenium*. Springer US, pp. 39-50.
- Sarathchandra S., Watkinson J. (1981) Oxidation of elemental selenium to selenite by *Bacillus megaterium*. *Science* **211**, 600-601.
- Schauble E.A. (2004) Applying Stable Isotope Fractionation Theory to New Systems. *Reviews in Mineralogy and Geochemistry* **55**, 65-111.
- Scheinost A.C., Charlet L. (2008) Selenite reduction by mackinawite, magnetite and siderite: XAS characterization of nanosized redox products. *Environ. Sci. Technol.* **42**, 1984-1989.
- Schilling K., Johnson T.M., Wilcke W. (2011a) Isotope Fractionation of Selenium During Fungal Biomethylation by *Alternaria alternata*. *Environ. Sci. Technol.* **45**, 2670-2676.
- Schilling K., Johnson T.M., Wilcke W. (2011b) Selenium Partitioning and Stable Isotope Ratios in Urban Topsoils. *Soil Sci. Soc. Am. J.* **75**, 1354-1364.
- Schlekat C.E., Dowdle P.R., Lee B.-G., Luoma S.N., Oremland R.S. (2000) Bioavailability of Particle-Associated Se to the Bivalve *Potamocorbula amurensis*. *Environ. Sci. Technol.* **34**, 4504-4510.
- Schröder T., Rienhöfer A., Andreesen J.R. (1999) Selenium-containing xanthine dehydrogenase from *Eubacterium barkeri*. *Eur. J. Biochem.* **264**, 862-871.
- Schrauzer G.N. (2000) Selenomethionine: A Review of Its Nutritional Significance, Metabolism and Toxicity. *The Journal of Nutrition* **130**, 1653-1656.
- Schroder I., Rech S., Krafft T., Macy J.M. (1997) Purification and Characterization of the Selenate Reductase from *Thauera selenatis*. *Journal of Biological Chemistry* **272**, 23765-23768.
- Schwartz K. (1977) Plenary Lecture-Essentiality versus Toxicity of Metals, in: Brown, S.S. (Ed.), *Clinical Chemistry and Chemical Toxicology of Metals*. Elsevier/North Holland, Amsterdam, pp. 3-22.
- Self W.T., Wolfe M.D., Stadtman T.C. (2003) Cofactor Determination and Spectroscopic Characterization of the Selenium-Dependent Purine Hydroxylase from *Clostridium purinolyticum*. *Biochemistry* **42**, 11382-11390.
- Stadtman T.C. (1974) Selenium Biochemistry. *Science* **183**, 915-922.
- Stadtman T.C. (1980) Selenium-Dependent Enzymes. *Annu. Rev. Biochem* **49**, 93-110.
- Stadtman T.C. (1990) Selenium Biochemistry. *Annu. Rev. Biochem* **59**, 111-127.
- Stadtman T.C. (1996) Selenocysteine. *Annu. Rev. Biochem* **65**, 83-100.
- Stams A.J.M., de Bok, Frank A. M., Plugge, Caroline M., van Eekert,

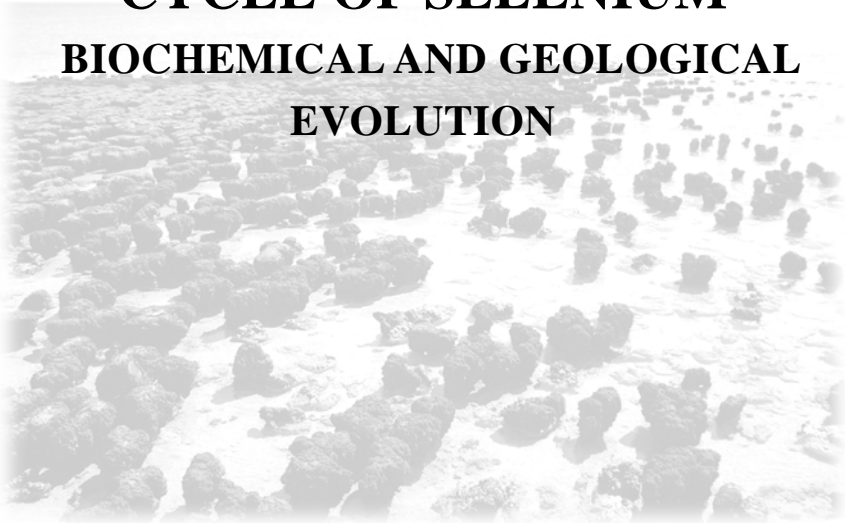
- Miriam H. A., Dolfing, Jan, Schraa, Gosse (2006) Exocellular electron transfer in anaerobic microbial communities. *Environ. Microbiol.* **8**, 371-382.
- Tan T., Beydoun D., Amal R. (2003a) Effects of organic hole scavengers on the photocatalytic reduction of selenium anions. *Journal of Photochemistry and Photobiology A: Chemistry* **159**, 273-280.
- Tan T., Beydoun D., Amal R. (2003b) Photocatalytic reduction of Se(VI) in aqueous solutions in UV/TiO₂ system: importance of optimum ratio of reactants on TiO₂ surface. *J. Mol. Catal. A: Chem.* **202**, 73-85.
- Tan T., Beydoun D., Amal R. (2003c) Photocatalytic Reduction of Se(VI) in Aqueous Solutions in UV/TiO₂ System: Kinetic Modeling and Reaction Mechanism. *Journal of Physical Chemistry B* **107**, 4296-4303.
- Taratus E.M., S.G. Eubanks, T.J. DiChristina (2000) Design and application of a rapid screening technique for isolation of selenite reduction-deficient mutants of *Shewanella putrefaciens*. *Microbiol. Res.* **155**, 79-85.
- Taylor S.R. (1964) Abundance of chemical elements in the continental crust: a new table. *Geochim. Cosmochim. Acta* **28**, 1273-1285.
- Tokunaga T.K., Lipton D.S., Benson S.M., Yee A.W., Oldfather J.M., Duckart E.C., Johannis P.W., Halvorsen K.E. (1991) Soil selenium fractionation, depth profiles and time trends in a vegetated site at Kesterson Reservoir. *Water, Air, & Soil Pollution* **57-58**, 31-41.
- Tomei F.A., Barton L.L., Lemanski C.L., Zocco T.G., Fink N.H., Sillerud L.O. (1995) Transformation of Selenate and Selenite to Elemental Selenium by *Desulfovibrio-Desulfuricans*. *J. Ind. Microbiol.* **14**, 329-336.
- Tudge A.P., Thode H.G. (1950) Thermodynamic properties of isotopic compounds of sulfur. *Can. J. Res.* **28**, 567-578.
- Turanov A.A., Xu X.-M., Carlson B.A., Yoo M.-H., Gladyshev V.N., Hatfield D.L. (2011) Biosynthesis of Selenocysteine, the 21st Amino Acid in the Genetic Code, and a Novel Pathway for Cysteine Biosynthesis. *Advances in Nutrition: An International Review Journal* **2**, 122-128.
- Von Damm K.L., Edmond J.M., Grant B., Measures C.I., Walden B., Weiss R.F. (1985) Chemistry of submarine hydrothermal solutions at 21 [deg]N, East Pacific Rise. *Geochim. Cosmochim. Acta* **49**, 2197-2220.
- Wachsmann M., Heumann K.G. (1992) Negative thermal ionization mass spectrometry of main group elements Part 2. 6th group: sulfur, selenium and tellurium. *Int. J. Mass Spectrom. Ion Processes* **114**, 209-220.
- Wang C., Lovell R.T. (1997) Organic selenium sources, selenomethionine and selenoyeast, have higher bioavailability than an inorganic selenium source, sodium selenite, in diets for channel catfish (*Ictalurus punctatus*). *Aquaculture* **152**, 223-234.
- Wang G., Jiang J., Zhu X. (2008) Study on the background level of selenium in soils and its sources,

- Guizhou Province. *Chinese Journal of Geochemistry* **27**, 178-182.
- Wang H., Zhang J., Yu H. (2007) Elemental selenium at nano size possesses lower toxicity without compromising the fundamental effect on selenoenzymes: Comparison with selenomethionine in mice. *Free Radical Biol. Med.* **42**, 1524-1533.
- Weiss H.V., Koide M., Goldberg E.D. (1971) Selenium and Sulfur in a Greenland Ice Sheet: Relation to Fossil Fuel Combustion. *Science* **172**, 261-263.
- Wen H., Carignan J. (2007) Reviews on atmospheric selenium: Emissions, speciation and fate. *Atmos. Environ.* **41**, 7151-7165.
- Wen H., Carignan J. (2011) Selenium isotopes trace the source and redox processes in the black shale-hosted Se-rich deposits in China. *Geochim. Cosmochim. Acta* **75**, 1411-1427.
- Wen H., Carignan J., Hu R., Fan H., Chang B., Yang G. (2007) Large selenium isotopic variations and its implication in the Yutangba Se deposit, Hubei Province, China. *Chin. Sci. Bull.* **52**, 2443-2447.
- Williams C.H., Arscott L.D., Müller S., Lennon B.W., Ludwig M.L., Wang P.-F., Veine D.M., Becker K., Schirmer R.H. (2000) Thioredoxin reductase. *Eur. J. Biochem.* **267**, 6110-6117.
- Woolfolk C.A., Whiteley H.R. (1962) Reduction of Inorganic Compounds with Molecular hydrogen by *Micrococcus lactulyticus* I.: Stoichiometry with Compounds of Arsenic, Selenium, Tellurium, Transition and Other Elements. *J. Bacteriol.* **84**, 647-658.
- Wrench J.J., Measures C.I. (1982) Temporal variations in dissolved selenium in a coastal ecosystem. *Nature* **299**, 431-433.
- Zawislanski P.T., McGrath, A.E. (1998) Selenium Cycle in Estuarine Wetlands: Overview and New Results from the San Francisco Bay, in: Frankenberger Jr., W.T., Engberg, R.A. (Ed.), *Environmental Chemistry of Selenium*. Marcel Dekker, INC., New York, pp. 223-242.
- Zehr J.P., Oremland R.S. (1987) Reduction of selenate to selenide by sulfate-respiring bacteria: experiments with cell suspensions and estuarine sediments. *Appl. Environ. Microbiol.* **53**, 1365-1369.
- Zhang J.-S., Gao X.-Y., Zhang L.-D., Bao Y.-P. (2001) Biological effects of a nano red elemental selenium. *BioFactors* **15**, 27-38.
- Zhang Y., Moore J.N. (1996) Selenium Fractionation and Speciation in a Wetland System. *Environ. Sci. Technol.* **30**, 2613-2619.
- Zhang Y., Zahir Z.A., Frankenberger W.T., Jr. (2004) Fate of Colloidal-Particulate Elemental Selenium in Aquatic Systems. *J Environ Qual* **33**, 559-564.
- Zhou X., Wang Y., Gu Q., Li W. (2009) Effects of different dietary selenium sources (selenium nanoparticle and selenomethionine) on growth performance, muscle composition and glutathione peroxidase enzyme activity of crucian carp (*Carassius auratus gibelio*). *Aquaculture* **291**, 78-81.

Zhu J.-M., Johnson T.M., Clark S.K.,
Zhu X.-K. (2008) High precision
measurement of selenium isotopic
composition by hydride
generation Multiple Collector
Inductively Coupled Plasma Mass
Spectrometry with a ^{74}Se - ^{77}Se
double spike. *Chinese J. Anal.
Chem.* **36**, 1385-1390.

CHAPTER 2

MARINE BIOGEOCHEMICAL CYCLE OF SELENIUM BIOCHEMICAL AND GEOLOGICAL EVOLUTION



KRISTEN MITCHELL, PAUL R. D. MASON, PHILIPPE VAN CAPPELLEN,
THOMAS M. JOHNSON, NOAH J. PLANAVSKY, SIMON W. POULTON,
EMMA U. HAMMARLUND, DONALD E. CANFIELD, GAWEN JENKIN

IN PREPARATION

THE IMAGE ON THE PREVIOUS PAGE IS OF STROMATOLITES, HAMELIN POOL, ON THE WAY TO MONKEY MIA, SHARK BAY AUSTRALIA. THIS IMAGE WAS DOWNLOADED FROM WIKIMEDIA COMMONS (COMMONS.WIKIMEDIA.ORG) A DATABASE OF 13,327,537 FREELY USABLE MEDIA FILES TO WHICH ANYONE CAN CONTRIBUTE UNDER CREATIVE COMMONS LICENSE (CREATIVECOMMONS.ORG).

ABSTRACT

Due to its redox sensitive behavior and chemical similarity to sulfur (S), the biogeochemical cycle of selenium (Se) and Se stable isotopes have recently enjoyed renewed interest. While the marine biogeochemical cycles of S and Se share some similarities, there are also major differences controlled by contrasting abundances, speciation and oceanic residence times. Here, we compare the marine S and Se cycles in relation to their distribution in the oceans, their role in biological cycles and the isotope fractionations that occur during biological uptake and reduction. The biochemical utilization of Se is reviewed in an evolutionary context. The geological evolution of the S cycle and S isotopic record is then used as a framework for discussing the Se isotopic compositions observed in marine sedimentary rocks spanning geological history. Selenium concentrations in marine shales are generally very low averaging around 5 ppm and cover a very limited isotopic range ($\delta^{82/76}\text{Se}=-2$ to $+2\%$). This suggests that assimilatory uptake and nutrient recycling has controlled the Se cycle throughout geologic time, despite biological evolution and major perturbations in the composition of the oceans and atmosphere.

2.1 SELENIUM AS MICRONUTRIENT

The availability and biogeochemical cycling of nutrient elements in the oceans through time has had a profound effect on the marine ecosystem. Selenium (Se) is an important micronutrient whose abundance in the modern oceans is principally controlled by biological uptake, carried out mainly by phytoplankton, and its subsequent recycling (Wrench, 1978; Price et al., 1987; Harrison, 1988). Selenium occurs in the oceans in multiple oxidation states, including Se(IV), Se(VI), Se(0) and Se(-II). Most aqueous and colloidal Se species are bioavailable and Se can be incorporated into cells by assimilatory reduction and used primarily as the amino acid selenocysteine, which is found all three domains of life (Copeland, 2005).

The six stable isotopes of Se (74, 76, 77, 78, 80 and 82) have the potential trace the Se cycle through time. The Se budget in the oceans is controlled by the balance between input from continental weathering, volcanic (hydrothermal) sources and atmospheric deposition, and output by sediment burial and volatilization. Each of the inputs has a distinct isotopic signature, as do the output fluxes. The Se isotopic composition of the oceans is thus controlled by the isotopic composition of the inputs and isotope fractionations that occur throughout the Se biogeochemical cycle. These processes together determine the isotopic composition of the material that is delivered to the sediments and preserved in the sedimentary rock record. Here we will compare the marine biogeochemical cycles of Se

and S with particular focus on the major biological pathways of both cycles, using the isotopic composition of marine sediments for each system as a guide to changes in these pathways through geological time.

2.2 BIOGEOCHEMISTRY OF SELENIUM: ANALOG OF SULFUR, OR NOT?

The biogeochemical cycle of sulfur (S) has been studied extensively and has informed our understanding of many aspects of Earth's evolution, including the emergence of life, major changes in ocean chemistry and the oxygenation of the atmosphere (Berner and Canfield, 1989; Canfield and Teske, 1996; Canfield and Raiswell, 1999; Canfield et al., 2000; Canfield, 2004; Canfield et al., 2007). More recently, there has been interest in providing complimentary geochemical information using other, novel, isotope systems such as Se. Selenium cycling and redox transitions are reflected in Se stable isotope variability and have been used as environmental tracers in modern and ancient environments (Johnson et al., 1999; Johnson et al., 2000; Rouxel et al., 2002; Rouxel et al., 2004; Wen et al., 2007; Wen and Carignan, 2011; Mitchell et al., 2012). While it is often instructive to use the similarities between S and Se to understand the Se cycle it is important to recognize the differences between the two biogeochemical cycles, which impact the use and interpretation of the Se isotope tracer.

Selenium is situated between sulfur and tellurium in Group VIA of the periodic table. Although it has physical and chemical

properties that are intermediate between those of metals and non-metals, it is usually characterized as a non-metal. Selenium is one of the rarest trace elements with a crustal average abundance of 0.05 ppm (Taylor, 1964), and is unevenly distributed on the surface of the Earth (Oldfield, 2002).

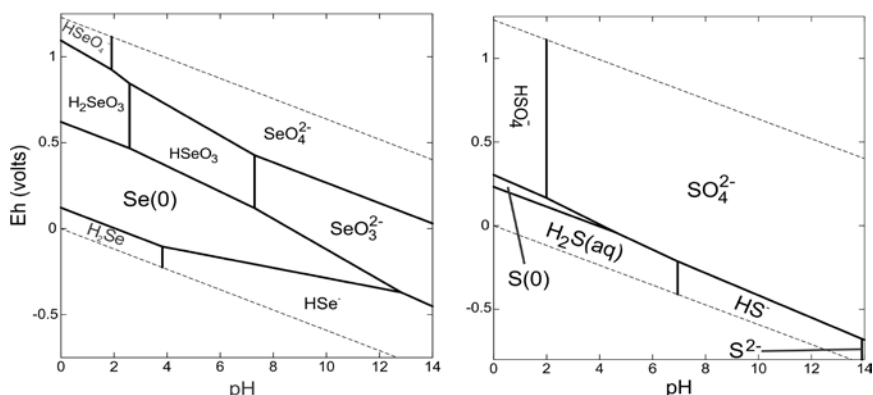


Figure 2.1 Thermodynamic stability diagrams for Se and S; total Se concentration is 10^{-8} and total sulfur concentration is 10^{-3} M, redrawn after Johnson and Bullen (2004). Notice the differences in stability for the elemental forms of Se and S as well as for selenate and sulfate. Elemental Se is stable over a much wider range than elemental S. Sulfate has a much larger stability field than does selenate, because selenite is stable over a wide range of redox potential.

Selenium is much less abundant than S, with a crustal Se/S ratio of 7.8×10^{-5} (mol/mol) (Taylor, 1964) and a ratio of 2.6×10^{-8} in modern seawater (mol/mol) (Rouxel et al., 2004). Selenium occurs naturally in the (-II), (0), (IV) and (VI) oxidation states. Sulfur can also be found in multiple oxidation states in nature including mainly (-II), (0), and (VI). The thermodynamic stability of elemental Se occurs over a wide range of redox potential and pH conditions in contrast to elemental S, which is only stable over a small window of redox and pH conditions (Figure 2.1; Seby et al., 2001; Johnson and

Bullen, 2004). In addition, under suboxic conditions selenite persists while oxyanions of sulfur are efficiently reduced (Cutter, 1982; Rue et al., 1997). Selenium has six stable isotopes ^{74}Se , ^{76}Se , ^{77}Se , ^{78}Se , ^{80}Se , and ^{82}Se , while S has only four; ^{32}S , ^{33}S , ^{34}S , and ^{36}S .

Selenium behaves as a nutrient element in the ocean, with concentrations below 2 nmol L^{-1} in deep waters (Measures, 1978; Measures and Burton, 1980b; Cutter and Bruland, 1984; Cutter and Cutter, 1995). Sulfur on the other hand exhibits near-conservative behavior, with a much higher average concentration of 28 mmol L^{-1} in modern seawater. The different abundances of S and Se are also reflected in contrasting ocean residence times of 8.7 million years for SO_4^{2-} and 26,000 years for Se (Broecker and Peng, 1982). The latter is the residence time for total Se, however. If we only consider reactive forms of Se, the reservoir estimates in Table 2.1 yield an oceanic residence time of ~2000 years.

Shrift (1964) was one of the first to recognize a Se cycle in nature, using the plant-soil system as a model. Over a decade later, Suzuki et al. (1979) described the marine Se cycle, identifying three factors controlling dissolved Se in the oceans: 1) exchanges between surface and deep waters, 2) biological assimilation of dissolved inorganic Se (DISE) into particulate organic (POSE) form, and 3) regeneration of dissolved inorganic and dissolved organic selenium (DOSe) from POSe and subsequent reoxidation of DOSe. Cutter and Bruland (1984) propose a similar model but expand it to include the uptake of DOSe by phytoplankton and speculate that $\text{Se}(0)$ may also

be bioavailable. Supporting evidence on Se(0) was unavailable at the time due to analytical limitations, however. Meanwhile, Doblin et al. (2006) showed Se(0) can be assimilated by algae, hence the model presented here accounts for uptake of DOSe and Se(0) (Figure 2.2). Table 2.1 summarizes the Se and S reservoirs and reservoir sizes. As can be seen from the table, Se reservoir sizes are much smaller than the corresponding S reservoirs.

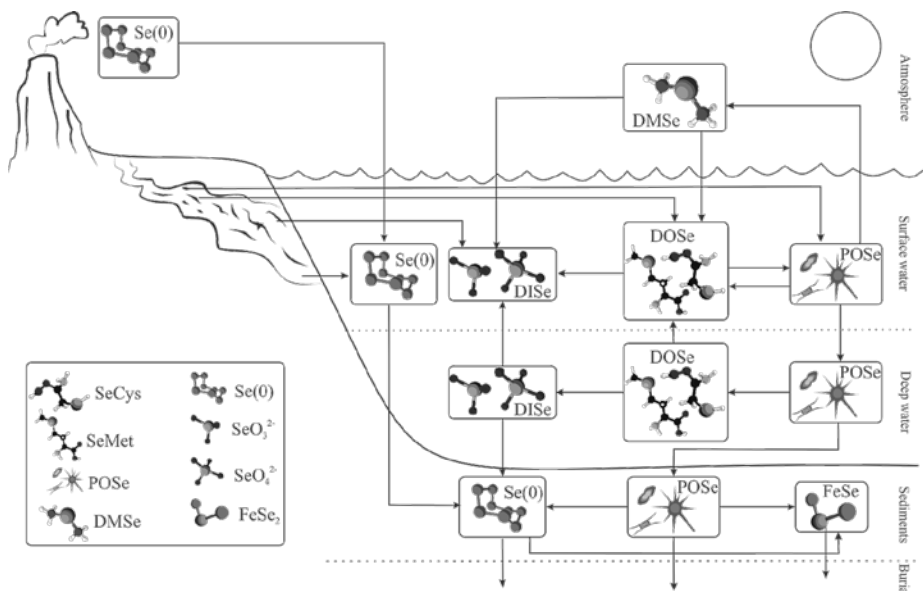


Figure 2.2 The oceanic selenium cycle. Dissolved inorganic selenium is represented by DISe and is comprised of selenate and selenite. DOSe denotes dissolved organic selenium, which is thought to be comprised mainly of selenomethionine and selenocysteine. POSe represents particulate organic selenium, which consists of living and dead organic materials.

Both Se and S are essential elements and play important roles in biology, but the differences in their abundances cause large differences in their biogeochemical cycles (Johnson, 2011). The high concentrations and long residence time of seawater sulfate mean that

SO_4^{2-} shows conservative behavior over long timescales despite being an essential element that is assimilated at high rates (Andreae, 1990). This behavior applies throughout the Phanerozoic and, probably since the start of the Proterozoic based on the inferred rise in sulfate concentration following global oxygenation at the start of the Proterozoic (Canfield and Teske, 1996; Canfield et al., 2000). In contrast, Se depth distributions show nutrient behavior, with low concentrations of selenium oxyanions and a major peak in organically-bound Se in surface waters. Marine Se on the modern Earth is dominated by biological cycling (Suzuki et al., 1979; Cutter and Bruland, 1984). The extent of this nutrient behavior through geological time has not been investigated to date, although preliminary studies show that assimilation by phytoplankton was likely the dominant control on Se isotopic variability throughout the Phanerozoic (Mitchell et al., 2012).

Sulfur is required by all domains of life. It is incorporated through the assimilatory pathway of sulfate reduction and found mainly as cysteine in organic matter (Figure 2.3). Sulfate is also widely used as a terminal electron acceptor for microbial respiration. Selenium is less abundant but is well-known as an essential micronutrient due to its incorporation into selenocysteine (the 21st amino acid) and selenoenzymes (Böck et al., 1991b). The gene coding for the synthesis of selenocysteine has been found in eukaryotes (mainly mammals), eubacteria and archaea (Xu et al., 2007).

Table 2.1 Marine reservoirs of selenium and sulfur.

Selenium (Se) Reservoirs	Se Mass (mol)	Sulfur (S) Reservoirs	S Mass (mol)	Se References	S References
Atmosphere, DMS _{Se}	1.4x10 ⁷	Atmosphere, DMS	9.0x10 ⁹	(Nriagu, 1989a)	(Mackenzie et al., 1979; Andreae and Raemdonck, 1983)
Surface Ocean, total	1.1x10¹¹	Surface Ocean, total	2.0x10¹⁸	(Nriagu, 1989a)	
Surface ocean, DIS _{Se}	6.5x10 ⁹	Surface ocean, DIS	2.0x10 ¹⁸	(Cutter and Bruland, 1984)	(Mackenzie et al., 1979)
Surface ocean, DOSe	4.1x10 ⁹	Surface ocean, DOS	1.2x10 ¹²	(Cutter and Bruland, 1984)	(Andreae, 1979; Mackenzie et al., 1979; Andreae, 1990)
Surface ocean, POSe	2.7x10 ⁹	Surface ocean, POS	1.6x10 ¹²	(Nriagu, 1989a)	(Mackenzie et al., 1979; Andreae, 1990)
Surface ocean, Se(0)	2.0x10 ⁶	Surface ocean, S(0)	0.0		
Deep ocean, total	1.6x10¹²	Deep ocean, total	3.6x10¹⁹	(Nriagu, 1989a)	
Deep Ocean, DIS _{Se}	1.5x10 ¹²	Deep Ocean, DIS	3.6x10 ¹⁹	(Cutter and Bruland, 1984)	(Mackenzie et al., 1979)
Deep Ocean, DOSe	1.2x10 ¹¹	Deep Ocean, DOS	1.2x10 ¹¹	(Cutter and Bruland, 1984)	(Mackenzie et al., 1979; Andreae, 1990)
Deep Ocean, POSe	3.2x10 ¹¹	Deep Ocean, POS	2.6x10 ¹²	(Buat-Menard and Chesselet, 1979; Mackenzie et al., 1979)	(Mackenzie et al., 1979; Andreae, 1990)
Sediments, Total	1.6x10¹¹	Sediments, Total	3.8x10²⁰	(Nriagu, 1989a)	
Sediments, Se(0)	5.3x10 ¹⁰	Sediments, S(0)	3.6x10 ¹⁴	(Wen and Qiu, 2002; Zhu et al., 2004)	(Mackenzie et al., 1979; Canfield et al., 2005)
Sediments, POSe	5.3x10 ¹⁰	Sediments, POS	1.8x10 ¹⁹	(Wen and Qiu, 2002; Zhu et al., 2004)	(Holser et al., 1989)
Sediments, FeSe	5. x10 ¹⁰	Sediments, FeS	2.5x10 ²⁰	(Wen and Qiu, 2002; Zhu et al., 2004)	(Holser et al., 1989)
		Sediments, SO ₄ ²⁻	1.1x10 ²⁰		(Garrels and Lerman, 1981)

Selenium oxyanions of Se(IV) and Se(VI), like sulfate, can be used as terminal electron acceptors (Zehr and Oremland, 1987; Oremland et al., 1989; Steinberg and Oremland, 1990; Oremland, 1994; Oremland et al., 1994; Blum et al., 1998; Herbel et al., 2000; Blum et al., 2001; Stolz et al., 2002; Clark and Johnson, 2008).

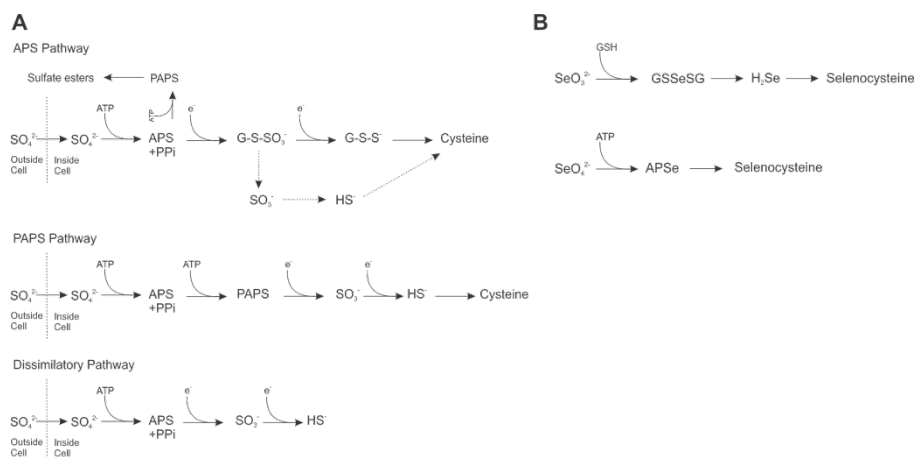


Figure 2.3 A) Uptake and reduction of sulfate. The steps shown are thought to be fundamentally the same for the uptake and incorporation of selenate into selenated proteins, where Se is substituted for sulfur in cysteine or methionine (Stadtman, 1974; Milne, 1998; Böck et al., 2006). The PAPS pathway is mainly used by archaea and bacteria. Figure drawn after Canfield et al. 2005 (APS, adenosine phosphosulfate; G-S-SO₃; organic thiosulfate; G-S-S⁻; reduced organic sulfur; PP_i, pyrophosphate; PAPS, phosphoadenosine-5'-phosphosulfate). B) Selenocysteine biosynthesis in plants, marine algae, and brewer's yeast, figure modified from Schrauzer (2000). This process may be slightly different in bacteria but follows the same general pathways. (GSH, glutathione; GSSeSG, selenogluthathione trisulfide; APSe, adenosine phosphoselenate).

2.3 BIOLOGICAL CYCLING OF SE AND S

The uptake of sulfur- or selenium oxyanions from seawater generally involves active uptake by cells which requires energy. Uptake is followed by reduction of the oxyanions to the -II oxidation state. Many prokaryotes also use compounds in addition to sulfate

including thiosulfate, polythionates and elemental sulfur to satisfy their biochemical sulfur requirements, which still requires reduction for incorporation into organic matter (Canfield et al., 2005). While S is generally incorporated as sulfate and processed through one of two possible reductive pathways (Figure 2.3; Canfield et al., 2005), there are multiple uptake pathways for Se which are less well known (Stadtman, 1974; Milne, 1998; Schrauzer, 2000; Böck et al., 2006). The uptake of selenium can involve multiple species including Se(IV), Se(VI), Se(0) and Se(-II) and depends on the local availability and speciation of Se, as well as organism specific needs. Reduced organic forms of Se have been shown to be bioavailable and possibly a major source of Se to some organisms, including marine phytoplankton (Shrift, 1964; Heider and Bock, 1993; Gobler et al., 1997; Baines and Fisher, 2001). Elemental Se also shows some bioavailability, again, mainly depending on the organism (Schlekat et al., 2000; Zhang et al., 2004; Wang et al., 2007). In many organisms, selenomethionine and selenocysteine, which occur in the -II oxidation state, appear to be the most bioavailable forms of Se, followed by dissolved selenite and selenate oxyanions (Heider and Bock, 1993; Baines, 2001).

The enzyme selenocysteine lyase is proposed to be the main enzyme in the recycling of micronutrient Se from degraded selenoproteins that contain selenocysteine (Stadtman, 1990; Omi et al., 2010; Mihara and Esaki, 2012). Selenocysteine lyase degradation of selenocysteine results in the end products H_2Se or elemental Se (Stadtman, 1990). Selenocysteine lyase, unlike cysteine desulfurases,

which can catalyze the release of both S and Se from cysteine and selenocysteine, only catalyzes the degradation of selenocysteine and is inert to cysteine (Mihara and Esaki, 2012). Two forms of selenocysteine lyase have thus far been isolated, one from bacteria and one from mammals, but it is likely that they are as widespread as their seleno-protein counterparts (Stadtman, 1990; Mihara and Esaki, 2012).

In the following sections we focus on the assimilatory and dissimilatory reduction of Se and S, mainly by prokaryotes, because these processes are major drivers of the cycling of Se and S and dissimilatory reduction imparts the largest isotope fractionations that can be traced in the rock record (Canfield, 2001a; Johnson and Bullen, 2004). In addition to biologically-mediated reduction there are many other pathways that are important to the cycling of both elements, including volatilization, microbial oxidation as well as high and low temperature abiotic pathways of oxidation and reduction that we will not discuss in great detail here as they are minor biogeochemical drivers in the marine system.

2.3.1 ASSIMILATORY REDUCTION

After uptake of sulfate, reduction proceeds along either the APS pathway (Figure 2.3A) which is mainly utilized by oxygen producing eukaryotes and a few cyanobacteria, or proceeds through the PAPS pathway (Figure 2.3A) found mainly in non-oxygen producing microbes (Canfield, 2001a). Details of the mechanisms of uptake and reduction of selenate and selenite are less well understood

but appear to partially follow the sulfate reduction pathways (APS or PAPS) or are reduced through the glutathione reduction pathways, selenate most likely follows the sulfate pathways due to their similar geometry (Figure 2.3B). The uptake of selenite appears to be more complex with multiple pathways possible (Stadtman, 1974; Schrauzer, 2000; Böck et al., 2006). However, it is assumed that the thioredoxin-glutathione system is involved in this initial step (Heider and Bock, 1993). However, some organisms seem to have non-specific mechanisms to take up selenite while others have specific mechanisms (Milne, 1998). Most evidence points to active transport of selenite but the mode of transport of selenite into the cell appears to be organism dependent (Heider and Bock, 1993; Obata et al., 2004). Selenite can be taken up into the sulfate reduction mechanism but only at elevated concentrations. After uptake into the cell selenate and selenite are reduced to selenide or selenophosphate presumably either through the sulfate reduction pathway or the glutathione pathway but other unknown pathways may also be important (Stadtman, 1974; Schrauzer, 2000). Selenocysteine is the first organic selenium compound formed which can eventually be converted to selenomethionine. Selenocysteine and selenomethionine can be incorporated into proteins and enzymes depending on function. Non-specific uptake results mainly in the excessive substitution of selenocysteine for cysteine and may be the cause for the toxicity of selenite (Heider and Bock, 1993).

Selenium can also be taken up in the form of dissolved organic compounds, presumably mainly as selenomethionine and/or selenocysteine (Heider and Bock, 1993; Baines, 2001). It is unclear how organic Se is transported across the cell membrane. Transport of organic S species across the cell membrane occurs through ABC (ATP-binding cassette) transporters but these are only active at low sulfate concentrations (Bykowski et al., 2002). The high sulfate concentrations in the oceans likely inhibit this pathway for S but there may be similar pathways for the uptake of organic Se.

Elemental Se has long been thought to be one of the least bioavailable forms of Se due to its decreased mobility after precipitation (Terry et al., 2000). However, uptake of elemental Se has been reported in invertebrates as well as mammals (Luoma et al., 1992; Wang and Lovell, 1997; Schlekot et al., 2000; Li et al., 2008; Zhou et al., 2009). In some mammals nanoparticulate Se(0) has been shown to be nearly as bioavailable as selenomethionine and selenite, but with less toxicity than selenomethionine (Zhang et al., 2001; Wang et al., 2008). There are only three known organisms that can oxidize elemental selenium to selenite and selenate; *Bacillus megaterium*, *Thiobacillus ASN-1*, and *Leptothrix MNB-1* (Sarithchandra and Watkinson, 1981; Dowdle and Oremland, 1998). This oxidation occurs enzymatically, thus the Se(0) is likely taken up into the cell. The direct uptake of Se(0) for assimilation in microorganisms has not yet been demonstrated to our knowledge. The ability of organisms to take up not only oxidized species of Se but also

reduced forms of Se is quite different from the uptake of S, which generally takes up only oxidized S species which require a subsequent reduction step (Bykowski et al., 2002; Canfield et al., 2005)

2.3.2 DISSIMILATORY REDUCTION

Sulfate reduction may account for half or more of the total organic carbon mineralization in modern marine environments (Canfield et al., 2005). Sulfate reducers are widely distributed and have a broad environmental tolerance with growth occurring in temperatures ranging from $-1.5\text{ }^{\circ}\text{C}$ to $105\text{ }^{\circ}\text{C}$, as well as over a wide range of salinity (Canfield et al., 2005). The conditions required for dissimilatory sulfate reduction include: the absence of molecular oxygen and a supply of appropriate electron donors, and are essentially the same as those required for dissimilatory selenate or selenite reduction. Most organisms that have been found to reduce selenium oxyanions are classified as nitrate reducers that can, in addition to nitrate, use other electron acceptors, such as arsenate, nitrite, thiosulfate and others to grow (Stolz and Oremland, 1999). The majority of selenate or selenite reducing organisms have been isolated from Se contaminated agricultural areas (i.e. San Joaquin Valley, Massie Slough) or extreme environments, such as soda lakes or hot springs (Blum et al., 1998; Huber et al., 2000; Blum et al., 2001).

Microorganisms capable of growth via dissimilatory reduction of selenium oxyanions can be placed in 4 groups, based on growth conditions and phylogeny: 1) hyperthermophilic archaea, 2) thermophilic bacteria, 3) mesophilic bacteria affiliated with the Gram-

positive bacteria and *Clostridia*, and 4) mesophilic gram-negative bacteria and γ -, δ - and ϵ -proteobacteria. The majority of the currently described species utilize organic electron donors in the form of short organic acids, alcohols or sugars. Thus far, a selenate reductase enzyme has only been isolated from *Thauera selenatis* (Schroder et al., 1997), thus most dissimilatory selenate reduction is carried out by microorganisms that are also able to metabolize with other electron acceptors (DeMoll-Decker and Macy, 1993; Kessi and Hanselmann, 2004).

The predominant end product of the reduction of selenium oxyanions is generally red amorphous elemental selenium (Oremland et al., 1989; Oremland et al., 2004). However, formation of considerable amounts of Se(-II) has been observed for selenite reduction by *Bacillus selenitireducens*, *Citrobacter freundii* and *Veillonella atypica* (Woolfolk and Whiteley, 1962; Herbel et al., 2003; Pearce et al., 2008). Production of Se(-II) occurs only after all selenite has been converted to Se(0). Elemental selenium is mainly deposited outside the cell. Therefore, it is likely that reduction of Se(0) to Se(-II) is achieved via an extracellular electron transfer mechanism.

2.4 ISOTOPE FRACTIONATION

2.4.1 FRACTIONATION ASSOCIATED WITH ASSIMILATORY REDUCTION

Assimilatory reduction processes are often not considered when considering the S isotope system, as the fractionations are relatively small when compared with fractionations accompanying dissimilatory reduction. Sulfur isotope fractionation ($\epsilon^{34}\text{S}$) during

assimilatory sulfate reduction is on the order of 1 to 5‰, while much larger fractionations are associated with dissimilatory reduction (see section 2.4.2) (Canfield, 2001a). The lack of a large fractionation is thought to be due to the small isotope fractionation associated with S uptake, and subsequent absence of exchange between internal and external S pools (Rees, 1973; Canfield, 2001a).

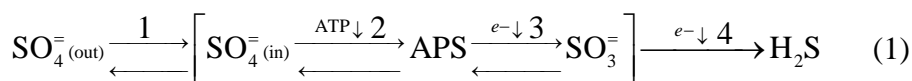
Few studies of assimilatory reduction of Se oxyanions have produced isotope fractionation data to date. Experiments of algal Se uptake have yielded fractionations ($\epsilon^{82/76}\text{Se}$) of 1.5 to 3.9‰ (Hagiwara, 2000). Phytoplankton in a freshwater lake were found to be only slightly fractionated ($\epsilon^{82/76}\text{Se}=0.74\text{‰}$) compared to the water (Clark and Johnson, 2010).

2.4.2 FRACTIONATION ASSOCIATED WITH DISSIMILATORY REDUCTION

The fractionation of sulfur isotopes during dissimilatory sulfate reduction has been studied extensively (Thode, 1951; Harrison and Thode, 1958; Kaplan and Rittenberg, 1964; Chambers, 1975; Habicht and Canfield, 1997). Experiments using pure cultures and natural populations produce S isotope fractionation ($\epsilon^{34}\text{S}$) ranging between 0 and 46‰ (Thode, 1951; Harrison and Thode, 1958; Kaplan and Rittenberg, 1964; Kemp and Thode, 1968; Chambers, 1975; Canfield et al., 2006a). This range of values is explained by differences in species of sulfate reducers (Detmers et al., 2001), the rate of sulfate reduction, as well as differences in environmental factors at the time of sulfate reduction, including electron donor supply, sulfate concentrations and temperature (Harrison and Thode,

1958; Kaplan and Rittenberg, 1964; Kemp and Thode, 1968; Detmers et al., 2001; Habicht et al., 2002a; Habicht et al., 2005; Canfield et al., 2006a; Hoek et al., 2006).

The standard model of sulfur isotope fractionation first proposed by Rees (1973), considers four main steps of dissimilatory sulfate reduction.



These steps are illustrated in Equation (1). They include: 1) transport of sulfate across the cell membrane, this step is associated with 3‰ fractionation, 2) activation of sulfate to APS, there is no isotope fractionation associated with this step, 3) reduction of APS to sulfite, which has associated fractionations of at least 25‰, and 4) reduction of sulfite to sulfide followed by transport of sulfide through the cell membrane, which has fractionation of a similar magnitude to step 3. This reaction network has been updated to account for mass flow to better describe fractionation in relation to multiple sulfur isotopes, electron donors, and temperature effects (Farquhar, 2003; Canfield et al., 2006a; Hoek et al., 2006; Mitchell et al., 2009) but it illustrates effectively the steps that impart the most S isotope fractionation.

The theory of sulfur isotope fractionation during dissimilatory reduction of sulfate provides the reference framework to contextualize the analogous Se isotope fractionation. Selenium isotopic fractionations associated with dissimilatory reduction by microorganisms are, on the whole, significantly smaller than those

found in the S isotope system. Most studies of isotope fractionation by dissimilatory selenate and selenite reduction have been done with pure cultures. Herbel et al. (2000) performed selenate and selenite experiments using growing cultures of *Sulfurospirillum barnesii* strain SES-3 and *Bacillus arenicoselenatis* strain EH1. In these experiments the authors observed final fractionations of 7.5‰ ($\epsilon^{82/76}\text{Se}$) in selenate experiments and up to 13.65‰ ($\epsilon^{82/76}\text{Se}$) in selenite reduction experiments.

Selenite reduction experiments, using sediment slurries with sediments from an intertidal mud flat in the northern reach of the San Francisco Estuary, show fractionations that are similar to those seen in pure culture studies ($\epsilon^{82/76}\text{Se}$; 8.25‰) and no dependence of fractionation on the concentration of selenium (Ellis et al., 2003). The latter implies that even at low Se concentrations Se isotope fractionations could be considerable, unlike S isotope fractionations which are significantly reduced at low S concentrations (Habicht et al., 2002b). Another study on an intact sediment core and agitated and non-agitated sediment slurries found much smaller fractionations than previous slurry experiments and pure microbial cultures (Clark and Johnson, 2008). The agitated slurries exhibited $\epsilon^{82/76}\text{Se}$ from 1.11 to 2.69‰, where unmixed slurries produced even smaller $\epsilon^{82/76}\text{Se}$ of 0.79‰. The intact sediment core gave a range of $\epsilon^{82/76}\text{Se}$ from -0.11‰ to 1.06‰. These results show more similarity to the limited range of $\delta^{82/76}\text{Se}$ in marine sedimentary rocks (see discussion below). Figure 2.4 summarizes the theoretical and experimentally observed

fractionations for both the Se and S isotope systems. A compilation of δ values for Se and S isotopes in sedimentary rocks is shown for comparison.

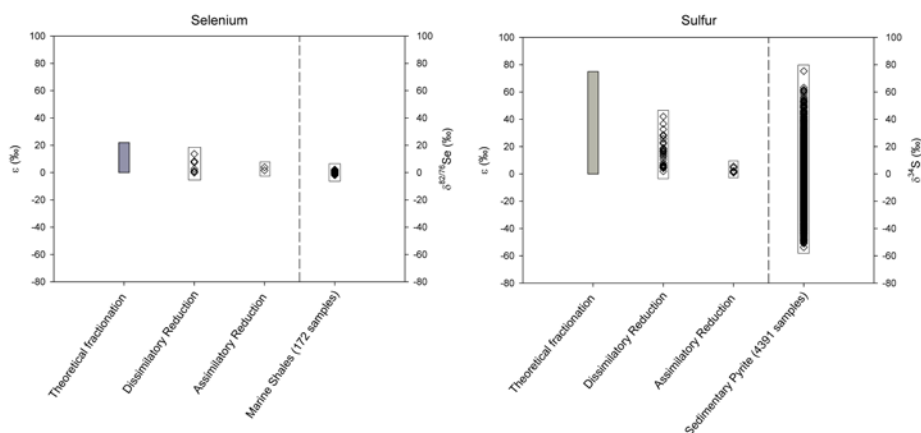


Figure 2.4 Isotope fractionation ranges for Se and S for theoretical fractionation, dissimilatory reduction, and assimilatory reduction, and δ values in sedimentary rocks. Data for assimilatory and dissimilatory reduction of Se is from (Johnson and Bullen, 2004). Theoretical calculation is from (Krouse and Thode, 1962). Marine shale $\delta^{82/76}\text{Se}$ data is from Mitchell et al. (2012) and this study. Data for dissimilatory reduction of S is from (Detmers et al., 2001). Data for assimilatory S reduction is from Canfield (2001a). Calculated theoretical fractionation is from Tudge and Thode (1950). Data for $\delta^{34}\text{S}$ is from Canfield and Raiswell (1999).

2.5 BIOCHEMICAL EVOLUTION OF SELENIUM

Selenocysteine, the 21st amino acid has changed our understanding of how the genetic code operates because it revealed the dual use of codons (Böck et al., 1991a; Gladyshev and Kryukov, 2001; Hatfield and Gladyshev, 2002; Turanov et al., 2011). Selenocysteine has similar functionality to that of its S homolog cysteine and the two can be exchanged for each other quite readily. The selenocysteine decoding equipment and selenoprotein genes are found in all 3 domains of life, though certain taxa may lack

this genetic information (Copeland, 2005). This indicates that the selenocysteine decoding machinery evolved before the division of the 3 domains of life but that these traits may have been lost and regained the latter, possibly by horizontal gene transfer (HGT) (Gladyshev and Kryukov, 2001; Romero et al., 2005; Zhang et al., 2006; Salinas et al., 2006). The dynamic loss, acquisition and maintenance of these genes indicate the utility and adaptability of selenocysteine usage.

It has been argued that Se was incorporated into the biochemistry of cells during the emergence and evolution of life before S (Hengeveld, 2007; Hengeveld and Fedonkin, 2007; Sun and Caetano-Anollés, 2009). This argument is based largely on the higher chemical reactivity of Se and its resistance to full oxidation that can potentially inactivate enzymes (Hengeveld, 2007; Hengeveld and Fedonkin, 2007; Ruggles et al., 2012). Hydrogenation of Se, specifically into a FeNiSe₂ complex, is postulated as the start of Se biochemistry (Hengeveld and Fedonkin, 2007); modern hydrogenases and dehydrogenases containing selenocysteine make up two of the major selenoprotein groups (Stadtman, 1980; Baltazar et al., 2011).

2.6 GENETICS: THE UGA CODON AND TRNA

Selenocysteine is co-translationally encoded by the UGA (UracilGuanineAdenine) codon, which also serves as a *stop* codon in the genetic code (Böck et al., 1991a; Böck et al., 1991b). When the genetic code was first deciphered, 20 amino acids were assigned to 61 of the 64 codons available in the triplet code, and 3 codons were assigned as stop codons. Thus each of the 64 possible codons was

assigned a function, and therefore did not allow for coding of additional amino acids. However, it was not until UGA was found to code for selenocysteine that it was considered possible that several codons could have more than one function (Böck et al., 1991a; Böck et al., 1991b).

Selenocysteine is the only known amino acid that is biosynthesized on its own transfer RNA (tRNA) (Turanov et al., 2011). Transfer RNA's main function is to deliver amino acids to the ribosome during protein synthesis. The tRNA coding for selenocysteine is the longest tRNA sequenced (90 basepairs) and also one of the most unique (Gladyshev and Hatfield, 2010). Due to the central role of tRNA in biochemistry, tRNA sequences retain significant ancestral and evolutionary information about protein biosynthesis (Eigen et al., 1989; Sun and Caetano-Anollés, 2009). The secondary structure of tRNA is characterized by its cloverleaf shape, which consists of the acceptor or amino acid stem and 4 arms: the D arm, the anticodon arm, the T arm, and the variable arm which is the site of the most variability. The long variable arm is a key characteristic of class II tRNAs which are found at the base of the phylogenetic tree, and it is proposed that modern attachment (charging) of amino acids began in Class II tRNA molecules with selenocysteine (Sun and Caetano-Anollés, 2009). It is also suggested that the stop codon UGA in mRNA, which also codes for selenocysteine, is the oldest codon to have a modern functional role in tRNA molecules (Sun and Caetano-Anollés, 2009). The

selenocysteine tRNA found in *Chlamydomonas reinhardtii*, a genus of unicellular green algae which is widely used as a model organism in cell and molecular biology and can be found in freshwater, soils, oceans and even snow, establishes a common ancestor of this tRNA for all domains of life (Rao et al., 2003).

Based on rRNA of 155 species whose entire genomes have been sequenced a total of 29 bacterial and 3 archaeal species were found to have selenocysteine decoding capabilities (Romero et al., 2005). Selenocysteine decoding capabilities are indicative of selenocysteine incorporation. Analysis of the genomes that possess the capability to incorporate selenocysteine suggests that this capability emerged at least once before the division of the three domains of life (Romero et al., 2005). There is also evidence for horizontal gene transfer (HGT) of some selenocysteine utilization traits, such as clustering of similar genes in distantly related species (Romero et al., 2005). HGT does not preclude the conclusion that selenocysteine utilization is ancient but exemplifies the continuing utility and adaptability of selenocysteine in modern organisms (Gladyshev and Kryukov, 2001; Romero et al., 2005; Zhang et al., 2006; Salinas et al., 2006).

2.7 SELENOCYSTEINE CONTAINING PROTEINS AND THEIR FUNCTIONALITY

There are 23 known selenoproteins which all have the shared feature of redox catalysis (Hatfield and Gladyshev, 2002). For those selenoproteins with known functions all are classified as

oxidoreductases, which as the name implies catalyze oxidation-reduction reactions (Hatfield and Gladyshev, 2002; Gladyshev, 2006; Gladyshev and Hatfield, 2010). However, there are many other selenoproteins whose functions are as yet unknown. Major selenoproteins are summarized in Table 2.2, and a few of the best studied selenoproteins are discussed in detail below.

Selenocysteine provides a catalytic advantage over cysteine in selenoproteins due to increased nucleophilicity and lower pKa (5.2) of SeH compared with SH (9.1) in cysteine (Harris and Turner, 2002; Copeland, 2005; Kim et al., 2006; Salinas et al., 2006). In some cases cysteine may not be reactive enough and therefore is replaced by selenocysteine, while in other cases selenocysteine may be too reactive and thus toxic, in which case cysteine is the preferred protein (Gladyshev and Hatfield, 2010). It has recently been found that the selenocysteine biosynthetic pathway can also synthesize cysteine, showing the flexibility of these two amino acids (Turanov et al., 2011).

Selenium has the ability to easily donate and accept electrons which gives it the ability to resist inactivation at the active site of selenocysteine (Hengeveld and Fedonkin, 2007; Ruggles et al., 2012). The ability to resist inactivation affords selenocysteine two specific properties: 1) it can easily be recycled to its original reduced form after oxidation, and 2) it is not oxidized by most oxidants to its highest VI+ oxidation state which would inactivate the enzyme.

Table 2.2 Selenoproteins and their functions.

Selenoprotein	Function	Additional information	References
<i>Proteins with labile Se cofactors</i>			
Xanthine dehydrogenase (XDH)	catalyzes oxidation of hypoxoxanthine and xanthine		(Schröder et al., 1999)
Nicotinic acid hydroxylase (NAH)	Reduces NADP ⁺ to NADPH	First step in fermentation of nicotinic acid to ammonia, propionate, acetate and CO ₂	(Stadtman, 1980; Gladyshev et al., 1996)
Purine hydroxylase (PH)	Fermentation of purines to CO ₂ , ammonia, acetate and formate		(Rother, 2012)
<i>Selenocysteine containing selenoproteins</i>			
[NiFeSe] hydrogenases	Catalyze the reversible oxidation of molecular hydrogen	Found in sulfate reducing or methanogenic microorganisms	(Baltazar et al., 2011)
Thioredoxin reductase (TR)	NADPH-dependent reduction of thioredoxin	Present in all organisms; used in redox signaling	(Arnér and Holmgren, 2000; Williams et al., 2000)
Glycine Reductase (selenoprotein A)	Reduces glycine to acetate	Only selenoprotein with no cysteine homolog	(Stadtman, 1996)
Glutathione peroxidase (GPx)	Reduces H ₂ O ₂	Part of the large glutathione peroxidase family	(Flohé and Brigelius-Flohé, 2012)
Formate Dehydrogenase	Oxidizes formate	Selenocysteine dependent forms mainly found in methanogens; 300 times more catalytically active than S homolog	(Stadtman, 1980; Stadtman, 1996)

The latter occurs with cysteine because S(IV) is unstable in most conditions unlike Se(IV) (Ruggles et al., 2012). The first property would make Se advantageous over its S homolog cysteine in the aerobic world while the second property, which does not require the presence of free oxygen, explains why selenocysteine usage could have originated in an early, anaerobic world (Ruggles et al., 2012).

Selenium occurs in selenoproteins in two main forms, as a labile cofactor and as the amino acid selenocysteine. Proteins with Se inserted post-translationally as a dissociable cofactor are a relatively rare form of selenated proteins, and have only been found in Mo-containing enzymes (Hatfield and Gladyshev, 2002), for this reason they will not be discussed further. Selenium can also be incorporated non-specifically into proteins through the cysteine or methionine biosynthetic pathways, resulting in the incorporation of selenocysteine in place of the S counterpart. This misincorporation of Se may be the cause of Se toxicity (Hatfield and Gladyshev, 2002).

2.7.1 NICKEL–IRON–SELENIUM HYDROGENASE

Russell and Hall (1997) suggest that FeS minerals studded with Ni formed the first semipermeable ‘catalytic boundary’ at the interface between hot (150°C) alkaline sulfide rich hydrothermal waters and a warm (90°C), iron rich Hadean ocean. This ‘catalytic boundary’ encouraged the synthesis of organic anions through hydrogenation, thus forming the first Fe–Ni–S hydrogenase. Hengeveld and Fedonkin (2007) modify Russell and Hall’s 1997 model by suggesting that Fe–Ni–selenides (FeNiS₂)_n were the key

minerals in this reaction rather than greigite. All [NiFeSe] hydrogenases are either periplasmic or membrane associated, and belong to one of 4 following classes of organisms: 1) δ -proteobacteria, 2) *Clostridia*, 3) *Methanococci*, and 4) *Methanopyrus*. The one exception is *Thermodesulfovibrio yellowstonii* from the Nitrospira class which is deep branching (Baltazar et al., 2011). Thus all organisms containing [NiFeSe] hydrogenases are either sulfate reducing bacteria or methanogenic archaea (Baltazar et al., 2011).

2.7.2 THIOREDOXIN REDUCTASE

Thioredoxin reductase (TR) and thioredoxin compose a major cellular redox system found in all organisms (Arnér and Holmgren, 2000; Novoselov and Gladyshev, 2003). Due to its universal incorporation thioredoxin reductase is the best candidate for an essential selenoprotein (Hatfield and Gladyshev, 2002). Even though this protein is found in all living organisms it was thought that the selenocysteine containing form only occurred in animals until recently when it was found in the alga *C. reinhardtii* (Hatfield and Gladyshev, 2002; Novoselov and Gladyshev, 2003). There are two types of thioredoxin reductase: 1) the small or bacterial type found in bacteria, archaea, plants and most unicellular eukaryotes 2) the large or animal type found in higher eukaryotes mainly animals (Williams et al., 2000; Novoselov and Gladyshev, 2003). The large form of TR generally contains a selenocysteine residue, while the small form contains only cysteine residue. It is thought that small TRs are ancient enzymes that were replaced with large TRs over time (Novoselov and Gladyshev,

2003). Large TRs have been found in *C. reinhardtii* along with 3 small TRs making it the only known organism to contain both large and small TRs (Novoselov and Gladyshev, 2003). Large TRs found in *C. reinhardtii* have both cysteine and selenocysteine containing proteins. Novoselov and Gladyshev (2003) conclude that the large TRs must have evolved in an organism that had the ability to insert selenocysteine before the split of the 3 domains and the large TRs was conserved in all organisms in which it is found.

2.7.3 GLUATHIONE PEROXIDASE

Glutathione peroxidase is found in all domains of life and is thought to act mainly as an anti-oxidant, protecting cells from oxidation due to hydrogen peroxide and organic peroxides. Selenocysteine containing active sites found mainly in vertebrates, while most terrestrial plants, yeasts, protozoa and bacteria have cysteine substituted glutathione peroxidases (Flohé and Brigelius-Flohé, 2012). An important exception to this rule is the green algae *C. reinhardtii* which contains selenocysteine glutathione peroxidase as well as nine other selenoproteins (Shigeoka et al., 1991; Novoselov et al., 2002).

2.8 GEOLOGICAL EVOLUTION

Sulfur isotopes have been widely used to identify early life in the form of sulfate reducing bacteria (SRB), as well as to track the global S cycle and oxygenation of the atmosphere and oceans. As discussed above (Section 2.4.2) dissimilatory sulfate reduction imparts large fractionations on S isotopes and this isotope fractionation is

dependent upon growth conditions. The S isotopic composition of sedimentary sulfides through time has been compiled by Canfield and co-workers (1996; 1999) and Shen and co-workers (2001) and is replotted in Figure 2.5A.

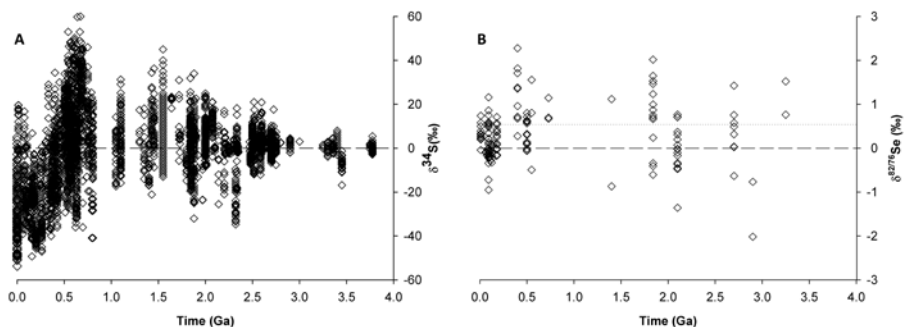


Figure 2.5 A) Sulfur isotopes through geologic time, replotted after Canfield and Raiswell (1999) and B) selenium isotopes through time, data from before 0.5 Ga from Mitchell et al. (2012); the rest of the Se data are from the present study, these are the same samples as plotted in Figure 2.4. See Mitchell et al. (2012) for detailed Se isotope methods. Note difference in δ scales between the two plots.

Sulfur isotopes show a wide range of isotope values in sulfides, from -50‰ to +50‰ that expands through time. During the Archean S isotopes were generally close to the mantle composition of 0‰, which has been attributed to low sulfate concentrations (Habicht et al., 2002b) and explained by a limited input of oxidized sulfur to the oceans due to low oxygen levels. Possible alternative sources of sulfate during the Archean were volcanic emanations that were hydrolyzed (Canfield and Raiswell, 1999) or photo-oxidized in the atmosphere (Farquhar et al., 2000), and the oxidation of primary mantle sulfide to sulfate during anoxygenic photosynthesis

(Schidlowski et al., 1989). Based on the S isotope record, non-limiting sulfate concentrations became widespread for the first time around 2.3 Ga, linked to the rise in atmospheric oxygen and independently supported by the loss of S isotope mass independent fractionation at approximately the same time (Canfield and Raiswell, 1999; Farquhar and Wing, 2003). The sulfur isotope record thus shows a clear evolution of the size of the marine sulfate reservoir through time and indicates the early evolution of microbial dissimilatory reduction.

A compilation of published and new selenium isotope data is shown for comparison in Figure 2.5B. These represent bulk isotope data for marine sedimentary rocks from a number of representative and previously well-characterized sites. Heavily weathered and hydrothermally-influenced samples have been excluded. Bulk rock samples were used due to the low Se (<100 ppm) concentrations. Selenium can occur in several different fractions in sediments including Se(0), kerogen and in sulfides (Zhu and Zheng, 2001; Zhu et al., 2004; Wen and Carignan, 2011). Despite this, recent studies of shales with high Se concentrations (>1000 ppm) show that different fractions of Se generally show similar isotopic compositions (Wen and Carignan, 2011) and our database can be used to give a first order interpretation of Se isotope evolution.

Overall, the range in $\delta^{82/76}\text{Se}$ in bulk sediments is within a relatively constant and very limited range of -3 to +3‰. The large fractionations in the S isotope record are attributed to the dissimilatory reduction of sulfate. The isotope fractionations of dissimilatory Se

reduction would also be expected to produce a (relatively) large range of isotopic compositions but this is not observed. Variations within individual geological formations are similar to the total range observed for all samples suggesting that fractionation is controlled by local rather than global processes, and that this does not significantly change through time. A similar range in $\delta^{82/76}\text{Se}$ is observed both before and after the great oxygenation event at 2.3 Ga which may reflect the insensitivity of the Se cycle to oxidative weathering. Selenium should be more resistant to oxidative weathering than sulfur, based on the thermodynamic stability of Se(0) (Figure 2.1). In addition, in areas where there are Se rich shales oxidative weathering of these sites often results in oxidation of organic Se to Se(0), which remains at the sites, and is generally not oxidized further even under fully oxic conditions (Kulp and Pratt, 2004; Zhu et al., 2004; Wen et al., 2006; Wen et al., 2007). It is also found that chemical weathering in some areas is not as important as physical weathering (Wen et al., 2006). However, chemical weathering of Se can be intensified under acidic conditions ($\text{pH}<4$) and at increased salinity (Presser and Swain, 1990). Weathering is also known to be able to produce large isotope fractionations, yielding isotope compositions as low as -14.2‰ (Wen et al., 2007; Zhu et al., 2008; Johnson, 2011). It is unknown at this time how much weathering inputs contribute to the marine biogeochemical cycle of Se, and thus to the isotope composition of marine sediments, or whether this would mainly affect local rather than global isotopic compositions.

Alternatively, the lack of isotopic variability may indicate a similar (bio)availability of Se under both oxic and anoxic atmospheric conditions, however this remains to be tested. Nonetheless, overall, the limited variability of the Se isotope record in marine sedimentary rocks is consistent with the assimilatory Se cycle. The oceanographic literature has long recognized the importance of the biological cycle of Se (Sugimura et al., 1976; Measures, 1978; Suzuki et al., 1979; Cutter and Bruland, 1984).

The Se isotope signature of seawater remains unknown. Due to the very low abundance of Se in sulfate minerals, (anhydrite has a Se/S ratio of 5.6×10^{-6} ; Nriagu, 1989), recreating the Se isotopic signature through time will be difficult at best. The lower limit of the $\delta^{82/76}\text{Se}$ in modern seawater can however be constrained by the phytoplankton value of 0.42‰ (Mitchell et al., 2012) and the range (0.04-0.42‰) determined by Rouxel et al. (2002) on seafloor Mn nodules, as both materials should have isotopic compositions close to that of modern seawater. Our data for marine sedimentary rocks show a similar range in $\delta^{82/76}\text{Se}$ and similar maximum and minimum values throughout geological history, suggesting a relatively constant Se isotopic composition for seawater since Archean times.

Similar to S, a major source of Se to Earth's surface is volcanism, which releases Se mainly in the forms of Se(0) and volatile Se species (Suzuoki, 1964). It is possible that these compounds are oxidized in the atmosphere or surface oceans as are S compounds (see above). Photo-oxidation of Se(IV) oxyanions by UV radiation has

been observed in the laboratory at a wavelength of 300 nm by Chen et al. (2005). However, photo-oxidation of Se(0) or other reduced Se species has not been studied in detail to our knowledge.

Selenium is present in seawater in several forms, including Se(0), dissolved organic Se (DOSe), and dissolved inorganic forms (DISe) including selenate (SeO_4^{2-}) and selenite (SeO_3^{2-}) (Cutter and Bruland, 1984). Organic Se is the most abundant form of dissolved Se in the surface ocean, accounting for up to 80% of total dissolved Se in marine surface waters (Wrench, 1983; Cutter, 1989; Cutter and Cutter, 1995; Baines, 2001). In addition, the uptake of organic selenium by phytoplankton has been observed, hence it may be a key pathway of Se uptake in marine surface waters and indicates efficient recycling of Se in surface oceans (Wrench and Measures, 1982; Cutter and Bruland, 1984; Cutter and Cutter, 1995; Baines, 2001). The organic Se delivered to the sediments is already in the lowest oxidation state, so any transformation to the FeSe state is not thought to induce isotope fractionation. The same is assumed for any oxidation to Se(0) that occurs because oxidation does not large induce isotope fractionations (Johnson et al., 1999).

The uptake of dissolved organic Se differentiates the cycling of Se from that of oceanic sulfur, where sulfate is the main oxidation state found throughout the water column. The biological activity that occurs in the surface ocean accounts for most of the Se delivered to the sediments, with only minor contributions from the dissimilatory cycle. The bioavailability of multiple forms of Se allows for the

uptake of Se from several different pools, thus changing the degree to which Se can be isotopically partitioned. The same is true for the end products in the Se cycle which can include Se(0), POSe, or FeSe. The Se isotopic cycle is thus more complex than the S isotopic cycle, as the latter is dominated by dissimilatory sulfate reduction and has a single input, sulfate, and a single end product, sulfide.

2.9 INTEGRATED BIOLOGICAL AND GEOLOGICAL EVOLUTION

By integrating the geochemical, biochemical and genetic information reviewed above, multiple lines of evidence emerge for the importance and antiquity of the assimilatory Se pathway and incorporation of Se into selenocysteine. The genes coding for the biosynthesis of selenocysteine show evidence for evolving before the split of the 3 domains of life, which occurred between 3.8 and 3.5 Ga (Eigen et al., 1989; Brocks et al., 2003; Sun and Caetano-Anollés, 2009). The genetic code is dated to be approximately 3.8 Ga, old enough to predate separation from the last common ancestor but not to exclude an extraterrestrial origin of the code (Eigen et al., 1989). tRNA evidence indicates that selenocysteine was around at the inception of the genetic code (Sun and Caetano-Anollés, 2009). Selenocysteine tRNA found in *C. reinhardtii* also firmly establishes a common ancestor for the tRNA found in all domains of life, suggesting, again, it evolved before the split of the 3 domains.

Nickel–iron–selenium hydrogenases only occur in sulfate reducers and methanogenic archaea, which are considered two of the oldest metabolisms on Earth suggesting that nickel–iron–selenium

hydrogenases may also be quite ancient (Kharecha et al., 2005; Canfield et al., 2006b; Baltazar et al., 2011). The coexistence of large thioredoxin reductases and small thioredoxin reductases in *C. reinhardtii* is the first reported occurrence of the two types in one organism which is living evidence that they evolved together, and the small thioredoxin reductases were lost in many organism through evolution (Novoselov et al., 2002; Novoselov and Gladyshev, 2003). Glutathione peroxidase is found in all domains of life however, the selenocysteine containing form occurs mainly in vertebrates but is also found in *C. reinhardtii* making it the only plant cell in which the selenocysteine containing glutathione peroxidase is found. There was no evidence for horizontal gene transfer for any of the selenoproteins found in *C. reinhardtii* implying that these proteins evolved at the least before the split of plants and animals, if not earlier (Novoselov et al., 2002).

Selenium is bioavailable in multiple forms including reduced organic forms, selenate, selenite, and as nano-particulate Se(0). The flexibility of uptake in the Se biochemical cycle could allow for any of the possible forms of Se to be taken up during evolution. The flexibility of Se to accept and donate electrons would facilitate early redox reactions and could explain why it is possible for nearly any form of Se to be incorporated into organic matter. Independence of Se isotope fractionation from Se concentration indicates that Se isotopes cannot provide any evidence concerning oxygenation, since as Se oxyanion concentrations increase, presumably due to increased

oxidative weathering resulting from increased free oxygen, the Se isotope fractionation will remain unchanged. Increased availability of sulfate at 2.3 Ga due to increased oxygenation, may have initiated the gradual shift from selenocysteine to cysteine in many organisms. The geochemical shift, which occurred after the split of the 3 domains of life, could account for the shift in the biochemical pathways and apparent loss of selenocysteine usage in so many phyla (Gladyshev and Kryukov, 2001; Zhang et al., 2006; Salinas et al., 2006).

Selenium isotope geochemistry appears to capture information over shorter time scales, as reflected by shorter residence times in the Se cycle compared with the S cycle, and over smaller geographic areas than the S isotope geochemistry which can capture basin scale changes over longer timescales. The antiquity of selenium as an essential micronutrient requires the availability of biologically-accessible forms in the oceans throughout geological history. Relative homogeneity in our preliminary reconstruction of secular Se isotope variability indicates that Se uptake and recycling in biomass has dominated the biogeochemical cycle of this element since the Archean.

REFERENCES

- Andreae M.O. (1979) Arsenic Speciation in Seawater and Interstitial Waters: The Influence of Biological-Chemical Interactions on the Chemistry of a Trace Element. *Limnol. Oceanog.* **24**, 440-452.
- Andreae M.O. (1990) Ocean-atmosphere interactions in the global biogeochemical sulfur cycle. *Mar. Chem.* **30**, 1-29.
- Andreae M.O., Raemdonck H. (1983) Dimethyl Sulfide in the Surface Ocean and the Marine Atmosphere: A Global View. *Science* **221**, 744-747.
- Arnér E.S.J., Holmgren A. (2000) Physiological functions of thioredoxin and thioredoxin reductase. *Eur. J. Biochem.* **267**, 6102-6109.
- Baines S.B., Fisher N.S. (2001) Interspecific differences in the bioconcentration of selenite by phytoplankton and their ecological implications. *Mar. Ecol. Prog. Ser.* **213**, 1-12.
- Baines S.B., Fisher, N.S., Doblin, M.A., Cutter, Gregory A. (2001) Uptake of dissolved organic selenides by marine phytoplankton. *Limnol. Oceanog.* **46**, 1936-1944.
- Baltazar C.S.A., Marques M.C., Soares C.M., DeLacey A.M., Pereira I.A.C., Matias P.M. (2011) Nickel–Iron–Selenium Hydrogenases – An Overview. *Eur. J. Inorg. Chem.* **2011**, 948-962.
- Berner R.A., Canfield D.E. (1989) A new model for atmospheric oxygen over Phanerozoic time. *Am J Sci* **289**, 333-361.
- Blum J.S., Bindi A.B., Buzzelli J., Stolz J.F., Oremland R.S. (1998) *Bacillus arsenicoselenatis*, sp. nov., and *Bacillus selenitireducens*, sp. nov.: two haloalkaliphiles from Mono Lake, California that respire oxyanions of selenium and arsenic. *Arch. Microbiol.* **171**, 19-30.
- Blum J.S., Stolz J.F., Oren A., Oremland R.S. (2001) *Selenihalanaerobacter shriftii* gen. nov., sp. nov., a halophilic anaerobe from Dead Sea sediments that respire selenate. *Arch. Microbiol.* **175**, 208-219.
- Böck A., Forchhammer K., Heider J., Baron C. (1991a) Selenoprotein synthesis: an expansion of the genetic code. *Trends Biochem. Sci* **16**, 463-467.
- Böck A., Forchhammer K., Heider J., Leinfelder W., Sawers G., Veprek B., Zinoni F. (1991b) Selenocysteine: the 21st amino acid. *Mol. Microbiol.* **5**, 515-520.
- Böck A., Rother M., Leibundgut M., Ban N. (2006) Selenium metabolism in prokaryotes, in: Hatfield, D.L., Berry, M.J., Gladyshev, V.N. (Eds.), *Selenium*. Springer US, pp. 9-28.
- Brocks J.J., Summons R.E., Heinrich D.H., Karl K.T. (2003) Sedimentary Hydrocarbons, Biomarkers for Early Life, *Treatise on Geochemistry*. Pergamon, Oxford, pp. 63-115.
- Broecker W.S., Peng T.H. (1982) *Tracers in the Sea*. Eldigio Press Lamont-Doherty Geological Survey, New York.
- Buat-Menard P., Chesselet R. (1979) Variable influence of the

- atmospheric flux on the trace metal chemistry of oceanic suspended matter. *Earth. Planet. Sci. Lett.* **42**, 399-411.
- Bykowski T., Ploeg J.R.v.d., Iwanicka-Nowicka R., Hryniewicz M.M. (2002) The switch from inorganic to organic sulphur assimilation in *Escherichia coli*: adenosine 5'-phosphosulphate (APS) as a signalling molecule for sulphate excess. *Mol. Microbiol.* **43**, 1347-1358.
- Canfield D.E. (2001) Biogeochemistry of Sulfur Isotopes. *Reviews in Mineralogy and Geochemistry* **43**, 607-636.
- Canfield D.E. (2004) The evolution of the Earth surface sulfur reservoir. *Am. J. Sci.* **304**, 839-861.
- Canfield D.E., Habicht K.S., Thamdrup B. (2000) The Archean sulfur cycle and the early history of atmospheric oxygen. *Science* **288**, 658-661.
- Canfield D.E., Kristensen E., Thamdrup B. (2005) The Sulfur Cycle, *Advances in Marine Biology*. Academic Press, pp. 313-381.
- Canfield D.E., Olesen C.A., Cox R.P. (2006a) Temperature and its control of isotope fractionation by a sulfate-reducing bacterium. *Geochim. Cosmochim. Acta* **70**, 548-561.
- Canfield D.E., Poulton S.W., Narbonne G.M. (2007) Late-Neoproterozoic Deep-Ocean Oxygenation and the Rise of Animal Life. *Science* **315**, 92-95.
- Canfield D.E., Raiswell R. (1999) The evolution of the sulfur cycle. *Am. J. Sci.* **299**, 697-723.
- Canfield D.E., Rosing M.T., Bjerrum C. (2006b) Early anaerobic metabolisms. *Philosophical transactions of the Royal Society of London. Series B, Biological sciences* **361**, 1819-1834; discussion 1835-1816.
- Canfield D.E., Teske A. (1996) Late Proterozoic rise in atmospheric oxygen concentration inferred from phylogenetic and sulphur-isotope studies. *Nature* **382**, 127-132.
- Chambers L. (1975) Fractionation of sulfur isotopes by continuous cultures of *Desulfovibrio desulfuricans*. *Can. J. Microbiol.* **21**, 1602-1607.
- Chen Y.-W., Zhou X.-L., Tong J., Truong Y., Belzile N. (2005) Photochemical behavior of inorganic and organic selenium compounds in various aqueous solutions. *Anal. Chim. Acta* **545**, 149-157.
- Clark S.K., Johnson T.M. (2008) Effective isotopic fractionation factors for solute removal by reactive sediments: A laboratory microcosm and slurry study. *Environ. Sci. Technol.* **42**, 7850-7855.
- Clark S.K., Johnson T.M. (2010) Selenium stable isotope investigation into selenium biogeochemical cycling in a lacustrine environment: Sweitzer Lake, Colorado. *Journal of Environmental Quality* **39**, 2200-2210.
- Copeland P. (2005) Making sense of nonsense: the evolution of selenocysteine usage in proteins. *Genome Biology* **6**, 221.

- Cutter G.A. (1982) Selenium in Reducing Waters. *Science* **217**, 829-831.
- Cutter G.A. (1989) The estuarine behaviour of selenium in San Francisco Bay. *Estuar. Coast. Shelf Sci.* **28**, 13-34.
- Cutter G.A., Bruland K.W. (1984) The marine biogeochemistry of selenium: A re-evaluation. *Limnol. Oceanogr.* **29**, 1179-1192.
- Cutter G.A., Cutter L.S. (1995) Behavior of dissolved antimony, arsenic, and selenium in the Atlantic Ocean. *Mar. Chem.* **49**, 295-306.
- DeMoll-Decker H., Macy J.M. (1993) The periplasmic nitrite reductase of *Thauera selenatis* may catalyze the reduction of selenite to elemental selenium. *Arch. Microbiol.* **160**, 241-247.
- Detmers J., Bruchert V., Habicht K.S., Kuever J. (2001) Diversity of sulfur isotope fractionations by sulfate-reducing prokaryotes. *Appl. Environ. Microbiol.* **67**, 888-894.
- Doblin M.A., Baines S.B., Cutter L.S., Cutter G.A. (2006) Sources and biogeochemical cycling of particulate selenium in the San Francisco Bay estuary. *Estuar. Coast. Shelf Sci.* **67**, 681-694.
- Dowdle P.R., Oremland R.S. (1998) Microbial oxidation of elemental selenium in soil slurries and bacterial cultures. *Environ. Sci. Technol.* **32**, 3749-3755.
- Eigen M., Lindemann B., Tietze M., Winkler-Oswatitsch R., Dress A., von Haeseler A. (1989) How old is the genetic code? Statistical geometry of tRNA provides an answer. *Science* **244**, 673-679.
- Ellis A.S., Johnson T.M., Herbel M.J., Bullen T.D. (2003) Stable isotope fractionation of selenium by natural microbial consortia. *Chem. Geol.* **195**, 119-129.
- Farquhar J. (2003) Multiple sulphur isotopic interpretations of biosynthetic pathways: implications for biological signatures in the sulphur isotope record. *Geobiology* **1**, 27-36.
- Farquhar J., Bao H.M., Thiemens M. (2000) Atmospheric influence of Earth's earliest sulfur cycle. *Science* **289**, 756-758.
- Farquhar J., Wing B.A. (2003) Multiple sulfur isotopes and the evolution of the atmosphere. *Earth. Planet. Sci. Lett.* **213**, 1-13.
- Flohé L., Brigelius-Flohé R. (2012) Selenoproteins of the Glutathione Peroxidase Family, in: Hatfield, D.L., Berry, M.J., Gladyshev, V.N. (Eds.), *Selenium*. Springer New York, pp. 167-180.
- Garrels R.M., Lerman A. (1981) Phanerozoic cycles of sedimentary carbon and sulfur. *Proceedings of the National Academy of Sciences of the United States of America* **78**, 4652-4656.
- Gladyshev V. (2006) Selenoproteins and selenoproteomes, in: Hatfield, D.L., Berry, M.J., Gladyshev, V.N. (Eds.), *Selenium*. Springer US, pp. 99-110.
- Gladyshev V.N., Hatfield D.L. (2010) Selenocysteine Biosynthesis, Selenoproteins, and Selenoproteomes, in: Atkins, J.F., Gesteland, R.F. (Eds.), *Recoding: Expansion of Decoding Rules Enriches Gene Expression*. Springer New York, pp. 3-27.

- Gladyshev V.N., Khangulov S.V., Stadtman T.C. (1996) Properties of the Selenium- and Molybdenum-Containing Nicotinic Acid Hydroxylase from *Clostridium barkeri*. *Biochemistry* **35**, 212-223.
- Gladyshev V.N., Kryukov G.V. (2001) Evolution of selenocysteine-containing proteins: Significance of identification and functional characterization of selenoproteins. *Biofactors* **14**, 87.
- Gobler C.J., Hutchins D.A., Fisher N.S., Cosper E.M., Sanudo-Wilhelmy S.A. (1997) Release and bioavailability of C, N, P, Se, and Fe following viral lysis of a marine chrysophyte. *Limnol. Oceanog.* **42**, 1492-1504.
- Habicht K.S., Canfield D.E. (1997) Sulfur isotope fractionation during bacterial sulfate reduction in organic-rich sediments. *Geochim. Cosmochim. Acta* **61**, 5351-5361.
- Habicht K.S., Gade M., Thamdrup B., Berg P., Canfield D.E. (2002a) Calibration of sulfate levels in the Archean Ocean. *Science* **298**, 2372-2374.
- Habicht K.S., Gade M., Thamdrup B., Berg P., Canfield D.E. (2002b) Calibration of Sulfate Levels in the Archean Ocean. *Science* **298**, 2372-2374.
- Habicht K.S., Salling L.L., Thamdrup B., Canfield D.E. (2005) Effect of low sulfate concentrations on lactate oxidation and isotope Fractionation during sulfate reduction by *Archaeoglobus fulgidus* strain Z. *Appl. Environ. Microbiol.* **71**, 3770-3777.
- Hagiwara Y. (2000) Selenium isotope ratios in marine sediments and algae. A reconnaissance study., MSc Thesis, University of Illinois at Urbana-Champaign.
- Harris T.K., Turner G.J. (2002) Structural Basis of Perturbed pKa Values of Catalytic Groups in Enzyme Active Sites. *IUBMB Life* **53**, 85-98.
- Harrison A.G., Thode H.G. (1958) Mechanism of the Bacterial Reduction of Sulphate from isotope fractionation studies. *Transactions of the Faraday Society* **53**, 84-92.
- Harrison P.J., Yu, P.W., Thompson, P.A., Price, N.M., Phillips, D.J. (1988) Survey of selenium requirements in marine phytoplankton. *Mar. Ecol. Prog. Ser.* **47**, 89-96.
- Hatfield D.L., Gladyshev V.N. (2002) How Selenium Has Altered Our Understanding of the Genetic Code. *Mol. Cell. Biol.* **22**, 3565-3576.
- Heider J., Bock A. (1993) Selenium Metabolism in Micro-organisms, in: Rose, A.H. (Ed.), *Advances in Microbial Physiology*. Academic Press, pp. 71-109.
- Hengeveld R. (2007) Two Approaches to the Study of the Origin of Life. *Acta Biotheoretica* **55**, 97-131.
- Hengeveld R., Fedonkin M. (2007) Bootstrapping the Energy Flow in the Beginning of Life. *Acta Biotheoretica* **55**, 181-226.
- Herbel M.J., Blum J.S., Oremland R.S., Borglin S.E. (2003) Reduction of elemental selenium to selenide: Experiments with anoxic sediments and bacteria that

- respire Se-oxyanions. *Geomicrobiol. J.* **20**, 587-602.
- Herbel M.J., Johnson T.M., Oremland R.S., Bullen T.D. (2000) Fractionation of selenium isotopes during bacterial respiratory reduction of selenium oxyanions. *Geochim. Cosmochim. Acta* **64**, 3701-3709.
- Hoek J., Reysenbach A.-L., Habicht K.S., Canfield D.E. (2006) Effect of hydrogen limitation and temperature on the fractionation of sulfur isotopes by a deep-sea hydrothermal vent sulfate-reducing bacterium. *Geochim. Cosmochim. Acta* **70**, 5831-5841.
- Holser W.T., Maynard J.B., Cruikshank K.M. (1989) Modelling the natural cycle of sulphur through Phanerozoic time, in: Brimblecombe, P., Lein, A.Y. (Eds.), *Evolution of the global biogeochemical sulphur cycle*. John Wiley & Sons Ltd, pp. 21-56.
- Huber R., Sacher M., Vollmann A., Huber H., Rose D. (2000) Respiration of Arsenate and Selenate by Hyperthermophilic Archaea. *Systematic and Applied Microbiology* **23**, 305-314.
- Johnson T.M. (2011) Stable Isotopes of Cr and Se as Tracers of Redox Processes in Earth Surface Environments Handbook of Environmental Isotope Geochemistry, in: Baskaran, M. (Ed.), *Advances in Isotope Geochemistry*. Springer Berlin Heidelberg, pp. 155-175.
- Johnson T.M., Bullen T.D. (2004) Mass-Dependent Fractionation of Selenium and Chromium Isotopes in Low-Temperature Environments. *Reviews in Mineralogy and Geochemistry* **55**, 289-317.
- Johnson T.M., Bullen T.D., Zawislanski P.T. (2000) Selenium stable isotope ratios as indicators of sources and cycling of selenium: Results from the northern reach of San Francisco Bay. *Environ. Sci. Technol.* **34**, 2075-2079.
- Johnson T.M., Herbel M.J., Bullen T.D., Zawislanski P.T. (1999) Selenium isotope ratios as indicators of selenium sources and oxyanion reduction. *Geochim. Cosmochim. Acta* **63**, 2775-2783.
- Kaplan I.R., Rittenberg S.C. (1964) Microbiological Fractionation of Sulphur Isotopes. *J. Gen. Microbiol.* **34**, 195-212.
- Kemp A.L.W., Thode H.G. (1968) The mechanism of the bacterial reduction of sulphate and of sulphite from isotope fractionation studies. *Geochim. Cosmochim. Acta* **32**, 71-91.
- Kessi J., Hanselmann K.W. (2004) Similarities between the Abiotic Reduction of Selenite with Glutathione and the Dissimilatory Reaction Mediated by *Rhodospirillum rubrum* and *Escherichia coli*. *J. Biol. Chem.* **279**, 50662-50669.
- Kharcha P., Kasting J., Siefert J. (2005) A coupled atmosphere-ecosystem model of the early Archean Earth. *Geobiology* **3**, 53-76.
- Kim H.-Y., Fomenko D.E., Yoon Y.-E., Gladyshev V.N. (2006) Catalytic Advantages Provided by Selenocysteine in Methionine-S-Sulfoxide Reductases†.

- Biochemistry* **45**, 13697-13704.
- Krouse H.R., Thode H.G. (1962) Thermodynamic properties and geochemistry of isotopic compounds of selenium. *Can. J. Chem.* **40**, 367-375.
- Kulp T.R., Pratt L.M. (2004) Speciation and weathering of selenium in upper cretaceous chalk and shale from South Dakota and Wyoming, USA. *Geochim. Cosmochim. Acta* **68**, 3687-3701.
- Li H., Zhang J., Wang T., Luo W., Zhou Q., Jiang G. (2008) Elemental selenium particles at nano-size (Nano-Se) are more toxic to Medaka (*Oryzias latipes*) as a consequence of hyper-accumulation of selenium: A comparison with sodium selenite. *Aquat. Toxicol.* **89**, 251-256.
- Luoma S.N., Johns C., Fisher N.S., Steinberg N.A., Oremland R.S., Reinfelder J.R. (1992) Determination of selenium bioavailability to a benthic bivalve from particulate and solute pathways. *Environ. Sci. Technol.* **26**, 485-491.
- Mackenzie F., Lantzy R., Paterson V. (1979) Global trace metal cycles and predictions. *Mathematical Geology* **11**, 99-142.
- Measures C., Burton, J.D. (1978) Behaviour and speciation of dissolved selenium in estuarine waters. *Nature* **273**, 293-295.
- Measures C.I., Burton J.D. (1980) The vertical distribution and oxidation states of dissolved selenium in the northeast Atlantic Ocean and their relationship to biological processes. *Earth. Planet. Sci. Lett.* **46**, 385-396.
- Mihara H., Esaki N. (2012) Selenocysteine Lyase: Mechanism, Structure, and Biological Role, in: Hatfield, D.L., Berry, M.J., Gladyshev, V.N. (Eds.), *Selenium*. Springer New York, pp. 95-105.
- Milne J.B. (1998) The Uptake and Metabolism of Inorganic Selenium Species, in: Frankenberger Jr., W.T., Engberg, R.A. (Ed.), *Environmental Chemistry of Selenium*. Marcel Dekker, New York, pp. 459-477.
- Mitchell K., Heyer A., Canfield D.E., Hoek J., Habicht K.S. (2009) Temperature effect on the sulfur isotope fractionation during sulfate reduction by two strains of the hyperthermophilic *Archaeoglobus fulgidus*. *Environ. Microbiol.* **11**, 2998-3006.
- Mitchell K., Mason P.R.D., Van Cappellen P., Johnson T.M., Gill B.C., Owens J.D., Diaz J., Ingall E.D., Reichart G.-J., Lyons T.W. (2012) Selenium as paleo-oceanographic proxy: A first assessment. *Geochim. Cosmochim. Acta* **89**, 302-317.
- Novoselov S.V., Gladyshev V.N. (2003) Non-animal origin of animal thioredoxin reductases: implications for selenocysteine evolution and evolution of protein function through carboxy-terminal extensions. *Protein science : a publication of the Protein Society* **12**, 372-378.
- Novoselov S.V., Rao M., Onoshko N.V., Zhi H., Kryukov G.V., Xiang Y., Weeks D.P., Hatfield D.L., Gladyshev V.N. (2002) Selenoproteins and selenocysteine insertion system in the model

- plant cell system,
Chlamydomonas reinhardtii.
EMBO J **21**, 3681-3693.
- Nriagu J. (1989) Global Cycling of Selenium, in: Inhat, M. (Ed.), *Occurrence and Distribution of Selenium*. CRC Press, Boca Raton, Florida, pp. 327-340.
- Obata T., Araie H., Shiraiwa Y. (2004) Bioconcentration Mechanism of Selenium by a Coccolithophorid, *Emiliania huxleyi*. *Plant and Cell Physiology* **45**, 1434-1441.
- Oldfield J.E. (2002) Selenium World Atlas. *Selenium-Tellurium Development Association*.
- Omi R., Kurokawa S., Mihara H., Hayashi H., Goto M., Miyahara I., Kurihara T., Hirotsu K., Esaki N. (2010) Reaction Mechanism and Molecular Basis for Selenium/Sulfur Discrimination of Selenocysteine Lyase. *J. Biol. Chem.* **285**, 12133-12139.
- Oremland R.S. (1994) Biogeochemical Transformations of Selenium in Anoxic Environments, in: Frankenberger Jr., W.T., Benson, S. (Ed.), *Selenium in the Environment*. Marcel Dekker, New York, pp. 389-419.
- Oremland R.S., Blum J.S., Culbertson C.W., Visscher P.T., Miller L.G., Dowdle P.R., Strohmaier F.E. (1994) Isolation, Growth, and Metabolism of an Obligately Anaerobic, Selenate-Respiring Bacterium, Strain Ses-3. *Appl. Environ. Microbiol.* **60**, 3011-3019.
- Oremland R.S., Herbel M.J., Blum J.S., Langley S., Beveridge T.J., Ajayan P.M., Sutto T., Ellis A.V., Curran S. (2004) Structural and spectral features of selenium nanospheres produced by se-respiring bacteria. *Appl. Environ. Microbiol.* **70**, 52-60.
- Oremland R.S., Hollibaugh J.T., Maest A.S., Presser T.S., Miller L.G., Culbertson C.W. (1989) Selenate Reduction to Elemental Selenium by Anaerobic-Bacteria in Sediments and Culture - Biogeochemical Significance of a Novel, Sulfate-Independent Respiration. *Appl. Environ. Microbiol.* **55**, 2333-2343.
- Pearce C.I., Coker V.S., Charnock J.M., Patrick R.A.D., Mosselmans J.F.W., Law N., Beveridge T.J., Lloyd J.R. (2008) Microbial manufacture of chalcogenide-based nanoparticles via the reduction of selenite using *Veillonella atypica*: an in situ EXAFS study. *Nanotechnology* **19**, 155603.
- Presser T.S., Swain W.C. (1990) Geochemical evidence for Se mobilization by the weathering of pyritic shale, San Joaquin Valley, California, U.S.A. *Appl. Geochem.* **5**, 703-717.
- Price N.M., Thompson P.A., Harrison P.J. (1987) Selenium: An Essential Element for Growth of the Coastal Marine Diatom *Thalassiosira pseudonana* (*Bacillariophyceae*)1,2. *Journal of Phycology* **23**, 1-9.
- Rao M., Carlson B.A., Novoselov S.V., Weeks D.P., Gladyshev V.N., Hatfield D.L. (2003) Chlamydomonas reinhardtii selenocysteine tRNA[Ser]Sec. *RNA* **9**, 923-930.
- Rees C.E. (1973) A steady-state

- model for sulphur isotope fractionation in bacterial reduction processes. *Geochim. Cosmochim. Acta* **37**, 1141-1162.
- Romero H., Zhang Y., Gladyshev V., Salinas G. (2005) Evolution of selenium utilization traits. *Genome Biology* **6**, R66.
- Rother M. (2012) Selenium Metabolism in Prokaryotes, in: Hatfield, D.L., Berry, M.J., Gladyshev, V.N. (Eds.), *Selenium*. Springer New York, pp. 457-470.
- Rouxel O., Fouquet Y., Ludden J.N. (2004) Subsurface processes at the lucky strike hydrothermal field, Mid-Atlantic ridge: evidence from sulfur, selenium, and iron isotopes. *Geochim. Cosmochim. Acta* **68**, 2295-2311.
- Rouxel O., Ludden J., Carignan J., Marin L., Fouquet Y. (2002) Natural variations of Se isotopic composition determined by hydride generation multiple collector inductively coupled plasma mass spectrometry. *Geochim. Cosmochim. Acta* **66**, 3191-3199.
- Rue E.L., Smith G.J., Cutter G.A., Bruland K.W. (1997) The response of trace element redox couples to suboxic conditions in the water column. *Deep Sea Res. I Oceanogr. Res. Pap.* **44**, 113-134.
- Ruggles E.L., Snider G.W., Hondal R.J. (2012) Chemical Basis for the Use of Selenocysteine Selenium, in: Hatfield, D.L., Berry, M.J., Gladyshev, V.N. (Eds.). Springer New York, pp. 73-83.
- Russell M.J., Hall A.J. (1997) The emergence of life from iron monosulphide bubbles at a submarine hydrothermal redox and pH front. *Journal of the Geological Society* **154**, 377-402.
- Salinas G., Romero H., Xu X.-M., Carlson B., Hatfield D., Gladyshev V. (2006) Evolution of selenocysteine decoding and the key role of selenophosphate synthetase in the pathway of selenium utilization, in: Hatfield, D.L., Berry, M.J., Gladyshev, V.N. (Eds.), *Selenium*. Springer US, pp. 39-50.
- Sarathchandra S., Watkinson J. (1981) Oxidation of elemental selenium to selenite by *Bacillus megaterium*. *Science* **211**, 600-601.
- Schidlowski M., Hayes J.M., Kaplan I.R. (1989) Evolution of The Sulphur Cycle in the Precambrian, in: Brimblecombe, P., Yu, A.L. (Eds.), *Evolution of the global biogeochemical sulphur cycle*. John Wiley & Sons, New York, pp. 3-19.
- Schlekat C.E., Dowdle P.R., Lee B.-G., Luoma S.N., Oremland R.S. (2000) Bioavailability of Particle-Associated Se to the Bivalve *Potamocorbula amurensis*. *Environ. Sci. Technol.* **34**, 4504-4510.
- Schröder T., Rienhöfer A., Andreesen J.R. (1999) Selenium-containing xanthine dehydrogenase from *Eubacterium barkeri*. *Eur. J. Biochem.* **264**, 862-871.
- Schrauzer G.N. (2000) Selenomethionine: A Review of Its Nutritional Significance, Metabolism and Toxicity. *The Journal of Nutrition* **130**, 1653-1656.
- Schroder I., Rech S., Krafft T., Macy

- J.M. (1997) Purification and Characterization of the Selenate Reductase from *Thauera selenatis*. *Journal of Biological Chemistry* **272**, 23765-23768.
- Seby F., Potin-Gautier M., Giffaut E., Borge G., Donard O.F.X. (2001) A critical review of thermodynamic data for selenium species at 25 degrees C. *Chem. Geol.* **171**, 173-194.
- Shen Y.A., Buick R., Canfield D.E. (2001) Isotopic evidence for microbial sulphate reduction in the early Archaean era. *Nature* **410**, 77-81.
- Shigeoka S., Takeda T., Hanaoka T. (1991) Characterization and immunological properties of selenium-containing glutathione peroxidase induced by selenite in *Chlamydomonas reinhardtii*. *Biochem. J.* **275**, 623-627.
- Shrift A. (1964) A Selenium Cycle in Nature? *Nature* **201**, 1304-1305.
- Stadtman T.C. (1974) Selenium Biochemistry. *Science* **183**, 915-922.
- Stadtman T.C. (1980) Selenium-Dependent Enzymes. *Annu. Rev. Biochem* **49**, 93-110.
- Stadtman T.C. (1990) Selenium Biochemistry. *Annu. Rev. Biochem* **59**, 111-127.
- Stadtman T.C. (1996) Selenocysteine. *Annu. Rev. Biochem* **65**, 83-100.
- Steinberg N.A., Oremland R.S. (1990) Dissimilatory Selenate Reduction Potentials in a Diversity of Sediment Types. *Appl. Environ. Microbiol.* **56**, 3550-3557.
- Stolz J.F., Basu P., Oremland R.S. (2002) Microbial transformation of elements: the case of arsenic and selenium. *International Microbiology* **5**, 201-207.
- Stolz J.F., Oremland R.S. (1999) Bacterial respiration of arsenic and selenium. *Fems Microbiology Reviews* **23**, 615-627.
- Sugimura Y., Suzuki Y., Miyake Y. (1976) The content of selenium and its Chemical Form in Seawater. *Journal of the Oceanographical Society of Japapn* **32**, 235-241.
- Sun F.J., Caetano-Anollés G. (2009) The evolutionary significance of the long variable arm in transfer RNA. *Complexity* **14**, 26-39.
- Suzuki Y., Miyake Y., Saruhashi K., Sugimura Y. (1979) A Cycle of Selenium in the Ocean. *Papers in Meteorology and Geophysics* **30**, 185-189.
- Suzuoki T. (1964) A geochemical study of selenium in volcanic exhalation and sulfur deposits. *Bull. Chem. Soc. Jpn.* **37**, 1200-1206.
- Taylor S.R. (1964) Abundance of chemical elements in the continental crust: a new table. *Geochim. Cosmochim. Acta* **28**, 1273-1285.
- Terry N., Zayed A.M., de Souza M.P., Tarun A.S. (2000) SELENIUM IN HIGHER PLANTS. *Annual Review of Plant Physiology and Plant Molecular Biology* **51**, 401-432.
- Thode H.G., Kleerkoper, H. and McElcheran, D.E. (1951) Sulfur Isotope Fractionation in the Bacterial Reduction of Sulfate. *Res. London* **4**, 581-522.
- Tudge A.P., Thode H.G. (1950) Thermodynamic properties of

- isotopic compounds of sulfur. *Can. J. Res.* **28**, 567-578.
- Turanov A.A., Xu X.-M., Carlson B.A., Yoo M.-H., Gladyshev V.N., Hatfield D.L. (2011) Biosynthesis of Selenocysteine, the 21st Amino Acid in the Genetic Code, and a Novel Pathway for Cysteine Biosynthesis. *Advances in Nutrition: An International Review Journal* **2**, 122-128.
- Wang C., Lovell R.T. (1997) Organic selenium sources, selenomethionine and selenoyeast, have higher bioavailability than an inorganic selenium source, sodium selenite, in diets for channel catfish (*Ictalurus punctatus*). *Aquaculture* **152**, 223-234.
- Wang G., Jiang J., Zhu X. (2008) Study on the background level of selenium in soils and its sources, Guizhou Province. *Chinese Journal of Geochemistry* **27**, 178-182.
- Wang H., Zhang J., Yu H. (2007) Elemental selenium at nano size possesses lower toxicity without compromising the fundamental effect on selenoenzymes: Comparison with selenomethionine in mice. *Free Radical Biol. Med.* **42**, 1524-1533.
- Wen H., Carignan J. (2011) Selenium isotopes trace the source and redox processes in the black shale-hosted Se-rich deposits in China. *Geochim. Cosmochim. Acta* **75**, 1411-1427.
- Wen H., Carignan J., Hu R., Fan H., Chang B., Yang G. (2007) Large selenium isotopic variations and its implication in the Yutangba Se deposit, Hubei Province, China. *Chin. Sci. Bull.* **52**, 2443-2447.
- Wen H., Carignan J., Qiu Y., Liu S. (2006) Selenium speciation in kerogen from two Chinese selenium deposits: Environmental implications. *Environ. Sci. Technol.* **40**, 1126-1132.
- Wen H., Qiu Y. (2002) Geology and geochemistry of Se-bearing formations in Central China. *International Geology Review* **44**, 164-178.
- Williams C.H., Arscott L.D., Müller S., Lennon B.W., Ludwig M.L., Wang P.-F., Veine D.M., Becker K., Schirmer R.H. (2000) Thioredoxin reductase. *Eur. J. Biochem.* **267**, 6110-6117.
- Woolfolk C.A., Whiteley H.R. (1962) Reduction of Inorganic Compounds with Molecular hydrogen by *Micrococcus lactulyticus* I.: Stoichiometry with Compounds of Arsenic, Selenium, Tellurium, Transition and Other Elements. *J. Bacteriol.* **84**, 647-658.
- Wrench J.J. (1978) Selenium metabolism in the Marine phytoplankters *Tetraselmis tetraele* and *Dunaliella minuta*. *Mar. Biol.* **49**, 231-236.
- Wrench J.J. (1983) Organic selenium in seawater: levels, origins and chemical forms. *Mar. Chem.* **12**, 237-237.
- Wrench J.J., Measures C.I. (1982) Temporal variations in dissolved selenium in a coastal ecosystem. *Nature* **299**, 431-433.
- Xu X.-M., Carlson B., Zhang Y., Mix H., Kryukov G., Glass R., Berry M., Gladyshev V., Hatfield D.

- (2007) New Developments in Selenium Biochemistry: Selenocysteine Biosynthesis in Eukaryotes and Archaea. *Biol. Trace Elem. Res.* **119**, 234-241.
- Zehr J.P., Oremland R.S. (1987) Reduction of selenate to selenide by sulfate-respiring bacteria: experiments with cell suspensions and estuarine sediments. *Appl. Environ. Microbiol.* **53**, 1365-1369.
- Zhang J.-S., Gao X.-Y., Zhang L.-D., Bao Y.-P. (2001) Biological effects of a nano red elemental selenium. *BioFactors* **15**, 27-38.
- Zhang Y., Romero H., Salinas G., Gladyshev V. (2006) Dynamic evolution of selenocysteine utilization in bacteria: a balance between selenoprotein loss and evolution of selenocysteine from redox active cysteine residues. *Genome Biology* **7**, R94.
- Zhang Y., Zahir Z.A., Frankenberger W.T., Jr. (2004) Fate of Colloidal-Particulate Elemental Selenium in Aquatic Systems. *J Environ Qual* **33**, 559-564.
- Zhou X., Wang Y., Gu Q., Li W. (2009) Effects of different dietary selenium sources (selenium nanoparticle and selenomethionine) on growth performance, muscle composition and glutathione peroxidase enzyme activity of crucian carp (*Carassius auratus gibelio*). *Aquaculture* **291**, 78-81.
- Zhu J.-M., Johnson T.M., Clark S.K., Zhu X.-K. (2008) High precision measurement of selenium isotopic composition by hydride generation Multiple Collector Inductively Coupled Plasma Mass Spectrometry with a ^{74}Se - ^{77}Se double spike. *Chinese J. Anal. Chem.* **36**, 1385-1390.
- Zhu J., Zheng B. (2001) Distribution of selenium in a mini-landscape of Yutangba, Enshi, Hubei Province, China. *Appl. Geochem.* **16**, 1333-1344.
- Zhu J., Zuo W., Liang X., Li S., Zheng B. (2004) Occurrence of native selenium in Yutangba and its environmental implications. *Appl. Geochem.* **19**, 461-467.

CHAPTER 3



**SELENIUM ISOTOPE
DISTRIBUTION IN THE OCEANS
A MASS BALANCE**

KRISTEN MITCHELL, SANNAN Z. MANSOOR, PAUL R.D. MASON,
THOMAS M. JOHNSON, PHILIPPE VAN CAPPELLEN

IN PREPARATION

THE IMAGE ON THE PREVIOUS PAGE WAS TAKEN BY THE GALILEO SPACECRAFT ON DECEMBER 7, 1992 ON ITS WAY TO EXPLORE THE JUPITER SYSTEM IN 1995-97. THIS FILE IS IN THE PUBLIC DOMAIN BECAUSE IT WAS CREATED BY NASA. NASA COPYRIGHT POLICY STATES THAT "NASA MATERIAL IS NOT PROTECTED BY COPYRIGHT UNLESS NOTED". THIS IMAGE WAS DOWNLOADED FROM WIKIMEDIA COMMONS (COMMONS.WIKIMEDIA.ORG) A DATABASE OF 13,327,537 FREELY USABLE MEDIA FILES TO WHICH ANYONE CAN CONTRIBUTE UNDER CREATIVE COMMONS LICENSE (CREATIVECOMMONS.ORG).

ABSTRACT

Selenium (Se) isotopes have proven less than straightforward as diagnostic indicators of biogeochemical processes mainly because of a generally limited range of isotopic compositions found in nature. In addition, paleo-oceanographic applications of Se isotope are hampered by the lack of independent determinations of the Se isotopic composition of seawater over time. Even for the present day no direct measure of the Se isotope composition ($\delta^{82/76}\text{Se}$) of seawater exists. The low concentrations (<1 nM or <0.08 ppb) and multiple oxidation states (Se(IV), Se(VI), Se(0) and Se(-II)) of Se in seawater present significant analytical difficulties. Modeling therefore may give us a first grasp of the Se isotopic systematics in the oceans using currently available Se isotope data. The mass balance Se isotope model developed here implies that the isotope dynamics are dominated by the very short residence times and response times of Se in the oceanic reservoirs. As a result, Se isotopes rapidly homogenize across reservoirs leading to small variations in $\delta^{82/76}\text{Se}$ between the reservoirs. The isotopic composition of bulk Se preserved in marine sediments is most sensitive to changes in the $\delta^{82/76}\text{Se}$ values of the continental inputs of Se to the ocean. The model provides an explanation for the small range in $\delta^{82/76}\text{Se}$ values observed in the marine sedimentary record.

3.1 INTRODUCTION

Selenium has recently gained much interest in the environmental sciences (Winkel et al., 2011). Selenium isotopes are used as tracers of point sources and for paleo-environmental reconstructions (Johnson et al., 1999; Johnson et al., 2000; Herbel et al., 2002; Clark, 2007; Wen et al., 2007; Johnson, 2011; Wen and Carignan, 2011; Schilling et al., 2011b; Mitchell et al., 2012). However, Se isotopes have proven to be a most challenging isotopic system for diagnostic evaluations of biogeochemical processes (Johnson et al., 1999; Johnson et al., 2000; Clark and Johnson, 2008; Clark and Johnson, 2010; Johnson, 2011), primarily because of the limited range of isotopic compositions and fractionations observed in natural settings (Clark and Johnson, 2008; Clark and Johnson, 2010; Schilling et al., 2011b; Mitchell et al., 2012). The paleo-oceanographic proxy potential of Se stable isotope signatures in sediments and sedimentary rocks spanning the Phanerozoic was recently assessed by Mitchell et al. (2012). A compilation of isotopic compositions of marine sediments and marine sedimentary rocks going back to 3.25 Ga is given in Figure 3.1. Despite the interest and effort, our understanding of Se isotope systematics remains far from a complete effort.

The isotopic composition of modern seawater has not yet been determined. This presents a major difficulty when attempting to use Se isotopes as a paleo-proxy because there is no starting point to work from.

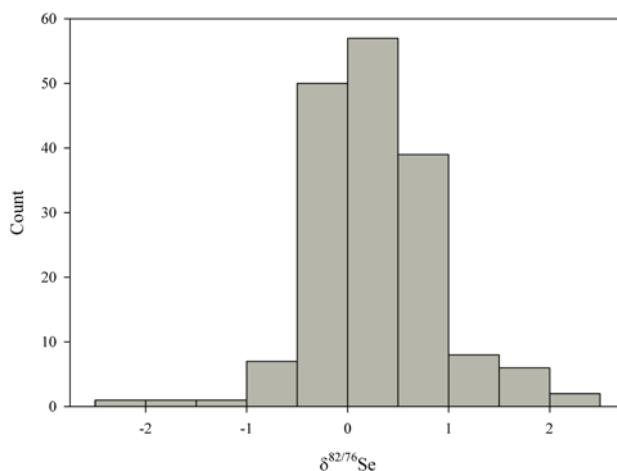


Figure 3.1 Frequency diagram of bulk Se isotope compositions (given as $\delta^{82/76}\text{Se}$ values) in 172 marine sedimentary rocks from 17 different sites ranging in age from present to 3.25 Ga. Note the relatively narrow range of isotopic compositions.

Because Se does not accumulate to a large extent in evaporite minerals (Nriagu, 1989b), it will also be difficult to trace the Se isotopic composition of seawater through geologic history, as done for seawater sulfate (Shen et al., 2001). This problem is compounded by the fact that there are multiple Se species in seawater, including organic and inorganic forms, with oxidation states ranging from +6 to -2. Measuring Se isotope compositions of different fractions in sediments is also difficult, even at relatively high bulk Se concentrations (Clark and Johnson, 2010; Wen and Carignan, 2011).

There are likely to be differences in Se isotopic composition of seawater depending on the sampling area. Selenium delivered to the oceans by rivers has already been extensively cycled upstream (Johnson et al., 2000). Isotopic compositions measured in marine nearshore environments tend to reflect the source and subsequent cycling of Se in the river (Johnson et al., 2000), thus recording local or

regional scale isotopic variations. Here, however, we focus on the global ocean isotopic dynamics as recorded by deep sea sediments. Anthropogenic Se inputs are changing the isotopic compositions of the oceans, however, this will be left to future research. Modeling gives us a first approximation of the Se isotopic distribution in the oceans using the currently available Se isotope data.

3.2 MODEL

A mass balance model, consisting of linear ordinary differential equations (ODEs), representing the 6 stable isotopes was implemented in MATLAB (MathWorks[®]) using the MATLAB “ode15s” solver, which is a variable order solver for the numerical differentiation. MATLAB was used as a modeling tool for its robustness and efficiency in solving complex numerical computations with high accuracy.

3.2.1 MODEL PARAMETERS

Figure 3.2 illustrates the oceanic biogeochemical Se cycle which was updated using the main components of the Se cycle suggested by Suzuki (1979) and Cutter and Bruland (1984). Selenium is present in seawater in several forms, including Se(0), dissolved organic Se (DOSe) which we assume to be composed of mainly of selenocysteine and selenomethionine and possibly other organic Se compounds, particulate organic Se (POSe), which we define as planktonic material containing Se, and dissolved inorganic forms (DISe) including selenate (SeO_4^{2-}) and selenite (SeO_3^{2-}).

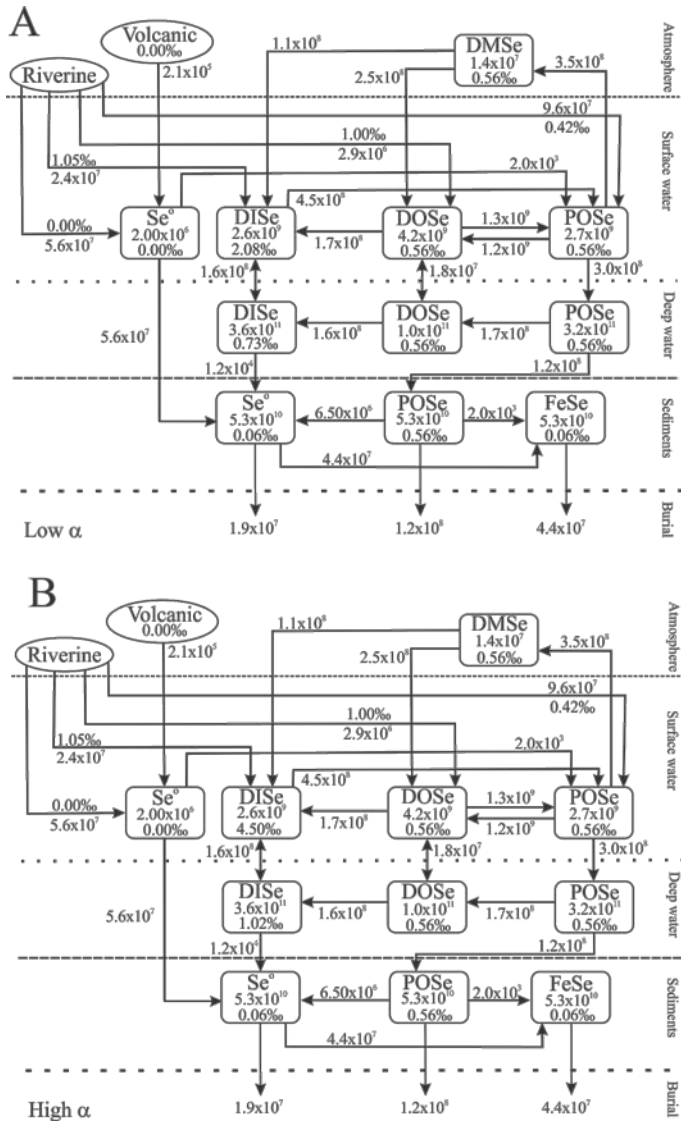


Figure 3.2 Steady state biogeochemical cycle of selenium in the oceans with $\delta^{82/76}\text{Se}$ values using A) a low α and B) a high α value for the assimilatory flux from surface DISE to surface POSe and the dissimilatory flux from deep water DISE to Se(0).

The initial parameters of the model are summarized in Table 3.1 which gives the initial bulk and isotopic values for each reservoir. Table 3.2 summarizes the initial bulk and isotopic fluxes. Mass

balance equations were set for each of the reservoirs, representing with output fluxes given by:

$$\left. \frac{d(\text{mass})}{dt} \right|_{OUT} = -k * \text{mass} \quad (1)$$

The steady state internal fluxes for each isotope were calculated based on the relative abundance of the isotopes, multiplied by the total steady state flux. The rate constant k for the internal fluxes, except for the assimilatory and dissimilatory reduction fluxes, and the diffusive fluxes, for each isotope were calculated based on the steady state flux out of the reservoir divided by the initial reservoir mass. The same concept was used to for output fluxes which include burial in sediments. The reservoirs for each isotope were initialized by using the percent abundance of each isotope multiplied by the total reservoir sizes. All reactions are first order reactions with respect to reservoir mass, except the diffusive fluxes. Diffusive fluxes for DISE and DOSE between surface and deep ocean layers were calculated based on the concentration difference between surface and deep ocean layers, and depth from midpoint of surface layer to midpoint of deep layer, as shown in Equation 2.

$$Flux = D \times \frac{(Concentration_{deep} - Concentration_{surface})}{depth} \times Ocean\ Surface\ Area \quad (2)$$

Where the value for diffusion coefficient was set at 3153.6 m²/yr (Krom et al., 1992). Depth from midpoint of surface to midpoint of deep layer was set to be 1800 m and surface area of

Table 3.1 Initial reservoir size and isotope reservoir sizes for the six isotopes, the percent abundance is shown for each isotope. These values were used to initialize the model, which was then run to steady state.

Reservoirs	Total mass (mol)	⁷⁴ Se (mol)	⁷⁶ Se (mol)	⁷⁷ Se (mol)	⁷⁸ Se (mol)	⁸⁰ Se (mol)	⁸² Se (mol)	Calculation or Explanation	References
Atmosphere, DMSe	1.4x10 ⁷	1.2x10 ⁵	1.3x10 ⁶	1.1x10 ⁶	3.3x10 ⁶	6.9x10 ⁶	1.2x10 ⁶		(Nriagu, 1989a)
Surface Ocean, total	1.3x10 ¹⁰	1.2x10 ⁹	1.2x10 ⁹	1.0x10 ⁹	3.1x10 ⁹	6.6x10 ⁹	1.2x10 ⁹		(Nriagu, 1989a)
Surface ocean, DISe	6.5x10 ⁹	5.7x10 ⁷	6.0x10 ⁸	4.9x10 ⁸	1.5x10 ⁹	3.2x10 ⁹	5.7x10 ⁸		(Cutter and Bruland, 1984)
Surface ocean, DOSe	4.1x10 ⁹	2.3x10 ⁷	2.5x10 ⁸	2.0x10 ⁸	6.3x10 ⁸	1.3x10 ⁹	2.3x10 ⁸		(Cutter and Bruland, 1984)
Surface ocean, POSe	2.7x10 ⁹	3.6x10 ⁷	3.8x10 ⁸	3.1x10 ⁸	9.8x10 ⁸	2.1x10 ⁹	3.7x10 ⁸	Estimate	
Surface ocean, Se(0)	2.0x10 ⁶	1.7x10 ⁴	1.9x10 ⁵	1.5x10 ⁵	4.7x10 ⁵	1.0x10 ⁶	1.8x10 ⁵	Estimate	
Deep ocean, total	2.0x10 ¹²	1.7x10 ¹⁰	1.8x10 ¹¹	1.5x10 ¹¹	4.7x10 ¹¹	9.8x10 ¹¹	1.5x10 ¹¹		(Nriagu, 1989a)
Deep Ocean, DISe	1.5x10 ¹²	1.3x10 ¹⁰	1.4x10 ¹¹	1.2x10 ¹¹	3.6x10 ¹¹	7.6x10 ¹¹	1.3x10 ¹¹		(Cutter and Bruland, 1984)
Deep Ocean, DOSe	1.2x10 ¹¹	1.0x10 ⁹	1.1x10 ¹⁰	8.7x10 ⁹	2.7x10 ¹⁰	5.7x10 ¹⁰	1.0x10 ¹⁰		(Cutter and Bruland, 1984)
Deep Ocean, POSe	3.2x10 ¹¹	2.8x10 ⁹	2.9x10 ¹⁰	2.4x10 ¹⁰	7.5x10 ¹⁰	1.6x10 ¹¹	2.8x10 ¹⁰	% particulate matter deep ocean x [Se] deep particulate matter	(Buat-Menard and Chesselet, 1979; Mackenzie et al., 1979)
Sediments, Total	1.6 x10 ¹¹	1.4x10 ⁹	1.5x10 ¹⁰	1.2x10 ¹⁰	3.8x10 ¹⁰	8.0x10 ¹⁰	1.4x10 ¹⁰		(Nriagu, 1989a)
Sediments, Se(0)	5.3x10 ¹⁰	4.6x10 ⁸	4.9x10 ⁹	4.0x10 ⁹	1.3x10 ¹⁰	2.6x10 ¹⁰	4.7x10 ⁹	33%, based on relative abundance oxidation states, first 10cm of sediments	(Wen and Qiu, 2002; Zhu et al., 2004)
Sediments, POSe	5.3x10 ¹⁰	4.6x10 ⁸	4.9x10 ⁹	4.0x10 ⁹	1.3x10 ¹⁰	2.6x10 ¹⁰	4.7x10 ⁹	same as above	(Wen and Qiu, 2002; Zhu et al., 2004)
Sediments, FeSe	5.3x10 ¹⁰	4.6x10 ⁸	4.9x10 ⁹	4.0x10 ⁹	1.3x10 ¹⁰	2.6x10 ¹⁰	4.7x10 ⁹	same as above	(Wen and Qiu, 2002; Zhu et al., 2004)

Table 3.2 Initial fluxes, and calculated isotope fluxes used to initialize the model. (SA=Surface area)

Fluxes	SS (mol/yr)	⁷⁴ Se (mol/yr)	⁷⁶ Se (mol/yr)	⁷⁷ Se (mol/yr)	⁷⁸ Se (mol/yr)	⁸⁰ Se (mol/yr)	⁸² Se (mol/yr)	Calculation or Explanation	References
Volcanic outgassing	2.1x10 ⁵	1.9x10 ³	2.0x10 ⁴	1.6x10 ⁴	5.1x10 ⁴	1.1x10 ⁴	1.9x10 ⁴		(Nriagu, 1989a)
Riverine input (total Particulate)									(Nriagu, 1989a)
Riverine input (POSe)	9.6x10 ⁷	8.3x10 ⁵	8.9x10 ⁶	7.3x10 ⁶	2.3x10 ⁷	4.8x10 ⁷	8.4x10 ⁶	63% of total	(Doblin et al., 2006)
Riverine input (Se(0))	5.6x10 ⁷	4.9x10 ⁵	5.2x10 ⁶	4.3x10 ⁶	1.3x10 ⁷	2.8x10 ⁷	5.0x10 ⁶	37% of total	(Doblin et al., 2006)
Riverine input (total dissolved)									(Nriagu, 1989a)
Riverine input (DISE)	2.4x10 ⁷	2.1x10 ⁵	2.2x10 ⁶	1.8x10 ⁶	5.6x10 ⁶	1.2x10 ⁷	2.1x10 ⁶	89% of total Se is inorganic	(Cutter and Cutter, 2004)
Riverine input (DOSe)	2.9x10 ⁶	2.5x10 ⁴	2.7x10 ⁵	2.2x10 ⁵	6.9x10 ⁵	1.5x10 ⁶	2.6x10 ⁵	11% of total Se is organic	(Cutter and Cutter, 2004)
Atmospheric deposition, total									(Nriagu, 1989a)
DISE from Atmosphere	1.0x10 ⁸	9.1x10 ⁵	9.7x10 ⁶	7.9x10 ⁶	2.5x10 ⁷	5.2x10 ⁷	9.2x10 ⁶	Estimate of 95% oxidation	
DOSe from Atmosphere	2.5x10 ⁸	2.1x10 ⁶	2.3x10 ⁷	1.9x10 ⁷	5.8x10 ⁷	1.2x10 ⁸	2.2x10 ⁷	Remainder of reduced Se	
Volatilization (DMSe)	3.5x10 ⁸	3.0x10 ⁶	3.2x10 ⁷	2.7x10 ⁷	8.3x10 ⁷	1.7x10 ⁸	3.1x10 ⁷	Reference	(Amouroux et al., 2001)
Surface, POSe to DOSe	1.2 x10 ⁹	1.1x10 ⁷	1.1x10 ⁸	9.2x10 ⁷	2.9x10 ⁸	6.1x10 ⁸	1.1x10 ⁸	33% total POSe(surface) yr ⁻¹	(Lee and Fisher, 1993)
Surface, POSe assimilation DISE	4.7x10 ⁸	See text for isotope flux calculation.						Estimate	(Nriagu, 1989a)
Surface, Reoxidation of DOSe	1.7x10 ⁸	1.5x10 ⁶	1.6x10 ⁷	1.3x10 ⁷	4.0x10 ⁷	8.4x10 ⁷	1.5x10 ⁷	Estimate	(Nriagu, 1989a)
Surface, POSe assimilation Se(0)	2.0x10 ³	1.7x10 ¹	1.9x10 ²	1.5x10 ²	4.7x10 ²	1.0x10 ³	1.8x10 ²	Estimate	
Surface, Uptake of DOSe to POSe	9.5x10 ⁸	1.1x10 ⁷	1.2x10 ⁸	9.9x10 ⁷	3.1x10 ⁸	6.5x10 ⁸	1.1x10 ⁸	Steady state	
POSe (surface to deep)	2.9x10 ⁸	2.6x10 ⁶	2.7x10 ⁷	2.2x10 ⁷	7.0x10 ⁷	1.5x10 ⁸	2.6x10 ⁷	13.5 ng cm ⁻² yr ⁻¹ x SA	(Buat-Menard and Chesselet, 1979; Mackenzie et al., 1979)
Upwelling to surface, total DISE	1.7x10 ⁸	1.5x10 ⁶	1.6x10 ⁷	1.3x10 ⁷	4.0x10 ⁷	8.5x10 ⁷	1.5x10 ⁷	Estimate	(Nriagu, 1989a)
Deep, dissolution POSe to DOSe	1.7x10 ⁸	1.3x10 ⁴	1.4x10 ⁵	1.2x10 ⁵	3.6x10 ⁵	7.6x10 ⁵	1.3x10 ⁵	Steady state	
Deep, oxidation of DOSe to DISE	1.7x10 ⁸	1.5x10 ⁶	1.6x10 ⁷	1.3x10 ⁷	4.1x10 ⁷	8.6x10 ⁷	1.5x10 ⁷	100% re-oxidation of DOSe _(deep)	(Cutter and Bruland, 1984)
Sedimentation, POSe	1.2x10 ⁸	1.5x10 ⁶	1.6x10 ⁷	1.3x10 ⁷	4.0x10 ⁷	8.5x10 ⁷	1.5x10 ⁷	20µmolC cm ⁻² yr ⁻¹ xSAxSe:C	(Emerson et al., 1985; Sherrard et al., 2004)
Se(0), surface to seds	5.6x10 ⁷	1.1x10 ⁶	1.1x10 ⁷	9.3x10 ⁶	2.9x10 ⁷	6.1x10 ⁷	1.1x10 ⁷	Estimate	
Dissimilatory reduction	5.0x10 ⁴	See text for isotope flux calculation.						Estimate	
Sediments, POSe to Se(0)	6.5x10 ⁶	4.4x10 ²	4.6x10 ³	3.8x10 ³	1.2x10 ⁴	2.5x10 ⁴	4.4x10 ³	Estimate	
Sediments, POSe to FeSe	2.0x10 ³	5.7x10 ⁴	6.0x10 ⁵	4.9x10 ⁵	1.5x10 ⁶	3.2x10 ⁶	5.7x10 ⁵	Estimate	
Sediments, Se(0) to FeSe	4.4x10 ⁷	1.7x10 ¹	1.9x10 ²	1.5x10 ²	4.7x10 ²	1.0x10 ³	1.8x10 ²	Estimate	
Burial, POSe	1.2x10 ⁸	1.0x10 ⁶	1.1x10 ⁷	8.8x10 ⁶	2.7x10 ⁷	5.8x10 ⁷	1.0x10 ⁷	Steady state	
Burial, FeSe	4.4x10 ⁷	3.8x10 ⁵	4.0x10 ⁶	3.3x10 ⁶	1.0x10 ⁷	2.2x10 ⁷	3.8x10 ⁶	Steady state	
Burial, Se(0)	1.9x10 ⁷	1.7x10 ⁵	1.8x10 ⁶	1.5x10 ⁶	4.6x10 ⁶	9.6x10 ⁶	1.7x10 ⁶	Steady state	

ocean was given a value of $3.61 \times 10^{14} \text{ m}^2$. Concentrations were calculated using the reservoir mass and surface ocean volume of $8 \times 10^{16} \text{ m}^3$, and a deep ocean volume of $1.3 \times 10^{18} \text{ m}^3$.

Because of the low concentration of Se in seawater, it is extensively recycled through the biological reservoirs in the surface ocean (Baines, 2001). This process is controlled by assimilatory reduction, the uptake of inorganic forms of Se (DISe) or organic forms (DOSe) to be used internally by the cell. Dissimilatory reduction is defined as the uptake of DISe which is not used to create biomass, and expelled from the cell, generally as Se(0). This process only occurs under oxygen limited conditions. The assimilatory (surface DISe to POSe) and the dissimilatory (deep DISe to Se(0) sediment) fluxes were created to include the isotope fractionation, ϵ as defined in Equation 3, where subscript A denotes the product and subscript B identifies the reactant associated with these processes and $\delta^{82/76}\text{Se}$ is the measured isotope composition.

$$\epsilon^{82/76}\text{Se} \cong \delta^{82/76}\text{Se}_A - \delta^{82/76}\text{Se}_B \quad (3)$$

$$\epsilon^{82/76} = (\alpha_{A-B} - 1) \quad (4)$$

The fractionation ϵ used for assimilatory and dissimilatory reduction were taken from Johnson and Bullen (2004): assimilatory reduction was assigned a low value $\epsilon^{82/76}$ of -1.5% and a high value of -3.9‰ and dissimilatory reduction was assigned a low value of -1.7% and a high value of -13.7‰. The high and low values of the fractionation factors were considered separately in the model to establish a range of possible isotopic values that could occur in nature.

The mass bias factor (β), which represents the difference in the reaction of each isotope based on its mass, was calculated using Equation 5 where M is the atomic mass of the isotope and can be used to determine the values of other mass ratios based on measured $\delta^{82/76}\text{Se}$ values (Albarede and Beard, 2004; Clark and Johnson, 2008).

$$\beta = \frac{\ln\left(\frac{\delta^{82/76}\text{Se}}{1000} + 1\right)}{\ln\left(\frac{{}^{82}\text{M}}{{}^{76}\text{M}}\right)} \quad (5)$$

The fractionation factor (α) is defined by Equation 6, and were calculated from the ε values above using Equation 4.

$$\alpha_{(A-B)} = \frac{\left(\frac{{}^{82}\text{Se}}{{}^{76}\text{Se}}\right)_A}{\left(\frac{{}^{82}\text{Se}}{{}^{76}\text{Se}}\right)_B} \quad (6)$$

The α values were converted from $^{82/76}\text{Se}$ ratios into ratios for each isotope relative to ^{76}Se using the mass bias factor (β ; Equation 7) and the mass fraction exponential (Albarede and Beard, 2004), where r_i is the ratio of the sample and R_i is the mass ratio of the standard:

$$r_i = R_i \left(\frac{M_{82}}{M_{76}}\right)^\beta \quad (7)$$

Once the fractionation factor α was calculated for each isotope, the values were then used to calculate the rate constant k_{76} , for the ^{76}Se isotope, using Equation 8, where k_T is the rate constant for the total flux and M_T is the total mass of the reservoir.

$$k_{76} = \frac{(k_T M_T)^{initial}}{[\alpha_{74} M_{74} + \alpha_{76} M_{76} + \alpha_{77} M_{77} + \alpha_{78} M_{78} + \alpha_{80} M_{80} + \alpha_{82} M_{82}]^{initial}} \quad (8)$$

The k_{76} value along with α values were then used to calculate the k values for each of the other isotopes. For example, the first order rate constant for ^{74}Se :

$$k_{74} = \alpha_{74} k_{76} \quad (9)$$

The k values were used to calculate assimilatory and dissimilatory fluxes for each respective isotope.

Each of the riverine and volcanic fluxes was assigned a $\delta^{82/76}\text{Se}$ value based on available literature values. The $\delta^{82/76}\text{Se}$ value of 1.05‰ was used for the riverine input of dissolved inorganic Se (DISe) in the model, based on average riverine values from the San Joaquin River and the Sacramento River in California (Johnson et al., 2000). Particulate organic Se (POSe) that is delivered by the rivers has been assigned a $\delta^{82/76}\text{Se}$ value of 0.42‰ based on the planktonic sample measured by Mitchell et al. (2012). Particulate inorganic Se (PISe), which we define as Se sorbed to clay materials is given the $\delta^{82/76}\text{Se}$ value of -0.42‰ based on marine clays measured by Rouxel et al. (2002), however this value is not explicitly incorporated into the model but is used to constrain other $\delta^{82/76}\text{Se}$ input values. Dissolved organic Se is assigned a $\delta^{82/76}\text{Se}$ value of 1.00‰ based on $\delta^{82/76}\text{Se}$ values of POSe, DISe and PISE. Riverine Se(0) input is assumed to have a $\delta^{82/76}\text{Se}$ value of 0‰. Volcanic input of Se(0) is also assumed to have a $\delta^{82/76}\text{Se}$ value of 0‰, assuming a mantle value of 0‰. These $\delta^{82/76}\text{Se}$ values for each input were used to calculate the input flux

value for each individual isotope to be used in the model. The $\delta^{82/76}\text{Se}$ values for the riverine and volcanic inputs were converted to fluxes of the six individual isotopes using the mass bias factor (Equation 5). First the δ values for each isotope relative to mass 76 was calculated from the literature $\delta^{82/76}\text{Se}$ value (i.e. $\delta^{80/76}\text{Se}$, $\delta^{78/76}\text{Se}$, $\delta^{77/76}\text{Se}$, $\delta^{74/76}\text{Se}$) using the mass fraction equation (Equation 7), then the ratios were multiplied to get the mass of each of the six isotopes. Six functions for each of the respective selenium isotopes, Se (74, 76, 77, 78, 80 and 82), were written with mass balance ODEs for each reservoir. The model is constructed so that the six isotopic computations occur separately for each isotope and therefore six separate models were computed simultaneously, each one corresponding to its respective Se isotope.

3.2.2 SENSITIVITY ANALYSIS AND RESPONSE TIMES

The factorial design method outlined by Kim et al. (2003) was used to test the sensitivity of the model to the $\delta^{82/76}\text{Se}$ input values. Sensitivity analysis was carried out on the $\delta^{82/76}\text{Se}$ values for the riverine and volcanic inputs described in section 3.2.1. The $\delta^{82/76}\text{Se}$ values for each of the five inputs were independently varied while the other input values remained unchanged. The magnitude of variation for each input was set to half the input value, the original input value, one and half times the input value, and twice the input value. The output after each variation in the input was the final $\delta^{82/76}\text{Se}$ value for each reservoir at the end of the steady state model simulation. The four final $\delta^{82/76}\text{Se}$ values for each reservoir were plotted against the

magnitude of the input change, and the slope of this graph was calculated and tabulated in a bar graph (Figure 3.3). The per unit changes in the final $\delta^{82/76}\text{Se}$ value for each reservoir represents the sensitivity of the final $\delta^{82/76}\text{Se}$ value to the unit change of the input $\delta^{82/76}\text{Se}$ value.

Response times were calculated for the fluxes to which the model was most sensitive, these were the riverine fluxes. The Se(0) riverine was excluded because it only affects three of the eleven reservoirs. The response time was calculated for the double the initial $\delta^{82/76}\text{Se}$ values.

3.3 RESULTS AND DISCUSSION

The initial model was run to steady state using high and low α values as described above to determine the isotopic compositions of the reservoirs; the results are shown in Figure 3.2. High and low α values produce largely the same $\delta^{82/76}\text{Se}$ values for each reservoir in the steady state model. The most notable exception is in the DISE reservoirs, where there is $\sim 2\%$ difference from the low α value to the high α value in the surface reservoir and a ~ 0.3 difference in the deep reservoir. The positive $\delta^{82/76}\text{Se}$ values found in the surface DISE reservoir (2.08-4.50‰) supports the suggestion by Mitchell et al. (2012) that the surface ocean may be slightly positive.

3.3.1 SENSITIVITY ANALYSIS AND RESPONSE TIME

The sensitivity analysis results are reported in Figure 3.3 for each input, with highest bars corresponding to the most sensitive selenium reservoir to unit input variation. The magnitude of the per

unit change in δ values is largest (1.0) when the riverine Se(0) input is changed (Figure 3.3). However, this change only significantly affects three of the reservoirs. Riverine POSe demonstrates the second highest per unit change (0.8), with eight reservoirs responding at approximately the same magnitude with two additional reservoirs affected to a lesser (0.08) degree. The only reservoir not influenced by the change in δ in the riverine POSe input is the Se(0) in the surface waters. Riverine DISe affects the same reservoirs but to a lesser degree overall (~ 0.2). Variation in riverine DOSe input show very small magnitudes of per unit change (~ 0.02), however it does affect ten of the eleven reservoirs similar to the results of the other riverine inputs. The least amount of change in the reservoirs is seen with the change in the input δ value of the volcanic input (< 0.00), and affects only three reservoirs, similar to the changes observed in Se(0) riverine input. Changes to the input $\delta^{82/76}\text{Se}$ values in riverine DOSe have the longest response times, with all reservoirs having response times over 10,000 years and up to nearly 20,000 years (Figure 3.4). Riverine DISe and POSe have response times that are much shorter than riverine DOSe. Changes to $\delta^{82/76}\text{Se}$ of riverine DISe have response times on the order of 10s of years to 1000s of years.

Response times to $\delta^{82/76}\text{Se}$ POSe changes are nearly instantaneous, with DMSe and the surface reservoir of POSe responding within one year and DOSe within 2 years; DISe responds within 8 years. The deep reservoirs respond on the order of hundreds of years, except POSe, which responds in ~ 60 years.

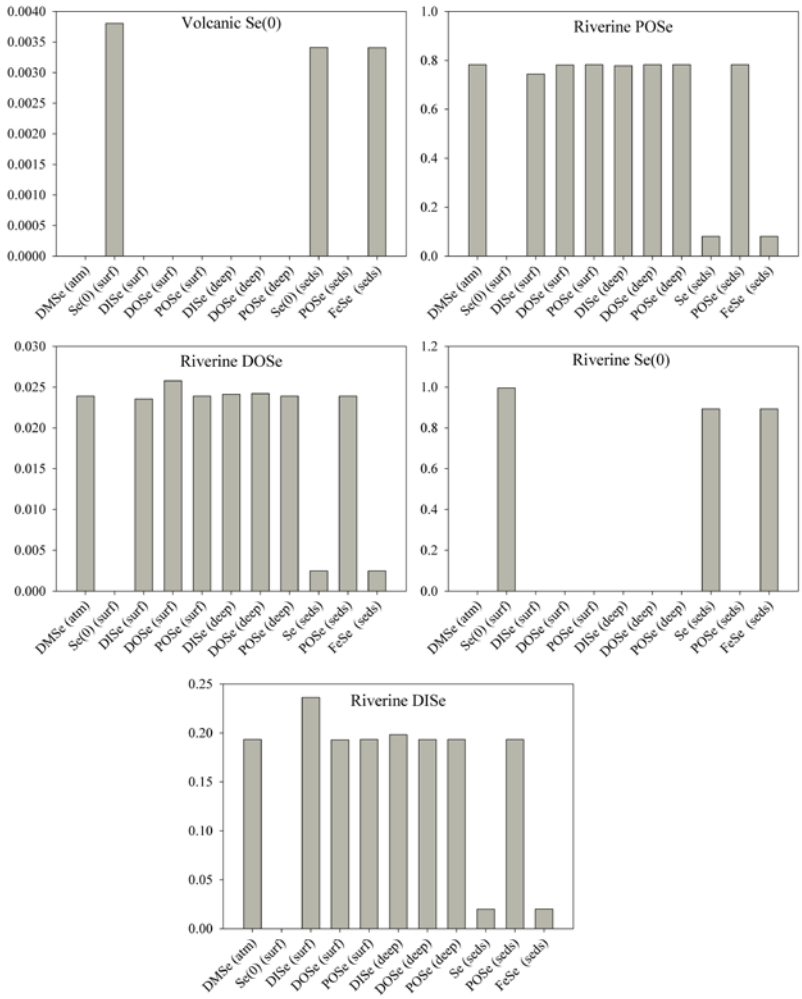


Figure 3.3 Sensitivity analysis of selenium input $\delta^{82/76}\text{Se}$ values, bars represent per unit change of final outputs relative to the input values.

The sedimentary reservoirs in these two cases respond on the order of 1000s of years which is similar to the other cases but with the exception of the POSe reservoir which responds in just over 200 years.

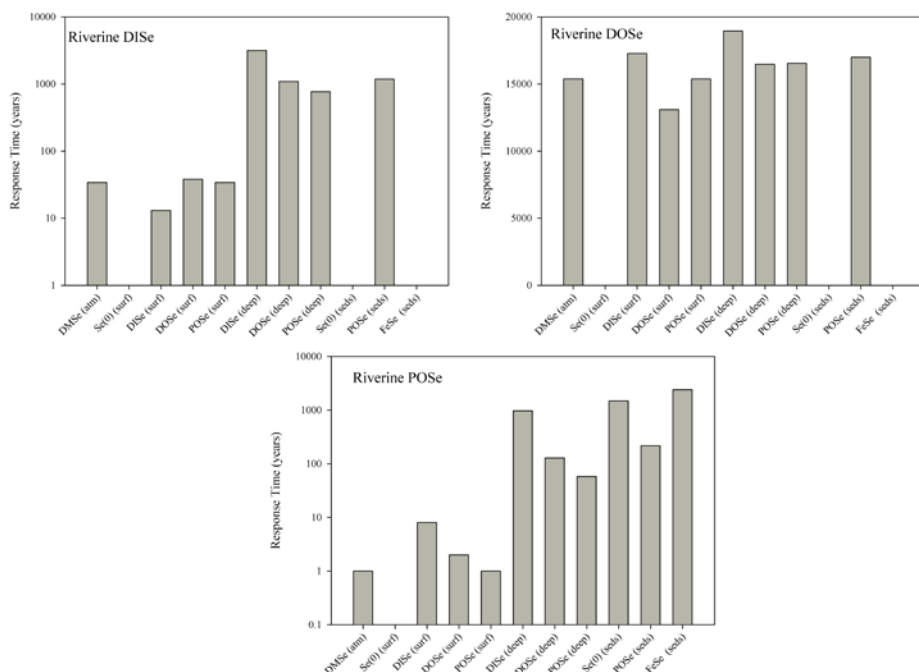


Figure 3.4 Response times after individually increasing input $\delta^{82/76}\text{Se}$ values of riverine DISe, DOSe and POSe by 2. Other fluxes, volcanic Se(0) and riverine Se(0), were not tested due to the low sensitivity of the model to changes in these fluxes. Zero response time indicates that there is no change in the reservoir. Note that response times for riverine DOSe are on a linear scale, the others on a log scale.

3.3.2 MODEL SCENARIOS

The model has such short residence times and response times that any perturbation to the system is rapidly recorded by all reservoirs (Table 3.3 and Figure 3.4). Therefore, model scenarios were implemented instantaneously on the steady state model to determine the magnitude of the response due to a given perturbation. Model scenarios include decreasing assimilatory fluxes, decreasing the fluxes of oxidation reactions to zero in the deep-ocean and sediments, and increasing dissimilatory reduction. These changes are also combined

as outlined below. In scenario 1, the assimilatory reduction flux from DISE to POSe in the surface waters is decreased from the steady state flux by two orders of magnitude. Scenario 2 simulates anoxic bottom water by decreasing the flux from DOSe to DISE in the deep water to zero and the flux from POSe to Se(0) in the sediments. For scenario 3 the dissimilatory reduction flux from DISE in the deep water to Se(0) in the sediments increased by two orders of magnitude.

Table 3.3 Residence times for the eleven reservoirs.

RESERVOIRS	RESIDENCE TIME (YEARS)
DMSe (atm)	0.040
Se(0) (surf)	0.035
DISE (surf)	5.7
DOSe (surf)	2.8
POSe (surf)	1.4
DISE (deep)	2326
DOSe (deep)	605
POSe (deep)	1076
Se(0) (seds)	844
POSe (seds)	434
FeSe (seds)	1218

Scenario 4 combines scenarios 1 to 3, with oxidation in the sediments and deep water reduced to zero, assimilation is decreased and dissimilatory reduction is increased as described above. In the last scenario, scenario 5, the assimilation flux is returned to the steady state value while oxidation in the sediments and deep water are attenuated to zero and the dissimilatory flux is increased by two orders of magnitude, as in scenario 3. Each of the model scenarios produces only a relatively small amount of change to the $\delta^{82/76}\text{Se}$ values for each reservoir (Table 3.4 and Table 3.5). Changes in the model produced more dramatic results in the high α cases for all scenarios (Table 3.4 and Table 3.5). Scenario 1 produces relatively large

changes in three reservoirs, $\text{DISE}_{\text{deep}}$, $\text{Se}(0)_{\text{sed}}$, and FeSe_{sed} in both the high and low α cases. $\text{DISE}_{\text{deep}}$ produces the largest change in the high α case ($\Delta\delta^{82/76}\text{Se}=3.2\text{‰}$), this appears to be due to a reversal of the diffusive flux between $\text{DISE}_{\text{surf}}$ and $\text{DISE}_{\text{deep}}$. However, the change in $\delta^{82/76}\text{Se}$ in the high α case is larger for all affected reservoirs (Table 3.5). The remaining reservoirs show only a very small amount of change ($\Delta\delta^{82/76}\text{Se} \approx -0.02\text{‰}$). The per mil (‰) change for scenario 2 is nearly identical for the high and low α cases, and the largest changes are seen in the same reservoirs as in scenario 1 ($\text{DISE}_{\text{deep}}$, $\text{Se}(0)_{\text{sed}}$, and FeSe_{sed}). The changes in $\delta^{82/76}\text{Se}$ values in the $\text{DISE}_{\text{deep}}$ reservoir are slightly larger for the high α case ($\Delta\delta^{82/76}\text{Se}=3.5\text{‰}$) and also for the low α case ($\Delta\delta^{82/76}\text{Se}=1.4\text{‰}$), than in scenario.

The change in $\delta^{82/76}\text{Se}$ values for $\text{Se}(0)_{\text{sed}}$, and FeSe_{sed} are also larger than in scenario 1 but still relatively small ($\sim 0.06\text{‰}$). Scenario 3 shows the most change in the sedimentary reservoirs, $\text{Se}(0)$ and FeSe , which become more negative, but POSe becomes more positive (Table 3.5). In the high and low α case of scenario 3 the $\delta^{82/76}\text{Se}$ remains unchanged in the individual sedimentary reservoirs. Scenario 4 produced the most change within the high α case for the sedimentary reservoirs and in $\text{DISE}_{\text{deep}}$.

Table 3.4 Steady state and scenario $\delta^{82/76}\text{Se}$ values.

RESERVOIRS	STEADY STATE		SCENARIO 1		SCENARIO 2		SCENARIO 3		SCENARIO 4		SCENARIO 5	
	High α	Low α	High α	Low α	High α	Low α	High α	Low α	High α	Low α	High α	Low α
	$\delta^{82/76}\text{Se}$ (‰)											
DMSe (atm)	0.5569	0.5558	0.5668	0.5556	0.5557	0.5557	0.6806	0.5699	1.2260	0.5658	0.5632	0.5558
Se(0) (surf)	0.0000	0.0000	0.0000	0.0000	0.0000	0.0000	0.0000	0.0000	0.0000	0.0000	0.0000	0.0000
DISE (surf)	4.4949	2.0828	4.5070	2.0826	4.5048	2.0939	4.6467	2.1004	5.4120	2.1114	4.5146	2.0941
DOSe (surf)	0.5578	0.5567	0.5677	0.5565	0.5565	0.5565	0.6813	0.5708	1.2256	0.5666	0.5640	0.5566
POSe (surf)	0.5569	0.5558	0.5668	0.5556	0.5557	0.5557	0.6806	0.5699	1.2260	0.5658	0.5632	0.5558
DISE (deep)	1.0159	0.7338	4.2295	1.9750	4.5057	2.0940	1.2330	0.7592	5.5044	2.1227	4.6069	2.1055
DOSe (deep)	0.5571	0.5559	0.5669	0.5557	0.5559	0.5558	0.6807	0.5701	1.2259	0.5659	0.5633	0.5559
POSe (deep)	0.5569	0.5558	0.5668	0.5556	0.5557	0.5557	0.6806	0.5699	1.2260	0.5658	0.5632	0.5558
Se(0) (seds)	0.0551	0.0572	0.0361	0.0578	-0.0002	0.0000	-0.1580	0.0403	-1.0965	0.0558	-0.0154	0.0007
POSe (seds)	0.5569	0.5558	0.5668	0.5556	0.5557	0.5557	0.6806	0.5699	1.2260	0.5658	0.5632	0.5558
FeSe (seds)	0.0551	0.0572	0.0361	0.0578	-0.0001	0.0000	-0.1579	0.0404	-1.0964	0.0559	-0.0154	0.0007

Table 3.5 Change in $\delta^{82/76}\text{Se}$ values from the steady state for high and low α cases for each scenario.

RESERVOIRS	SCENARIO 1		SCENARIO 2		SCENARIO 3		SCENARIO 4		SCENARIO 5	
	High α	Low α	High α	Low α	High α	Low α	High α	Low α	High α	Low α
$\Delta\delta^{82/76}\text{Se}$ (‰)										
DMSe (atm)	0.0099	-0.0002	-0.0012	-0.0001	0.1237	0.0141	0.6691	0.0100	0.0063	0.0000
Se(0) (surf)	0.0000	0.0000	0.0000	0.0000	0.0000	0.0000	0.0000	0.0000	0.0000	0.0000
DISE (surf)	0.0121	-0.0002	0.0098	0.0111	0.1518	0.0175	0.9171	0.0285	0.0197	0.0113
DOSe (surf)	0.0099	-0.0002	-0.0013	-0.0002	0.1235	0.0141	0.6678	0.0100	0.0062	-0.0001
POSe (surf)	0.0099	-0.0002	-0.0012	-0.0001	0.1237	0.0141	0.6691	0.0100	0.0063	0.0000
DISE (deep)	3.2137	1.2412	3.4898	1.3602	0.2171	0.0254	4.4885	1.3889	3.5910	1.3717
DOSe (deep)	0.0098	-0.0002	-0.0012	-0.0001	0.1237	0.0141	0.6689	0.0100	0.0063	0.0000
POSe (deep)	0.0099	-0.0002	-0.0012	-0.0001	0.1237	0.0141	0.6691	0.0100	0.0063	0.0000
Se(0) (seds)	-0.0191	0.0006	-0.0553	-0.0572	-0.2131	-0.0169	-1.1516	-0.0014	-0.0705	-0.0565
POSe (seds)	0.0099	-0.0002	-0.0012	-0.0001	0.1237	0.0141	0.6691	0.0100	0.0063	0.0000
FeSe (seds)	-0.0191	0.0006	-0.0553	-0.0572	-0.2131	-0.0169	-1.1515	-0.0014	-0.0705	-0.0565

DISe_{deep} shows the most change in any reservoir for any scenario with a 4.5‰ increase in the $\delta^{82/76}\text{Se}$ value, however this is due largely to increased mixing from the DISe_{surf} reservoir; Se(0)_{sed}, and FeSe_{sed} are 1.2‰ lighter and POSe_{sed} is 0.7‰ heavier (Table 3.5).

Scenario 5 is similar to scenario 1 and 2 in that the most significantly affected reservoirs are DISe_{deep}, Se(0)_{sed}, and FeSe_{sed}, the changes in this scenario are even larger (3.6‰) for DISe_{deep} and (0.07‰) for Se(0)_{sed}, and FeSe_{sed} in the high α case. The bulk sediment $\delta^{82/76}\text{Se}$ value for all cases remains the same as the input value.

The responses to the imposed perturbations are relatively small (Table 3.4 and Table 3.5) and are on the order of $\delta^{82/76}\text{Se}$ values observed in marine sediments and marine sedimentary rocks, though the most positive values (5.5‰) in the high α cases in the water column are higher than what has been observed in marine sediments (max 2.3‰). The low α cases produce positive $\delta^{82/76}\text{Se}$ values of 2.1‰ in the water column which are closer to what is observed in the sedimentary record but do not produce any negative $\delta^{82/76}\text{Se}$ values. However, these positive surface water values do not appear to be reflected in the sediments in the model, other than slight increases seen in the POSesed reservoir (max=1.22‰), which is within the range of measured sedimentary $\delta^{82/76}\text{Se}$ values (Figure 3.1). The lowest $\delta^{82/76}\text{Se}$ value found in the model scenarios is -1.10‰, found in scenario 4, for the Se(0) and FeSe sedimentary reservoirs, this is similar to the lowest $\delta^{82/76}\text{Se}$ value observed in marine sediments is -

2.0‰. However, this would only be found in a bulk sediment if the relative abundance of Se(0) and FeSe in the sediments were greater than that of POSe in the sediments.

Changes in the $\delta^{82/76}\text{Se}$ in the sediments would not be detectable using current analytical techniques. The different Se reservoirs would have to be separated to be able to see the $\delta^{82/76}\text{Se}$ changes. The highest $\delta^{82/76}\text{Se}$ value for the sediments is found in the POSe reservoir in scenario 4 (1.2‰), however, in this same case the most negative values are also found for Se(0) (-1.10‰) and FeSe (-1.10‰) in the sediments. If the three sedimentary species of Se were separated, scenario 4 would reveal rather different $\delta^{82/76}\text{Se}$ values between the Se(0) and FeSe compared with the POSe $\delta^{82/76}\text{Se}$ values. However, at the low Se concentrations found in marine sedimentary rocks and sediments, this process is currently very difficult and has not yet been successful to date for these samples.

The effects of changing the $\delta^{82/76}\text{Se}$ values of the inputs are still relatively small with unit input variation, less than ~ 1 for all inputs tested in the sensitivity analysis. Therefore, to create significant changes in the $\delta^{82/76}\text{Se}$ values, especially of the sediment, in the model, dramatic changes in the inputs are necessary, either by changing multiple inputs or changing one dramatically. The most sensitive input is the riverine POSe input, thus changing the $\delta^{82/76}\text{Se}$ value to a reasonably negative value (-4‰) will create a bulk sediment value similar to what is found in marine sediments (-2.0‰); the lowest marine sediment $\delta^{82/76}\text{Se}$ value reported is -2.0‰ (Figure 3.1). The other possibility is to change multiple inputs, which may be more

realistic due to the rapid mixing of Se across reservoirs. To obtain a negative $\delta^{82/76}\text{Se}$ in the sediment, values for $\delta^{82/76}\text{Se}$ riverine inputs could be as follows: POSe=-2.5‰; DOSe=-2.0‰; Se(0)=0.00‰ and DISe=-2.0‰. These input values would give a bulk sediment $\delta^{82/76}\text{Se}$ value of -1.65‰, again similar to the lowest observed shale value. This is of course just one of many possible combinations.

The only inputs which are likely to vary enough in $\delta^{82/76}\text{Se}$ composition in nature are weathering products which can yield isotope compositions as low as -13‰ and as high as 5‰ (Wen et al., 2007; Zhu et al., 2008; Johnson, 2011). In shale with high Se contents, oxidative weathering of these sites often results in oxidation of reduced organic Se to Se oxyanions which are then reduced back to Se(0), which remains at the sites and is generally not oxidized further even under fully oxic modern conditions (Kulp and Pratt, 2004; Zhu et al., 2004; Wen et al., 2006; Wen et al., 2007). However, chemical weathering of Se can be intensified under acidic conditions (pH<4) and at increased salinity (Presser and Swain, 1990). Most of input effects would only be observed locally however.

3.4 CONCLUSIONS

The model reflects both mixing processes and processes of Se isotope fractionation. The very short residence time of Se in most reservoirs appears to allow for rapid homogenization of the isotopes, thus the $\delta^{82/76}\text{Se}$ values do not change dramatically with flux perturbations in the system. The model is most sensitive to changes in $\delta^{82/76}\text{Se}$ inputs. Therefore, it seems that most of the isotopic

differences seen in the rock record are due to local effects, probably due to changing input $\delta^{82/76}\text{Se}$ values, or the proportion of each of the inputs. The bulk sediment reservoir $\delta^{82/76}\text{Se}$ is controlled largely by the POSe $\delta^{82/76}\text{Se}$ value in the sediments, and even when there are large differences in the individual reservoirs the bulk value remains unchanged due to the opposite effects of the POSe reservoir and the Se(0) and FeSe reservoirs.

REFERENCES

- Albarede F., Beard B. (2004) Analytical Methods for Non-Traditional Isotopes. *Reviews in Mineralogy and Geochemistry* **55**, 113-152.
- Amouroux D., Liss P.S., Tessier E., Hamren-Larsson M., Donard O.F.X. (2001) Role of oceans as biogenic sources of selenium. *Earth. Planet. Sci. Lett.* **189**, 277-283.
- Baines S.B., Fisher, N.S., Doblin, M.A., Cutter, Gregory A. (2001) Uptake of dissolved organic selenides by marine phytoplankton. *Limnol. Oceanog.* **46**, 1936-1944.
- Buat-Menard P., Chesselet R. (1979) Variable influence of the atmospheric flux on the trace metal chemistry of oceanic suspended matter. *Earth. Planet. Sci. Lett.* **42**, 399-411.
- Clark S.K. (2007) Selenium stable isotope ratios in wetlands: Insights into biogeochemical cycling and how a diffusive barrier affects the measured fractionation factor. PhD Thesis, University of Illinois at Urbana-Champaign.
- Clark S.K., Johnson T.M. (2008) Effective isotopic fractionation factors for solute removal by reactive sediments: A laboratory microcosm and slurry study. *Environ. Sci. Technol.* **42**, 7850-7855.
- Clark S.K., Johnson T.M. (2010) Selenium stable isotope investigation into selenium biogeochemical cycling in a lacustrine environment: Sweitzer Lake, Colorado. *Journal of Environmental Quality* **39**, 2200-2210.
- Cutter G.A., Bruland K.W. (1984) The marine biogeochemistry of selenium: A re-evaluation. *Limnol. Oceanog.* **29**, 1179-1192.
- Cutter G.A., Cutter L.S. (2004) Selenium biogeochemistry in the San Francisco Bay estuary: changes in water column behavior. *Estuar. Coast. Shelf Sci.* **61**, 463-476.
- Doblin M.A., Baines S.B., Cutter L.S., Cutter G.A. (2006) Sources and biogeochemical cycling of particulate selenium in the San Francisco Bay estuary. *Estuar. Coast. Shelf Sci.* **67**, 681-694.
- Emerson S., Fischer K., Reimers C., Heggie D. (1985) Organic carbon dynamics and preservation in deep-sea sediments. *Deep Sea Research Part A. Oceanographic Research Papers* **32**, 1-21.
- Herbel M.J., Johnson T.M., Tanji K.K., Gao S.D., Bullen T.D. (2002) Selenium stable isotope ratios in California agricultural drainage water management systems. *J. Environ. Qual.* **31**, 1146-1156.
- Johnson T.M. (2011) Stable Isotopes of Cr and Se as Tracers of Redox Processes in Earth Surface Environments Handbook of Environmental Isotope Geochemistry, in: Baskaran, M. (Ed.), *Advances in Isotope Geochemistry*. Springer Berlin Heidelberg, pp. 155-175.
- Johnson T.M., Bullen T.D. (2004)

- Mass-Dependent Fractionation of Selenium and Chromium Isotopes in Low-Temperature Environments. *Reviews in Mineralogy and Geochemistry* **55**, 289-317.
- Johnson T.M., Bullen T.D., Zawislanski P.T. (2000) Selenium stable isotope ratios as indicators of sources and cycling of selenium: Results from the northern reach of San Francisco Bay. *Environ. Sci. Technol.* **34**, 2075-2079.
- Johnson T.M., Herbel M.J., Bullen T.D., Zawislanski P.T. (1999) Selenium isotope ratios as indicators of selenium sources and oxyanion reduction. *Geochim. Cosmochim. Acta* **63**, 2775-2783.
- Kim I.S., Son K.J., Yang Y.S., Yaragada P.K.D.V. (2003) Sensitivity analysis for process parameters in GMA welding processes using a factorial design method. *International Journal of Machine Tools and Manufacture* **43**, 763-769.
- Krom M.D., Brenner S., Kress N., Neori A., Gordon L.I. (1992) Nutrient dynamics and new production in a warm-core eddy from the Eastern Mediterranean Sea. *Deep Sea Research Part A. Oceanographic Research Papers* **39**, 467-480.
- Kulp T.R., Pratt L.M. (2004) Speciation and weathering of selenium in upper cretaceous chalk and shale from South Dakota and Wyoming, USA. *Geochim. Cosmochim. Acta* **68**, 3687-3701.
- Lee B.-G., Fisher N., S. (1993) Release rates of trace elements and protein from decomposing planktonic debris. 1. Phytoplankton debris. *J. Mar. Res.* **51**, 391-421.
- Mackenzie F., Lantzy R., Paterson V. (1979) Global trace metal cycles and predictions. *Mathematical Geology* **11**, 99-142.
- Mitchell K., Mason P.R.D., Van Cappellen P., Johnson T.M., Gill B.C., Owens J.D., Diaz J., Ingall E.D., Reichart G.-J., Lyons T.W. (2012) Selenium as paleo-oceanographic proxy: A first assessment. *Geochim. Cosmochim. Acta* **89**, 302-317.
- Nriagu J. (1989a) Global Cycling of Selenium, in: Inhat, M. (Ed.), *Occurrence and Distribution of Selenium*. CRC Press, Boca Raton, Florida, pp. 327-340.
- Nriagu J. (1989b) Selenium in Geological Materials, in: Inhat, M. (Ed.), *Occurrence and Distribution of Selenium*. CRC Press, Boca Raton.
- Presser T.S., Swain W.C. (1990) Geochemical evidence for Se mobilization by the weathering of pyritic shale, San Joaquin Valley, California, U.S.A. *Appl. Geochem.* **5**, 703-717.
- Rouxel O., Ludden J., Carignan J., Marin L., Fouquet Y. (2002) Natural variations of Se isotopic composition determined by hydride generation multiple collector inductively coupled plasma mass spectrometry. *Geochim. Cosmochim. Acta* **66**, 3191-3199.
- Schilling K., Johnson T.M., Wilcke W. (2011) Selenium Partitioning and Stable Isotope Ratios in Urban Topsoils. *Soil Sci. Soc. Am. J.* **75**, 1354-1364.

- Shen Y.A., Buick R., Canfield D.E. (2001) Isotopic evidence for microbial sulphate reduction in the early Archaean era. *Nature* **410**, 77-81.
- Sherrard J.C., Hunter K.A., Boyd P.W. (2004) Selenium speciation in subantarctic and subtropical waters east of New Zealand: trends and temporal variations. *Deep Sea Res. I Oceanogr. Res. Pap.* **51**, 491-506.
- Suzuki Y., Miyake Y., Saruhashi K., Sugimura Y. (1979) A Cycle of Selenium in the Ocean. *Papers in Meteorology and Geophysics* **30**, 185-189.
- Wen H., Carignan J. (2011) Selenium isotopes trace the source and redox processes in the black shale-hosted Se-rich deposits in China. *Geochim. Cosmochim. Acta* **75**, 1411-1427.
- Wen H., Carignan J., Hu R., Fan H., Chang B., Yang G. (2007) Large selenium isotopic variations and its implication in the Yutangba Se deposit, Hubei Province, China. *Chin. Sci. Bull.* **52**, 2443-2447.
- Wen H., Carignan J., Qiu Y., Liu S. (2006) Selenium speciation in kerogen from two Chinese selenium deposits: Environmental implications. *Environ. Sci. Technol.* **40**, 1126-1132.
- Wen H., Qiu Y. (2002) Geology and geochemistry of Se-bearing formations in Central China. *International Geology Review* **44**, 164-178.
- Winkel L.H.E., Johnson C.A., Lenz M., Grundl T., Leupin O.X., Amini M., Charlet L. (2011) Environmental Selenium Research: From Microscopic Processes to Global Understanding. *Environ. Sci. Technol.* **46**, 571-579.
- Zhu J.-M., Johnson T.M., Clark S.K., Zhu X.-K. (2008) High precision measurement of selenium isotopic composition by hydride generation Multiple Collector Inductively Coupled Plasma Mass Spectrometry with a ^{74}Se - ^{77}Se double spike. *Chinese J. Anal. Chem.* **36**, 1385-1390.
- Zhu J., Zuo W., Liang X., Li S., Zheng B. (2004) Occurrence of native selenium in Yutangba and its environmental implications. *Appl. Geochem.* **19**, 461-467.

CHAPTER 4

SELENIUM AS PALEO- OCEANOGRAPHIC PROXY A FIRST ASSESSMENT

KRISTEN MITCHELL, PAUL R. D. MASON, PHILIPPE VAN CAPPELLEN,
THOMAS M. JOHNSON, BENJAMIN C. GILL, JEREMY D. OWENS, JULIA
DIAZ, ELLERY D. INGALL, GERT-JAN REICHART, TIMOTHY W. LYONS

THIS CHAPTER WAS PUBLISHED IN *GEOCHIMICA ET COSMOCHIMICA ACTA*
ON 15 JULY 2012, VOL. 89, 302-317, doi: 10.1016/j.gca.2012.03.038.

THE IMAGE ON THE PREVIOUS PAGE IS FROM IMAGEGEO ([HTTP://WWW.IMAGGEO.NET/](http://www.imaggeo.net/)) THE ONLINE OPEN ACCESS GEOSCIENCES IMAGE REPOSITORY OF THE EUROPEAN GEOSCIENCES UNION UNDER CREATIVE COMMONS LICENSE ([CREATIVECOMMONS.ORG](http://creativecommons.org)). TOTAL LUNAR ECLIPSE, MARCH 2007, COUNTRY: FRANCE, CONTINENT: EUROPE, SUBMITTED ON MARCH 29, 2010. IMAGE BY: BRUNO THIEN, DISTRIBUTED BY EGU UNDER A CREATIVE COMMONS LICENSE.

ABSTRACT

Selenium (Se) is an essential trace element, which, with multiple oxidation states and six stable isotopes, has been suggested as a potentially powerful paleoenvironmental proxy. In this study, bulk Se concentrations and isotopic compositions were analyzed in a suite of about 120 samples of fine-grained marine sedimentary rocks and sediments spanning the entire Phanerozoic. While the Se concentrations vary greatly (0.22 to 72 ppm), the $\delta^{82/76}\text{Se}$ values fall in a fairly narrow range from -1 to +1‰ (relative to NIST SRM3149), with the exception of laminated black shales from the New Albany Shale formation (Late Devonian), which have $\delta^{82/76}\text{Se}$ values of up to +2.20‰. Black Sea sediments (Holocene) and sedimentary rocks from the Alum Shale formation (Late Cambrian) have Se to total organic carbon ratios (Se/TOC) and $\delta^{82/76}\text{Se}$ values close to those found in modern marine plankton ($1.72 \pm 0.15 \times 10^{-6}$ mol/mol and $0.42 \pm 0.22\%$). For the other sedimentary sequences and sediments, the Se/TOC ratios show Se enrichment relative to modern marine plankton. Additional input of isotopically light terrigenous Se may explain the Se/TOC and $\delta^{82/76}\text{Se}$ data measured in recent Arabian Sea sediments (Pleistocene). The very high Se concentrations in sedimentary sequences that include the Cenomanian-Turonian Oceanic Anoxic Event (OAE) 2 may reflect an enhanced input of volcanogenic Se to the oceans. As the latter has an isotopic composition not greatly different from marine plankton, the volcanogenic source does not impart a distinct signature to the sedimentary Se isotope record. The lowest average $\delta^{82/76}\text{Se}$ values are observed in the OAE2 samples from Demerara Rise

and Cape Verde Basin cores ($\delta^{82/76}\text{Se} = -0.14 \pm 0.45\text{‰}$) and could reflect fractionation associated with microbial or chemical reduction of Se oxyanions in the euxinic water column. In contrast, a limiting availability of seawater Se during periods of increased organic matter production and burial may be responsible for the elevated $\delta^{82/76}\text{Se}$ values and low Se/TOC ratios in the black shales of the New Albany Shale formation. Overall, our results indicate that to unlock the full proxy potential of marine sedimentary Se records, we need to gain a much more detailed understanding of the sources, chemical speciation, isotopic fractionations and cycling of Se in the marine environment.

4.1 INTRODUCTION AND BACKGROUND

Selenium (Se) exhibits four major oxidation states in the environment: -II, 0, +IV, and +VI. It also has six stable isotopes: ^{74}Se , ^{76}Se , ^{77}Se , ^{78}Se , ^{80}Se , and ^{82}Se . Given the multiple oxidation states and multiple isotopes, Se has the potential to be a powerful paleoenvironmental proxy. Selenium isotopes have a long history among the ‘non-traditional’ stable isotopes, starting with the original study of Krouse and Thode (1962). Selenium isotope ratios were first measured using gas source mass spectrometry (Krouse and Thode, 1962). This technique was relatively sensitive but it required large sample quantities ($>10\ \mu\text{g Se}$). The advent of the multi-collector inductively coupled plasma mass spectrometer (MC-ICP-MS) resulted in a dramatic reduction in sample sizes, enabling a wider range of applications (Rouxel et al., 2002). However, although selenium isotopes are proving to be useful environmental (Johnson et al., 1999; Johnson et al., 2000; Herbel et al., 2002; Clark and Johnson, 2008; Clark and Johnson, 2010) and geological tracers (Rouxel et al., 2002; Rouxel et al., 2004; Wen et al., 2006; Wen et al., 2007; Zhu et al., 2008; Wen and Carignan, 2011), much work remains to be done to fully delineate the isotopic fractionations associated with the biogeochemical Se cycle (for reviews, see Johnson and Bullen, (2004), and Johnson, (2004)). Here, we present a first evaluation on whether Se concentrations and isotope signatures ($\delta^{82/76}\text{Se}$) in marine shales and mudstones can yield information on the prevailing environmental conditions during sediment deposition.

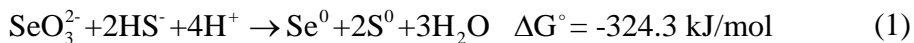
The biogeochemical cycle of Se is often compared to that of sulfur (S) (Zehr and Oremland, 1987; Stolz et al., 2002; Hoefs, 2009). However, while the two elements share chemical similarities, their oceanic cycles exhibit marked differences. Dissolved total Se concentrations in seawater are very low (<1 nM or <0.08 ppb, Cutter and Bruland, 1984) in contrast to the high abundance of sulfate (~28 mM). Major inputs of selenium to the ocean are atmospheric deposition (i.e. dust and volcanic ash), hydrothermal inputs, and riverine discharge (Suzuoki, 1964; Von Damm et al., 1985b; Von Damm et al., 1985a; Auclair, 1987; Nriagu, 1989a; Von Damm, 1991; Rouxel et al., 2002; German and Von Damm, 2003b; Rouxel et al., 2004). Dissolved Se in the water column exists as Se(VI) plus Se(IV) oxyanions and as dissolved organic Se, with the latter often dominating total dissolved Se in oxic and anoxic marine waters (Cutter, 1982; Cutter and Bruland, 1984; Cutter, 1992; Baines, 2001). Selenium oxyanions exhibit nutrient-like depth distributions in the ocean, unlike sulfate, which behaves conservatively in the water column (Measures and Burton, 1980a, b; Measures et al., 1983; Cutter and Bruland, 1984; Cutter and Cutter, 1995; Johnson, 2004). Assimilatory uptake by plankton accounts for most of the dissolved Se removal in the surface ocean (Cutter and Bruland, 1984). Selenium is generally taken up as selenate (SeO_4^{2-}) or selenite (SeO_3^{2-}) during assimilatory reduction, although dissolved organic Se can also be directly assimilated from seawater (Baines, 2001).

The major supply of Se to modern marine sediments is the deposition of organic detritus at the seafloor (Wrench and Measures,

1982; Cutter and Bruland, 1984; Ohlendorf, 1989; Baines and Fisher, 2001; Borchers et al., 2005; Böning et al., 2005). Selenium in organic compounds is mainly under the $-II$ oxidation state (Rother, 2012). Evidence from sediments collected in the NW Pacific show that Se deposited at the seafloor as organic Se remains largely bound to organic matter throughout early diagenesis (Sokolova and Pilipchuck, 1973). Organically-bound Se is also frequently the dominant form of Se in ancient shales. Kulp and Pratt (2004), for instance, determined that on average 64% of Se in shales from South Dakota and Wyoming is in the organic fraction. The other main form of Se in marine and freshwater sediments is elemental Se, which can be produced by reductive or oxidative processes in the water column or in the sediments (Cutter and Bruland, 1984; Velinsky and Cutter, 1990, 1991). Organic matter has been suggested to be the parent material of elemental Se found in carbonaceous shales (Martens and Suarez, 1997a; Wen and Qiu, 1999, 2002; Zhu et al., 2004; Wen et al., 2006; Wen et al., 2007; Zhu et al., 2008; Wen and Carignan, 2011).

Selenium oxyanions can be reduced via dissimilatory reduction processes, which are carried out by a number of different microbes (Oremland et al., 1989; Oremland et al., 1990; Oremland, 1991, 1994). While elemental Se is typically the predominant end-product of microbial Se reduction, $Se(0)$ can be further reduced to selenide, $Se(-II)$ (Herbel et al., 2003). Abiotic redox reactions also play an important role in Se cycling. For example, under sulfidic conditions selenite can reductively precipitate as elemental Se (Eq. 1)

and possibly also form polysulfidic Se and thiol-bound Se (Weres et al., 1989; Hockin and Gadd, 2003; Breynaert et al., 2008).



Selenate and selenite oxyanions sorb to organic matter, iron oxides and iron sulfides (Balistrieri and Chao, 1987; Bruggeman et al., 2005; Scheinost and Charlet, 2008). Selenite, however, tends to bind far more strongly than selenate. Adsorption of selenite on pyrite (FeS_2) is followed by reduction to elemental Se (Bruggeman et al., 2005). Selenite sorbed to mackinawite (FeS) is reduced to either elemental Se or Se(-II) in the form of FeSe , depending on pH (Scheinost and Charlet, 2008). Thus, the available evidence indicates that diverse pathways may lead to burial in marine sediments of Se under the form of organic selenide, sorbed selenite, elemental Se and iron-bound selenide.

Redox transformations can fractionate the stable isotopes of Se. Reported ranges of fractionation factors (given as ϵ values) are summarized in the lower part of Figure 4.1.

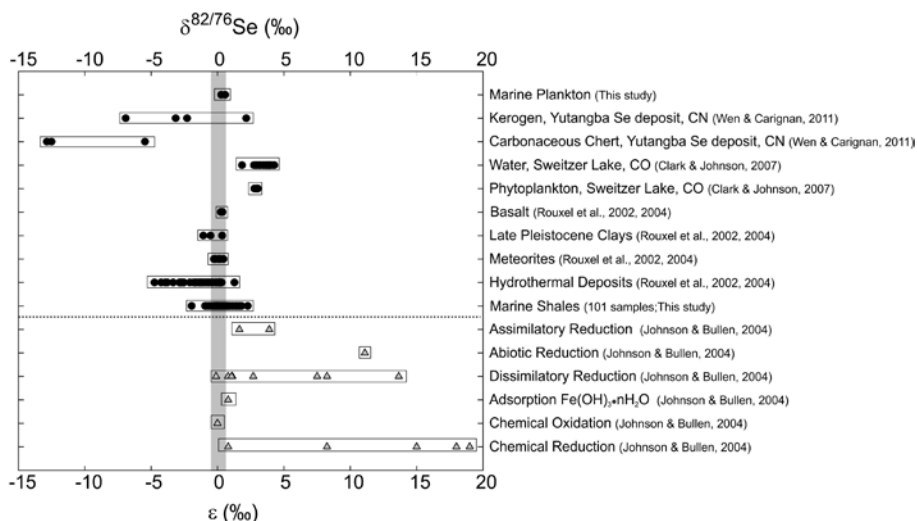


Figure 4.1 Compilation of $^{82/76}\text{Se}$ isotope fractionations (ϵ ; grey triangles), and $^{82/76}\text{Se}$ isotopic compositions (δ ; solid circles) of natural materials, including rocks, sediments, ore deposits, plankton and natural waters. Note that the fractionations reported as $^{80/76}\text{Se}$ by Johnson and Bullen (2004) are converted to $^{82/76}\text{Se}$ using the relationship $\epsilon_{80/76} = 2/3 \epsilon_{82/76}$.

The redox pathways that have been shown to produce significant Se isotope fractionation include biotic dissimilatory reduction and abiotic reduction of Se(VI) and Se(IV) oxyanions by green rust (Herbel et al., 2000; Herbel et al., 2002; Johnson and Bullen, 2003; Ellis et al., 2003; Johnson and Bullen, 2004). Large isotope fractionations have also been observed in chemical reduction experiments performed under highly acidic conditions and at high temperatures (Krouse and Thode, 1962; Rees and Thode, 1966; Rashid and Krouse, 1985). Although the reduction of selenite by

sulfide (Eq. 1) is expected to produce significant fractionations, this has yet to be demonstrated.

Isotope fractionations associated with assimilatory processes are often disregarded in stable isotope studies, because they are generally small in comparison to isotope fractionation resulting from dissimilatory processes. However, as can be seen in Figure 4.1, in the Se isotope system even limited fractionation during assimilatory reduction may be significant because of the fairly narrow overall range of isotope fractionation, up to 15‰ for $\epsilon^{82/76}\text{Se}$ compared to 72‰ for $\epsilon^{34}\text{S}$ (Tudge and Thode, 1950; Krouse and Thode, 1962; Canfield et al., 2005). In one laboratory study of algal uptake of selenate and selenite by the freshwater species *Chlamydomonas reinhardtii* $\epsilon^{82/76}\text{Se}$ values between 1.5 and 3.90‰ were obtained (Hagiwara, 2000).

Our study focuses on Se in well-characterized marine shale and mudstone sequences from various Phanerozoic time intervals, as well as their modern counterparts. Fine grained sediments and sedimentary rocks are selected because of their relatively high Se concentrations (Turekian and Wedepohl, 1961). The bulk Se concentrations measured in the samples analyzed in this study vary widely, from 0.22 to 72 ppm. Much higher Se concentrations have been observed in shale formations from China (Wen et al., 2007; Zhu et al., 2008; Wen and Carignan, 2011). However, these exceptional Se enrichments, which are also accompanied by wide ranges in Se isotopic composition, are clearly the result of secondary redistribution

processes (Wen and Carignan, 2011) and are, therefore, excluded from our study.

The Phanerozoic sequences we analyzed all include black shale horizons. The usually high organic carbon concentrations and increased burial rates of organic carbon associated with black shales have been proposed to result from 1) increased primary productivity and/or 2) enhanced preservation of organic carbon due to anoxic conditions (Arthur et al., 1987). Generally, some combination of these two factors are thought to accompany the formation of black shale sequences, though this is still a matter of debate (Jenkyns, 2010). Increased productivity may be caused by an increase in the availability of limiting nutrients due to increased supply from the continents or more efficient nutrient recycling in the oceans (Wignall, 1994; Van Cappellen and Ingall, 1994, 1996). Enhanced respiratory oxygen demand resulting from the increased supply of organic matter may in turn enhance the expansion of anoxic bottom waters (Wignall, 1994). Because of the multiple controls on the organic matter content of marine sediments, which include but are not exclusively dependent on bottom water oxygenation, paleo-redox conditions are generally assessed using a variety of geochemical (e.g., iron speciation and trace element enrichments), sedimentological (e.g., laminations) and ecological characteristics (e.g., abundance and depth distributions of benthic organisms).

Periods of time when oxygen-depleted waters covered large areas of the seafloor are known as Oceanic Anoxic Events or OAEs. They are typically recognized by extensive black shale stratigraphic

horizons transcending local basins (Schlanger and Jenkyns, 1976). Major Phanerozoic OAEs occurred during the Toarcian (~183 Ma), the Early Aptian (OAE1a; ~120 Ma), and the Cenomanian-Turonian (OAE2; ~93 Ma) (Jenkyns, 2010). Here, sedimentary sequences that comprise the following three OAEs are investigated: OAE2, the Toarcian OAE and the Steptoean Positive Carbon Isotope Excursion or SPICE. Also included in this study are samples from the New Albany Shale (Devonian-Mississippian) that were deposited under oscillating bottom water redox conditions, as well as modern sediments from the anoxic-sulfidic (euxinic) Black Sea and oxic to suboxic Arabian Sea. The data are used to assess to what extent Se concentrations and $\delta^{82/76}\text{Se}$ stable isotope ratios reflect (paleo-)depositional conditions, including redox conditions at the seafloor.

4.2 MATERIALS

4.2.1 MARINE PLANKTON

A plankton sample was obtained from the oligotrophic central North Pacific Ocean (138.9999°W, 32.0002°N) using a plankton net with a mesh size of 200 μm on board *R/V Kilo Moana* in July 2008. The sample consists of 10-15% zooplankton, with phytoplankton making up the remainder, including but not limited to *Trichodesmium sp.*, *Hemiaulus sp.* and *Ethmodiscus sp.* (Watkins-Brandt, 2010; Fujieki et al., 2011; Brzezinski et al., 2011). The sample was freeze-dried, split into two separate sub-samples of equal weight. The two sub-samples were processed following the same procedures as the sediment and rock samples (described below).

4.2.2 BLACK SEA: MODERN EUXINIC BASIN

The Black Sea is the largest existing euxinic basin and serves as an analog for ancient deposition and preservation of organic matter under euxinic conditions (Lyons and Kashgarian, 2005). The Black Sea represents a quasi-steady state system with anoxic deep-water replacement times on the order of 2,000 years. Numerous geochemical proxies have been validated in the Black Sea, including reactive plus total iron concentrations and the degree of pyritization (Canfield et al., 1996; Raiswell and Canfield, 1998; Lyons and Kashgarian, 2005), molecular biomarkers (Sinninghe Damsté et al., 1993), and molybdenum isotopes (Arnold et al., 2004).

Black Sea sediments were collected during Leg 4 of the 1988 *R/V Knorr* Black Sea Oceanographic Expedition using a box corer (Lyons, 1991; Lyons et al., 1993). Sediments from stations 3, 4, 9, 14 and 16 were analyzed in this study. Samples from station 9 and 14 contain unit 1 (non-‘turbiditic’) sediments (Degens and Ross, 1974). Stations 3 and 4 are located west of the Bosphorus, Station 16 is in the Bay of Sinop. For detailed site and sedimentological descriptions, see Lyons (1991). Sediments deposited under oxic bottom waters have total organic carbon (TOC) contents of ~1 wt.%, those from the deep anoxic (euxinic) basin have significantly higher TOC contents of around 5 wt.%. The sediments are all of Holocene age.

4.2.3 ARABIAN SEA: MODERN OXYGEN MINIMUM ZONE (OMZ)

Circulation in the Arabian Sea is controlled by seasonal shifts of the monsoon winds, causing upwelling of nutrient-rich water along

both coasts of the Arabian Sea (Calvert et al., 1995). Increased productivity accompanies the seasonal upwelling of nutrient-rich water. A strong oxygen minimum zone (OMZ) is present across the entire Arabian Sea at intermediate water depths (Calvert et al., 1995), with dissolved oxygen concentrations dropping to suboxic levels ($\sim 4.5 \mu\text{M}$) (Morrison et al., 1999).

Sediment samples were taken from two piston cores (463 & 464) collected on Murray Ridge in the northern Arabian Sea during the Netherlands Indian Ocean Program (NIOP) in 1992. Core 463 is located within the present-day OMZ; core 464 was collected below the oxygen-poor waters. The geochemistry and chronology of the cores are described in detail elsewhere (Reichart et al., 1998; Sinninghe-Damsté et al., 2002; van der Weijden et al., 2006). The sediments used in the present study were deposited between 60 and 150 ky ago. The organic carbon profiles show precession-related variations that are more pronounced in core 463 than in core 464 (van der Weijden et al., 2006). The maximum TOC concentrations in core 463 are on the order of 6 wt.%, with an average of ~ 2 wt.%.

4.2.4 DEMERARA RISE AND CAPE VERDE BASIN: OAE2

Sediment samples were obtained from ODP (Ocean Drilling Program) Leg 207 core 1258A on the Demerara Rise, a submarine plateau located in the western equatorial Atlantic Ocean off the coast of Suriname (Erbacher et al., 2005). Cape Verde Basin sediments were collected during DSDP (Deep Sea Drilling Project) Leg 41 at Site 367 off the coast of Senegal (Kuypers et al., 2002). The sediments

deposited during OAE2 are captured in the Demerara Rise core, but only the first half of OAE2 is recorded in the topmost portion of the Cape Verde Basin core.

The Demerara Rise sediments are mostly laminated black shales containing up to 29 wt.% TOC (averaging 12 wt.%). The Cape Verde Basin sediments contain terrigenous silicates and clay minerals. High TOC concentrations of up to 40 wt.% (average TOC = 18 wt. %) are observed in the samples corresponding to OAE2 (Herbin et al., 1986; Kuypers et al., 2002). Organic matter in the Demerara Rise and Cape Verde Basin sediments is principally of marine origin (Kuypers et al., 2002; Erbacher et al., 2005). Further details on the trace element geochemistry of the sediments from both sites can be found elsewhere (Brumsack, 1986; Hetzel et al., 2009).

Anoxic water column conditions likely existed prior to OAE2, and often reached upward to the photic zone moving the chemocline significantly (Kuypers et al., 2002). Sulfidic conditions in the water column during OAE2 also appear to have reached the photic zone and may have been present sporadically before the anoxic event (Kuypers et al., 2002).

4.2.5 POSIDONIA SHALE: EARLY JURASSIC (TOARCIAN OCEANIC ANOXIC EVENT)

The Posidonia Shale was deposited in a shallow epicontinental sea and is characterized by very well preserved fossils and high TOC contents (Röhl et al., 2001). The samples for this study are from a quarry located in Dotternhausen, SW Germany, and span the Lower Toarcian *Tenuicostatum paltum* to the *Bifrons commune* ammonite

zones (Schmid-Röhl et al., 2002). The bottom 2 meters of the section consist of organic-poor (<1 wt.% TOC) grey marlstones. The next 4.5 meters up-core comprise organic-rich laminated shales with very thin silty layers attributed to the Toarcian OAE; TOC concentrations are between 10 and 14 wt.%. The topmost 2.5 meters of the core are mostly bituminous mudstones, with an average TOC of ~7 wt.%.

The high degree of preservation of organic matter within the organic-rich portions of the Posidonia Shale has generally been ascribed to the presence of permanently anoxic and, possibly, even euxinic bottom waters (Raiswell and Berner, 1985; Raiswell et al., 1993; Schouten et al., 2000). However, there are indications of brief periods of oxygenation during otherwise long periods of anoxia (Fisher and Hudson, 1987). A proposed mechanism for these oxygenation events are shifts between estuarine and anti-estuarine circulation (Röhl et al., 2001). During high river discharge accompanying monsoon rains, increased nutrient availability and decreased salinity led to the establishment of a redox boundary in the water column. This redox boundary persisted throughout the year when sea level stand was low. However, as sea level rose, the redox boundary was largely destroyed during the winter when anti-estuarine circulation dominated. Enrichment in trace metals supports a marked influence of fluvial input during Posidonia shale deposition (Brumsack, 1991).

4.2.6 NEW ALBANY SHALE: STRATIFIED BASIN

Core material was obtained from the Camp Run Member of the New Albany Shale in Central Indiana (North American Exploration Hole INJK-I3 Sec. 9, T. 6N, R. 5E, Jackson County, Indiana). The core consists of alternating, and clearly separated, bioturbated and laminated shale layers. The laminated, black shales have relatively high TOC contents (average 8.2 wt.%) (Ingall et al., 1993; Calvert et al., 1996). The bioturbated, grey shales show evidence of burrowing and have low TOC contents (average 0.5 wt.%).

The Late Devonian-Early Mississippian New Albany Shale formed under conditions of eustatic sea level rise (Ingall et al., 1993). The geochemical characteristics of the Camp Run Member of the New Albany Shale indicate that the laminated shales were deposited under dysoxic to anoxic rather than euxinic conditions (Beier and Hayes, 1989). The repeated vertical shift of the anoxic/oxic interface at the basin margin is thought to have created the closely alternating layers of interbedded black and light colored shales (Cluff, 1980; Calvert et al., 1996).

4.2.7 ALUM SHALE: LATE CAMBRIAN SPICE

The Scandinavian Alum Shale Formation, deposited during the Middle Cambrian to Lower Ordovician, consists mainly of dark grey to black mudstones and the Alum Shale. The latter is enriched in TOC (10–20 wt.%), syngenetic pyrite, phosphate and trace elements (Ahlberg et al., 2009b; Gill et al., 2011). Sedimentary iron speciation

data along with the absence of bioturbation, suggests euxinic conditions during deposition of the Alum Shale (Thickpenny, 1984, 1987; Gill et al., 2011). Bulk rock samples for this study were obtained from Andrarum-3 Drill Core in Sweden (Ahlberg et al., 2009b; Gill et al., 2011).

The studied portion of the Alum shale formation contains the SPICE (Steptoean Positive Carbon Isotope Excursion) event defined by a marked shift in $\delta^{13}\text{C}$ of the organic carbon (Ahlberg et al., 2009b). The carbon isotope excursion has been observed in several locations throughout the world, including Kazakhstan, China, Australia, Eastern and Western North America (Glumac and Walker, 1998; Saltzman et al., 1998). The widespread observation of this event is thought to have been due to a transient global shift in carbon and sulfur cycling, which coincided with a global trilobite extinction event and the spread of euxinic conditions throughout the ocean (Saltzman et al., 1998; Saltzman et al., 2000; Gill et al., 2011).

4.3 METHODS

4.3.1 SAMPLE DIGESTION

Sample preparation followed the procedure outlined in Zhu et al. (2008). Freeze-dried plankton, rock, and sediment powders were weighed to 0.5 g per aliquot. Each aliquot was pre-digested in a 7 ml PFA beaker with 2.5 ml of concentrated nitric acid at 100°C for 3 hours to oxidize the organic matter. After the pre-digestion the sample was transferred to a 23 ml PTFE liner using an additional 0.5 ml of concentrated nitric acid to rinse the PFA beaker (total of 3 ml HNO_3).

The liner was then placed in a Parr bomb and heated at 165°C for 10 hours (Zhu et al., 2008; Clark and Johnson, 2010). After cooling, the sample was moved to a 15 ml conical centrifuge tube and the PTFE liner was rinsed with 1 ml H₂O; the rinse was also transferred to the centrifuge tube. The resulting suspension was centrifuged for 20 minutes at 3000 RPM, and the supernatant liquid was decanted into a clean 7 ml PFA beaker. The remaining sample powder was rinsed with 2 ml of 8 M HNO₃, and the powder was re-suspended by mixing on a vortexer. The suspension was centrifuged a second time using the same procedure, and the supernatant was added to the same 7 ml PFA beaker containing the first extraction. The sample was then placed on a 100°C hot plate (inner beaker temperature ~70°C) and heated to incipient dryness.

Once dry, the sample was re-suspended in 5 ml of 5 M HCl and ultra-sonicated for 15 min. Subsequently, it was filtered through a 0.45 µm pore size syringe filter and into a clean 30 ml borosilicate glass test tube with a PFA lined cap. The filter was rinsed into the same test tube using an additional 5 ml of 5 M HCl. The sample was then heated for 1 hour at 100°C in an aluminum block to convert any Se(VI) to Se(IV).

4.3.2 ANALYTICAL TECHNIQUES

4.3.2.1 SELENIUM CONCENTRATIONS

After the digestion the total Se concentrations were determined via atomic fluorescence spectrometry (AFS). A small aliquot (900 µl) from the digest was diluted to a total of 20 ml with 30% HCl. The

concentration was measured on a PSA 10.055 Millennium Excalibur Atomic Fluorescence Spectrometer equipped with a continuous flow hydride generator (HG) and a boosted discharge hollow cathode Se lamp. The Se concentration standard used was a single element ICP standard ($1.000 \mu\text{g mL}^{-1}$ Se in dilute HNO_3 , Ultra Scientific). Concentrations measured on 5 separate leaches of the U.S. Geological Survey (USGS) certified reference material Green River Shale (SGR-1b; $n=16$) yielded an average of 3.54 ppm Se, standard deviation (2σ) of ± 0.70 ppm and a relative standard deviation (RSD) of 9.9%. The relative error on these measurements was $\pm 2\%$, based on the USGS certificate of analysis (recommended Se value = 3.5 ppm).

4.3.2.2 SELENIUM ISOTOPE NOTATION

All Se isotope ratios and fractionations presented in this paper are relative to NIST SRM 3149 (Carignan and Wen, 2007). Values that were reported by other authors relative to the MERCK standard, were converted to the NIST scale according to Carignan and Wen (2007), which requires the addition of +1.54‰ to the MERCK value. The isotope notations are analogous to those of Canfield (2001a) for the sulfur system. The isotopic fractionation factor for a given biogeochemical process (α) is defined as follows:

$$\alpha_{(A-B)} = \frac{\left(\frac{{}^{82}\text{Se}}{{}^{76}\text{Se}}\right)_A}{\left(\frac{{}^{82}\text{Se}}{{}^{76}\text{Se}}\right)_B} \quad (2)$$

where A is the reactant and B is the product. Isotopic compositions are expressed in per mil (‰) units and are expressed in the standard delta (δ) notation (Coplen, 2011):

$$\delta^{82/76}Se = \left[\frac{\left(\frac{^{82}Se}{^{76}Se} \right)_{Sam}}{\left(\frac{^{82}Se}{^{76}Se} \right)_{Std}} - 1 \right] \quad (3)$$

Isotopic fractionations are expressed in terms of ϵ values, also with units of (‰):

$$\epsilon_{A-B} = (\alpha_{A-B} - 1) \quad (4)$$

The epsilon notation is convenient because ϵ is roughly equal to the difference between the δ values for two compounds:

$$\epsilon_{A-B} \cong \delta^{82/76}Se_A - \delta^{82/76}Se_B \quad (5)$$

4.3.2.3 SELENIUM ISOTOPIC ANALYSIS

The $^{74/77}Se$ double isotope spike was first added to the samples, in order to correct for any fractionation that might occur during the thiol cotton fiber (TCF) separation. The TCF was used for the chemical separation of Se from the dissolved matrix (i.e., separation from Fe, Ge, etc.) prior to isotopic analysis. The preparation of the thiol cotton fiber followed a procedure modified after Yu et al. (2001). A mixture was prepared by combining 20 ml thioglycolic acid (96-99%), 14 ml acetic anhydride (99.9%), 6.4 ml glacial acetic acid, 0.064 ml sulfuric acid (97.5%) and 2.5 ml 18 M Ω water. Medical grade hydrophilic cotton (6 g) was added to the mixture. The separation of the Se via the TCF followed the detailed protocol of Zhu et al. (2008) based on Rouxel et al. (2002).

Selenium isotope determinations were measured by Hydride Generation Multi Collector Inductively Coupled Plasma Mass

Spectrometry (HG-MC-ICP-MS), using a double focusing Nu Plasma MC-ICP-MS (Wrexham, North Wales, UK), located at the Department of Geology, University of Illinois at Urbana-Champaign. The HG-MC-ICP-MS method was modified from Rouxel et al. (2002). The reductant used for the hydride generation was 0.3% NaBH₄ in 0.3% NaOH. The sample and reductant were introduced into the hydride generator at a flow rate of 0.25 ml min⁻¹. The hydrides generated were carried into the instrument with argon as the carrier gas.

The Se isotope standard solution was NIST SRM 3149 (Carignan and Wen, 2007). The mass difference between ⁷⁴Se and ⁸²Se is greater than between ⁸²Se and ⁷⁶Se, but ⁷⁴Se is far less abundant (0.87%) than ⁷⁶Se (9.02), hence, the ^{82/76}Se ratio is used preferably (Krouse and Thode, 1962). The low abundance of ⁷⁴Se also makes the double spike technique used here ideal. The ⁷⁴Se + ⁷⁷Se double spike approach corrects for instrumental mass bias and for any isotopic fractionation occurring during the sample preparation steps. ⁷⁴Se-enriched and ⁷⁷Se-enriched spikes were purchased from ISOFLEX, USA, and mixed to create a Se isotope double spike (⁷⁴Se/⁷⁷Se), which was added in the Se(IV) form to all samples and well mixed prior to the TCF separation procedure. The amount of spike was chosen to attain a ⁷⁷Se/⁷⁸Se ratio of roughly 2. The samples for isotope analysis were prepared so as to yield about 20 mL of solution containing 4-6 ng ml⁻¹ selenium, producing ⁷⁸Se intensity between 12 and 20 pA (1.2 to 2.0 V). Between each sample the hydride generator apparatus was rinsed with 2 M HCl until the normal background signal was

retrieved, and on-peak baseline measurements were subtracted, in order to avoid memory effects between samples. NIST SRM 3149 was measured approximately every five samples to account for instrument drift, and results were normalized to interpolated NIST SRM-3149 values.

The analytical data were first corrected for interferences (for detailed discussion, see Electronic Annex Zhu et al., 2008; Clark and Johnson, 2010; supporting information; Schilling et al., 2011a; supporting information). The different isotopic ratios ($^{74}\text{Se}/^{78}\text{Se}$, $^{76}\text{Se}/^{78}\text{Se}$, $^{77}\text{Se}/^{78}\text{Se}$, $^{80}\text{Se}/^{78}\text{Se}$, and $^{82}\text{Se}/^{78}\text{Se}$) were then entered into an iterative data reduction procedure that extracted the sample's $^{82}\text{Se}/^{76}\text{Se}$ and $^{82}\text{Se}/^{78}\text{Se}$ ratios from the measurements on the sample-spike mixture. Replicate analyses (repeat TCF preparation and analysis) were carried out on 7 samples. This yields a precision estimate of $\pm 0.16\%$, calculated as two times the root mean square of the differences. Replicate analyses of SGR-1 ($n=11$) yield $\delta^{82/76}\text{Se} = -0.20\% \pm 0.10\%$ (2σ), which differs from Rouxel et al. (2002) published value by -0.65% .

4.4 RESULTS

In this first assessment of the Se proxy in marine sediments and sedimentary rocks, we focus on general trends in the entire data set. The analysis presented in the next section relies primarily on the average values of bulk Se concentrations and isotopic compositions, together with average TOC and Se/TOC ratios, summarized in Figure 4.2. The complete data set is presented in the supplementary material

(Electronic Annex), which also provides detailed descriptions of the results for each individual set of samples.

In Figure 4.2, the results for each sampling location are grouped in two or three categories described in the following text. For the Black Sea, we separate the sediments from the oxic basin margin (open symbols) from those collected in the deep euxinic basin (filled symbols). For the Arabian Sea, the two categories correspond to core 464 (open) and core 463 (filled). For the Demerara Rise and Cape Verde Basin sediments, we distinguish the sediments that were deposited just before (open, B), during OAE2 (filled) and after OAE2 (open, A). Similarly, for the Posidonia Shale and Alum Shale Formations, samples from before (open, B), during (filled) and after (open, A) the Toarcian OAE and SPICE, are grouped together, respectively. The OAEs and SPICE events are defined based on the $\delta^{13}\text{C}$ excursions described in the literature (See Figs. EA2, EA3, and EA5). Finally, for the New Albany Shale, the bioturbated (open) and laminated shales (filled) define the two categories.

The average Se concentrations vary by more than one order of magnitude (Figure 4.2A). Selenium concentrations in the Demerara Rise and Cape Verde Basin sediments are significantly higher than for the other sites. They are also well above the world shale average of 0.6 ppm (Turekian and Wedepohl, 1961). As expected, for any given location, the sediments deposited under the more reducing conditions (filled symbols) are on average more enriched in TOC (Figure 4.2B). The OAE2 sequences show the highest average TOC concentrations, while the lowest TOC concentrations are seen in the Black Sea and

Arabian Sea sediments as well as in the bioturbated layers of the New Albany Shale.

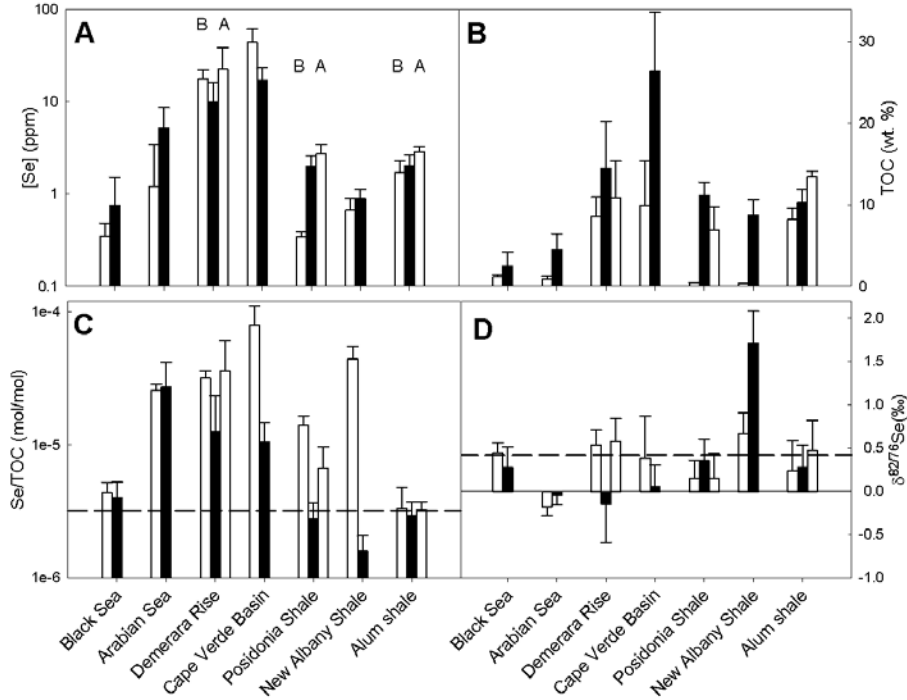


Figure 4.2 Average values in the sediments and sedimentary rocks of A) total selenium concentrations (ppm), B) total organic carbon concentrations (TOC, wt.%), C) molar Se/TOC ratios – the dashed line indicates the average Se/TOC ratio in phytoplankton ($3.6 \pm 1.7 \times 10^{-6}$ mol/mol; Doblin et al., 2006), and D) the Se isotopic composition, expressed as $\delta^{82/76}\text{Se}$ (‰) – the dashed line indicates the isotopic composition of modern plankton collected in the Pacific Ocean (+0.42‰; this study). For the Black Sea, we separate the sediments from the oxic basin margin (open symbols) from those collected in the deep euxinic basin (filled symbols). For the Arabian Sea, the two categories correspond to core 464 (open) and core 463 (filled). For the Demerara Rise and Cape Verde Basin sediments, we distinguish the sediments that were deposited just before (open, B), during OAE2 (filled) and after OAE2 (open, A). Similarly, for the Posidonia Shale and Alum Shale Formations, samples from before (open, B), during (filled) and after (open, A) the Toarcian OAE and SPICE, are grouped together, respectively. For New Albany Shale, the bioturbated (open) and laminated shales (filled). Error bars indicate standard deviations (1σ).

The Se to organic carbon ratios (Se/TOC) vary by about two orders of magnitude (Figure 4.2C). The average Se/TOC values for the Black Sea sediments, the Alum Shale Formation, the Toarcian OAE and the laminated New Albany shale layers are close to or slightly below the average literature value for modern marine phytoplankton ($3.6 \pm 1.7 \times 10^{-6}$ mol/mol; Doblin et al., 2006). The phytoplankton sample from the oligotrophic Pacific Ocean measured in this study has a Se/TOC value of 1.7×10^{-6} mol/mol, which is toward the low end of Se/TOC values found in the shales. The Arabian Sea cores, the non-OAE samples of the Demerara Rise and Cape Verde Basin and the bioturbated New Albany Shale layers have average Se/TOC ratios far above those of modern marine phytoplankton. Note, however, that the differences in average Se/TOC ratios between non-OAE2 and OAE2 sediments, and between the bioturbated and laminated layers of the New Albany Shale, are primarily due to concentration differences of TOC, rather than Se (Figure 4.2A-C).

In contrast to the Se concentrations and Se/TOC ratios, the average $\delta^{82/76}\text{Se}$ values only exhibit a narrow range (-0.14 to 1.71‰; Figure 4.2D). Most values fall close to or below the isotopic composition we measured on modern plankton (0.42‰) from the (open) Pacific Ocean (Figure 4.2D). The notable exceptions are the New Albany Shale with significantly heavier $\delta^{82/76}\text{Se}$ values, and the Arabian Sea sediments and OAE2 samples from the Demerara Rise, which have negative average $\delta^{82/76}\text{Se}$ values.

4.5 DISCUSSION

The average Se/TOC ratio of modern marine plankton provides a reference point to which sediment Se/TOC ratios can be compared (Figure 4.2C). The lowest marine plankton Se/TOC ratios previously measured (1.8×10^{-6} mol/mol) have been reported for Subantarctic Surface Water (SASW) and Subtropical Surface Water (STW) (Sherrard et al., 2004). The plankton sample from the oligotrophic Pacific Ocean measured in this study has a comparable Se/TOC value of 1.7×10^{-6} mol/mol. Cultured phytoplankton have somewhat higher Se/TOC values around $3.2 \pm 6.2 \times 10^{-6}$ mol/mol (Doblin et al., 2006). The cultured plankton have a similar Se/TOC content to plankton collected from estuarine seston tows which range from $3.6 \pm 1.7 \times 10^{-6}$ up to $5.7 \pm 2.9 \times 10^{-6}$ (Doblin et al., 2006). The higher values probably reflect luxury uptake (i.e., Se uptake in excess of the minimum requirement for growth) by phytoplankton in these areas (Vandermeulen and Foda, 1988; Baines and Fisher, 2001).

For the modern and ancient marine sediments analyzed in this study, the sediment Se/TOC values are either similar or greater than the values observed for modern marine plankton (Figure 4.2C). The most depleted Se/TOC ratios are found in the laminated black shales of the New Albany formation, with values at the lower end of the modern plankton range. The Se/TOC values of the Black Sea, Alum Shale, and Toarcian OAE samples are close to the average Se/TOC of modern marine phytoplankton. All the remaining sediments and sedimentary rocks are enriched in Se relative to marine plankton,

suggesting selective enrichment processes or additional sources of Se to the sediment.

The Se isotopic data may potentially help explain the observed variations in the sediment Se/TOC ratios. Compared to the relatively large Se isotope fractionations reported in laboratory studies, especially fractionations associated with reductive processes, the range of $\delta^{82/76}\text{Se}$ values in the sediments and sedimentary rocks analyzed here is remarkably narrow (Figure 4.2D and Figure 4.3). In addition, most $\delta^{82/76}\text{Se}$ values fall fairly close to the $\delta^{82/76}\text{Se}$ value of plankton collected in the oligotrophic Pacific Ocean ($\delta^{82/76}\text{Se} = 0.42\text{‰}$, this study). This observation is particularly true for the Black Sea sediments and Alum Shale samples, which also exhibit Se/TOC ratios that are indistinguishable from those of modern marine plankton.

Direct measurements in the water column of the Black Sea show that organic selenide is the dominant form of dissolved Se, both in the surface and the deeper anoxic waters (Cutter, 1992). The persistence of organic selenide throughout the water column supports the idea that the main flux of Se to the sediments is particulate organic matter, which releases dissolved organic selenide as it sinks to the seafloor. Because Se is already in reduced form when reaching the sediments, no significant further reduction of Se and accompanying fractionation effects are expected, while reoxidation of organic selenide in shallower sediments deposited under oxic bottom waters would only produce small fractionations (Figure 4.1). Under these conditions, the early diagenetic redistribution of deposited organic Se,

for example into mineral selenide or elemental selenium should preserve the original planktonic Se isotopic composition (Thomson et al., 1998; Mercone et al., 1999).

The proposed interpretation of the Black Sea selenium data implies that the corresponding sediment $\delta^{82/76}\text{Se}$ values primarily reflect surface ocean water values, with a small offset due to the fractionation accompanying reductive assimilation of Se by phytoplankton. By analogy with the limited fractionation observed during assimilatory sulfate uptake (Canfield, 2001a), reductive assimilation of Se is assumed to only impart a small fractionation, especially when compared to the fractionation accompanying dissimilatory reduction. The assumption is further supported by a number of laboratory and field studies. In culture experiments with the freshwater alga *Chlamydomonas reinhardtii*, Hagiwara (2000) found fractionations between biomass and medium of $\epsilon^{82/76}\text{Se} = 1.5\text{--}3.90\text{‰}$ (Figure 4.1). Fractionations in natural aquatic environments are likely smaller, as Se uptake may in part be due to non-reductive assimilation of dissolved organic Se. For example, phytoplankton collected in a freshwater lake in Colorado, USA, has a $\delta^{82/76}\text{Se}$ value only 0.6‰ lower than the mean $\delta^{82/76}\text{Se}$ value of coexisting aqueous selenate (Clark and Johnson, 2010). Similarly small differences are observed between organically bound selenium extracted from modern sediments from a variety of settings and the coexisting waters (Johnson et al., 2000; Herbel et al., 2002; Clark and Johnson, 2010).

Assuming that fractionation during Se assimilation by marine plankton is (relatively) small, the $\delta^{82/76}\text{Se}$ values determined for

modern marine plankton ($0.42 \pm 0.22\%$) should provide a lower limit for surface seawater $\delta^{82/76}\text{Se}$ from the central North Pacific Ocean. These oligotrophic, Se-limited surface waters previously subjected to extensive Se assimilation would further be expected to have somewhat heavier $\delta^{82/76}\text{Se}$ compositions than deeper water masses or surface waters in upwelling zones. Our marine plankton value (0.42%) agrees remarkably well with the range of $\delta^{82/76}\text{Se}$ values of 0.04% to 0.42% measured by Rouxel et al. (2002) on manganese nodules, which, presumably, record seawater isotopic compositions with negligible fractionation. (Note: the original $\delta^{82/76}\text{Se}$ values of Rouxel et al. reported relative to the MERCK standard are converted to NIST SRM 3149 values using the conversion factor, $+1.54\%$, from Carignan and Wen, 2007. These indirect constraints on modern ocean $\delta^{82/76}\text{Se}$, however, will need to be verified by direct determinations of the Se isotopic composition of seawater.

Weathering on land is expected to yield isotopically light alteration products (solids). For example, extreme Se enrichments in supergene ore deposits have $\delta^{82/76}\text{Se}$ values as low as -14.2% (Wen et al., 2007; Zhu et al., 2008). Typical $\delta^{82/76}\text{Se}$ values of land-derived materials are likely less negative. Rouxel et al. (2002), for instance, report an average $\delta^{82/76}\text{Se}$ of $-0.42 \pm 0.72\%$ for clay-dominated samples from the Izu-Bonin-Mariana Margin (ODP Leg 185, Site 1149, Late Pleistocene). This value is probably more representative of continental weathering products delivered to the oceans.

Terrigenous Se input may be the source of the relatively light isotopic signatures of the Arabian Sea sediments (Figure 4.2). If the

average $\delta^{82/76}\text{Se}$ value of terrigenous matter mentioned above (-0.42‰) and that of marine plankton measured in this study (+0.42‰) are representative for the Arabian Sea, then isotopic balance implies that more than 50% of the Se in cores 463 and 464 is of terrigenous origin. Major contributions of terrigenous Se are in agreement with the Al and Se concentrations reported by van der Weijden et al. (2006) for the same sediments. Bottom-water oxygenation inferred from biomarkers indicates that the sediments of Arabian Sea core 463 were deposited under predominantly anoxic conditions, while core 464 experienced mostly oxic conditions (Sinninghe-Damsté et al., 2002). Despite the difference in bottom-water oxygenation, the average Se/TOC and $\delta^{82/76}\text{Se}$ values are very similar for the two cores. This similarity is consistent with the inferred predominance of a (common) terrigenous Se source at both locations in the Arabian Sea.

Significant terrestrial inputs of trace elements have also been proposed for the Posidonia Shale sequence (Brumsack, 1991), and could thus account for the excess Se/TOC and relatively light Se isotopic compositions observed in the samples deposited before and after the Toarcian OAE. The shift toward planktonic Se/TOC and $\delta^{82/76}\text{Se}$ values during the Toarcian OAE (Figure 4.3) may then reflect an increased contribution of marine organic matter deposition and preservation to total sedimentary Se burial.

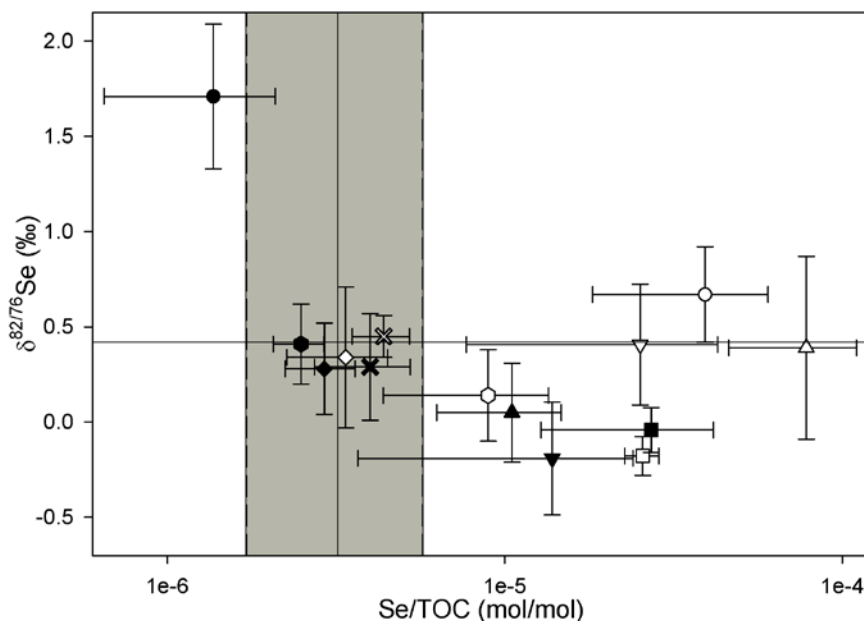


Figure 4.3 Average Se/TOC ratios versus average $\delta^{82/76}\text{Se}$ values. The solid vertical line indicates average Se/TOC of phytoplankton (Doblin et al., 2006). The shading encompasses the range of Se/TOC ratios observed in modern phytoplankton (upper limit, Doblin et al., 2006; lower limit, this study). The solid horizontal line indicates the average $\delta^{82/76}\text{Se}$ of oligotrophic open Pacific Ocean plankton (this study). Symbols: X=Black Sea; circles=New Albany Shale; hexagon=Posidonia Shale; diamond=Alum Shale; square=Arabian Sea; triangle, down=Demerara Rise; triangle, up=Cape Verde Basin. Open and filled symbols correspond to the categories used in Figure 4.2, with the exception of the OAE sequences where the before and after OAE data have been combined (see section 4 in text for more details). Error bars indicate the standard deviations (1σ) of the average values Se/TOC and $\delta^{82/76}\text{Se}$ values.

In contrast to the Arabian Sea sediments and Posidonia Shale samples, the laminated black shales of the New Albany Shale formation exhibit $\delta^{82/76}\text{Se}$ values that shift away from the modern planktonic value in the positive direction. In addition to the most positive $\delta^{82/76}\text{Se}$ values, the laminated New Albany shale layers also exhibit the lowest Se/TOC ratios (Figure 4.3). One possible explanation is that the Se signatures in the laminated shales reflect

high primary productivity (Ingall et al., 1993; Ingall and Jahnke, 1997) under extreme water column Se limitation due to increased assimilatory Se demand. The reduced availability of Se would not only have led to the burial of Se-depleted organic matter but could also have decreased the extent of fractionation during assimilatory Se uptake. The black shale isotopic compositions would then yield a minimum estimate of $\delta^{82/76}\text{Se}$ of Late Devonian-Early Mississippian seawater of $1.7\pm 0.5\%$. Alternatively, the positive $\delta^{82/76}\text{Se}$ values of the laminated New Albany shales could represent a local, productivity-driven enrichment of heavy Se in the water column of a semi-isolated depositional basin with restricted connection to the global ocean. Lower primary productivity during deposition of the bioturbated shales of the New Albany Shale sequence would have alleviated Se limitation and delivered isotopically lighter organically bound Se to the sediments. The relatively higher Se/TOC ratios in the bioturbated New Albany Shale samples could be accounted for by additional Se deposition, for example, as Se sorbed to settling iron oxides, or by preferential retention of Se by iron oxides at the seafloor. As for assimilation, sorption to ferric iron oxyhydroxides is expected to result in slightly lighter Se being buried in the sediments ($\epsilon \approx 0.8\%$, Johnson et al., 1999; Johnson and Bullen, 2004).

Increased volcanism may have played a major role in triggering OAE2 (Schlanger et al., 1981; Schlanger et al., 1987; Sinton and Duncan, 1997; Kerr, 1998; Turgeon and Creaser, 2008; Jenkyns, 2010; Adams et al., 2010). Elevated levels of trace elements have been cited as evidence for intense volcanic activity (Snow et al.,

2005; Turgeon and Creaser, 2008; Adams et al., 2010). Volcanogenic Se input could thus produce the high Se/TOC ratios in the Demerara Rise and Cape Verde Basin sediments (Figure 4.2C and Figure 4.3). Volcanic (sub-aerial and sub-marine) and hydrothermal activity releases Se principally as nano-particulate Se(0) and volatile Se compounds (Suzuoki, 1964; Von Damm et al., 1985b; Von Damm et al., 1985a; Rubin, 1997; Snow et al., 2005). However, much of the Se released by seafloor hydrothermal vents is likely deposited nearby, and is presumably a minor source of Se to the oceans (Auclair, 1987; Rouxel et al., 2004). Nano-particulate Se(0) could be incorporated directly into marine sediments (Velinsky and Cutter, 1990), while volatile Se would increase the availability of Se in the water column, which may cause luxury Se uptake phytoplankton (Vandermeulen and Foda, 1988; Baines and Fisher, 2001), hence increasing the Se/TOC ratio of deposited organic matter. Excess Se may also have been removed from the water column as selenite sorbed to settling mineral and organic matter, further enriching the sediments in Se.

Ocean basalts have isotopic compositions very near that of modern marine plankton ($\delta^{82/76}\text{Se} = 0.25\text{‰}$; Rouxel et al., 2004). Most likely, the isotopic compositions of the volatile and nano-particulate Se associated with marine volcanism are close to the basaltic values. Hence, bulk sediment $\delta^{82/76}\text{Se}$ values should not differentiate between marine planktonic and volcanogenic Se sources. The average $\delta^{82/76}\text{Se}$ values of the sediments deposited during OAE2 are distinctly lower than those of the sediments deposited before and after the event, however (Figure 4.3). We attribute this pattern to the microbial or

chemical reduction of excess Se(VI) and Se(IV) oxyanions within the euxinic water column of OAE2. Both biotic and abiotic reduction in the water column would result in the production of isotopically light particulate Se(0) or FeSe, which would subsequently settle to the seafloor. During the less reducing conditions before and after OAE2, however, sorbed Se oxyanions would be delivered to the sediments where early diagenetic Se reduction would occur in the semi-closed sediment system, hence preserving the bulk isotopic signature of the deposited Se.

Taken together, our data imply marked differences between the stable isotope systematics of selenium and sulfur. The narrow range of $\delta^{82/76}\text{Se}$ values in the sediments and sedimentary rocks analyzed in this study stands in stark contrast to the sedimentary sulfide $\delta^{34}\text{S}$ geological record, which shows large variations through time (Canfield and Raiswell, 1999; Shen et al., 2001). To a great extent, the latter can be attributed to the dominant imprint of dissimilatory sulfate reduction, and the corresponding wide range of fractionations, on the sulfur isotopic signatures in marine sediments (Canfield et al., 2000; Canfield, 2005). In contrast, we propose that the sedimentary $\delta^{82/76}\text{Se}$ record is dominated by the relatively small fractionations accompanying assimilatory uptake of Se and the delivery of organically-bound selenide to the seafloor. The latter severely limits the extent to which early diagenetic reductive processes can modify the bulk isotopic composition of deposited Se. The $\delta^{82/76}\text{Se}$ variations observed here can to a large degree be explained by variations in terrigenous inputs and the degree of surface

water Se limitation. The narrow range of $\delta^{82/76}\text{Se}$ further argues against large variations in the selenium isotopic composition of seawater over the course of the Phanerozoic, probably as a result of the very efficient recycling of assimilated Se within the ocean system (Cutter and Bruland, 1984; Cutter, 1992).

The Se concentrations and isotopic variability of our study also contrast with those reported by Wen et al. (2007) and Wen and Carignan (2011) for Se deposits hosted in black shale formations in China. These authors explain the observed Se enrichments by the following three mechanisms: 1) primary hydrothermal Se deposition (Zunyi Ni-Mo-Se deposit), 2) secondary hydrothermal alteration (La'erma Se-Au deposit), and 3) supergene alteration (Yutangba deposit). Primary hydrothermal enrichment results in high Se concentrations of up to 99 ppm in black shales, and 1900 ppm in the associated ore deposits. Secondary hydrothermal alteration shows enrichments of Se between the host rocks and the ores of about one order of magnitude (Wen and Carignan, 2011), while supergene alteration produces the highest Se enrichments with Se concentrations >4500 ppm (Wen et al., 2007). The supergene alteration is also accompanied by the largest range of Se isotopic composition reported for a single sedimentary formation, with $\delta^{82/76}\text{Se}$ values between -14.20‰ and 9.13‰ (Wen et al., 2007; Zhu et al., 2008; Wen and Carignan, 2011).

According to Zhu and coworkers (2008), the large spread in $\delta^{82/76}\text{Se}$ values of the Yutangba shales and ores results from repeated cycles of oxidative mobilization and reductive precipitation of Se.

Selenium oxidation occurs in the surficial soil zone of the ore deposit and along fast-flowing fractures to an unknown depth below the surface (possibly on the order of 1 m). As the selenium seeps downward, the water eventually becomes anoxic, and Se reprecipitates as Se(-II) or Se(0), producing a selenium enriched layer. Upon subsequent exposure of this layer at the earth's surface, the cycle of supergene alteration repeats itself, hence increasing the degree of isotopic fractionation (Wen and Carignan, 2011). Isotopic compositions measured on drill core samples show a progressive narrowing of the range in the $\delta^{82/76}\text{Se}$ values, which converge to a typical shale value of $\sim 0\%$ at about 50 m depth (Zhu et al., 2008). The exceptional Se enrichments and large ranges in Se isotopic compositions observed in the black-shale hosted Se deposits of China are therefore the result of secondary redistribution of Se by alteration processes and, hence, not indicative of the paleoenvironmental conditions during sediment deposition.

Our current conceptual understanding of the biogeochemical cycling of Se and Se isotopes in the oceans, under variable redox regimes is summarized in Figure 4.4. The panels in the figure are based on the selenium isotopic ratios and Se/TOC values observed in the marine sediments and sedimentary rocks discussed above. For each of the redox regimes, we suggest that the main dissolved Se species in the water column is organic Se (Cutter, 1982; Cutter and Bruland, 1984; Cutter, 1992), and that assimilation is the main driving mechanism of Se cycling in the surface oceans. The figure also includes dimethyl selenide (DMSe) efflux as a possible pathway for

the removal of Se from the oceans (Amouroux et al., 2001). This process is unlikely to impart a significant isotopic shift, as little fractionation is associated with volatilization (Schilling et al., 2011a).

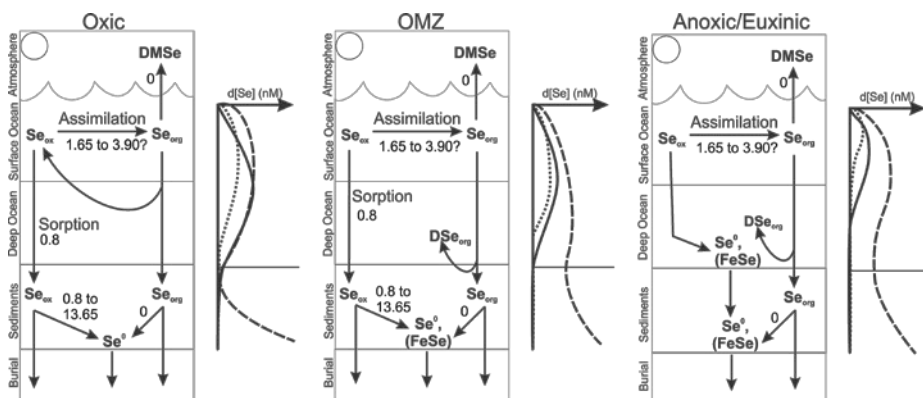


Figure 4.4 Proposed Se cycling under various water column redox conditions. Depth profiles of dissolved Se species concentrations are shown schematically next to each ocean panel: dotted line indicates Se(VI), solid line indicates Se(IV), long dash indicates dissolved organic Se (DSe_{org}). On the panels, Se_{ox} includes Se(VI) and Se(IV), DSe_{org} stands for dissolved organic Se, $DMSe$ refers to dimethyl selenide. All numerical values shown are ϵ values (‰), with zero values indicating unknown but presumably small fractionation. The ϵ values for assimilation are from Hagiwara (2000); values for dissimilatory reduction are from the compilation by Johnson and Bullen (2004) and the values given for adsorption are from Johnson (1999).

The transport of Se to the sediments is dominantly in the form of settling organic matter in all three redox regimes, with some input of oxidized Se species in the oxic and OMZ water column scenarios and elemental Se and FeSe in the anoxic/euxinic scenario. In the anoxic/euxinic water column there is no input of oxidized Se species to the sediments, as they are reduced in the water column. Further early diagenetic redistribution leads to the ultimate burial of a mix of predominantly organic Se, elemental Se and sorbed Se.

Admittedly, many of the proposed interpretations of the data and the conceptual diagrams of Figure 4.4 remain highly speculative. Their verification will require a far more comprehensive characterization of the chemical speciation and isotopic composition of the key sediment Se pools. So far there have been very few studies that have successfully analyzed the isotopic compositions of the different forms of Se in sediments and sedimentary rocks. Wen and Carignan (2011) analyzed the Se isotopic composition of different fractions extracted from rock samples; their samples, however, were significantly more enriched in Se (100 to 10000 ppm) than our sediments and sedimentary rocks (≤ 75 ppm). Clark and Johnson (2010) successfully analyzed Se isotopic signatures of samples with lower Se concentrations (≤ 40 ppm), but they relied on relatively large sample sizes (~ 3 g). Both studies report some mass balance discrepancies after extraction steps, as also reported by others (Wright et al., 2003; Lenz et al., 2008). Thus, there remains ample room for methodological improvements to fully unlock the Se and Se isotopic proxies.

4.6 CONCLUSIONS

This study provides a first assessment of the paleo-oceanographic insights that may eventually be extracted from selenium records in fine-grained marine sediments and sedimentary rocks. The Se concentrations and Se/TOC ratios show significant variations, which are interpreted in terms of changes over time in the sources, water column availability and sedimentary sinks of Se. The

small variations in $\delta^{82/76}\text{Se}$ provide further constraints on the sources and cycling of Se under different oceanographic regimes. For example, the large Se/TOC ratios (compared to modern marine plankton) and the negative $\delta^{82/76}\text{Se}$ excursion observed for black shales deposited during OAE2 are explained by an enhanced supply of volcanogenic Se to the oceans accompanied by reduction of excess Se(VI, IV) oxyanions in the euxinic water column and subsequent burial as elemental Se and iron-bound selenide. A similar isotopic signature is not observed in modern sediments deposited under euxinic bottom waters in the Black Sea, presumably because of a much lower water column availability of Se.

The interpretations proposed to explain the observed Se concentration and isotopic records in the sediments and sedimentary rocks analyzed are speculative and non-unique. In a large measure, this reflects the wide diversity of oxidation states and geochemical forms of Se. Bulk sediment Se concentrations and isotopic signatures therefore only offer a partial window into the depositional conditions and biogeochemical processes that control the incorporation of Se into marine sediments. Quantitative information on the speciation of Se in marine sediments and sedimentary rocks would significantly strengthen the Se proxy, especially if the chemical differentiation of the sedimentary pools of Se is coupled to their isotopic fingerprints. Equally important, however, is the effort to fully characterize all end-member sources that contribute Se to marine sediments. The existing datasets on Se contents, speciation and isotopic ratios of end-member sources, such as marine and terrestrial organic matter, continental

weathering products, river run-off, and volcanic plus hydrothermal inputs, are limited at best. Similarly, many gaps remain in our understanding of the isotopic fractionations associated with key processes in the marine Se cycle, such as the reduction of selenite by free sulfide and iron sulfide minerals.

The results of our study clearly caution against the common assumption that selenium is an analog of sulfur. The narrow range of $\delta^{82/76}\text{Se}$ values in marine sediments and sedimentary rocks contrasts with the large variations in sedimentary $\delta^{34}\text{S}$ over geological time. We believe this reflects the dominant imprints of assimilatory and reduction dissimilatory processes on the sedimentary records of $\delta^{82/76}\text{Se}$ and $\delta^{34}\text{S}$, respectively. This further implies that bulk $\delta^{82/76}\text{Se}$ values may only be weakly affected by redox conditions at the seafloor, unless Se is present in large excess in the water column. The sedimentary records of Se and S therefore encode distinct, and possibly complementary, paleo-oceanographic information. The results presented in this study should be useful in prioritizing further research efforts in the field of Se biogeochemistry and isotope geochemistry to more firmly develop the proxy potential of this element.

REFERENCES

- Adams D.D., Hurtgen M.T., Sageman B.B. (2010) Volcanic triggering of a biogeochemical cascade during Oceanic Anoxic Event 2. *Nature Geosci* **3**, 201-204.
- Ahlberg P.E.R., Axheimer N., Babcock L.E., Eriksson M.E., Schmitz B., Terfelt F. (2009) Cambrian high-resolution biostratigraphy and carbon isotope chemostratigraphy in Scania, Sweden: first record of the SPICE and DICE excursions in Scandinavia. *Lethaia* **42**, 2-16.
- Amouroux D., Liss P.S., Tessier E., Hamren-Larsson M., Donard O.F.X. (2001) Role of oceans as biogenic sources of selenium. *Earth. Planet. Sci. Lett.* **189**, 277-283.
- Arnold G.L., Anbar A.D., Barling J., Lyons T.W. (2004) Molybdenum Isotope Evidence for Widespread Anoxia in Mid-Proterozoic Oceans. *Science* **304**, 87-90.
- Arthur M.A., Schlanger S.O., Jenkyns H.C. (1987) The Cenomanian-Turonian Oceanic Anoxic Event, II. Palaeoceanographic controls on organic-matter production and preservation. *Geol. Soc. Spec. Pub.* **26**, 401-420.
- Auclair G., Fouquet, Y. and Bohn, M. (1987) Distribution of selenium in high-temperature hydrothermal sulfide deposits at 13° north, East Pacific Rise. *Can. Mineral.* **25**, 577-587.
- Baines S.B., Fisher N.S. (2001) Interspecific differences in the bioconcentration of selenite by phytoplankton and their ecological implications. *Mar. Ecol. Prog. Ser.* **213**, 1-12.
- Baines S.B., Fisher, N.S., Doblin, M.A., Cutter, Gregory A. (2001) Uptake of dissolved organic selenides by marine phytoplankton. *Limnol. Oceanog.* **46**, 1936-1944.
- Balistrieri L.S., Chao T.T. (1987) Selenium adsorption by goethite. *Soil Sci. Soc. Am. J.* **51**, 1145-1151.
- Beier J.A., Hayes J.M. (1989) Geochemical and isotopic evidence for paleoredox conditions during deposition of the Devonian-Mississippian New Albany Shale, southern Indiana. *Geol. Soc. Am. Bull.* **101**, 774-782.
- Böning P., Cuyper S., Grunwald M., Schnetger B., Brumsack H.-J. (2005) Geochemical characteristics of Chilean upwelling sediments at ~36°S. *Mar. Geol.* **220**, 1-21.
- Borchers S.L., Schnetger B., Böning P., Brumsack H.J. (2005) Geochemical signatures of the Namibian diatom belt: Perennial upwelling and intermittent anoxia. *Geochem. Geophys. Geosyst.* **6**, Q06006.
- Breyneart E., Bruggeman C., Maes A. (2008) XANES-EXAFS analysis of Se solid-phase reaction products formed upon contacting Se(IV) with FeS₂ and FeS. *Environ. Sci. Technol.* **42**, 3595-3601.
- Bruggeman C., Maes A., Vancluysen J., Vandemussele P. (2005) Selenite reduction in Boom clay: Effect of FeS₂, clay minerals and

- dissolved organic matter. *Environ. Pollut.* **137**, 209-221.
- Brumsack H.-J. (1991) Inorganic geochemistry of the German 'Posidonia Shale': palaeoenvironmental consequences. *Geological Society, London, Special Publications* **58**, 353-362.
- Brumsack H.J. (1986) The inorganic geochemistry of Cretaceous black shales (DSDP Leg 41) in comparison to modern upwelling sediments from the Gulf of California. *Geol. Soc. Spec. Pub.* **21**, 447-462.
- Brzezinski M.A., Krause J.W., Church M.J., Karl D.M., Li B., Jones J.L., Updyke B. (2011) The annual silica cycle of the north Pacific subtropical gyre. *Deep Sea Res. I Oceanogr. Res. Pap.* **58**, 988-1001.
- Calvert S.E., Bustin R.M., Ingall E.D. (1996) Influence of water column anoxia and sediment supply on the burial and preservation of organic carbon in marine shales. *Geochim. Cosmochim. Acta* **60**, 1577-1593.
- Calvert S.E., Pedersen T.F., Naidu P.D., von Stackelberg U. (1995) On the organic carbon maximum on the continental slope of the eastern Arabian Sea. *J. Mar. Res.* **53**, 269-296.
- Canfield D.E. (2001) Biogeochemistry of Sulfur Isotopes. *Reviews in Mineralogy and Geochemistry* **43**, 607-636.
- Canfield D.E. (2005) The early history of atmospheric oxygen: Homage to Robert A. Garrels. *Annu. Rev. Earth Planet. Sci.* **33**, 1-36.
- Canfield D.E., Habicht K.S., Thamdrup B. (2000) The Archean sulfur cycle and the early history of atmospheric oxygen. *Science* **288**, 658-661.
- Canfield D.E., Kristensen E., Thamdrup B. (2005) The Sulfur Cycle. *Advances in Marine Biology*. Academic Press, pp. 313-381.
- Canfield D.E., Lyons T.W., Raiswell R. (1996) A model for iron deposition to euxinic Black Sea sediments. *Am. J. Sci.* **296**, 818-834.
- Canfield D.E., Raiswell R. (1999) The evolution of the sulfur cycle. *Am. J. Sci.* **299**, 697-723.
- Carignan J., Wen H. (2007) Scaling NIST SRM 3149 for Se isotope analysis and isotopic variations of natural samples. *Chem. Geol.* **242**, 347-350.
- Clark S.K., Johnson T.M. (2008) Effective isotopic fractionation factors for solute removal by reactive sediments: A laboratory microcosm and slurry study. *Environ. Sci. Technol.* **42**, 7850-7855.
- Clark S.K., Johnson T.M. (2010) Selenium stable isotope investigation into selenium biogeochemical cycling in a lacustrine environment: Sweitzer Lake, Colorado. *Journal of Environmental Quality* **39**, 2200-2210.
- Cluff R.M. (1980) Paleoenvironment of the New Albany Shale Group (Devonian-Mississippian) of Illinois. *J. Sediment. Res.* **50**, 767-780.
- Coplen T.B. (2011) Guidelines and recommended terms for expression of stable-isotope-ratio

- and gas-ratio measurement results. *Rapid Commun. Mass Spectrom.* **25**, 2538-2560.
- Cutter G.A. (1982) Selenium in Reducing Waters. *Science* **217**, 829-831.
- Cutter G.A. (1992) Kinetic controls on metalloid speciation in seawater. *Mar. Chem.* **40**, 65-80.
- Cutter G.A., Bruland K.W. (1984) The marine biogeochemistry of selenium: A re-evaluation. *Limnol. Oceanog.* **29**, 1179-1192.
- Cutter G.A., Cutter L.S. (1995) Behavior of dissolved antimony, arsenic, and selenium in the Atlantic Ocean. *Mar. Chem.* **49**, 295-306.
- Degens E.T., Ross D.A. (1974) The Black Sea-Geology, Chemistry and Biology. American Association of Petroleum Geologists, Tulsa, p. 633.
- Doblin M.A., Baines S.B., Cutter L.S., Cutter G.A. (2006) Sources and biogeochemical cycling of particulate selenium in the San Francisco Bay estuary. *Estuar. Coast. Shelf Sci.* **67**, 681-694.
- Ellis A.S., Johnson T.M., Herbel M.J., Bullen T.D. (2003) Stable isotope fractionation of selenium by natural microbial consortia. *Chem. Geol.* **195**, 119-129.
- Erbacher J., Friedrich O., Wilson P.A., Birch H., Mutterlose J. (2005) Stable organic carbon isotope stratigraphy across Oceanic Anoxic Event 2 of Demerara Rise, western tropical Atlantic. *Geochem. Geophys. Geosyst.* **6**, Q06010.
- Fisher I.S.J., Hudson J.D. (1987) Pyrite formation in Jurassic shales of contrasting biofacies. *Geol. Soc. Spec. Pub.* **26**, 69-78.
- Fujieki L.A., Santiago-Mandujano F., Lethaby P., Lukas R., Karl D. (2011) Hawaii Ocean Time-series Data Report 20: 2008. University of Hawaii, Honolulu, Hawaii, p. 395.
- German C.R., Von Damm K.L. (2003) Hydrothermal Processes, *Treatise on Geochemistry*. Pergamon, Oxford, pp. 181-222.
- Gill B.C., Lyons T.W., Young S.A., Kump L.R., Knoll A.H., Saltzman M.R. (2011) Geochemical evidence for widespread euxinia in the Later Cambrian ocean. *Nature* **469**, 80-83.
- Glumac B., Walker K.R. (1998) A Late Cambrian positive carbon-isotope excursion in the Southern Appalachians; relation to biostratigraphy, sequence stratigraphy, environments of deposition, and diagenesis. *J. Sediment. Res.* **68**, 1212-1222.
- Hagiwara Y. (2000) Selenium isotope ratios in marine sediments and algae. A reconnaissance study., MSc Thesis, University of Illinois at Urbana-Champaign.
- Herbel M.J., Blum J.S., Oremland R.S., Borglin S.E. (2003) Reduction of elemental selenium to selenide: Experiments with anoxic sediments and bacteria that respire Se-oxyanions. *Geomicrobiol. J.* **20**, 587-602.
- Herbel M.J., Johnson T.M., Oremland R.S., Bullen T.D. (2000) Fractionation of selenium isotopes during bacterial respiratory reduction of selenium oxyanions. *Geochim. Cosmochim. Acta* **64**, 3701-3709.
- Herbel M.J., Johnson T.M., Tanji K.K., Gao S.D., Bullen T.D. (2002) Selenium stable isotope

- ratios in California agricultural drainage water management systems. *J. Environ. Qual.* **31**, 1146-1156.
- Herbin J.P., Montadert L., Muller C., Gomez R., Thurow J., Wiedmann J. (1986) Organic-rich sedimentation at the Cenomanian-Turonian boundary in oceanic and coastal basins in the North Atlantic and Tethys. *Geol. Soc. Spec. Pub.* **21**, 389-422.
- Hetzel A., Böttcher M.E., Wortmann U.G., Brumsack H.-J. (2009) Paleo-redox conditions during OAE 2 reflected in Demerara Rise sediment geochemistry (ODP Leg 207). *Palaeogeogr., Palaeoclimatol., Palaeoecol.* **273**, 302-328.
- Hockin S.L., Gadd G.M. (2003) Linked redox precipitation of sulfur and selenium under anaerobic conditions by sulfate-reducing bacterial biofilms. *Appl. Environ. Microbiol.* **69**, 7063-7072.
- Hoefs J. (2009) *Stable Isotope Geochemistry*, 6th ed. Springer-Verlag, Berlin, Heidelberg.
- Ingall E.D., Bustin R.M., Van Cappellen P. (1993) Influence of water column anoxia on the burial and preservation of carbon and phosphorus in marine shales. *Geochim. Cosmochim. Acta* **57**, 303-316.
- Ingall E.D., Jahnke R. (1997) Influence of water-column anoxia on the elemental fractionation of carbon and phosphorus during sediment diagenesis. *Mar. Geol.* **139**, 219-229.
- Jenkyns H.C. (2010) Geochemistry of oceanic anoxic events. *Geochem. Geophys. Geosyst.* **11**, Q03004.
- Johnson T.M. (2004) A review of mass-dependent fractionation of selenium isotopes and implications for other heavy stable isotopes. *Chem. Geol.* **204**, 201-214.
- Johnson T.M., Bullen T.D. (2003) Selenium isotope fractionation during reduction by Fe(II)-Fe(III) hydroxide-sulfate (green rust). *Geochim. Cosmochim. Acta* **67**, 413-419.
- Johnson T.M., Bullen T.D. (2004) Mass-Dependent Fractionation of Selenium and Chromium Isotopes in Low-Temperature Environments. *Reviews in Mineralogy and Geochemistry* **55**, 289-317.
- Johnson T.M., Bullen T.D., Zawislanski P.T. (2000) Selenium stable isotope ratios as indicators of sources and cycling of selenium: Results from the northern reach of San Francisco Bay. *Environ. Sci. Technol.* **34**, 2075-2079.
- Johnson T.M., Herbel M.J., Bullen T.D., Zawislanski P.T. (1999) Selenium isotope ratios as indicators of selenium sources and oxyanion reduction. *Geochim. Cosmochim. Acta* **63**, 2775-2783.
- Kerr A.C. (1998) Oceanic plateau formation: a cause of mass extinction and black shale deposition around the Cenomanian-Turonian boundary? *Journal of the Geological Society* **155**, 619-626.
- Krouse H.R., Thode H.G. (1962) Thermodynamic properties and geochemistry of isotopic

- compounds of selenium. *Can. J. Chem.* **40**, 367-375.
- Kulp T.R., Pratt L.M. (2004) Speciation and weathering of selenium in upper cretaceous chalk and shale from South Dakota and Wyoming, USA. *Geochim. Cosmochim. Acta* **68**, 3687-3701.
- Kuypers M.M.M., Pancost R.D., Nijenhuis I.A., Sinninghe Damsté J.S. (2002) Enhanced productivity led to increased organic carbon burial in the euxinic North Atlantic basin during the late Cenomanian oceanic anoxic event. *Paleoceanography* **17**, 1051.
- Lenz M., van Hullebusch E.D., Farges F., Nikitenko S., Borca C.N., Grolimund D., Lens P.N.L. (2008) Selenium speciation assessed by X-Ray absorption spectroscopy of sequentially extracted anaerobic biofilms. *Environ. Sci. Technol.* **42**, 7587-7593.
- Lyons T.W. (1991) Upper Holocene sediments of the Black Sea: Summary of Leg 4 Box Cores (1988 Black Sea Oceanographic Expedition), in: Izdar, E., Murray, J.W. (Eds.), *Black Sea Oceanography*. Kluwer Academic Publisher, pp. 401-441.
- Lyons T.W., Berner R.A., Anderson R.F. (1993) Evidence for large pre-industrial perturbations of the Black Sea chemocline. *Nature* **365**, 538-540.
- Lyons T.W., Kashgarian M. (2005) Paradigm lost, paradigm found-The Black Sea-black shale connection as viewed from the anoxic basin margin. *Oceanography* **18**, 86-99.
- Martens D.A., Suarez D.L. (1997) Selenium Speciation of Marine Shales, Alluvial Soils, and Evaporation Basin Soils of California. *J. Environ. Qual.* **26**, 424-432.
- Measures C.I., Burton J.D. (1980a) Gas chromatographic method for the determination of selenite and total selenium in sea water. *Anal. Chim. Acta* **120**, 177-186.
- Measures C.I., Burton J.D. (1980b) The vertical distribution and oxidation states of dissolved selenium in the northeast Atlantic Ocean and their relationship to biological processes. *Earth. Planet. Sci. Lett.* **46**, 385-396.
- Measures C.I., Grant B.C., Mangum B.J., Edmond J.M. (1983) The relationship of the distribution of dissolved selenium IV and VI in three oceans to the physical and biological process, in: Wong, C.S., Boyle, E., Bruland, K.W., Burton, J.D., Goldberg, E.D. (Ed.), *Trace Metals In Seawater*. Plenum Press, New York.
- Mercone D., Thomson J., Croudace I.W., Troelstra S.R. (1999) A coupled natural immobilisation mechanism for mercury and selenium in deep-sea sediments. *Geochim. Cosmochim. Acta* **63**, 1481-1488.
- Morrison J.M., Codispoti L.A., Smith S.L., Wishner K., Flagg C., Gardner W.D., Gaurin S., Naqvi S.W.A., Manghnani V., Prosperie L., Gundersen J.S. (1999) The oxygen minimum zone in the Arabian Sea during 1995. *Deep Sea Res. II Top. Stud. Oceanogr.* **46**, 1903-1931.
- Nriagu J. (1989) Global Cycling of Selenium, in: Inhat, M. (Ed.),

- Occurrence and Distribution of Selenium*. CRC Press, Boca Raton, Florida, pp. 327-340.
- Ohlendorf H.M. (1989) Bioaccumulation and Effects of Selenium on Wildlife, in: Jacobs, L.W. (Ed.), *Selenium in Agriculture and the Environment*. American Society of Agronomy, Madison, pp. 133-177.
- Oremland R.S. (1991) In situ bacterial selenate reduction in the agricultural drainage systems of western Nevada. *Appl. Environ. Microbiol.* **57**, 615-617.
- Oremland R.S. (1994) Biogeochemical Transformations of Selenium in Anoxic Environments, in: Frankenberger Jr., W.T., Benson, S. (Ed.), *Selenium in the Environment*. Marcel Dekker, New York, pp. 389-419.
- Oremland R.S., Hollibaugh J.T., Maest A.S., Presser T.S., Miller L.G., Culbertson C.W. (1989) Selenate Reduction to Elemental Selenium by Anaerobic-Bacteria in Sediments and Culture - Biogeochemical Significance of a Novel, Sulfate-Independent Respiration. *Appl. Environ. Microbiol.* **55**, 2333-2343.
- Oremland R.S., Steinberg N.A., Maest A.S., Miller L.G., Hollibaugh J.T. (1990) Measurement of in Situ Rates of Selenate Removal by Dissimilatory Bacterial Reduction in Sediments. *Environ. Sci. Technol.* **24**, 1157-1164.
- Raiswell R., Berner R.A. (1985) Pyrite formation in euxinic and semi-euxinic sediments. *Am. J. Sci.* **285**, 710-724.
- Raiswell R., Bottrell S.H., Al-Biatty H.J., Tan M.M. (1993) The influence of bottom water oxygenation and reactive iron content on sulfur incorporation into bitumens from Jurassic marine shales. *Am. J. Sci.* **293**, 569-596.
- Raiswell R., Canfield D.E. (1998) Sources of iron for pyrite formation in marine sediments. *Am. J. Sci.* **298**, 219-245.
- Rashid K., Krouse H.R. (1985) Selenium isotopic fractionation during SeO_3^{2-} reduction to Se^0 and H_2Se . *Can. J. Chem.* **63**, 3195-3199.
- Rees C.E., Thode H.G. (1966) Selenium isotope effects in the reduction of sodium selenite and of sodium selenate. *Can. J. Chem.* **44**, 419-427.
- Reichert G.J., Lourens L.J., Zachariasse W.J. (1998) Temporal Variability in the northern Arabian Sea Oxygen Minimum Zone (OMZ) during the last 225,000 years. *Paleoceanography* **13**, 607-621.
- Röhl H.-J., Schmid-Röhl A., Oschmann W., Frimmel A., Schwark L. (2001) The Posidonia Shale (Lower Toarcian) of SW-Germany: an oxygen-depleted ecosystem controlled by sea level and palaeoclimate. *Palaeogeogr., Palaeoclimatol., Palaeoecol.* **165**, 27-52.
- Rother M. (2012) Selenium Metabolism in Prokaryotes, in: Hatfield, D.L., Berry, M.J., Gladyshev, V.N. (Eds.), *Selenium*. Springer New York, pp. 457-470.
- Rouxel O., Fouquet Y., Ludden J.N. (2004) Subsurface processes at the lucky strike hydrothermal

- field, Mid-Atlantic ridge: evidence from sulfur, selenium, and iron isotopes. *Geochim. Cosmochim. Acta* **68**, 2295-2311.
- Rouxel O., Ludden J., Carignan J., Marin L., Fouquet Y. (2002) Natural variations of Se isotopic composition determined by hydride generation multiple collector inductively coupled plasma mass spectrometry. *Geochim. Cosmochim. Acta* **66**, 3191-3199.
- Rubin K. (1997) Degassing of metals and metalloids from erupting seamount and mid-ocean ridge volcanoes: Observations and predictions. *Geochim. Cosmochim. Acta* **61**, 3525-3542.
- Saltzman M.R., Ripperdan R.L., Brasier M.D., Lohmann K.C., Robison R.A., Chang W.T., Peng S., Ergaliev E.K., Runnegar B. (2000) A global carbon isotope excursion (SPICE) during the Late Cambrian: relation to trilobite extinctions, organic-matter burial and sea level. *Palaeogeogr., Palaeoclimatol., Palaeoecol.* **162**, 211-223.
- Saltzman M.R., Runnegar B., Lohmann K.C. (1998) Carbon isotope stratigraphy of Upper Cambrian (Steptoean Stage) sequences of the eastern Great Basin: Record of a global oceanographic event. *Geol. Soc. Am. Bull.* **110**, 285-297.
- Scheinost A.C., Charlet L. (2008) Selenite reduction by mackinawite, magnetite and siderite: XAS characterization of nanosized redox products. *Environ. Sci. Technol.* **42**, 1984-1989.
- Schilling K., Johnson T.M., Wilcke W. (2011) Isotope Fractionation of Selenium During Fungal Biomethylation by *Alternaria alternata*. *Environ. Sci. Technol.* **45**, 2670-2676.
- Schlanger S.O., Arthur M.A., Jenkyns H.C., Scholle P.A. (1987) The Cenomanian-Turonian Oceanic Anoxic Event, I. Stratigraphy and distribution of organic carbon-rich beds and the marine $\delta^{13}\text{C}$ excursion. *Geol. Soc. Spec. Pub.* **26**, 371-399.
- Schlanger S.O., Jenkyns H.C. (1976) Cretaceous oceanic anoxic events: causes and consequences. *Neth. J. Geosci.* **55**, 179-184.
- Schlanger S.O., Jenkyns H.C., Premoli-Silva I. (1981) Volcanism and vertical tectonics in the Pacific Basin related to global Cretaceous transgressions. *Earth. Planet. Sci. Lett.* **52**, 435-449.
- Schmid-Röhl A., Röhl H.-J., Oschmann W., Frimmel A., Schwark L. (2002) Palaeoenvironmental reconstruction of Lower Toarcian epicontinental black shales (Posidonia Shale, SW Germany): global versus regional control. *Geobios* **35**, 13-20.
- Schouten S., van Kaam-Peters H.M.E., Rijpstra W.I.C., Schoell M., Sinninghe Damste J.S. (2000) Effects of an oceanic anoxic event on the stable carbon isotopic composition of early Toarcian carbon. *Am. J. Sci.* **300**, 1-22.
- Shen Y.A., Buick R., Canfield D.E. (2001) Isotopic evidence for microbial sulphate reduction in the early Archaean era. *Nature* **410**, 77-81.

- Sherrard J.C., Hunter K.A., Boyd P.W. (2004) Selenium speciation in subantarctic and subtropical waters east of New Zealand: trends and temporal variations. *Deep Sea Res. I Oceanogr. Res. Pap.* **51**, 491-506.
- Sinninghe-Damsté J.S., Rijpstra W.I.C., Reichart G.J. (2002) The influence of oxic degradation on the sedimentary biomarker record II. Evidence from Arabian Sea sediments. *Geochim. Cosmochim. Acta* **66**, 2737-2754.
- Sinninghe Damsté J.S., Wakeham S.G., Kohnen M.E.L., Hayes J.M., de Leeuw J.W. (1993) A 6,000-year sedimentary molecular record of chemocline excursions in the Black Sea. *Nature* **362**, 827-829.
- Sinton C.W., Duncan R.A. (1997) Potential links between ocean plateau volcanism and global ocean anoxia at the Cenomanian-Turonian boundary. *Economic Geology* **92**, 836-842.
- Snow L.J., Duncan R.A., Bralower T.J. (2005) Trace element abundances in the Rock Canyon Anticline, Pueblo, Colorado, marine sedimentary section and their relationship to Caribbean plateau construction and oxygen anoxic event 2. *Paleoceanography* **20**, PA3005.
- Sokolova Y.G., Pilipchuck M.F. (1973) Geochemistry of Selenium in sediments in the NW part of the Pacific Ocean. *Geokhimiya (Geochemistry International)* **10**, 1537-1546.
- Stolz J.F., Basu P., Oremland R.S. (2002) Microbial transformation of elements: the case of arsenic and selenium. *International Microbiology* **5**, 201-207.
- Suzuoki T. (1964) A geochemical study of selenium in volcanic exhalation and sulfur deposits. *Bull. Chem. Soc. Jpn.* **37**, 1200-1206.
- Thickpenny A. (1984) The sedimentology of the Swedish Alum Shales. *Geol. Soc. Spec. Pub.* **15**, 511-525.
- Thickpenny A. (1987) Palaeo-oceanography and depositional environment of the Scandinavian Alum Shales: sedimentological and geochemical evidence., in: Leggett, J.K., Zuffa, G.G. (Eds.), *Marine Clastic Sedimentology—Concepts and Case Studies*. Graham & Trotman, London, pp. 156-171.
- Thomson J., Jarvis I., Green D.R.H., Green D.A., Clayton T. (1998) Mobility and immobility of redox-sensitive elements in deep-sea turbidites during shallow burial. *Geochim. Cosmochim. Acta* **62**, 643-656.
- Tudge A.P., Thode H.G. (1950) Thermodynamic properties of isotopic compounds of sulfur. *Can. J. Res.* **28**, 567-578.
- Turekian K.K., Wedepohl K.H. (1961) Distribution of the elements in some major units of the Earth's crust. *Geol. Soc. Am. Bull.* **72**, 175-192.
- Turgeon S.C., Creaser R.A. (2008) Cretaceous oceanic anoxic event 2 triggered by a massive magmatic episode. *Nature* **454**, 323-326.
- Van Cappellen P., Ingall E.D. (1994) Benthic phosphorus regeneration, net primary production, and ocean anoxia: A model of the coupled

- marine biogeochemical cycles of carbon and phosphorus. *Paleoceanography* **9**, 677-692.
- Van Cappellen P., Ingall E.D. (1996) Redox stabilization of the atmosphere and oceans by phosphorus-limited marine productivity. *Science* **271**, 493-496.
- van der Weijden C.H., Reichart G.J., van Os B.J.H. (2006) Sedimentary trace element records over the last 200 kyr from within and below the northern Arabian Sea oxygen minimum zone. *Mar. Geol.* **231**, 69-88.
- Vandermeulen J.H., Foda A. (1988) Cycling of selenite and selenate in marine phytoplankton. *Mar. Biol.* **98**, 115-123.
- Velinsky D.J., Cutter G.A. (1990) Determination of elemental selenium and pyrite-selenium in sediments. *Anal. Chim. Acta* **235**, 419-425.
- Von Damm K.L. (1991) Controls on the Chemistry and Temporal Variability of Seafloor Hydrothermal Fluids, *Seafloor Hydrothermal Systems: Physical, Chemical, Biological, and Geological Interactions*. American Geophysical Union.
- Von Damm K.L., Edmond J.M., Grant B., Measures C.I., Walden B., Weiss R.F. (1985a) Chemistry of submarine hydrothermal solutions at 21 [deg]N, East Pacific Rise. *Geochim. Cosmochim. Acta* **49**, 2197-2220.
- Von Damm K.L., Edmond J.M., Measures C.I., Grant B. (1985b) Chemistry of submarine hydrothermal solutions at Guaymas Basin, Gulf of California. *Geochim. Cosmochim. Acta* **49**, 2221-2237.
- Watkins-Brandt K.S. (2010) Phosphorus control of Nitrogen Fixation. MSc Thesis, Oregon State University.
- Wen H., Carignan J. (2011) Selenium isotopes trace the source and redox processes in the black shale-hosted Se-rich deposits in China. *Geochim. Cosmochim. Acta* **75**, 1411-1427.
- Wen H., Carignan J., Hu R., Fan H., Chang B., Yang G. (2007) Large selenium isotopic variations and its implication in the Yutangba Se deposit, Hubei Province, China. *Chin. Sci. Bull.* **52**, 2443-2447.
- Wen H., Carignan J., Qiu Y., Liu S. (2006) Selenium speciation in kerogen from two Chinese selenium deposits: Environmental implications. *Environ. Sci. Technol.* **40**, 1126-1132.
- Wen H., Qiu Y. (1999) Organic and inorganic occurrence of selenium in Laerma Se-Au deposit. *Science in China Series D: Earth Sciences* **42**, 662-669.
- Wen H., Qiu Y. (2002) Geology and geochemistry of Se-bearing formations in Central China. *International Geology Review* **44**, 164-178.
- Weres O., Jaouni A.-R., Tsao L. (1989) The distribution, speciation and geochemical cycling of selenium in a sedimentary environment, Kesterson Reservoir, California, U.S.A. *Appl. Geochem.* **4**, 543-563.
- Wignall P.B. (1994) *Black Shales*. Oxford University Press, Oxford.
- Wrench J.J., Measures C.I. (1982) Temporal variations in dissolved

- selenium in a coastal ecosystem. *Nature* **299**, 431-433.
- Wright M.T., Parker D.R., Amrhein C. (2003) Critical evaluation of the ability of sequential extraction procedures to quantify discrete forms of selenium in sediments and soils. *Environ. Sci. Technol.* **37**, 4709-4716.
- Yu M., Tian W., Sun D., Shen W., Wang G., Xu N. (2001) Systematic studies on adsorption of 11 trace heavy metals on thiol cotton fiber. *Anal. Chim. Acta* **428**, 209-218.
- Zehr J.P., Oremland R.S. (1987) Reduction of selenate to selenide by sulfate-respiring bacteria: experiments with cell suspensions and estuarine sediments. *Appl. Environ. Microbiol.* **53**, 1365-1369.
- Zhu J.-M., Johnson T.M., Clark S.K., Zhu X.-K. (2008) High precision measurement of selenium isotopic composition by hydride generation Multiple Collector Inductively Coupled Plasma Mass Spectrometry with a ^{74}Se - ^{77}Se double spike. *Chinese J. Anal. Chem.* **36**, 1385-1390.
- Zhu J., Zuo W., Liang X., Li S., Zheng B. (2004) Occurrence of native selenium in Yutangba and its environmental implications. *Appl. Geochem.* **19**, 461-467.

SUPPLEMENTAL INFORMATION

The Supplementary Material presents the individual data sets for each of the sampling locations. The data includes selenium concentrations and isotopic compositions determined in this study, as well as ancillary data from the literature. Also included is a more detailed description of the selenium isotope interferences and calculations.

4.7 SITE DATA

4.7.1 BLACK SEA

The selenium concentrations in the sediments from the oxic sites range from 0.22 to 0.49 ppm, with an average value of 0.35 ± 0.13 ppm (1σ). For the deep basin sites, the corresponding range is 0.35 to 2.35 ppm, with an average concentration of 0.76 ± 0.7 ppm. Although the average $^{82/76}\text{Se}$ isotopic composition at the oxic sites is slightly heavier than at the deep basin sites ($0.45 \pm 0.11\text{‰}$ versus $0.29 \pm 0.28\text{‰}$), the $\delta^{82/76}\text{Se}$ ranges essentially overlap. Both the Se/TOC ratios and the $\delta^{82/76}\text{Se}$ values of the Black Sea samples are comparable to the values measured on modern marine phytoplankton.

Table EA 1 Black Sea (Data for stations 3, 4, δ^{16} from (Lyons et al., 1993) and data from stations 9 & 14 from (Lyons and Berner, 1992).

Sample Name	[Se] (ppm)	$\delta^{82/76}\text{Se}$ (‰)	Se/TOC (mol/mol)	TOC (wt.%)	Pyrite S (wt.%)	Total S (wt.%)	Depositional environment
BS4 STA9 BC1b 20-22 cm	2.39	0.26	6.36×10^{-6}	5.71	1.62	1.62	euxinic unit 1
BS4 STA14 BC1 20-22 cm	1.42	-0.04	4.63×10^{-6}	4.65	0.76	0.76	euxinic unit 1
BS4 STA3 BC- 1b 6-8	0.43	0.22	4.87×10^{-6}	1.33	3.19	3.19	paleo- chemocline
BS4 STA3 BC- 1b 8-10	0.30	0.25	3.17×10^{-6}	1.40	3.23	3.23	paleo- chemocline
BS4 STA3 BC- 1b 12-14	0.25	0.31	2.43×10^{-6}	1.42	1.19	1.19	paleo- chemocline
BS4 STA4 BC- 1a 8-10	0.47	0.20	3.88×10^{-6}	1.85	2.28	2.28	paleo- chemocline
BS4 STA4 BC- 1a 10-12	0.40	0.74	2.94×10^{-6}	2.04	2.4	2.4	paleo- chemocline
BS4 STA4 BC- 1a 14-16	0.42	-	3.64×10^{-6}	1.74	1.39	1.39	paleo- chemocline
BS4 STA4 BC- 1a 2-4	0.43	0.58	4.99×10^{-6}	1.31	-	-	oxic
BS4 STA16 BC1 0-2 cm	0.27	0.50	4.15×10^{-6}	1.00	0.09	0.09	oxic
BS4 STA16 BC1 16-18 cm	0.22	0.33	3.29×10^{-6}	1.01	0.01	0.019	oxic
BS4 STA3 BC- 1b 2-4	0.49	0.39	5.10×10^{-6}	1.47	0.12	0.121	oxic

4.7.2 ARABIAN SEA

The data for both Arabian Sea cores are displayed in Figure EA 1. The selenium concentrations fall mostly in the range 1-4 ppm, except for sediments from the 100-125 kyr time interval in core 463, which exhibit Se concentrations of up to ~11 ppm. Sediments from both cores show a very limited range in isotopic composition (< 0.5‰). The $\delta^{82/76}\text{Se}$ values are among the most negative ones in the entire data set, with most values falling below 0‰. The molar Se/TOC ratios of the Arabian Sea sediments (2.01×10^{-5} to 3.44×10^{-5}) exceed those measured on marine phytoplankton (3.2×10^{-6}).

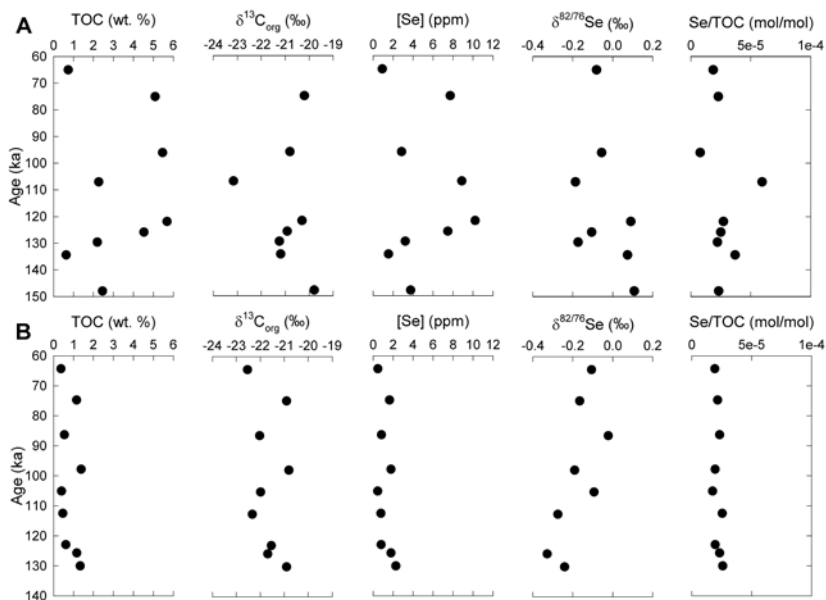


Figure EA 1 Arabian Sea data from A) NIOP Core 463 and B) NIOP Core 464 on the Murray Ridge. For detailed descriptions of the sites, cores and $\delta^{13}\text{C}$ and TOC data, see Reichart et al. (1997) and Sinninghe-Damsté et al. (2002).

Table EA 2 Arabian Sea selenium concentration, isotope and Se/TOC data. For detailed descriptions of the sites, cores and $\delta^{13}\text{C}$, TOC and Total S data, see Reichart et al. (1997) and Sinninghe-Damsté et al. (2002).

Sample Name	Age (kyr)	[Se] (ppm)	$\delta^{82/76}\text{Se}$ (‰)	Se/TOC (mol/mol)	TOC (wt.%)	$\delta^{13}\text{C}$ (‰)	Total S (wt.%)
NIOP 463 113	65.00	0.91	-0.08‰	1.88×10^{-5}	0.74	-	0.60
NIOP 463 104	75.00	7.72	-	2.30×10^{-5}	5.09	-20.20	1.00
NIOP 463 82	96.00	2.85	-0.06‰	7.93×10^{-6}	5.46	-20.80	0.60
NIOP 463 88	107.00	8.89	-0.19‰	5.96×10^{-5}	2.27	-23.16	0.90
NIOP 463 73	121.85	10.22	0.09‰	2.73×10^{-5}	5.69	-20.30	1.50
NIOP 463 70	125.83	7.49	-0.11‰	2.51×10^{-5}	4.53	-20.92	1.00
NIOP 463 68	129.60	3.22	-0.17‰	2.23×10^{-5}	2.19	-21.24	0.60
NIOP 463 65	134.39	1.54	0.07‰	3.70×10^{-5}	0.63	-21.19	0.40
NIOP 463 56	147.92	3.76	0.11‰	2.33×10^{-5}	2.45	-19.79	0.80
NIOP 464 148	64.30	0.48	-0.11‰	1.93×10^{-5}	0.37	-22.53	-
NIOP 464 136	74.74	1.65	-0.17‰	2.16×10^{-5}	1.16	-20.90	0.20
NIOP 464 124	86.32	0.84	-0.02‰	2.33×10^{-5}	0.55	-22.03	0.40
NIOP 464 116	97.81	1.78	-0.19‰	1.96×10^{-5}	1.39	-20.80	0.20
NIOP 464 112	105.07	0.46	-0.09‰	1.74×10^{-5}	0.40	-21.99	0.50
NIOP 464 108	112.50	0.78	-0.27‰	2.55×10^{-5}	0.46	-22.33	0.20
NIOP 464 104	122.92	0.80	-	1.96×10^{-5}	0.62	-21.54	0.70
NIOP 464 101	125.69	1.79	-0.33‰	2.33×10^{-5}	1.17	-21.69	0.30
NIOP 464 97	130.00	2.28	-0.24‰	2.59×10^{-5}	1.34	-20.90	0.60
NIOP 464 93	136.03	3.93	-0.08‰	1.70×10^{-5}	3.52	-	0.50

4.7.3 DEMERARA RISE AND CAPE VERDE BASIN

Very high selenium concentrations are observed in the Demerara Rise and the Cape Verde Basin samples (Figure EA 2), compared to the typical concentrations measured on the other rocks and sediment shales presented in this study. The maximum concentrations in the Demerara Rise (> 30 ppm) and Cape Verde Basin samples (> 70 ppm) are found after and before OAE2, respectively. During OAE2, the selenium concentrations drop to values 2-3 times lower than those before and after the event. Together with the increase in TOC, this leads to a major drop in the Se/TOC ratios during OAE2.

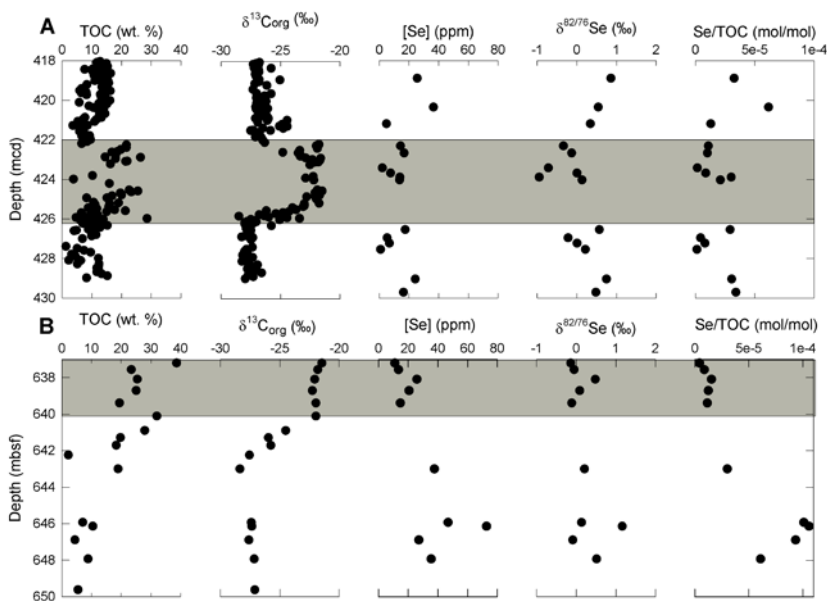


Figure EA 2 Data from the A) Demerara Rise and B) Cape Verde Basin cores. Grey bars indicate OAE2 as defined by the $\delta^{13}\text{C}_{\text{org}}$ excursion. Data for TOC and $\delta^{13}\text{C}$ for Demerara Rise are from Erbacher et al. (2005) and for Cape Verde Basin from Kuypers et al. (2002).

Table EA 3 Demerara Rise selenium concentration, isotope and Se/TOC data. Data for sulfur, TOC and $\delta^{13}\text{C}$ for Demerara Rise are from Erbacher et al. (2005), depth has been updated after MacLeod (2008).

Sample Name	Depth (mcd)	[Se] (ppm)	$\delta^{82/76}\text{Se}$ (‰)	Se/TOC (mol/mol)	TOC (wt.%)	$\delta^{13}\text{C}$ (‰)	Total S (wt.%)	$\delta^{34}\text{S}_{\text{py}}$ (‰)
207 1258A 42-4 18-20	418.89	25.61	0.86‰	3.27×10^{-5}	13.52	-26.88	3.23	-13.73
207 1258A 42-5 18-20	420.35	36.55	0.54‰	6.17×10^{-5}	13.47	-27.09	3.24	-13.87
2071258A 42-5 102-103	421.19	4.85	0.34‰	1.30×10^{-5}	5.65	-24.49	1.47	-24.40
207 1258A 42-6 82-83	422.31	14.39	-0.34‰	1.10×10^{-5}	19.88	-21.90	5.80	-26.79
2071258A 42-6 118-119	422.67	16.77	-0.13‰	1.01×10^{-5}	25.11	-23.44	7.49	-25.69
207 1258A 42-7 53-54	423.42	2.10	0.72‰	1.72×10^{-6}	18.58	-22.53	4.54	-22.52
207-1258A 42-7 79-80	423.68	7.63	0.00‰	8.76×10^{-6}	13.24	-22.39	-	-
207-1258A 42-7 100-101	423.89	13.97	0.95‰	3.02×10^{-5}	7.02	-22.89	-	-
207-1258A 42-7 114-115	424.03	13.71	0.13‰	2.11×10^{-5}	9.86	-22.20	-	-
2071258A 42 CC 4-5	426.54	17.53	0.57‰	2.93×10^{-5}	9.09	-	1.85	-5.46
207-1258A 43-1 41-42	426.96	5.35	-0.22‰	4.42×10^{-6}	18.40	-22.45	-	-
207-1258A 43-1 75-76.5	427.23	6.84	0.00‰	8.09×10^{-6}	12.85	-21.88	-	-
207 1258A 43-1 106-107	427.54	0.95	0.22‰	1.37×10^{-6}	10.50	-23.10	-	-
207 1258A 43-3 2-3	429.04	24.27	0.75‰	3.06×10^{-5}	12.04	-28.12	-	-
207 1258A 43- 3 68.5-70	429.71	16.32	0.48‰	3.41×10^{-5}	7.26	-27.94	-	-
207 1258A 43-3 101-103	430.03	16.02	0.34‰	3.58×10^{-5}	6.80	-27.77	-	-
207 1258A 43- 4 39-40.5	430.46	13.82	0.59‰	2.61×10^{-5}	8.04	-27.65	-	-

Table EA 4 Cape Verde Basin selenium concentration, isotope and Se/TOC data, $\delta^{13}\text{C}$ (‰) from Kuypers et al. (2002).

Sample Name	Depth (mbsf)	[Se] (ppm)	$\delta^{82/76}\text{Se}$ (‰)	Se/TOC (mol/mol)	TOC (wt.%)	$\delta^{13}\text{C}$ (‰)
ODP 367 18-1 120-124 cm	637.20	11.00	-0.14‰	4.32×10^{-6}	38.65	-21.45
ODP 367 18-2 6-9	637.56	13.49	-0.06‰	8.74×10^{-6}	23.43	-21.80
ODP 367 18-2 59-62 cm	638.09	25.89	0.48‰	1.55×10^{-5}	25.43	-22.05
ODP 367 18-2 121-125	638.71	20.63	0.09‰	1.25×10^{-5}	25.06	-22.25
ODP 367 18-3 39-42	639.39	14.77	-0.12‰	1.15×10^{-5}	19.44	-21.95
ODP 367 18-5 100-106 cm	643.00	37.60	0.21‰	3.01×10^{-5}	18.95	-28.35
ODP 367 19-1 143-147	645.93	46.88	0.13‰	1.01×10^{-4}	7.06	-27.40
ODP 367 19-2 14-18	646.14	72.80	1.16‰	1.06×10^{-4}	10.45	-27.35
ODP 367 19-2 89-94 cm	646.89	27.21	-0.09‰	9.34×10^{-5}	4.42	-27.60
ODP 367 19-3 43-47 cm	647.93	35.48	0.51‰	6.09×10^{-5}	8.85	-27.15

The shales deposited at Demerara Rise during OAE2 have the most negative $\delta^{82/76}\text{Se}$ compositions of the entire dataset collected in this study, with a minimum $\delta^{82/76}\text{Se}$ value of -0.72‰. The Demerara Rise core also shows the largest isotopic shift between samples. The average $\delta^{82/76}\text{Se}$ during OAE2 is $-0.14 \pm 0.45\%$, before the event it is $0.54 \pm 0.17\%$, and after the event $0.58 \pm 0.26\%$. The general trend in $\delta^{82/76}\text{Se}$ in the Cape Verde Basin core is similar, but less pronounced,

than for the Demerara Rise. The average $\delta^{82/76}\text{Se}$ values before and during OAE2 are $0.39\pm 0.48\text{‰}$ and $0.05\pm 0.26\text{‰}$, respectively. Note, however, that only the lower portion of OAE2 is captured by the available Cape Verde Basin core material; that is, the data may not be representative for the entire OAE2.

4.7.4 POSIDONIA SHALE

If we exclude the organic-poor mudstones at the bottom of the core, the selenium concentrations and isotopic compositions vary little along the core (Figure EA 3). The selenium concentrations tend to be slightly lower during the OAE (average: 2.01 ± 0.59 ppm), compared to after the event (average: $2.72\pm 0.70\text{‰}$). The Se/TOC ratios are distinctly lower during the Toarcian OAE, primarily because of the higher TOC concentrations. The $\delta^{82/76}\text{Se}$ values range over approximately 1‰ and are, on average, higher during ($0.36\pm 0.25\text{‰}$) than before ($0.15\pm 0.21\text{‰}$) or after the event ($0.15\pm 0.29\text{‰}$).

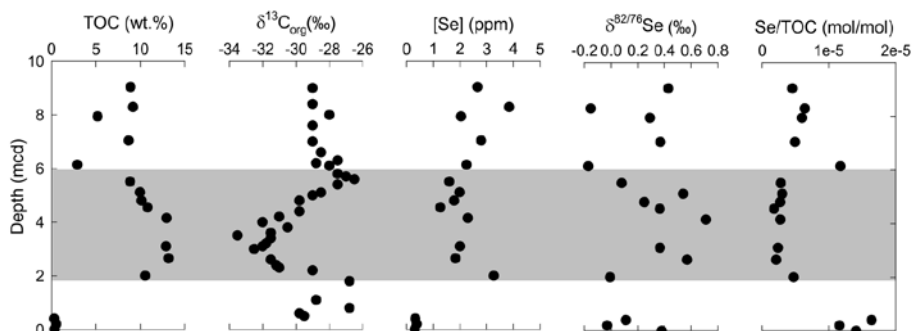


Figure EA 3 Posidonia Shale. Grey bar indicates Toarcian OAE based on $\delta^{13}\text{C}$ values. TOC data from B. Gill, personal communication and $\delta^{13}\text{C}_{\text{org}}$ data from Schmid-Röhl et al. (2002).

Table EA 5 Posidonia Shale selenium concentration, isotope and Se/TOC data. TOC data from B. Gill, personal communication and $\delta^{13}\text{C}_{\text{org}}$ data from Schmid-Röhl et al. (2002).

Sample Name	Depth (mcd)	[Se] (ppm)	$\delta^{82/76}\text{Se}$ (‰)	Se/TOC (mol/mol)	TOC (wt. %)	$\delta^{13}\text{C}$ (‰)	Total S (wt.%)	Pyrite S (wt.%)	$\delta^{34}\text{S}_{\text{py}}$ (‰)
DO-1	0.0	0.31	0.38	1.41×10^{-5}	0.34	-29.5	1.13	0.86	-34.6
DO-2	0.2	0.39	-0.03	1.16×10^{-5}	0.52	-29.8	1.00	1.15	-3.2
DO-3	0.4	0.33	0.11	1.64×10^{-5}	0.31	-26.8	1.61	2.15	-25.3
DO-11 PS	2.0	3.27	-0.01	4.71×10^{-6}	10.53	-26.8	3.67	3.12	-26.4
DO-13	2.7	1.83	0.57	2.11×10^{-6}	13.16	-31.5	4.74	3.61	3.4
DO-15	3.1	2.01	0.37	2.36×10^{-6}	12.90	-32.0	3.80	3.22	-24.6
DO-20	4.2	2.30	0.71	2.70×10^{-6}	12.95	-31.0	3.77	2.87	-24.1
DO-23 PS	4.6	1.27	0.37	1.79×10^{-6}	10.83	-29.8	3.25	2.49	-27.4
DO-25	4.8	1.78	0.25	2.67×10^{-6}	10.13	-29.8	3.04	3.01	-27.6
DO-27	5.1	2.00	0.54	3.04×10^{-6}	9.98	-28.5	3.94	3.30	-29.8
DO-30	5.5	1.61	0.08	2.76×10^{-6}	8.85	-27.0	4.07	3.31	-29.6
DO-34	6.1	2.25	-0.17	1.18×10^{-5}	2.91	-28.0	3.19	2.84	-36.1
DO-38	7.0	2.80	0.37	4.91×10^{-6}	8.66	-29.0	2.66	2.12	-31.2
DO-43	7.9	2.04	0.29	5.97×10^{-6}	5.19	-28.0	2.12	1.67	-
DO-45	8.3	3.85	-0.15	6.36×10^{-6}	9.19	-29.0	2.83	1.55	-30.0
DO-48	9.0	2.66	0.43	4.54×10^{-6}	8.90	-29.0	2.33	2.77	-28.8

4.7.5 NEW ALBANY SHALE

On average, the bioturbated grey shales have slightly lower selenium concentrations than the laminated black shales (0.67 ± 0.28 versus 0.89 ± 0.12 ppm) (Figure EA 4). The Se/TOC ratios are much higher in the bioturbated layers, however, because of the much lower TOC concentrations. Systematic differences in the selenium isotopic compositions are also observed between shale layers deposited under oxic and anoxic conditions: bioturbated shales are lighter with an average $\delta^{82/76}\text{Se}$ value of 0.67 ± 0.80 ‰ versus 1.71 ± 0.48 ‰ for the laminated shales.

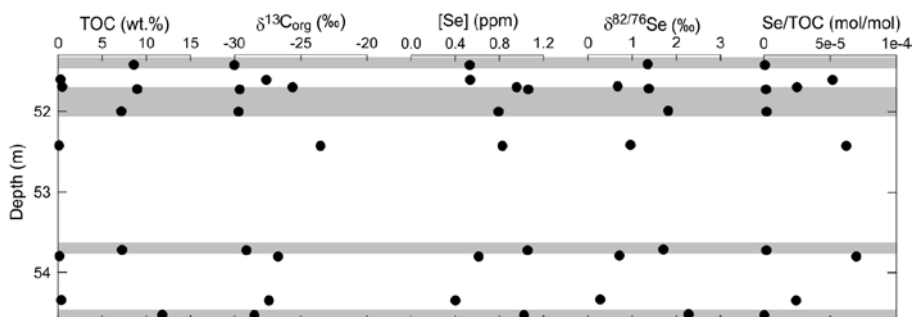


Figure EA 4 New Albany Shale. Grey bars indicate laminated black shales; white sections indicate bioturbated grey shales. TOC data are from Ingall et al. (1993) and $\delta^{13}\text{C}_{\text{org}}$ data are from Calvert et al. (1996).

Table EA 6 New Albany Shale selenium concentration, isotope and Se/TOC data. TOC and Total S are from Ingall et al. (1993) and $\delta^{13}\text{C}_{\text{org}}$ data are from Calvert et al. (1996)

Sample Name	Depth (mcd)	[Se] (ppm)	$\delta^{82/76}\text{Se}$ (‰)	Se/TOC (mol/mol)	TOC (wt. %)	$\delta^{13}\text{C}$ (‰)	Total S (wt.%)
6 CR168.7	51.42	0.53	1.36	9.36×10^{-7}	8.6	-30.0	3.79
9 CR169.3	51.60	0.53	0.71	2.62×10^{-5}	0.31	-27.6	0.56
12 CR169.6	51.69	0.96	0.67	3.03×10^{-5}	0.48	-25.6	1.63
13 CR169.7	51.72	1.06	1.38	1.80×10^{-6}	8.96	-29.6	3.48
17 CR170.6	52.00	0.79	1.82	1.68×10^{-6}	7.17	-29.7	3.44
22 CR172.0	52.43	0.83	0.96	9.67×10^{-5}	0.13	-23.5	1.19
46 CR176.25	53.72	1.05	1.71	2.21×10^{-6}	7.24	-29.1	2.32
47 CR176.5	53.80	0.61	0.72	5.16×10^{-5}	0.18	-26.7	0.42
59 CR178.3	54.35	0.40	0.28	1.60×10^{-5}	0.38	-27.4	1.39
63 CR178.9	54.53	1.02	2.28	1.31×10^{-6}	11.83	-28.5	3.30

4.7.6 ALUM SHALE

The SPICE event is accompanied by a lowering of the selenium concentrations and $\delta^{82/76}\text{Se}$ values (Figure EA 5). The average selenium concentration during the event is 2.03 ± 0.61 ppm. Before SPICE the average concentration is 1.71 ± 0.60 ppm, while after SPICE it increases to 2.88 ± 0.35 ppm. The molar Se/TOC ratios remain fairly constant along the core ($3.33 \times 10^{-6} \pm 1.47 \times 10^{-6}$ to $3.26 \times 10^{-6} \pm 4.77 \times 10^{-7}$), with values close to those of modern marine phytoplankton. The selenium isotopic composition at the bottom of the core is relatively light ($\delta^{82/76}\text{Se} = 0.24 \pm 0.35\text{‰}$). The $\delta^{82/76}\text{Se}$ values

increase before the anoxic event, with a peak value at 0.79‰. Within SPICE, $\delta^{82/76}\text{Se}$ values exhibit a local minimum that coincides with the maximum in $\delta^{13}\text{C}_{\text{org}}$ and the minimum in selenium concentration. The average $\delta^{82/76}\text{Se}$ during SPICE is 0.28 ± 0.26 ‰. After SPICE, $\delta^{82/76}\text{Se}$ increases to 0.65 ± 0.06 ‰.

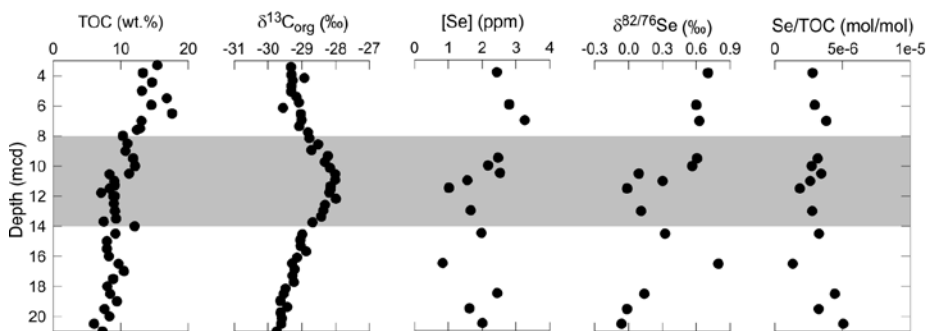


Figure EA 5 Alum Shale. Grey bar indicates the SPICE event based on $\delta^{13}\text{C}$ data. Data for TOC (Gill et al., 2011) and $\delta^{13}\text{C}_{\text{org}}$ from Ahlberg et al. (2009a).

Table EA 7 Alum Shale selenium concentration, isotope and Se/TOC data. Data for TOC and sulfur from Gill et al. (2011) and $\delta^{13}\text{C}_{\text{org}}$ from Ahlberg et al. (2009a).

Sample Name	Depth (mcd)	[Se] (ppm)	$\delta^{82/76}\text{Se}$ (‰)	Se/TOC (mol/mol)	TOC (wt.%)	$\delta^{13}\text{C}$ (‰)	Pyrite S (wt.%)	Total S (wt.%)	$\delta^{34}\text{S}_{\text{py}}$ (‰)
Alum47	20.5	2.01	-0.06	5.04×10^{-6}	6.06	-29.61	4.42	5.13	3.5
Alum49	19.5	1.63	-0.01	3.25×10^{-6}	7.60	-29.53	4.09	5.26	1.8
Alum51	18.5	2.45	0.14	4.43×10^{-6}	8.41	-29.53	4.64	5.91	4.0
Alum55	16.5	0.84	0.80	1.32×10^{-6}	9.67	-29.28	4.56	5.51	7.0
Alum59	14.5	1.60	0.32	2.64×10^{-6}	9.22	-28.98	4.26	5.69	7.0
Alum62	13	2.41	0.11	3.99×10^{-6}	9.18	-28.39	4.33	5.65	14.4
Alum65	11.5	1.02	-0.01	1.86×10^{-6}	8.34	-28.16	3.45	4.60	21.6
Alum66	11	1.56	0.30	2.61×10^{-6}	9.08	-28.08	5.1	5.64	18.3
Alum67	10.5	2.53	0.09	3.43×10^{-6}	11.22	-28.09	4.82	5.49	20.1
Alum68	10	2.18	0.57	2.72×10^{-6}	12.13	-30.04	6.16	7.45	16.1
Alum69	9.5	2.47	0.61	3.17×10^{-6}	11.83	-28.28	6.18	7.95	14.3
Alum74	7	3.26	0.63	3.80×10^{-6}	13.03	-29.04	3.75	5.73	0.3
Alum76	5.95	2.80	0.60	2.93×10^{-6}	14.51	-29.32	3.02	4.10	-1.7
Alum78	5	3.03	-0.05	3.51×10^{-6}	13.10	-29.31	4.02	4.85	0.5
Alum80	3.8	2.44	0.71	2.79×10^{-6}	13.28	-29.31	3.97	4.90	-3.8

4.8 SELENIUM ISOTOPE ANALYTICAL INTERFERENCES AND DOUBLE SPIKE CALCULATIONS

4.8.1 ISOBARIC INTERFERENCES

MC-ICP-MS analysis of Se involves correction for numerous isobaric interferences (Table EA8). For example, the Ar-based plasma generates polyatomic ions ($^{40}\text{Ar}^{40}\text{Ar}^+$), Kr is a ubiquitous trace gas in compressed Ar, and atmospheric Kr diffuses into sample solutions. Traces of Ge, As, and Br also occur in prepared samples, causing additional interferences. Interferences are monitored and corrected for when necessary. Many are eliminated or reduced in size by measuring signal intensities on blank solutions (on-mass zeros) and subtracting them from the measured intensities.

Table EA 8 Isobaric interferences for Se isotope analysis

74	76	77	78	80	82
^{74}Ge	$^{40}\text{Ar}^{36}\text{Ar}$	$^{40}\text{Ar}^{37}\text{Cl}$	$^{40}\text{Ar}^{38}\text{Ar}$	$^{40}\text{Ar}^{40}\text{Ar}$	^{82}Kr
^{58}NiO	$^{38}\text{Ar}^{38}\text{Ar}$	^{76}SeH	^{78}Kr	^{80}Kr	^{81}BrH
	^{76}Ge	^{61}NiO	^{77}SeH	^{79}BrH	
	^{75}AsH		^{62}NiO		
	^{60}NiO				

The $^{40}\text{Ar}^{40}\text{Ar}^+$ ion produces a very large interference that is roughly the same size as the measured ^{80}Se signal. Fluctuations of Ar intensity preclude its subtraction with sufficient precision to obtain precise ^{80}Se data. With ^{74}Se and ^{77}Se as the spike isotopes, the Se isotope ratios determined in the samples are $^{82}\text{Se}/^{76}\text{Se}$ (reported) and $^{82}\text{Se}/^{78}\text{Se}$ (not reported; used to detect certain types of errors).

Smaller ArAr^+ ion beams interfere with measurements of ^{78}Se and ^{76}Se but were removed almost completely by subtracting on-mass zeros. Drift in the intensities of the ArAr^+ signals was not captured by the on-mass zeros and was determined by monitoring beam intensity

at mass 80 and subtraction of calculated ^{80}Se intensity to arrive at an estimate of residual ArAr^+ intensity. Natural Ar isotope abundances and the double-spike-derived mass bias were used to correct the signals at $m/z = 78$ and 76 for residual ArAr^+ contributions.

Two isotopes of Ge, ^{74}Ge and ^{76}Ge (35.9% and 7.4% abundance, respectively) interfere with Se isotope measurements. A Ge correction was determined via measurement of the ^{73}Ge signal using an ion counter, and calculation of ^{74}Ge and ^{76}Ge using assumed natural abundances and the mass bias determined by the Se double spike procedure (see below).

Three isotopes of Kr can interfere with Se measurements: ^{78}Kr , ^{80}Kr , and ^{82}Kr (0.35%, 2.28% 11.58% of total Kr, respectively). Trace Kr is present in the Ar gas used to generate the plasma, and significant interferences can be generated from Kr dissolved into sample solutions from the atmosphere. Subtraction of on-mass zeros effectively removes Kr interferences, provided ^{84}Kr is monitored to ensure the Ar supply is not unusually Kr-contaminated and the sample and blank solutions are both equilibrated with Kr in the atmosphere prior to analysis. Similarly, a small interference by ArCl^+ at mass 77 has a negligible effect provided the HCl concentration in the samples matches within 5% the HCl concentration in the blank used to measure on-peak zeros.

Hydride interferences from $^{75}\text{AsH}^+$, $^{76}\text{SeH}^+$, $^{77}\text{SeH}^+$, $^{79}\text{BrH}^+$, and $^{81}\text{BrH}^+$ at masses 76, 77, 78, 80, and 81 are generally very small, but are corrected for by measurement of As, Se, and Br intensities and

calculation of the respective hydrides based on measured AsH^+/As , SeH^+/Se , and BrH^+/Br ratios. Typically, As concentrations are so low that a correction is not required, however in several of the rock samples large concentrations were observed and a correction was applied. Large Br and BrH^+ signals were occasionally observed and appeared to be related to generation of a volatile Br species, possibly BrCl , formed during digestion. The sample solutions were bubbled with N_2 for 20 min to remove the Br species.

The sample cone and skimmer cone are made of Ni, and a small amount of NiO^+ signal is likely at 74, 76, 77, 78, and 80, but it is very small and constant enough in intensity so that the on-mass zero subtraction removes it effectively.

Signals for each run were recorded using nine Faraday detectors on all masses from 74 through 82. After applying Ge, BrH , AsH , and SeH corrections, the data were processed via an iterative reduction algorithm described below.

4.8.2 DOUBLE ISOTOPE SPIKE AND DATA REDUCTION

A double isotope spike is employed to correct for isotopic discrimination in mass spectrometry and sample preparation. During mass spectrometry, the instrument has a strong but nearly constant bias in favor of heavier isotopes relative to lighter ones; this is known as instrumental mass bias. It can be measured and corrected for by adding two stable spike isotopes to the sample in known proportions (Eugster et al., 1969; Russell et al., 1978). The measured ratio of the spiked isotopes in the mixture is sensitive to the mass bias and can

thus be used to correct for it. The use of the $^{74}\text{Se} + ^{77}\text{Se}$ spike is detailed in the methods section of the main text.

The double spike has the added benefit of allowing correction for any isotopic fractionation that occurs during sample preparation. Because the spike is added as early as possible during sample preparations and its valence is same as that of the analyzed Se, isotopic fractionation that may occur during subsequent steps of the sample preparation is corrected for along with the mass bias correction. Purification of Se by the TCF method used in this study likely causes isotopic fractionation which is removed by the double spike procedure.

The data reduction method is based on that of Johnson et al. (1999) and follows an iterative procedure similar to previously published double isotope spike techniques (Eugster et al., 1969; Russell et al., 1978) to determine the sample's ratios of $^{82}\text{Se}/^{76}\text{Se}$ and $^{82}\text{Se}/^{78}\text{Se}$ from the ratios measured for the sample-spike mixture. The natural abundances of Se isotopes reported by Wachsmann and Heumann (1992) were used as the starting value for the iterative reduction program. The calculations follow a nested iteration scheme whereby the instrumental discrimination and natural isotope composition are successively refined:

1. A trial value for the $^{74}\text{Se}/^{77}\text{Se}$ ratio of the double spike, with the natural Se removed, is calculated:

$$\left(\frac{^{74}\text{Se}}{^{77}\text{Se}}\right)_{s, \text{ trial}} = \frac{\left(\frac{^{74}\text{Se}}{^{78}\text{Se}}\right)_n - \left(\frac{^{74}\text{Se}}{^{78}\text{Se}}\right)_m \times \left[\frac{\left(\frac{^{77}\text{Se}}{^{78}\text{Se}}\right)_m / \left(\frac{^{77}\text{Se}}{^{78}\text{Se}}\right)_s - 1}{\left(\frac{^{77}\text{Se}}{^{78}\text{Se}}\right)_n - \left(\frac{^{77}\text{Se}}{^{78}\text{Se}}\right)_m} \times \left[\frac{\left(\frac{^{74}\text{Se}}{^{78}\text{Se}}\right)_m / \left(\frac{^{74}\text{Se}}{^{78}\text{Se}}\right)_s - 1}{\left(\frac{^{74}\text{Se}}{^{78}\text{Se}}\right)_n - \left(\frac{^{74}\text{Se}}{^{78}\text{Se}}\right)_m} - 1\right]}{\left(\frac{^{77}\text{Se}}{^{78}\text{Se}}\right)_n - \left(\frac{^{77}\text{Se}}{^{78}\text{Se}}\right)_m} \times \left[\frac{\left(\frac{^{74}\text{Se}}{^{78}\text{Se}}\right)_m / \left(\frac{^{74}\text{Se}}{^{78}\text{Se}}\right)_s - 1}{\left(\frac{^{74}\text{Se}}{^{78}\text{Se}}\right)_n - \left(\frac{^{74}\text{Se}}{^{78}\text{Se}}\right)_m} - 1\right]}{\left(\frac{^{77}\text{Se}}{^{78}\text{Se}}\right)_n - \left(\frac{^{77}\text{Se}}{^{78}\text{Se}}\right)_m} \times \left[\frac{\left(\frac{^{74}\text{Se}}{^{78}\text{Se}}\right)_m / \left(\frac{^{74}\text{Se}}{^{78}\text{Se}}\right)_s - 1}{\left(\frac{^{74}\text{Se}}{^{78}\text{Se}}\right)_n - \left(\frac{^{74}\text{Se}}{^{78}\text{Se}}\right)_m} - 1\right]}{\left(\frac{^{77}\text{Se}}{^{78}\text{Se}}\right)_n - \left(\frac{^{77}\text{Se}}{^{78}\text{Se}}\right)_m} \times \left[\frac{\left(\frac{^{74}\text{Se}}{^{78}\text{Se}}\right)_m / \left(\frac{^{74}\text{Se}}{^{78}\text{Se}}\right)_s - 1}{\left(\frac{^{74}\text{Se}}{^{78}\text{Se}}\right)_n - \left(\frac{^{74}\text{Se}}{^{78}\text{Se}}\right)_m} - 1\right]} \quad (\text{EA1})$$

where the m , n , and s refer to the measured mixture, the assumed natural Se composition, and the assumed double spike composition, respectively. The $^{82}\text{Se}/^{76}\text{Se}$ ratios are obtained by multiplying $^{82}\text{Se}/^{78}\text{Se}$ by $^{78}\text{Se}/^{76}\text{Se}$.

2. The trial $^{74}\text{Se}/^{77}\text{Se}$ ratio of the double spike is compared to the known ratio to calculate the discrimination. An exponential discrimination law is used; in other words, the measured ratio r is related to the true ratio r_0 by:

$$r = r_0 \left(\frac{m_1}{m_2} \right)^\beta \quad (\text{EA2})$$

where m_1 and m_2 are the masses of the two isotopes and β is the parameter that determines the degree of discrimination.

3. Using the calculated value for β , the measured ratios are corrected for mass bias.
4. Step 1 above is performed using the corrected ratios; steps 1 through 3 are repeated iteratively until the values converge.
5. A trial value for the sample's $^{82}\text{Se}/^{76}\text{Se}$ or $^{82}\text{Se}/^{78}\text{Se}$ ratio, with the double spike subtracted, is calculated. Using this result (Step 2) and the assumed natural composition, trial values for the sample's $^{74}\text{Se}/^{82}\text{Se}$ and $^{77}\text{Se}/^{82}\text{Se}$ are calculated.
6. A new series of iterations that refine the instrumental discrimination are then performed using the sample's revised isotopic composition.
7. Several series of iterations are performed until the sample's isotopic composition converges.

REFERENCES

- Ahlberg P., Axheimer N., Babcock L.E., Eriksson M.E., Schmitz B., Terfelt F. (2009) Cambrian high-resolution biostratigraphy and carbon isotope chemostratigraphy in Scania, Sweden: first record of the SPICE and DICE excursions in Scandinavia. *Lethaia* **42**, 2-16.
- Calvert S.E., Bustin R.M., Ingall E.D. (1996) Influence of water column anoxia and sediment supply on the burial and preservation of organic carbon in marine shales. *Geochim. Cosmochim. Acta* **60**, 1577-1593.
- Erbacher J., Friedrich O., Wilson P.A., Birch H., Mutterlose J. (2005) Stable organic carbon isotope stratigraphy across Oceanic Anoxic Event 2 of Demerara Rise, western tropical Atlantic. *Geochem. Geophys. Geosyst.* **6**, Q06010.
- Eugster O., Tera F., Wasserbu.G. (1969) Isotopic Analyses of Barium in Meteorites and in Terrestrial Samples. *Journal of Geophysical Research* **74**, 3897-3908.
- Gill B.C., Lyons T.W., Young S.A., Kump L.R., Knoll A.H., Saltzman M.R. (2011) Geochemical evidence for widespread euxinia in the Later Cambrian ocean. *Nature* **469**, 80-83.
- Ingall E.D., Bustin R.M., Van Cappellen P. (1993) Influence of water column anoxia on the burial and preservation of carbon and phosphorus in marine shales. *Geochim. Cosmochim. Acta* **57**, 303-316.
- Johnson T.M., Herbel M.J., Bullen T.D., Zawislanski P.T. (1999) Selenium isotope ratios as indicators of selenium sources and oxyanion reduction. *Geochim. Cosmochim. Acta* **63**, 2775-2783.
- Kuypers M.M.M., Pancost R.D., Nijenhuis I.A., Sinninghe Damsté J.S. (2002) Enhanced productivity led to increased organic carbon burial in the euxinic North Atlantic basin during the late Cenomanian oceanic anoxic event. *Paleoceanography* **17**, 1051.
- Lyons T.W., Berner R.A. (1992) Carbon-sulfur-iron systematics of the uppermost deep-water sediments of the Black Sea. *Chem. Geol.* **99**, 1-27.
- Lyons T.W., Berner R.A., Anderson R.F. (1993) Evidence for large pre-industrial perturbations of the Black Sea chemocline. *Nature* **365**, 538-540.
- MacLeod K.G., Martin E.E., Blair S.W. (2008) Nd isotopic excursion across Cretaceous ocean anoxic event 2 (Cenomanian-Turonian) in the tropical North Atlantic. *Geology* **36**, 811-814.
- Reichart G.J., den Dulk M., Visser H.J., van der Weijden C.H., Zachariasse W.J. (1997) A 225 kyr record of dust supply, paleoproductivity and the oxygen minimum zone from the Murray Ridge (northern Arabian Sea). *Palaeogeogr., Palaeoclimatol., Palaeoecol.* **134**, 149-169.

- Russell W.A., Papanastassiou D.A., Tombrello T.A. (1978) Ca isotope fractionation on the Earth and other solar system materials. *Geochim. Cosmochim. Acta* **42**, 1075-1090.
- Schmid-Röhl A., Röhl H.-J., Oschmann W., Frimmel A., Schwark L. (2002) Palaeoenvironmental reconstruction of Lower Toarcian epicontinental black shales (Posidonia Shale, SW Germany): global versus regional control. *Geobios* **35**, 13-20.
- Sinninghe-Damsté J.S., Rijpstra W.I.C., Reichert G.J. (2002) The influence of oxic degradation on the sedimentary biomarker record II. Evidence from Arabian Sea sediments. *Geochim. Cosmochim. Acta* **66**, 2737-2754.
- Wachsmann M., Heumann K.G. (1992) Negative thermal ionization mass spectrometry of main group elements Part 2. 6th group: sulfur, selenium and tellurium. *Int. J. Mass Spectrom. Ion Processes* **114**, 209-220.

CHAPTER 5

SELENIUM SORPTION AND ISOTOPE FRACTIONATION IRON OXIDES VERSUS IRON SULFIDES



KRISTEN MITCHELL, RAOUL-MARIE COUTURE, THOMAS M. JOHNSON,
PAUL R. D. MASON, PHILIPPE VAN CAPPELLEN

THIS CHAPTER WAS SUBMITTED TO *CHEMICAL GEOLOGY* ON AUGUST 1,
2012.

THE PHOTO ON THE PREVIOUS PAGE WAS TAKEN DURING SORPTION EXPERIMENTS BY RAOUL-MARIE COUTURE.

ABSTRACT

Sorption and reduction are important processes influencing the environmental mobility and cycling of Se. In this study, we determined the rates of reaction and isotopic fractionations of Se(IV) and Se(VI) during sorption to iron oxides (2-line ferrihydrite, hematite and goethite) and iron sulfides (mackinawite and pyrite) at pH 7 and room temperature ($22\pm 2^\circ\text{C}$). More than 80% of aqueous Se(IV) was removed from solution in the presence of the mineral phases, except for hematite where only 40% of aqueous Se(IV) was sorbed. In contrast, less than 20% of aqueous Se(VI) was removed in the mineral suspensions, except for 2-line ferrihydrite where approximately 50% removal was observed. While XANES spectra revealed no change in Se oxidation state when Se(IV) and Se(VI) sorbed to iron oxides, they showed evidence of reduction in the presence of iron sulfides. Selenium isotopic fractionations, expressed as $\epsilon^{82/76}\text{Se}$, were always less than 1‰ in the experiments with iron oxides (mean $\epsilon^{82/76}\text{Se}$: 0.2‰). Fractionations were significantly higher in the experiments with iron sulfides, with $\epsilon^{82/76}\text{Se}$ values of up to $\sim 10\%$ in the Se(IV)-pyrite system, and a mean $\epsilon^{82/76}\text{Se}$ value of 2.3‰ for all sorption experiments with iron sulfides combined. The larger fractionations in the experiments with iron sulfides reflect the chemical reduction of Se(IV) and Se(VI). The highest isotope fractionation observed in the Se(IV)-FeS₂ system (9.7‰) is comparable to that previously reported for Se(VI) reduction by green rust (11.1‰).

5.1 INTRODUCTION

There has been much recent interest in the biogeochemical processes controlling the mobility of selenium (Se) in natural settings (Bruggeman et al., 2005; Bruggeman et al., 2007; Charlet et al., 2007; Scheinost and Charlet, 2008; Breynaert et al., 2008; Scheinost et al., 2008; Missana et al., 2009; Chakraborty et al., 2010; Han et al., 2011; Winkel et al., 2011; Pettine et al., 2012). While the microbiological reduction of Se(VI) and Se(IV) oxyanions and the corresponding isotope fractionations have been studied in some detail (Johnson et al., 1999; Herbel et al., 2000; Ellis et al., 2003; Clark and Johnson, 2008; Clark and Johnson, 2010; Schilling et al., 2011a), the isotope fractionations associated with sorption and abiotic reduction have received far less attention (Johnson et al., 1999; Johnson and Bullen, 2003). Selenium(VI) and Se(IV) oxyanions sorb to organic matter, iron oxides and iron sulfides (Balistrieri and Chao, 1987; Bruggeman et al., 2005; Scheinost and Charlet, 2008), and these reactions may impart as yet unknown isotope fractionations.

Goethite and hematite are the most widespread iron (Fe) oxides in soils and sediments. Nanogoethite is thought to be the dominant authigenic Fe(III) phase in freshwater and marine sediments (Schwertmann and Cornell, 2000; van der Zee et al., 2003). Ferrihydrite is highly reactive and a preferential substrate for dissimilatory iron reduction (Bonneville et al., 2009). It may form as the initial product of Fe(II) oxidation, then transform into more stable Fe(III) oxides. Iron(III) oxyhydroxides significantly impact the mobility and distribution of Se. Sorption of Se to iron oxides is well

documented (Balistrieri and Chao, 1987; Hayes et al., 1987; Hayes et al., 1988; Balistrieri and Chao, 1990; Zhang and Sparks, 1990; Manceau and Charlet, 1994; Zingaro et al., 1997; Wijnja and Schulthess, 2000; Duc et al., 2003; Duc et al., 2006; Catalano et al., 2006; Rovira et al., 2008), but only for hydrous ferric oxyhydroxide (HFO) has an isotopic fractionation been reported. The corresponding $\epsilon^{82/76}\text{Se}$ value is quite small, 0.8‰, compared to isotope fractionations associated with microbial reduction of Se(IV) or Se(VI) for which $\epsilon^{82/76}\text{Se}$ can reach values of up to ~14‰ (Johnson et al., 1999; Herbel et al., 2000).

Abiotic reduction of Se is another important process that affects the fate and transport of Se in the environment. Iron sulfides are widespread in marine sediments and in other settings including lake sediments, swamps and aquifers (Rickard et al., 1995; Rickard and Morse, 2005). Sorption of Se(IV) by pyrite (FeS_2) results in reduction to elemental Se or FeSe_2 (Bruggeman et al., 2005; Charlet et al., 2012). Depending on pH, sorption of Se(IV) to mackinawite (FeS) has been shown to result in reduction to either Se(0) or Se(-II) in the form of iron selenides (Scheinost and Charlet, 2008). Johnson and Bullen (2003) investigated the reduction of Se(IV) by green rust, an Fe(II) and Fe(III) bearing mineral with sulfate layers, and obtained a $\epsilon^{82/76}\text{Se}$ value of 11.1‰. To our knowledge this is the only abiotic Se reduction study conducted with an environmentally relevant mineral for which isotopic fractionation was monitored.

The precipitation of elemental selenium and elemental sulfur has been observed in cultures of *Desulfomicrobium norvegicum*

isolated from an estuarine sediment (Hockin and Gadd, 2003). However, the mechanism appears to be abiotic reduction of Se(IV) ions by aqueous sulfide, a reaction favored over the formation of iron monosulfide (Hockin and Gadd, 2003). The abiotic reaction between Se(IV) and aqueous sulfide has been independently verified by mixing Na_2SeO_3 and Na_2S in a carbonate buffered solution at pH 8.2 (Breynaert et al., 2008). Zingaro et al. (1997) observed the formation of elemental, trigonal grey Se by reacting SeO_4^{2-} or SeO_3^{2-} with aqueous Fe(II) added under the form of $\text{Fe}(\text{NH}_4)_2(\text{SO}_4)_2$.

The isotopic signatures of sorption and abiotic reduction processes relevant to the biogeochemical cycling of Se may help unlock the potential of this element as an environmental and paleotracer of redox conditions (Johnson, 2011; Mitchell et al., 2012). Therefore, in this study, we measured the rates and extent of sorption, plus the associated isotopic fractionations of Se(IV) and Se(VI) in the presence of the iron oxides goethite, hematite, and 2-line ferrihydrite, as well as the iron sulfides mackinawite (FeS) and pyrite (FeS_2).

5.2 METHODS

5.2.1 IRON MINERALS

5.2.1.1 IRON(III) OXIDES

Two-line ferrihydrite was synthesized following the procedure outlined in Schwertmann and Cornell (2000). A solution of 0.4 M $\text{FeCl}_3 \cdot 6 \text{H}_2\text{O}$ was neutralized with 1M NaOH and then dialyzed to remove Na^+ and Cl^- ions using dialysis tubing (6000-8000 Dalton dialysis membrane; Spectra/Por) in a vessel containing ~10 L ultrapure water (18 M Ω). The water was replaced until the

conductivity dropped to that of ultrapure water. The dialysis procedure required about two weeks. The mineral was recovered from the dialysis tubing, freeze-dried and kept at 4°C in an amber glass bottle. The synthesis protocol of Schwertmann and Cornell (2000) yields a 2-line ferrihydrite with a specific surface area of 200 m²g⁻¹. Low surface area (LSA) hematite (Bayferrox 105M) with a reported surface area of 12 m²g⁻¹ (Bonneville et al., 2004) and goethite (Bayferrox 910) with a reported surface area of 15 m²g⁻¹ (Bonneville et al., 2009) were obtained commercially (bayferrox.com). Immediately before the sorption experiments, the goethite and hematite were washed several times with ultrapure O₂-free water.

5.2.1.2 IRON SULFIDES

Nanocrystalline mackinawite (FeS) was synthesized by adapting the protocol of Wolthers et al. (2005) as follows. In an anaerobic chamber, 200 mL of 10⁻³ M Na₂S solution was added to 200 mL of 10⁻³ M Fe(SO₄)₂(NH₄)₂•6H₂O solution, both being prepared in a 0.01 M tri-sodium citrate pH-buffer (pH 6.00 ± 0.01). The black precipitate was left to age in the flask for one hour and then transferred to air-tight PTFE tubes (Oakridge, 30ml). The tubes were centrifuged for 15 minutes at 4000g, the supernatant was discarded and the precipitate rinsed with ultrapure O₂-free water; this procedure was repeated 5 times. The precipitate was freeze-dried under N₂ for 48h. The mineral was kept in an anaerobic chamber in an amber glass bottle. Wolthers et al. (2003) report a specific surface area of the mackinawite of 350 m²g⁻¹. Pyrite (FeS₂; Strem Chemical, 41.7 m²g⁻¹)

was selected based on the work of Bostick and Fendorf (2003) and prepared for sorption experiments according to their protocols.

5.2.2 EXPERIMENTS

The background solutions for all sorption experiments were made from O₂-free ultrapure 18 MΩ water adjusted to an ionic strength of 0.05 M with NaCl and a pH of 7 using 3-morpholinopropanesulfonic acid (MOPS, Merck) (Bostick and Fendorf, 2003). Minerals were rinsed with ultrapure water, and then used to prepare 2 g L⁻¹ slurries with the background solution in an anaerobic chamber. After preparation of the suspensions, the serum bottles were crimped-sealed and placed on a shaker outside the anaerobic chamber at room temperature (22±2 °C). The experiments were started by injecting either a Na₂SeO₃ or Na₂SeO₄ solution into the serum bottles. The initial concentrations of aqueous selenium were fixed at 100 μM for Se(VI) and 75 μM for Se(IV). Selenium(IV) reduction experiments by aqueous sulfide and Fe(II) were carried out in identical fashion by making 500 μM Na₂S or Fe(SO₄)₂(NH₄)₂•6H₂O solutions using the background solution described above in an anaerobic chamber. Sub-samples of 1 ml were taken using syringes, filtered (0.2 μm pore size polysulfone membrane) and delivered to HDPE conical centrifuge tubes to which 100 μl of concentrated HCl was then added. Iron oxide experiments were sampled immediately after injection of the Se stock solution, then every 10 minutes for the first hour, then hourly for the next 8 hours and finally at 24 hours. Sub-samples for the iron sulfide and the homogenous aqueous

experiments were taken immediately after injection of the Se stock solution, at 10, 20, 40 minutes, 1 hour, then at 2, 6, 9, and 24 hours.

Additional Se(IV)-FeS sorption experiments were run in 5 parallel batches in order to recover enough solid phase for Se isotope analysis. Five 30 ml PTFE Oak Ridge centrifuge tubes were filled with 2 g L⁻¹ in MOPS buffer, and Se(IV) was added to achieve a concentration of 75 µM. Experiments were terminated by centrifuging the samples and separating the aqueous phase from the solids. The first sub-sample was collected within the first 2 minutes of Se(IV) addition. Samples were then taken every 20 minutes for the first hour and the last sample was taken at 24 hours. Aqueous samples were filtered through a 0.2 µm pore size syringe filter into a 50 ml conical centrifuge tube to which 200 µl of concentrated HCl was then added. Solid phase samples were transferred to 7 ml PTFE beakers. The solid phase was digested in 3 ml concentrated HNO₃ amended with 0.2 ml H₂O₂ and heated on a hot plate at 100°C for 3 hours.

5.2.3 ANALYTICAL TECHNIQUES

5.2.3.1 SELENIUM CONCENTRATIONS

Selenium concentrations were measured on a PS Analytical 10.055 Millennium Excalibur Atomic Fluorescence Spectrometer (AFS) equipped with a continuous flow hydride generator (HG) and a boosted discharge hollow cathode Se lamp. The Se concentration standard used was a single element ICP standard (1.000 µg mL⁻¹ Se in dilute HNO₃, Ultra Scientific). The relative standard deviation (RSD) associated with the concentration measurements was 9.9%. For the iron oxide experiments, Se(IV) concentrations were determined

directly after sub-sampling via hydride generation atomic fluorescence spectrometry (HG-AFS) by diluting a small aliquot (100 μ l) of the filtered sample with 30% HCl. Note that hydride generation only measures Se(IV). The Se(VI) concentration was determined after a 100 μ l aliquot was added to 5 ml 5 M HCl and heated for one hour to reduce the Se(VI) to Se(IV), followed by dilution to 30% HCl prior to analysis with HG-AFS. For the iron sulfide and homogenous aqueous experiments, Se(IV) or Se(VI) concentrations were determined as above. An additional aliquot was analyzed for total Se concentration after chemical oxidation by taking a 100 μ l aliquot of the sub-sample which was heated for one hour at 100°C in 2 M NaOH and 7% H₂O₂. After the sample cooled to room temperature concentrated HCl was added to reach 4.3 M HCl and then the sample was heated again for one hour at 100°C to ensure all Se was in the Se(IV) form for HG-AFS analysis. The sample was then diluted to 30% HCl for HG-AFS analysis.

5.2.3.2 SELENIUM ISOTOPE RATIOS

Thiol cotton fiber (TCF) was used for the chemical separation of Se from potential interferences in the dissolved matrix prior to isotopic analysis, following the procedure outlined in Mitchell et al. (2012) after Zhu et al. (2008). Selenium isotope determinations were carried out on a Hydride Generation Multi Collector Inductively Coupled Plasma Mass Spectrometer (HG-MC-ICP-MS), using a double focusing Nu Plasma MC-ICP-MS (Wrexham, North Wales, UK), located at the Department of Geology, University of Illinois at Urbana-Champaign. The reductant used for the hydride generation

was 0.3% NaBH₄ in 0.3% NaOH. The sample and reductant were introduced into the hydride generator at a flow rate of 0.25 ml min⁻¹. The hydrides generated were carried into the instrument using argon as the carrier gas.

The Se isotope standard solution was NIST SRM 3149. The mass difference between ⁷⁴Se and ⁸²Se is greater than between ⁸²Se and ⁷⁶Se, but ⁷⁴Se is far less abundant (0.87%) than ⁷⁶Se (9.02%) so that determination of the ^{82/76}Se ratio is preferred (Krouse and Thode, 1962). The low abundance of ⁷⁴Se also makes the double spike technique used here ideal. ⁷⁴Se-enriched and ⁷⁷Se-enriched spikes were purchased from ISOFLEX, USA, and mixed to create a Se isotope double spike (⁷⁴Se/⁷⁷Se), which was added to all samples and well mixed prior to sample preparation and TCF separation procedure. The samples for isotope analysis were prepared so as to contain 4-6 µg ml⁻¹ Se, producing between 1.2 and 2 volts for ⁷⁸Se. To achieve normal background signal the hydride generator apparatus was rinsed with 2 M HCl between each sample in order to avoid memory effects between samples. An isotope standard was measured approximately every 5 samples to account for instrument drift.

5.2.3.3 X-RAY DIFFRACTION

Iron minerals were characterized using powder X-ray diffraction (XRD), which was performed using a PANalytical X-Pert PRO MPD X-ray diffractometer equipped with a cobalt source and an X-Celerator detector. All scans were collected from front-packed powder samples over the range of 10–90° 2θ at a scan rate of 0.6° per minute. The diffraction patterns were compared to the reference

powder diffraction file (PDF) for goethite (#29-0713), and hematite (#33-0664). The identity of the 2-line ferrihydrite was confirmed by the two very broad characteristic peaks, and was compared to the PDF #29-0712 (six-line ferrihydrite). Mackinawite was shown to be amorphous, but no standard was available in the PDF database for comparison (Brezonik and Arnold, 2011).

5.2.3.4 X-RAY ABSORPTION SPECTROSCOPY

Solid phase samples were collected at the end of the sorption experiments by centrifugation and dried over N₂ in an anaerobic chamber. The samples were transported to the beamline in N₂-filled sealed test tubes protected by an O₂-free Bio-Bag™. X-ray Absorption Near-Edge (XANES) spectra were collected at the Hard X-ray Micro-Analysis (HXMA) beamline (CLS06ID-1) of the Canadian Light Source (Saskatoon, Canada). The samples and reference materials (sodium selenite, sodium selenate and elemental Se) were mixed with boron nitride and pressed into a pellet under N₂-atmosphere, placed in the sample holder, sealed with Kapton® tape and transferred to the cryostat by placing the sample holder in the N₂-saturated vapours boiling off a liquid N₂ Dewar. Analyses were carried out at T<15K in a helium (He) cryostat to limit Se photo redox reactions under the beam (Huggins and Sanei, 2011).

The X-ray energy resolution was maintained by a double crystal monochromator, equipped with Si(111) and Si(220), and the energy calibration was based on a Se metal standard using the main edge crest of 12662.5 eV. Between 6 and 15 spectra were collected in transmission mode using an ionization chamber or in fluorescence

mode using a 4-element array Si solid-state detector. In order to attenuate scattered principle energy X-rays from entering the fluorescence detector, soller slits, and an absorbing filter (As) were placed between the sample and the fluorescence. Data were collected in constant steps of 10eV from 12404 eV until 12623 eV, of 0.56 eV from 12623 eV to 12686 eV and in increasing steps of 1.1 eV to 5 eV from 12687 eV until 13296 eV. All spectra were edge normalized and background corrected using the auto-bk algorithm implemented in the ATHENA software package (Ravel and Newville, 2005).

5.2.4 DATA ANALYSIS

5.2.4.1 KINETIC MODELING

Multiple processes occur, either simultaneously or in sequence, when aqueous Se oxyanions are brought into contact with Fe minerals, including fast reversible binding to surface sites, molecular rearrangement at sorption sites, coprecipitation and slow diffusion into the lattice or mineral aggregate (Zhang and Selim, 2005). In the case of selenium, a redox active element, the Se(IV) or Se(VI) added to the mineral slurries can additionally undergo changes in oxidation state, either in solution or at the mineral surface (Charlet et al., 2007; Han et al., 2011). Because of the multiplicity of possible reaction steps, we extracted reaction parameters using a versatile sorption model based on the mixed kinetic-equilibrium modeling approach described in Zhang and Stanforth (2005). The model is schematically illustrated in Figure 5.1.

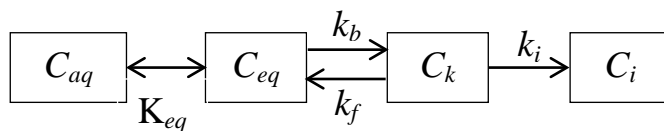


Figure 5.1 Consecutive reaction model used to extract equilibrium and kinetic parameters for the Se sorption reactions. C_{aq} is the concentration of selenium in solution, C_{eq} , C_k , and C_i are the quantities sorbed to equilibrium, reversible kinetic, and irreversible kinetic sites, respectively, where K_{eq} , k_f , k_b , and k_i are the corresponding reaction parameters. The initial uptake from solution is assumed to be instantaneous and reversible, hence, this step is represented by an equilibrium constant (K_{eq}).

The K_{eq} , k_b , k_f and k_i parameter values were extracted for each experiment using inverse modeling of the time series of dissolved Se concentration measured (Table 5.1). The equilibrium constant K_{eq} corresponds to the initial uptake from solution, which is assumed to be near instantaneous and reversible. All kinetically controlled steps are assumed to follow first-order rate equations. Hence, the rate constants k_f , k_b and k_i all have units of inverse time. The equations were implemented in Microsoft Excel and the subset of parameters that best described the dataset was constrained using the Solver function. Minimization of the root mean square error (RMSE) was used to select the subset of parameters yielding to the best fit between the model and the data.

Table 5.1 Equilibrium constant (K_{eq}) and forward (k_f), backward (k_b), and irreversible rate constants extracted from time-series of Se sorbed onto Fe-oxides and Fe-sulfides using the consecutive reaction model.

Se species	Fe mineral	Log K_{eq}	k_f (hr^{-1})	k_b (hr^{-1})	k_i (hr^{-1})	RMSE
<i>Iron oxides</i>						
Se(VI)	2-line ferrihydrite	0.1	0.4	1.3	2.0×10^{-3}	1.48
	Hematite	–	–	–	–	5.30 ^a
	Goethite	–	–	–	–	3.23 ^a
Se(IV)	2-line ferrihydrite	0.5	1.0	2.0	1.0×10^{-4}	1.13

	Hematite	1.0	0.01	3.4	4.0×10^{-4}	2.59
	Goethite	11.5	0.1	1.5	3.0×10^{-4}	0.49
<i>Iron sulfides</i>						
Se(VI)	Mackinawite (FeS)	-1.0	2.8	10.0	1.0×10^{-3}	3.03
	Pyrite (FeS ₂)	-1.0	0.01	4.8	3.0×10^{-3}	3.34
Se(IV)	Mackinawite (FeS)	-0.4	3.8	0.01	1.0×10^{-4}	7.24
	Pyrite (FeS ₂)	0	0.07	0.1	3.4×10^{-4}	2.78

^aThe results are best reproduced without reaction

5.2.4.2 SELENIUM ISOTOPES

The analytical data were first corrected for interferences as described in Zhu et al. (2008). The different isotopic ratios ($^{74}\text{Se}/^{78}\text{Se}$, $^{76}\text{Se}/^{78}\text{Se}$, $^{77}\text{Se}/^{78}\text{Se}$, $^{80}\text{Se}/^{78}\text{Se}$, and $^{82}\text{Se}/^{78}\text{Se}$) were then reduced using an iterative procedure to obtain the $^{82}\text{Se}/^{76}\text{Se}$ and $^{82}\text{Se}/^{78}\text{Se}$ ratios. Replicate analyses (TCF preparation and analysis) were conducted on 19 samples, yielding a precision estimate of $\pm 0.05\%$, calculated as two times the root mean square of the differences. Replicate analyses of USGS reference material SGR-1 (n=20) yielded $\delta^{82/76}\text{Se} = -0.18 \pm 0.13\%$ (2σ).

The isotope notation used for the selenium system follows that used for sulfur by Canfield (2001b). The fractionation factor is defined as:

$$\alpha_{(A-B)} = \frac{\left(\frac{^{82}\text{Se}}{^{76}\text{Se}} \right)_A}{\left(\frac{^{82}\text{Se}}{^{76}\text{Se}} \right)_B} \quad (1)$$

where A is the reactant and B the reaction product. Isotopic compositions are expressed in per mil (‰) and are presented in the standard delta notation reporting the 82/76 ratio relative to the NIST SRM 3149 standard:

$$\delta^{82/76}Se = \left[\frac{\left(\frac{^{82}Se}{^{76}Se} \right)_{Sam}}{\left(\frac{^{82}Se}{^{76}Se} \right)_{Std}} - 1 \right] \quad (2)$$

Fractionations are expressed in terms of ϵ , also in ‰ units, where A and B are defined as above:

$$\epsilon^{82/76}Se = (\alpha_{A-B} - 1) \quad (3)$$

The epsilon notation is convenient because ϵ is roughly equal to the difference between the δ values of the reactant and product:

$$\epsilon^{82/76}Se \cong \delta^{82/76}Se_A - \delta^{82/76}Se_B \quad (4)$$

Isotopic compositions ($\delta^{82/76}Se$) of sorbed and reduced Se were inferred from the $\delta^{82/76}Se$ values measured on the aqueous phase assuming isotopic mass balance. Uncertainties in $\epsilon^{82/76}Se$ were determined by calculating the uncertainties of the slopes using standard linear estimation methods (Basu and Johnson, 2012).

5.3 RESULTS

5.3.1 REACTION KINETICS

Selenium(IV) sorbed rapidly on all Fe(III) oxides studied (Figure 5.2a,c,e), as expected given the known affinity of Se(IV) for iron oxide surfaces (Balistrieri and Chao, 1987, 1990; Zhang and Sparks, 1990; Peak and Sparks, 2002). In the first few minutes of reaction, >99% of Se(IV) sorbed to goethite and 2-line ferrihydrite (Figure 5.2 a,e; Table 5.2). In contrast, only about 50% of the added Se(IV) sorbed to hematite during the 24 hour experiment (Figure 5.2c; Table 5.2). As expected from previous work (Balistrieri and Chao,

1987; Duc et al., 2003), Se(VI) did not sorb as strongly as Se(IV) on iron oxides. Approximately 50% of Se(VI) sorbed to 2-line ferrihydrite (Figure 5.2b), while hardly any sorption to either hematite or goethite was observed (Figure 5.2 d,f). The Se(IV) and Se(VI) sorbed to the iron oxide minerals exhibited no evidence of changes in oxidation state, as shown by the white-line peaks of the XANES 1st derivative spectra at the Se K-edge (Figure 5.3; Table 5.3) of the sorbed Se, which remained aligned with the corresponding peaks of the respective initial Se species. XANES spectra could not be obtained for Se(VI) sorbed to hematite or goethite because insufficient Se sorbed to the mineral phases.

The rates of reduction of Se(IV) with aqueous Fe(II) and H₂S were determined to provide a basis for comparison with the reduction rates with the iron sulfide minerals.

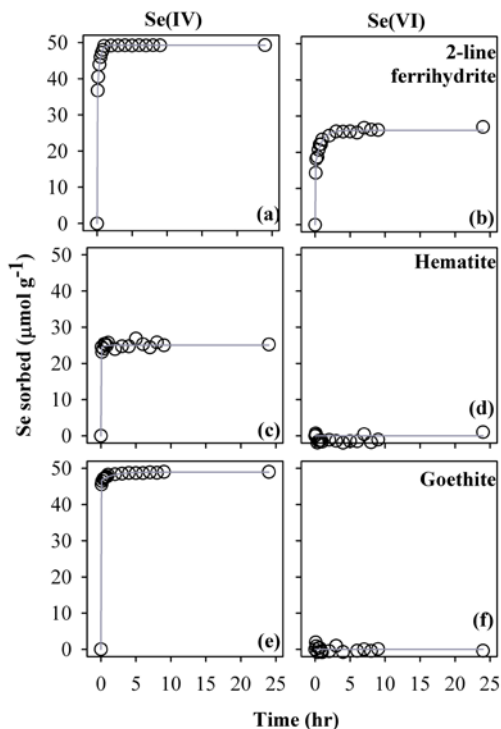


Figure 5.2 Measured (open circles) and modeled (solid line) Se sorbed to 2-line ferrihydrite (a,b), hematite (c,d), goethite (e,f) as a function of time in pH 7 MOPS-buffered slurries (2 g L^{-1}) containing initial concentrations of $100 \text{ }\mu\text{M}$ Se(VI) or $75 \text{ }\mu\text{M}$ Se(IV).

The reaction with aqueous sulfide was considerably faster than with aqueous Fe(II): aqueous Se(IV) half-life was 2 minutes when reacting with $\text{H}_2\text{S}_{\text{aq}}$ and 12 hours with Fe(II). The reaction between sulfide and Se(IV) was near-100% complete, whereas only 81% of aqueous Se(IV) was consumed in the Fe(II) solution (Table 5.2). In the experiments with aqueous sulfide, less than 5% of the Se remaining in solution was in the original +IV oxidation state, while for the experiments with Fe(II) >95% of the remaining aqueous Se was still present as Se(IV) (Table SI-5.2).

Table 5.2 Isotopic compositions, total sorption, half-life and final oxidation state of iron oxide and iron sulfide experiments. Maximum ϵ values are the highest values found during the course of each experiment.

Experiment	$t_{1/2}$ (min)	Total Se removed (%)	Reduction observed	ϵ_{\max} (‰)	Relative error (‰)
<i>Iron oxides</i>					
Se(VI)					
Hematite	–	14	N	–	–
Goethite	–	17	N	–	–
2-line ferrihydrite	35	46	N	0.08	± 1.2
Se(IV)					
Hematite	42	41	N	0.14	± 2.4
Goethite	3.6	99	N	0.45	± 0.6
2-line ferrihydrite	15	>99	N	0.93	± 0.4
<i>Iron sulfides</i>					
Se(VI)					
Mackinawite (FeS)	60 hrs	20	Y	3.0	± 0.2
Pyrite (FeS ₂)	69 hrs	13	Y	–	–
Se(IV)					
Mackinawite (FeS)	3.4	98	Y	3.7 ^a	± 0.3
Pyrite (FeS ₂)	9 hrs	96	Y	9.7	± 0.0

^acalculated using measured $\delta^{82/76}\text{Se}$ of solid phase

In the mackinawite (FeS) suspension, aqueous Se(IV) exhibited a half-life of less than 4 minutes (Figure 5.4a; Table 5.2). In addition, near-complete Se(IV) removal from solution was observed. In contrast, only 25% of aqueous Se(VI) was removed from solution after 24h contact with FeS (Figure 5.4b; Table 5.2). The XANES spectra at the Se K-edge of the solid samples from the FeS experiments showed a white line at ~ 12660 eV, implying that reaction of Se(IV) and Se(VI) with FeS resulted in Se reduction (Figure 5.3). At the end of the Se(IV)-FeS experiment, approximately 20% of Se remaining in solution was in the form of Se(IV), with the remainder being reduced Se, presumably Se(0) or Se(-II) (Table SI-5.3). Note

that the XANES spectra did not allow us to distinguish between Se(0) and Se(-II), as also reported by previous workers (Lenz et al., 2008; Charlet et al., 2012).

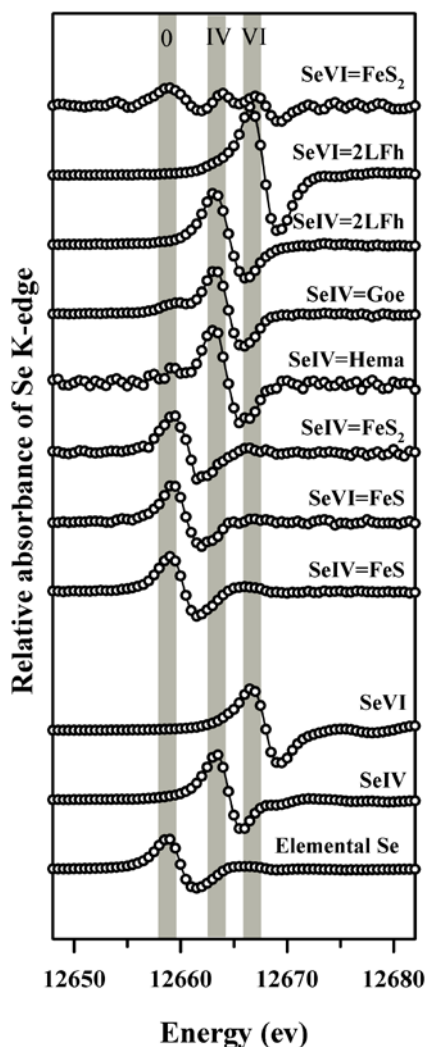


Figure 5.3 First derivatives of Se K-edge XANES spectra for selected reference compounds as well as for the solid samples from sorption experiments. The shaded areas indicate the first derivative XANES peak of elemental Se(0) (at 12659 eV), Se(IV)-O (at 12664 eV), Se(VI)-O (at 12667 eV), respectively.

Table 5.3 Position (eV) of the edge crest and 1st derivative of normalized XANES spectra at the Se K-edge for the sorption complex and the reference materials for Se(0), Se(IV) and Se(VI).

Samples	Normalized XANES	1 st Derivative
Se(IV) Mackinawite (FeS)	12659.69	12657.86
Se(VI) Mackinawite (FeS)	12660.27	12658.21
Se(IV) Pyrite (FeS ₂)	12660.32	12658.50
Se(IV) Hematite	12663.99	12662.13
Se(IV) Goethite	12664.05	12662.50
Se(IV) 2-line ferrihydrite	12664.32	12662.50
Se(VI) 2-line ferrihydrite	12667.55	12666.00
Se(VI) Pyrite (FeS ₂)	12667.89	12657.98
Reference		
Se(0) metal	12659.26	12659.32
Se(IV) oxide	12664.30	12662.48
Se(VI) oxide	12667.40	12665.90

In the presence of pyrite it took nearly 24 hours for most of the Se(IV) to react (Figure 5.4a,c). The XANES spectrum for this experiment confirmed that Se bound to pyrite was in a reduced oxidation state, either as Se(0) or Se(-II) (Figure 5.3 and Table 5.3). Only about 13% of aqueous Se(VI) was removed from solution in the presence of pyrite (Table 5.2). The XANES spectrum for the Se(VI)-FeS₂ experiment showed the presence of Se(VI), Se(IV) and Se(0)/Se(-II) after 24 hours (Figure 5.3).

5.3.2 SELENIUM ISOTOPE FRACTIONATIONS

All the $\delta^{82/76}\text{Se}$ values measured on the aqueous samples collected during the sorption and homogeneous solution experiments are listed in Tables SI-5.1 and SI-5.2 of the Supplemental Information, while Table SI-5.3 provides the solid-phase $\delta^{82/76}\text{Se}$ values measured in the Se(IV)-FeS system. For each $\delta^{82/76}\text{Se}$ determination in a given The $\epsilon^{82/76}\text{Se}$ values for the Se(IV)-FeS system derived from the the solid-phase samples agreed well with those derived from the aqueous

samples. experiment a corresponding value for the fractionation $\epsilon^{82/76}\text{Se}$ was calculated.

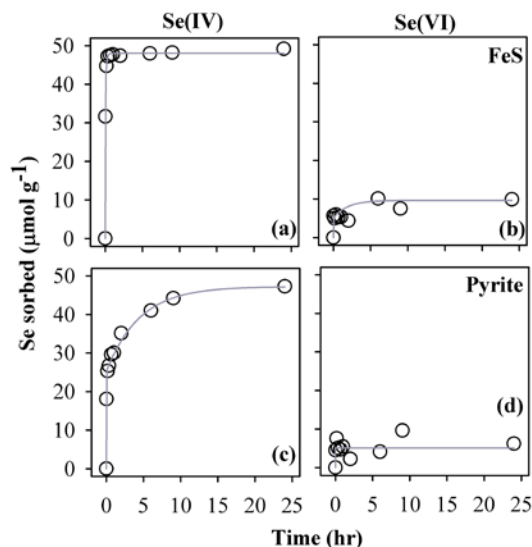


Figure 5.4 Measured (open circles) and modeled (solid line) sorbed Se in the presence of FeS or FeS₂ as a function of time in pH 7 MOPS-buffered slurries (2 g L⁻¹) containing an initial concentration of 100 μM of either Se(VI) or Se(IV).

The ranges of $\epsilon^{82/76}\text{Se}$ values obtained with the iron oxide and iron sulfide minerals are summarized in Figure 5.5, while the maximum $\epsilon^{82/76}\text{Se}$ values observed in the different experiments are given in Table 5.2.

Figure 5.5 and Table 5.2 do not include fractionations for the Se(VI)-hematite, Se(VI)-goethite and Se(VI)-pyrite experiments, as too little sorption occurred in these systems to calculate precise fractionations. A meaningful $\epsilon^{82/76}\text{Se}$ value could not be obtained for the Se(IV)-H₂S system either, but in this case because of the extremely fast and complete reaction between Se(IV) and aqueous sulfide in homogeneous solution.

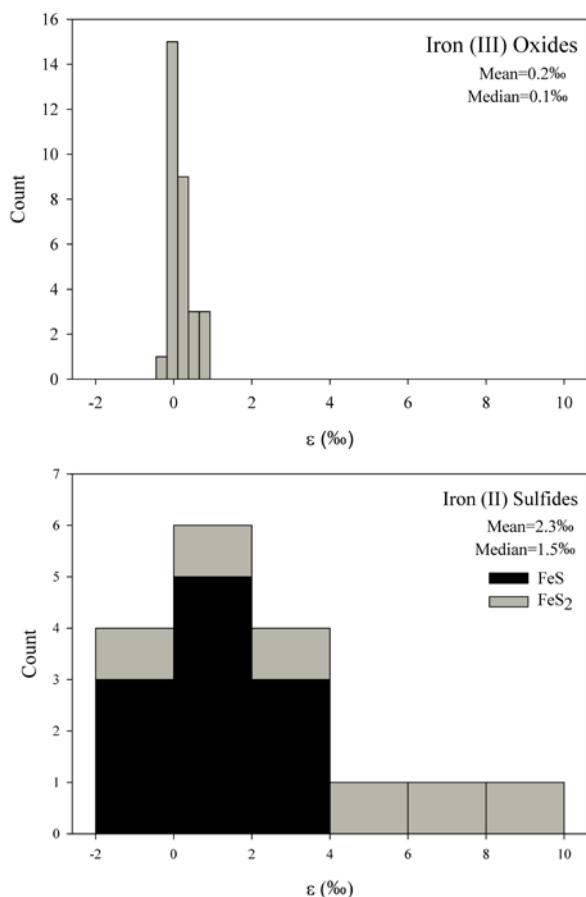


Figure 5.5 Frequency diagrams of isotope fractionations ($\epsilon^{82/76}\text{Se}$) for Se(IV) and Se(VI) on iron oxides (31 samples) and iron sulfides (17 samples).

The aqueous $\delta^{82/76}\text{Se}$ measurements resulted in a maximum $\epsilon^{82/76}\text{Se}$ value of 0.44‰ for the Se(IV)-Fe(II) system. The reliability of this $\epsilon^{82/76}\text{Se}$ estimate is questionable, however, because it may be biased by the inclusion of colloidal precipitate material in the filtered samples.

Sorption of Se(IV) and Se(VI) to the iron oxides yielded very small fractionations (mean $\epsilon^{82/76}\text{Se}$: 0.2‰). Sorption to the iron sulfide minerals showed significantly larger fractionations, with a maximum

$\epsilon^{82/76}\text{Se}$ of 9.7‰ and a mean of 2.3‰. The range of fractionations observed in the sorption experiments with the iron oxides was also much narrower than that obtained with the iron sulfides (Figure 5.5). The largest Se fractionation was observed for reaction between Se(IV) and pyrite (9.7‰).

In the experiments with 2-line ferrihydrite and pyrite, the spread in the fraction of sorbed Se(IV) was sufficient to test whether Se fractionation follows the standard Rayleigh model. As shown in Figure 5.6, the data for the two systems could be fitted by the Rayleigh fractionation model, except for the highest fractions of sorbed Se (i.e., when less than 5% of total Se remained in solution).

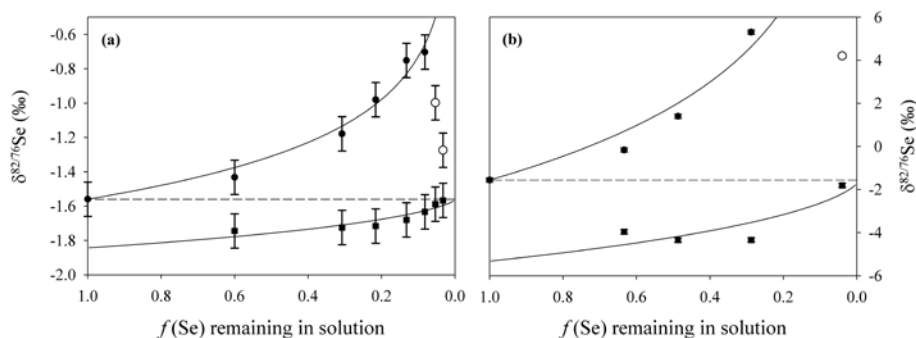


Figure 5.6 a) Se(IV) sorption to 2-line ferrihydrite b) Se(IV) sorption and reduction on FeS₂. Filled circles show measured isotopic compositions of Se remaining in solution, open circles indicate samples that were not used to fit the Rayleigh model. Filled squares represent the calculated isotopic composition of the Se(IV) on the solid. Error bars indicate the precision of the $\delta^{82/76}\text{Se}$ measurements.

5.4 DISCUSSION

Our results on sorption of Se (VI) and Se(IV) to Fe(III) oxyhydroxides are in agreement with previous work: oxyanions of Se(IV) sorb strongly to these minerals, those of Se(VI) far less (e.g., Ballistrieri and Chao, 1987; Catalano et al., 2006; Duc et al., 2006).

Uptake of Se(IV) and Se(VI) to 2-line-ferrihydrate is best modeled as a multistep process, with at least one slower reaction step following initial fast adsorption. Possibly, the slower step represents diffusion into the ferrihydrate particle aggregates, in line with the reported large inter-particle porosity and internal surface area of ferrihydrate (Cornell and Schwertmann, 2003). In contrast, the modeled sorption curve for the Se(IV)-goethite system is dominated by the large equilibrium constant ($\log K_{\text{eq}}=11.5$), which suggests fast adsorption to a fairly homogenous set of surface sites. While Se(IV) sorption to hematite is modeled with a significantly lower equilibrium constant than for goethite ($\log K_{\text{eq}}=1.0$), the very small values of the rate constants k_f and k_i similarly suggest that Se remains bound to the initial adsorption sites at the mineral surface. The total removal of aqueous Se(IV) in the presence of hematite (41%) is smaller than reported by Duc et al. (2006) who found that 95% of Se(IV) sorbed to hematite within 24 hours at pH 7. These authors, however, used a slurry containing 8 times more hematite (16 g L^{-1}) than in our experiment.

The largest fractionation for Se(IV) sorption to the Fe oxyhydroxides is observed for 2-line ferrihydrate, which is consistent with the inferred multi-step mechanism of Se(IV) sorption to 2-line ferrihydrate. Multi-step mechanisms tend to produce larger fractionations, because each step may contribute to the overall fractionation (Johnson and Bullen, 2003). Nonetheless, selenium isotope fractionations accompanying sorption to Fe oxyhydroxides are very small, as previously observed by Johnson and Bullen (2004) for Se(IV) sorption to hydrous ferric oxide. The latter authors report a

$\epsilon^{82/76}\text{Se}$ value of 0.8‰, which falls within the range obtained here. All the data existing to date thus indicate that sorption to Fe oxyhydroxide minerals produces little to no Se isotopic fractionation.

Inverse modeling of the removal of aqueous Se(IV) by the iron sulfide minerals yields small equilibrium constants, implying that removal of the Se oxyanions is kinetically controlled, which, in turn, is consistent with the observed reduction of Se(IV). The reaction of Se(IV) with pyrite is markedly slower than with mackinawite. The latter mineral is fairly soluble and releases sulfide and Fe(II) to solution (Wolthers et al., 2003), both of which have been shown to reduce Se(IV) to Se(0) (Zingaro et al., 1997; Hockin and Gadd, 2003; Breynaert et al., 2008; Pettine et al., 2012). The observed removal of Se in the FeS suspension is much faster than expected for reduction by aqueous Fe(II), but comparable with the rate of reduction of Se(IV) by aqueous sulfide. Thus, sulfide is the likely reductant of Se(IV) in the FeS suspension. While Se(0) is probably the main Se(IV) reduction product, Scheinost et al. (2008) showed that, while the reduction of Se(IV) by mackinawite first produces Se(0), subsequent formation of FeSe at the mineral surface also occurs.

As for the experiments with the iron oxyhydroxides, Se(VI) shows a much lower reactivity toward iron sulfide minerals than Se(IV). This is again consistent with previous work. Han et al. (2011), for instance, showed that, for comparable experimental conditions (initial Se(VI) concentration of 127 μM ; 1 g L⁻¹ FeS, pH 8), only about 25% of aqueous Se was removed after 40 hours, further increasing to 50% after 100 hours. Similarly, in a recent study

(Charlet et al., 2012) found that even after 336 hours only ~25% of the initial aqueous Se(VI) reacted with pyrite, indicating that this reaction does not go to completion even on relatively long time scales.

Sorption by iron sulfide minerals is accompanied by generally higher $\epsilon^{82/76}\text{Se}$ values than sorption by iron oxide minerals. The larger fractionations undoubtedly reflect the reduction of Se (Johnson and Bullen, 2003; Bruggeman et al., 2005; Scheinost and Charlet, 2008; Breynaert et al., 2008). As for sulfur, kinetic fractionation accompanies the breakage of the Se-O bond during reduction (Rees, 1973; Johnson and Bullen, 2003). The highest $\epsilon^{82/76}\text{Se}$ value obtained here (9.7‰) is of the same magnitude as reported for Se(VI) reduction by green rust (Johnson and Bullen, 2003). The $\epsilon^{82/76}\text{Se}$ range of low-temperature abiotic Se reduction largely overlaps that reported for dissimilatory selenium reduction (0.3-13.7‰; Herbel et al., 2000). Selenium isotopic signatures recorded in sediments and soils therefore do not provide a straightforward proxy to distinguish between biotic and abiotic reduction processes (Mitchell et al., 2012).

In the sorption experiments with FeS and FeS₂, reduced Se accumulates in the aqueous phase. This is particularly true for the Se(IV)-FeS system where nearly 80% of aqueous Se appears to be in reduced form. The reduced Se present in solution possibly represents nano-particulate Se(0) that is not retained on the 0.2 μm pore size filters (Charlet et al., 2007), or reduced Se bound to particles of amorphous mackinawite smaller than 0.2 μm (Wolthers et al., 2005). Either way, the accumulation of reaction product in the operationally defined aqueous phase implies that the calculated isotope

fractionations reported here for the experiments with the Fe sulfide minerals are minimum estimates of the true $\epsilon^{82/76}\text{Se}$ values. Further research is therefore needed to more definitely delineate the range in fractionation accompanying reductive sorption of Se oxyanions.

5.5 CONCLUSIONS

Until now, little quantitative information was available on Se isotope fractionations accompanying environmentally relevant abiotic reactions, hence seriously limiting our ability to use Se isotopic signatures as environmental tracers in contemporary and ancient settings (Mitchell et al., 2012). Here, we significantly expand the number of literature values of Se(IV) and, to a lesser extent, Se(VI) isotope fractionations associated with sorption to representative Fe oxyhydroxide and sulfide minerals. The iron oxide minerals investigated 2-line ferrihydrite, goethite and hematite, are widespread and represent major sorbents of Se in natural aquatic environments. Sorption of Se to these minerals produces very little fractionation ($\epsilon^{82/76}\text{Se} < 1\%$). In the presence of the iron sulfide minerals mackinawite and pyrite, Se(IV) and Se(VI) are reduced, which results in significantly larger fractionations, with $\epsilon^{82/76}\text{Se}$ values of up to $\sim 10\%$. Reductive sorption of Se(IV) to pyrite produces the largest fractionation of all of the reaction systems investigated. Thus, while Se isotopic signatures in environmental samples may record reduction processes, in and by themselves may not allow one to distinguish abiotic and biotic reduction pathways of Se.

REFERENCES

- Balistrieri L.S., Chao T.T. (1987) Selenium adsorption by goethite. *Soil Sci. Soc. Am. J.* **51**, 1145-1151.
- Balistrieri L.S., Chao T.T. (1990) Adsorption of selenium by amorphous iron oxyhydroxide and manganese dioxide. *Geochim. Cosmochim. Acta* **54**, 739-751.
- Basu A., Johnson T.M. (2012) Determination of Hexavalent Chromium Reduction Using Cr Stable Isotopes: Isotopic Fractionation Factors for Permeable Reactive Barrier Materials. *Environ. Sci. Technol.* **46**, 5353-5360.
- Bonneville S., Behrends T., Van Cappellen P. (2009) Solubility and dissimilatory reduction kinetics of iron(III) oxyhydroxides: A linear free energy relationship. *Geochim. Cosmochim. Acta* **73**, 5273-5282.
- Bonneville S., Van Cappellen P., Behrends T. (2004) Microbial reduction of iron(III) oxyhydroxides: effects of mineral solubility and availability. *Chem. Geol.* **212**, 255-268.
- Bostick B.C., Fendorf S. (2003) Arsenite sorption on troilite (FeS) and pyrite (FeS₂). *Geochim. Cosmochim. Acta* **67**, 909-921.
- Breynaert E., Bruggeman C., Maes A. (2008) XANES-EXAFS analysis of Se solid-phase reaction products formed upon contacting Se(IV) with FeS₂ and FeS. *Environ. Sci. Technol.* **42**, 3595-3601.
- Brezonik P.L., Arnold W.A. (2011) *Water Chemistry: An Introduction to the Chemistry of Natural and Engineered Aquatic Systems*. Oxford University Press, Inc., Oxford.
- Bruggeman C., Maes A., Vancluysen J. (2007) The interaction of dissolved Boom Clay and Gorleben humic substances with selenium oxyanions (selenite and selenate). *Appl. Geochem.* **22**, 1371-1379.
- Bruggeman C., Maes A., Vancluysen J., Vandemussele P. (2005) Selenite reduction in Boom clay: Effect of FeS₂, clay minerals and dissolved organic matter. *Environ. Pollut.* **137**, 209-221.
- Canfield D.E. (2001) Biogeochemistry of sulfur isotopes, in: Valley, J.W., Cole, D.R. (Eds.), *Stable Isotope Geochemistry*. Mineralogical Society of America, Washington, DC., pp. 607-636.
- Catalano J.G., Zhang Z., Fenter P., Bedzyk M.J. (2006) Inner-sphere adsorption geometry of Se(IV) at the hematite (100)-water interface. *J. Colloid Interface Sci.* **297**, 665-671.
- Chakraborty S., Bardelli F., Charlet L. (2010) Reactivities of Fe(II) on Calcite: Selenium Reduction. *Environ. Sci. Technol.* **44**, 1288-1294.
- Charlet L., Kang M., Bardelli F., Kirsch R., Géhin A., Grenèche J.-M., Chen F. (2012) Nanocomposite Pyrite-Greigite Reactivity toward Se(IV)/Se(VI). *Environ. Sci. Technol.* **46**, 4869-4876.
- Charlet L., Scheinost A.C., Tournassat C., Grenèche J.M., Gehin A., Fernandez-Martínez A., Coudert S., Tisserand D., Brendle J. (2007) Electron

- transfer at the mineral/water interface: Selenium reduction by ferrous iron sorbed on clay. *Geochim. Cosmochim. Acta* **71**, 5731-5749.
- Clark S.K., Johnson T.M. (2008) Effective isotopic fractionation factors for solute removal by reactive sediments: A laboratory microcosm and slurry study. *Environ. Sci. Technol.* **42**, 7850-7855.
- Clark S.K., Johnson T.M. (2010) Selenium stable isotope investigation into selenium biogeochemical cycling in a lacustrine environment: Sweitzer Lake, Colorado. *Journal of Environmental Quality* **39**, 2200-2210.
- Cornell R.M., Schwertmann U. (2003) *The iron oxides: structure, properties, reactions, occurrences, and uses*, 2nd, completely rev. and extended ed. ed. Weinheim : Wiley-VCH
- Duc M., Lefèvre G., Fédoroff M. (2006) Sorption of selenite ions on hematite. *J. Colloid Interface Sci.* **298**, 556-563.
- Duc M., Lefevre G., Fedoroff M., Jeanjean J., Rouchaud J.C., Monteil-Rivera F., Dumonceau J., Milonjic S. (2003) Sorption of selenium anionic species on apatites and iron oxides from aqueous solutions. *Journal of Environmental Radioactivity* **70**, 61-72.
- Ellis A.S., Johnson T.M., Herbel M.J., Bullen T.D. (2003) Stable isotope fractionation of selenium by natural microbial consortia. *Chem. Geol.* **195**, 119-129.
- Han D.S., Batchelor B., Abdel-Wahab A. (2011) Sorption of selenium(IV) and selenium(VI) to mackinawite (FeS): Effect of contact time, extent of removal, sorption envelopes. *J. Hazard. Mater.* **186**, 451-457.
- Hayes K.F., Papelis C., Leckie J.O. (1988) Modeling ionic strength effects on anion adsorption at hydrous oxide/solution interfaces. *J. Colloid Interface Sci.* **125**, 717-726.
- Hayes K.F., Roe A.L., Brown G.E., JR., Hodgson K.O., Leckie J.O., Parks G.A. (1987) In Situ X-ray Absorption Study of Surface Complexes: Selenium Oxyanions on α -FeOOH. *Science* **238**, 783-786.
- Herbel M.J., Johnson T.M., Oremland R.S., Bullen T.D. (2000) Fractionation of selenium isotopes during bacterial respiratory reduction of selenium oxyanions. *Geochim. Cosmochim. Acta* **64**, 3701-3709.
- Hockin S.L., Gadd G.M. (2003) Linked redox precipitation of sulfur and selenium under anaerobic conditions by sulfate-reducing bacterial biofilms. *Appl. Environ. Microbiol.* **69**, 7063-7072.
- Huggins F.E., Sanei H. (2011) Synchrotron-radiation-induced oxidation of selenite to selenate in coal-derived fly ash. *Journal of Synchrotron Radiation* **18**.
- Johnson T.M. (2011) Stable Isotopes of Cr and Se as Tracers of Redox Processes in Earth Surface Environments Handbook of Environmental Isotope Geochemistry, in: Baskaran, M. (Ed.), *Advances in Isotope Geochemistry*. Springer Berlin Heidelberg, pp. 155-175.

- Johnson T.M., Bullen T.D. (2003) Selenium isotope fractionation during reduction by Fe(II)-Fe(III) hydroxide-sulfate (green rust). *Geochim. Cosmochim. Acta* **67**, 413-419.
- Johnson T.M., Herbel M.J., Bullen T.D., Zawislanski P.T. (1999) Selenium isotope ratios as indicators of selenium sources and oxyanion reduction. *Geochim. Cosmochim. Acta* **63**, 2775-2783.
- Krouse H.R., Thode H.G. (1962) Thermodynamic properties and geochemistry of isotopic compounds of selenium. *Can. J. Chem.* **40**, 367-375.
- Lenz M., van Hullebusch E.D., Farges F., Nikitenko S., Borca C.N., Grolimund D., Lens P.N.L. (2008) Selenium speciation assessed by X-Ray absorption spectroscopy of sequentially extracted anaerobic biofilms. *Environ. Sci. Technol.* **42**, 7587-7593.
- Manceau A., Charlet L. (1994) The Mechanism of Selenate Adsorption on Goethite and Hydrated Ferric Oxide. *J. Colloid Interface Sci.* **168**, 87-93.
- Missana T., Alonso U., Scheinost A.C., Granizo N., García-Gutiérrez M. (2009) Selenite retention by nanocrystalline magnetite: Role of adsorption, reduction and dissolution/co-precipitation processes. *Geochim. Cosmochim. Acta* **73**, 6205-6217.
- Mitchell K., Mason P.R.D., Van Cappellen P., Johnson T.M., Gill B.C., Owens J.D., Diaz J., Ingall E.D., Reichart G.-J., Lyons T.W. (2012) Selenium as paleo-oceanographic proxy: A first assessment. *Geochim. Cosmochim. Acta* **89**, 302-317.
- Peak D., Sparks D.L. (2002) Mechanisms of Selenate Adsorption on Iron Oxides and Hydroxides. *Environ. Sci. Technol.* **36**, 1460-1466.
- Pettine M., Gennari F., Campanella L., Casentini B., Marani D. (2012) The reduction of selenium (IV) by hydrogen sulfide in aqueous solutions. *Geochim. Cosmochim. Acta* **83**, 37-47.
- Ravel B., Newville M. (2005) ATHENA, ARTEMIS, HEPHAESTUS: data analysis for X-ray absorption spectroscopy using IFEFFIT. *J. Synchrot. Radiat.* **12**, 537-541.
- Rees C.E. (1973) A steady-state model for sulphur isotope fractionation in bacterial reduction processes. *Geochim. Cosmochim. Acta* **37**, 1141-1162.
- Rickard D., Morse J.W. (2005) Acid volatile sulfide (AVS). *Mar. Chem.* **97**, 141-197.
- Rickard D., Schoonen Martin A.A., Luther G.W. (1995) Chemistry of Iron Sulfides in Sedimentary Environments, *Geochemical Transformations of Sedimentary Sulfur*. American Chemical Society, pp. 168-193.
- Rovira M., Giménez J., Martínez M., Martínez-Lladó X., de Pablo J., Martí V., Duro L. (2008) Sorption of selenium(IV) and selenium(VI) onto natural iron oxides: Goethite and hematite. *J. Hazard. Mater.* **150**, 279-284.
- Scheinost A.C., Charlet L. (2008) Selenite reduction by mackinawite, magnetite and siderite: XAS characterization of nanosized redox products.

- Environ. Sci. Technol.* **42**, 1984-1989.
- Scheinost A.C., Kirsch R., Banerjee D., Fernandez-Martinez A., Zaenker H., Funke H., Charlet L. (2008) X-ray absorption and photoelectron spectroscopy investigation of selenite reduction by Fe^{II}-bearing minerals. *J. Contam. Hydrol.* **102**, 228-245.
- Schilling K., Johnson T.M., Wilcke W. (2011) Isotope Fractionation of Selenium During Fungal Biomethylation by *Alternaria alternata*. *Environ. Sci. Technol.* **45**, 2670-2676.
- Schwertmann U., Cornell R.M. (2000) *Iron oxides in the laboratory: preparation and characterization*, 2nd ed. Wiley-VCH.
- van der Zee C., Roberts D.R., Rancourt D.G., Slomp C.P. (2003) Nanogoethite is the dominant reactive oxyhydroxide phase in lake and marine sediments. *Geology* **31**, 993-996.
- Wijnja H., Schulthess C.P. (2000) Vibrational Spectroscopy Study of Selenate and Sulfate Adsorption Mechanisms on Fe and Al (Hydr)oxide Surfaces. *J. Colloid Interface Sci.* **229**, 286-297.
- Winkel L.H.E., Johnson C.A., Lenz M., Grundl T., Leupin O.X., Amini M., Charlet L. (2011) Environmental Selenium Research: From Microscopic Processes to Global Understanding. *Environ. Sci. Technol.* **46**, 571-579.
- Wolthers M., Charlet L., van Der Linde P.R., Rickard D., van Der Weijden C.H. (2005) Surface chemistry of disordered mackinawite (FeS). *Geochim. Cosmochim. Acta* **69**, 3469-3481.
- Wolthers M., Van der Gaast S.J., Rickard D. (2003) The structure of disordered mackinawite. *Am. Mineral.* **88**, 2007-2015.
- Zhang H., Selim H.M. (2005) Kinetics of arsenate adsorption-desorption in soils. *Environ. Sci. Technol.* **39**, 6101-6108.
- Zhang P., Sparks D.L. (1990) Kinetics of selenate and selenite adsorption/desorption at the goethite/water interface. *Environ. Sci. Technol.* **24**, 1848-1856.
- Zhu J.-M., Johnson T.M., Clark S.K., Zhu X.-K. (2008) High precision measurement of selenium isotopic composition by hydride generation Multiple Collector Inductively Coupled Plasma Mass Spectrometry with a ⁷⁴Se-⁷⁷Se double spike. *Chinese J. Anal. Chem.* **36**, 1385-1390.
- Zingaro R.A., Carl Dufner D., Murphy A.P., Moody C.D. (1997) Reduction of oxoselenium anions by iron(II) hydroxide. *Environment International* **23**, 299-304.

SUPPLEMENTAL INFORMATION**Table SI-5.1 Measured Se concentrations and isotope compositions for iron oxide experiments.**

Experiment	Time Elapsed (h)	[Se] (μM)	$\delta^{82/76}\text{Se}_{\text{aq}}$ (‰)
Se(IV)- 2 line ferrihydrite	0.00	75.6	-1.56
	0.01	45.3	-1.43
	0.08	23.3	-1.18
	0.17	16.3	-0.98
	0.33	10.0	-0.75
	0.50	6.2	-0.70
	0.67	4.0	-1.00
	0.83	2.5	-1.28
Se(VI)- 2 line ferrihydrite	0.00	111.3	-1.21
	0.01	76.0	–
	0.08	64.7	-1.26
	0.17	57.6	-1.43
	0.33	56.6	-1.17
Se(IV)-Hematite	0.00	75.6	-1.42
	0.01	46.0	-1.65
	0.08	45.8	-1.65
	0.17	48.4	-1.61
	0.33	46.7	-1.61
	0.50	44.1	-1.64
	0.67	44.4	-1.65
	0.83	45.1	-1.61
Se(VI)-Hematite	0.00	111.3	-1.21
	0.01	90.0	-1.32
	0.08	90.0	-1.76
	0.17	90.8	-1.36
	0.33	94.7	-1.42
Se(IV)-Goethite	0.00	75.5	-1.56
	0.01	7.6	-1.15
	0.08	6.9	1.80
	0.17	5.3	0.71
	0.33	4.2	0.28
	0.50	3.8	-0.20
	0.67	3.2	0.21
	0.83	2.9	-0.06
Se(VI)-Goethite	0.00	111.3	-1.21
	0.01	89.3	-1.25
	0.08	87.6	-1.37
	0.17	89.6	-1.39
	0.33	92.7	-1.29

Table SI-5.2 Measured Se concentrations and isotope compositions for iron sulfide experiments and homogenous solution experiments. Total [Se] refers to the total concentrations of Se in the aqueous sample.

Experiment	Time Elapsed (h)	Total [Se] (μM)	[Se(IV) or Se(VI)] (μM)	$\delta^{82/76}\text{Se}_{\text{aq}}$ (‰)
Se(IV)- FeS	0.00	75.6	75.6	-1.56
	0.02	27.0	3.4	-1.08
	0.17	7.0	1.1	0.00
	2.00	3.0	–	-2.19
	24.00	1.6	–	-2.09
Se(VI)-FeS	0.00	111.3	111.3	-1.21
	0.02	98.6	92.4	-1.04
	24.00	88.9	67.6	-0.62
Se(IV)-FeS ₂	0.00	75.6	75.6	-1.56
	0.02	47.9	37.2	-0.17
	0.17	36.8	29.8	1.38
	2.00	21.7	20.3	5.34
	24.00	3.1	0.91	4.20
Se(VI)-FeS ₂	0.00	111.3	111.3	-1.21
	0.02	101.1	88.5	-1.15
	24.00	97.3	104.3	-1.22
Se(IV)-Fe(II) _(aq)	0.00	75.6	75.6	-1.56
	0.02	47.1	45.3	-1.39
	1.00	47.4	45.4	-1.41
	24.00	14.0	9.6	-1.53
Se(IV)-H ₂ S _(aq)	0.00	75.6	75.6	-1.56
	0.02	17.6	0.85	–
	1.00	1.6	0.86	-2.46
	24.00	1.7	0.75	-2.62

Table SI-5.3 Total Se and Se(IV) concentration and isotopic data for solid phase from Se(IV)-FeS experiments.

Experiment	Time Elapsed (h)	Total [Se] (μM)	[Se(IV)] (μM)	$\delta^{82/76}\text{Se}$ (‰) aqueous phase	Solid [Se] ($\mu\text{g/g}$)	$\delta^{82/76}\text{Se}$ (‰) solid phase
Se(IV)- FeS	0.00	61.8	61.8	-1.56	–	–
	0.02	32.7	2.2	0.01	495.7	-2.32
	0.33	6.8	1.0	1.22	455.7	-2.50
	0.67	3.6	0.7	-0.20	1025.3	-1.35
	1.00	3.0	0.7	-0.80	1148.8	-0.97
	24.00	2.7	0.8	-2.35	995.6	-1.17

CHAPTER 6

CONCLUSIONS AND FUTURE RESEARCH DIRECTIONS



THE IMAGE ON THE PREVIOUS PAGE IS FROM IMAGEGEO ([HTTP://WWW.IMAGGEO.NET/](http://www.imaggeo.net/)) THE ONLINE OPEN ACCESS GEOSCIENCES IMAGE REPOSITORY OF THE EUROPEAN GEOSCIENCES UNION UNDER CREATIVE COMMONS LICENSE (CREATIVECOMMONS.ORG). LUNAR ECLIPSE DURING THE AUGUST FULLMOON OF AUGUST 16TH 2008, CAPTURED NORTH OF THE WATERFALLS OF LIVADITIS, IN NE GREECE. CREDIT: EVANGELOS KARAGEORGOS , LABORATORY OF ATMOSPHERIC POLLUTION AND POLLUTION CONTROL ENGINEERING, DUTH , XANTHI – GREECE.

6.1 CONCLUSIONS

The marine selenium (Se) cycle is dominated by biological cycling in surface waters which is reflected in the limited Se isotopic variability observed in marine sediments. Isotopic signatures found in marine sediments over wide spatial and temporal timescales occur over a narrow range and do not reflect large scale processes, such as the great oxidation event 2.2 Ga (GOE) or global ocean anoxic events (OAEs). Thus, we conclude that Se isotopic signatures in marine sediments reflect local scale variations over short timescales due to the rapid mixing of Se reservoirs in the surface oceans, which causes a lack of long term isotopic memory of biogeochemical cycling processes. On geological timescales, the marine sediments near instantaneously record the isotopic signature of the Se inputs to the oceans.

The biological cycle of Se is a major part of the marine Se cycle. The biochemical utilization of Se has a long evolutionary history that possibly predates the use of sulfur (S) in biochemical molecules. The essential need for Se in biochemical molecules and the low Se concentrations in seawater make Se a micronutrient element. The narrow range of Se isotope compositions found in marine sediments is consistent with the fact that reductive assimilation of Se does not impart significant fractionation.

Selenium isotope fractionations associated with sorption and abiotic reduction of Se under environmental conditions are poorly known. Selenium readily sorbs to iron (III) oxides, which is one pathway for Se to enter and leave the ocean system. The isotopic

fractionation associated with this process is very small, thus the Se isotopic compositions of sorbed Se is likely to very closely represent the isotopic composition of the source water. Sorption and subsequent reduction of Se by iron sulfide minerals is associated with much larger fractionations and could be a source of variability in Se isotopic compositions observed in marine sediments.

The major input of Se to marine sediments is under the form of Se associated with organic detritus. During early diagenesis most of this organic Se remains in the organic matter pool while a minor amount may be transformed to Se(0) and even less to FeSe. Hence, Se accumulation in marine sediments differs fundamentally from that of S. Sulfur, as sulfide, is the main component in pyrite and mackinawite, while sulfate constitutes the main component of gypsum and anhydrite. Because S and Se do not aggregate in the same sedimentary mineral phases, they record different environmental conditions and biogeochemical processes. Selenium and sulfur do however aggregate in hydrothermal minerals, thus their coexistence may help to rule out low temperature environments.

Processes that fractionate Se isotope significantly, such as dissimilatory reduction of Se oxyanions and reduction by iron sulfide minerals, do not appear to play a dominant role in the marine environment. At best, they have only a small influence on Se isotope fractionations, because most Se is delivered to the seafloor under reduced form with organic matter. Even if dissimilatory and abiotic processes occur, it is likely that the isotopic fractionation observed is

muted, because of the very small Se reservoir size (Clark and Johnson, 2008).

Because Se isotopes have several limitations as a paleo-proxy, it is important to consider these limitations carefully before undertaking a project including selenium isotopes. A key question ask before starting the labor intensive process of measuring Se isotope compositions, is: Will Se isotopes give us new information about the (paleo-)environments of interest or will they just confirm what we already know?

Selenium isotopes are difficult to analyze due to limitations in sample preparation and interferences on MC-ICP-MS. The most significant interference in our studies was the presence of arsenic. Low concentrations of selenium in relevant materials are an issue and make it even harder to separate chemical species of selenium. Separation methods of different fractions of Se have their own limitations (Martens and Suarez, 1997b; Wright et al., 2003; Lenz et al., 2008; Clark and Johnson, 2010). However, even when chemical Se species are separated, they do not show large differences in isotopic composition (Clark, 2007; Wen and Carignan, 2011). The older the rocks the more difficult it is to make accurate Se isotope measurements, due to the extremely low Se concentrations and possible increased arsenic interferences, which are difficult to eliminate.

6.2 FUTURE WORK

Selenium and Se isotopes appear to be appropriate for investigating local scale processes over short time periods. When

working with selenium, the researcher should be prepared for setbacks and the sometimes erratic behavior of selenium, the teenager of the periodic table. With that in mind what follows are ideas for future work with selenium that would expand our knowledge of the biogeochemistry of Se and Se isotopes.

- 1) Se isotope fractionations and isotopic compositions in extreme environments, such as Mono Lake and hydrothermal waters in areas like Yellowstone National Park, have not yet been explored.
- 2) The role of Se in the origin of life is a fascinating subject, which is still in its infancy. The coupling of the biochemistry of selenium and the biogeochemical cycling of selenium may provide insights into this micronutrient's biological evolution.
- 3) Selenium could be a limiting micronutrient in the marine systems, like iron, phosphorus or nitrogen. The role of Se in controlling primary productivity should be evaluated.
- 4) The study of the photoredox chemistry of selenium, may provide new insights into the atmospheric cycling of selenium and selenium isotope fractionations that may occur during these transformations.
- 5) The selenium isotopic composition of modern seawater has yet to be determined. Measuring selenium isotope compositions with depth may reveal anthropogenic inputs into the oceans, and how they have affected the Se biogeochemical cycle and the isotopic distribution of Se.

- 6) The bioavailability of more species of Se, including Se(0) and organic selenides for assimilatory uptake and incorporation into selenocysteine, should be evaluated to more fully understand the cycling of Se in marine surface waters.
- 7) Investigating the early diagenetic redistribution of Se could help determine which sedimentary pools Se is preserved in the sedimentary record.
- 8) Extraction procedures for individual species, including organic, elemental and iron selenide fractions from natural samples need to be developed to be able to assemble useful information from marine sediments similar to SEDEX method for phosphorus (Ruttenberg, 1992).

REFERENCES

- Clark S.K. (2007) Selenium stable isotope ratios in wetlands: Insights into biogeochemical cycling and how a diffusive barrier affects the measured fractionation factor. PhD Thesis, University of Illinois at Urbana-Champaign.
- Clark S.K., Johnson T.M. (2008) Effective isotopic fractionation factors for solute removal by reactive sediments: A laboratory microcosm and slurry study. *Environ. Sci. Technol.* **42**, 7850-7855.
- Clark S.K., Johnson T.M. (2010) Selenium stable isotope investigation into selenium biogeochemical cycling in a lacustrine environment: Sweitzer Lake, Colorado. *Journal of Environmental Quality* **39**, 2200-2210.
- Lenz M., van Hullebusch E.D., Farges F., Nikitenko S., Borca C.N., Grolimund D., Lens P.N.L. (2008) Selenium speciation assessed by X-Ray absorption spectroscopy of sequentially extracted anaerobic biofilms. *Environ. Sci. Technol.* **42**, 7587-7593.
- Martens D.A., Suarez D.L. (1997) Selenium Speciation of Soil/Sediment Determined with Sequential Extractions and Hydride Generation Atomic Absorption Spectrophotometry. *Environ. Sci. Technol.* **31**, 133-139.
- Ruttenberg K.C. (1992) Development of a sequential extraction method for different forms of phosphorus in marine sediments. *Limnol. Oceanog.* **37**, 1460-1482.
- Wen H., Carignan J. (2011) Selenium isotopes trace the source and redox processes in the black shale-hosted Se-rich deposits in China. *Geochim. Cosmochim. Acta* **75**, 1411-1427.
- Wright M.T., Parker D.R., Amrhein C. (2003) Critical evaluation of the ability of sequential extraction procedures to quantify discrete forms of selenium in sediments and soils. *Environ. Sci. Technol.* **37**, 4709-4716.

ACKNOWLEDGEMENTS

“IT IS NOT SO MUCH OUR FRIENDS' HELP THAT HELPS US AS THE CONFIDENT KNOWLEDGE THAT THEY WILL HELP US”

~EPICURUS

It has been a long road that has spanned multiple countries and several universities.

I would first like to thank my promoter Philippe Van Cappellen and supervisor Paul Mason. As well as my thesis assessment committee: Laurent Charlet, Greg Cutter, Tom Johnson, Tim Lyons, and Jack Middelburg.

I would also like to thank all the others who provided scientific guidance during my PhD experience:

Tom Johnson

Don Canfield

Jian-Ming Zhu

Ellery Ingall

Scott Clark

Tim Lyons

I would like to thank my paranimfs Suzanne Hangx and Desiree Roerdink for their help with preparations for the defense and the thesis defense ceremony.

Thanks to my colleagues and friends who offered support and fun times:

Emma Hammarlund and colleagues at the University of Southern Denmark
Suzanne Hangx, Emilia Liteanu, Lori Palasse, Marjoijn Stam, Sander van den Boorn, Desiree Roerdink, and the others at Utrecht University
Amanda Raddatz, Charles Bopp and others at the University of Illinois
Kate Cerully, Kate Salome, Krystal Persaud, Shruti Bhide and the rest at Georgia Tech

Ana Lima and Helen Powley and the rest at University of Waterloo

Lindsay Gulanes, Farina Situmorang and Kristel Jeffereies at Fearless Heart Yoga for keeping me sane during thesis writing time

Most of all I would like to thank Brad Lawrason who dealt with moving to three different countries and three universities so I could finish my PhD. He did this while also dealing with long nights in the lab, trips to Illinois and endless talk about selenium, but most importantly making sure I was fed. And thanks to my mom, and sister who visited every country and university and sent care packages far and wide. To my Dad who pretended he cared what I was talking about when I tried to explain my research to him. Thanks to Pop-Pop who helped make it all possible.

CURRICULUM VITAE

Kristen Ann Mitchell graduated from Plymouth-Whitemarsh High School in June 2001. In August of 2001 she began her undergraduate degree at Eckerd College in St. Petersburg, FL. In May of 2005 she completed her Bachelor of Science in Marine Science in the marine chemistry track. She finished with a thesis entitled “A Comparison of Modern and Fossil Coral Climatology in the Western Pacific Warm Pool”, which was completed at the University of South Florida in St. Petersburg, FL with Dr. Terry Quinn in the pale-oceanography and paleoclimatology lab.

After graduating from Eckerd College, Kristen accepted a Student Fulbright Fellowship which she completed in 2005-2006 at the University of Southern Denmark with Dr. Don Canfield where she completed two research projects: Temperature Effect on the Sulfur Isotope Fractionation during Sulfate Reduction by Two Strains of the Hyperthermophilic *Archaeoglobus fulgidus*, and Sulfur Isotope Fractionation in Gypsum Crusts from Eilat, Israel.

After completing her Fulbright Fellowship Kristen began her PhD at Utrecht University in August of 2006 with Dr. Paul Mason and Prof. dr. Philippe Van Cappellen. In September of 2007, Kristen completed her Master of Science degree, a Prestige Masters in System Earth Modeling, from which she graduated with distinction with a focus in biogeochemistry. The first chapter of her master’s thesis was published in Environmental Microbiology in December 2009.

In August of 2008 Kristen moved to Georgia Institute of Technology, Atlanta, Georgia, USA, to continue her PhD project with Prof. Dr. Philippe Van Cappellen. In May of 2011 Kristen completed her second Master of Science degree in geochemistry in the School of Earth and Atmospheric Sciences at Georgia Institute of Technology. In June of 2011, Kristen moved to the University of Waterloo, Waterloo, ON, CA as a Research Associate to finish her PhD thesis with Prof. Dr. Philippe Van Cappellen.

